

ON THE STRUCTURAL ANALYSIS OF

HIGHWAY PAVEMENTS:

An Application of Variational Methods

by

^{Dr}
M.E. Fleming, B.Sc.

Thesis presented for the Degree of
Doctor of Philosophy

Department of Civil Engineering

The University of Leeds

March, 1968



IMAGING SERVICES NORTH

Boston Spa, Wetherby

West Yorkshire, LS23 7BQ

www.bl.uk

**CONTAINS
PULLOUTS**

TABLE OF CONTENTS

	Page
INTRODUCTION	1
PRESENT STATE OF PAVEMENT STRUCTURAL ANALYSIS	2
Introduction	2
Idealization of the Pavement/Subgrade System	14
Established Analyses of the Pavement/Subgrade System	26
Summary and Discussion	48
PROPOSED RESEARCH PROGRAM	54
STRUCTURAL ANALYSIS OF THE HIGHWAY PAVEMENT	57
Introduction	57
A Thick Plate Theorem in Elasticity	64
Specifications and Assumptions of the Structural Analysis	70
Analysis of the Pavement with Full Interface Contact	77
Preserved	
Analysis of the Pavement Including Possible Loss of	86
Interface Contact	
Discussion	92
SOLUTION TO THE DIFFERENTIAL EQUATIONS OF THE	94
STRUCTURAL ANALYSIS	
General Approach to the Solution of the Equations	95
Application of Power Series	96
Application of Chebyshev Polynomials	105
Application of Fourier Series	117

	Page
Summary	123
FUNCTIONS DESCRIBING THE APPLIED TRANSVERSE WHEEL-LOAD	124
Development of the Loading Functions	126
Numerical Computation of the Loading Functions	142
Comparison of the Loading Function Representations	161
Discussion	172
COMPUTATION OF THE PAVEMENT STRESSES AND DEFORMATIONS	174
Setting-up the Algebraic Form of the Differential Equations	175
Solution of the Algebraic Equations	186
Determination of Stresses, Strains and Deflections	192
Discussion	210
A LIMITED EXPERIMENTAL APPLICATION OF THE STRUCTURAL ANALYSIS	212
Design of the Experimental Investigation	214
Elastic Properties of the Plate and Foundation Materials	218
Obtaining the Analytical Results	226
Discussion of Analytical and Experimental Results	229
CONCLUSIONS	235
RECOMMENDATIONS FOR FURTHER RESEARCH	239
SELECTED REFERENCES	241
ACKNOWLEDGEMENTS	250
APPENDIX A: NOMENCLATURE	251

	Page
APPENDIX B: PROGRAMS TO DETERMINE THE FUNCTIONS DESCRIBING THE APPLIED TRANSVERSE WHEEL-LOAD	260
APPENDIX C: PROGRAMS FOR THE COMPUTATION OF PAVEMENT STRESSES AND DEFORMATIONS	275

INTRODUCTION

Because of the high financial cost involved in highway construction, it is essential that the most economic methods of design and construction are employed in roadworks. From the design aspect, a road must perform its required function for a specified number of years and the extent to which a pavement fulfils this requirement is largely dependent upon the structural method of design employed. Such a method should be economical, completely reliable, and easily applicable. The main difficulty which arises is that there are a great many parameters involved in any pavement design procedure. These vary from those created by pavement frost effects to those resulting from vehicle wheel configurations. The magnitudes and effects of several of these variables are also difficult to determine quantitatively.

In the light of present knowledge it is generally accepted that the ultimate pavement design method will be principally empirical in nature. However, the use of a structural analysis of the pavement as a basis of such an empirical approach is advisable. The analysis should be used to determine the critical stresses, strains and deflections occurring in a pavement and should cover as many as possible of the determinate parameters. This theoretical analysis might then also provide a tool with which the effect of these parameters could be investigated.

PRESENT STATE OF PAVEMENT STRUCTURAL ANALYSIS

Introduction

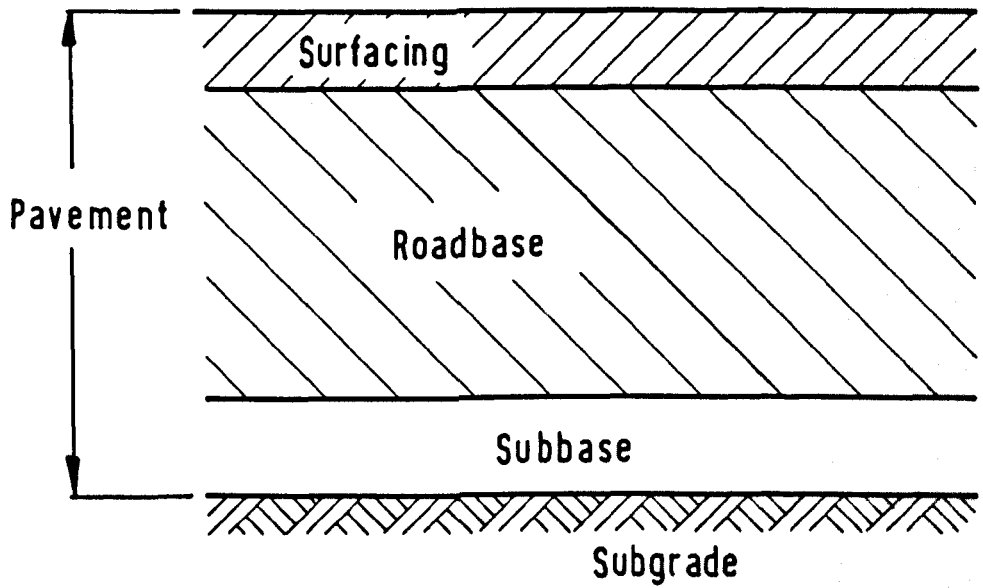
Pavement and foundation

The basic problem in highway pavement design is to provide, as economically as possible, a road structure capable of carrying an estimated amount of traffic, for a given number of years, over the soil occurring along the proposed route.

The structural elements of a pavement and foundation are shown in Figure 1. A typical pavement and foundation cross-section may include the natural in-place subgrade, a compacted subgrade, a compacted subbase, a compacted roadbase of treated or plain gravel or crushed stone, and a surfacing of one or more layers of asphalt. The roadbase and/or surface layers may be replaced by one layer of reinforced or plain concrete. Thus a pavement is a structure consisting of superimposed layers of selected and processed materials whose primary function is to distribute concentrated vehicle wheel-loads to the supporting subgrade so that the reduced pressure transmitted does not exceed the supporting capacity of the subgrade and, at the same time, structural failure of the pavement itself does not occur.

Rigid and flexible pavements are the two main types of road

Figure 1. The basic structural elements of a pavement.



structure. They are defined by the manner in which they distribute the applied wheel-loads to the subgrade. The distinguishing feature of a flexible pavement is that the reduction of transmitted pressure is accomplished through the lateral distribution of the concentrated load with depth rather than by the flexural action of the pavement itself. In rigid pavements, on the other hand, flexural action is dominant and therefore such a structure can bridge over localized discontinuous or inadequate support.

Pavement design factors

The main causes of failure which need to be taken into account when designing a pavement are as follows:

1. Excessive stresses due to traffic. These may be transmitted to the subgrade and lead to excessive deformation with consequent failure of the layers above. Large stresses in the road-base or subbase may also lead to failure of the road even though the subgrade does not become excessively deformed.
2. Excessive stresses from other causes. Temperature or moisture changes in any part of the pavement may possibly, in the case of rigid pavements constructed of concrete, create stresses which cause the break-up of the pavement.
3. Stripping of the surfacing. This may occur through an insufficient adhesive bond being developed between either individual particles of mineral aggregate in the surfacing or between the surfacing and roadbase. Failures of this type are usually confined to bituminous surfacings.

4. Deterioration of the subgrade after construction. A change in the moisture content of the subgrade can result in a loss of support for the pavement. An increase in moisture content usually causes a loss in subgrade strength, while a decrease in moisture content may result in shrinkage of the subgrade. Repeated wheel-loads can cause compaction and consolidation of the subgrade so that localized areas of pavement are left unsupported. The action of frost can often cause damage to the pavement and allow water to enter the subgrade through cracks formed in the surfacing.

Pavement deterioration due to excessive traffic stresses is probably the most important cause of failure and is therefore the only one considered in many methods of pavement design. 'Ideal' methods of design, which attempt to design on the basis of resistance to traffic stresses, should normally try to take account of the following relevant factors:

- a. The magnitudes of the applied wheel-loads.
- b. The wheel contact pressures with the road surface.
- c. The shape of the tyre-carriageway contact area.
- d. Possible combinations of single, dual and tandem wheel configurations.
- e. The dynamic nature of wheel-loads and, thus, the dynamic properties of the pavement and foundation.
- f. The impact effect on the pavement and subgrade due to vehicles encountering irregularities in the surfacing.

- g. The cumulative effect of repeated applications of wheel-loads.
- h. The distribution of stress throughout the pavement and subgrade.
- i. The distribution of wheel-loads across the road width.
- j. The effects of temperature.

Again, ideally, such methods should give the thickness and type of construction that will most economically ensure the desired life of pavement structure. Unfortunately all of these factors cannot yet be taken into account when designing a highway pavement.

Approaches to pavement structural design

There are a great many methods of pavement design which not only differ considerably in their approach to the problem but also in their reliability. Most methods consider only some of the possible causes of failure. Because of the complexity of the problem and its relatively recent consideration, no single method has been shown to be completely acceptable. Even though existing methods are so diverse, they can be classified into the five following main groups (1):

Group 1. Empirical methods based purely on precedent. The highway engineer's personal judgement, using his past knowledge of traffic and climatic conditions in the area, is still used to a certain extent to determine required pavement thicknesses. These methods are only justifiable in the 'design' of the most minor of roads and, even then, should be based on intimate knowledge and past experience of

of highways in the locality.

Group 2. Empirical methods using soil classification tests. With these procedures the thickness of construction over a given subgrade is determined from past experience of the thicknesses required for similar wheel-loads on similarly classified soil subgrades. The classification tests used for this purpose are, normally, the particle-size analysis and the liquid and plastic limit tests. The justification for these methods is that if the moisture content of a soil is controlled and an adequate dry unit weight is obtained in the subgrade through compaction, then the thickness of construction required to withstand given traffic stresses depends largely on the composition and structure of the basement soil. The Group Index method of design (2) is an example of a procedure which utilizes this approach in the design of both flexible and rigid pavements.

Group 3. Empirical methods using a soil strength test. In these methods a test is used to classify the 'strength' of a subgrade soil. The test used, which is commonly a penetration or bearing test, is frequently only applicable to its associated design method. The strength test is considered to stress the subgrade in a standard way and then the thickness of pavement is determined on the basis of experience of the thicknesses required on top of subgrades of similar strength in the past. The best known of these design methods is the California Bearing Ratio method (3). It is used for both flexible and rigid pavement thickness design purposes.

Group 4. Methods based partly on theory and partly on experience. These methods require that the fundamental stress/strain properties of the subgrade soil and the pavement materials be determined by shear or bearing tests so that the results may be employed in a simplified or modified theory of stress distribution which has been found to have some experimental justification. The reasoning here is that, in order to overcome the difficulty of analysing the true stress/strain characteristics of the soil and the true distribution of stress in the layers under the wheel-load, a method in this group is justified in making certain assumptions and neglecting some factors in order to produce a simplified theory which can be easily handled at the design stage. The assumptions and neglected factors involved in any method of this group are generally proved reasonable by experience.

A theory of stress distribution in a concrete pavement which has been used as a basis of some methods in this group is that due to H.M. Westergaard (4). These methods have mainly given consideration to the stresses within the concrete, and the subgrade has only been considered in so far as it effects these stresses.

The Westergaard formulae simply provide a method of calculating the stresses within a given thickness of slab. Such matters as joint spacing, slab width, reinforcement, etc., are considered separately within the design method. In Westergaard's analysis the concrete slab is assumed to be an elastic solid. The reaction of the subgrade is assumed to be vertical and to be proportional to the deflection of the slab. Thus Westergaard's subgrade is assumed to be elastic and to

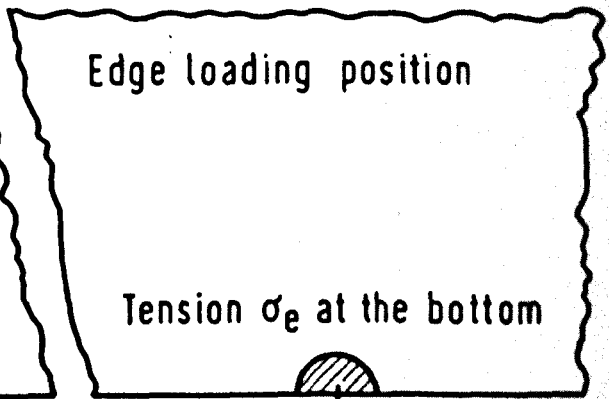
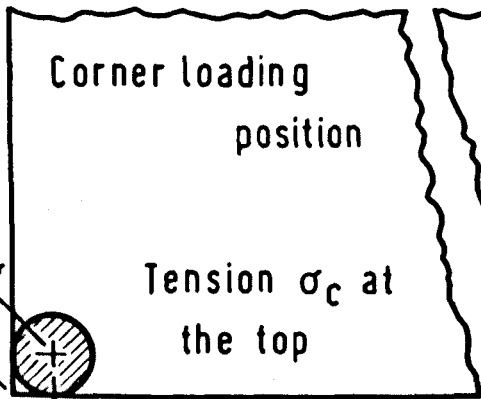
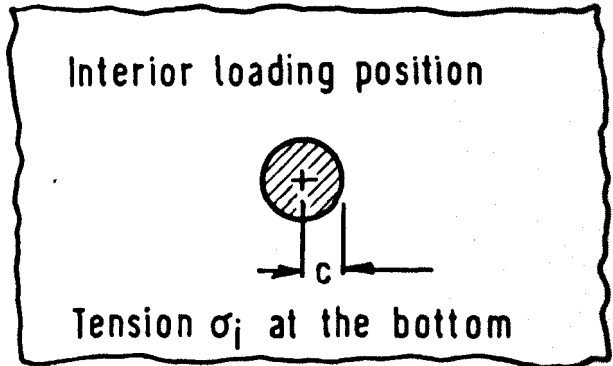
act in a similar manner to a set of vertical springs. This idealization of a foundation is referred to as a Winkler foundation.

In his analysis Westergaard assumed that each wheel-load was uniformly distributed over a circular wheel contact area and obtained formulae for the maximum tensile stresses in the concrete for the loading positions shown in Figure 2. As can be seen, these locations were at a corner, at an edge and at some distance from an edge of the slab. He also (5) studied the problem of warping stresses due to a temperature gradient through the slab on the assumption that this gradient was a straight line. An improvement to Westergaard's work on this latter subject was later made by Tomlinson (6).

The elastic constant used to describe the stress/strain relationship of the Winkler foundation is the modulus of subgrade reaction, k , and is defined as the pressure required to cause a unit deflection of the subgrade surface. It is normally measured in units of $\text{lb./in.}^2/\text{in.}$ and is determined by a plate bearing test. The most usual method of determining k is according to the procedure laid down by the U.S. Corps of Engineers (7).

A number of improvements have been made on Westergaard's original stress analysis which make it agree more closely with experimental work. Thus, Kelley (8) suggested an improved formula for determining the maximum tensile stress for the corner loading case after comparing the value given by Westergaard's formula with experimental highway pavements; his work is especially applicable when the slab

Figure 2. The three loading positions on a slab which were analysed by Westergaard.



corner is not in complete contact with the subgrade due to upward warping of the slab. Spangler (9), after conducting large-scale indoor experimental tests, confirmed Kelley's formula for corner loading and suggested a simplification of the formula which yields substantially the same results.

Pickett (10) noted that several of the theoretical and empirical formulae developed for corner stresses in concrete pavements had obvious limitations to their range of application. For example, he pointed out that the Westergaard, Kelley and Spangler equations all indicate the maximum stress to be zero when the ratio of the radius of the loading area to the radius of relative stiffness is unity. The radius of relative stiffness is a constant representing the slab/foundation system and was first defined by Westergaard, in terms of the slab thickness, the Poissons ratio of the slab, the slab's modulus of elasticity, and the modulus of subgrade reaction of the subgrade. Because of these observations, Pickett worked toward the development of a formula which had the same shape and characteristics of the Westergaard equation but which had less limitations on its use and also gave approximately the same stresses as the Kelley and Spangler equations within their range of application.

Both Spangler and Pickett attempted to allow for the non-uniform distribution of moments along sections perpendicular to the bisector of the corner angle whereas Westergaard assumed this distribution to be uniform. Pickett through his semi-empirical equation also allowed

for lack of subgrade support near the corner due to warping.

Group 5. Wholly theoretical methods. These procedures are based entirely on mathematical analyses of the stresses and strains throughout the pavement and subgrade and on the true stress/strain characteristics of the various materials. The best known theoretical analysis in this group is that due to Burmister (11) and it is this which forms the basis of most design approaches in this group.

Burmister analysed the stresses and strains in a two-layer system which consisted of an elastic slab, infinite in the horizontal plane only, placed on a semi-infinite solid of lower modulus of elasticity; he considered the system to be subjected to a uniformly distributed load acting over a circular area and applied to the upper surface of the slab. The interface between the two layers was assumed to be either perfectly rough or perfectly smooth. Using these assumptions Burmister was then able to compute the vertical displacement at the surface under the centre of the applied load for various pavement thicknesses and elastic constants.

Burmister suggested a pavement design method based on the results of his analysis. For flexible pavement design purposes he considered the pavement as the top layer of a two-layer system and the subgrade as the bottom layer. The thickness of the top layer was then determined so that the displacement under the wheel was limited to an arbitrarily selected quantity. It is here that empiricism really entered into Burmister's design procedure since not only does difficulty

arise in obtaining satisfactory values for the elastic properties of the pavement and subgrade which are required by the procedure but, in addition, the value for the limiting displacement is chosen with no direct account being taken of the stresses in the materials. No account is also taken of the traffic intensity or of deformation due to traffic consolidation and compaction. In summary it can perhaps be said that the method is not very practical, especially as it is extremely sensitive to the value of limiting displacement chosen.

From the above brief discussion it can be seen that there is, as yet, no one design method which is generally accepted. There are over forty design methods, many of them having little in common with one another either in the assumptions they make or in the results they produce. It is possible, however, that a structural analysis of the pavement/subgrade system may be used in the future as the basis of one generally accepted rational design method. What is clearly required in that case is a method of analysis which includes as many of the design parameters as possible and which would thus help to forecast pavement behaviour more accurately. Some of the relevant existing methods of structural analysis are examined briefly in a later section of this chapter. Before this, it is necessary to discuss the possible idealisations which are applicable to a pavement/subgrade system.

Idealization of the Pavement/Subgrade System

The vertical variation in the material composition of a highway structure, coupled with the complex nature of the behaviour under load of the individual materials, has hindered the development of a rational analysis for the stresses and displacements provided by traffic loads. Because of these and other difficulties, analysts have found it necessary to idealize the pavement/subgrade system into mathematically tractable forms. Some of the idealizations which have been made are now discussed.

Wheel/pavement contact area and pressure distribution

The actual contact area between a wheel and a pavement surfacing is somewhere between an ellipse and a rectangle, depending upon the type of tyre and the tyre pressure. The distribution of pressure over this contact area depends upon many factors including the type of tyre, the tyre pressure and the stiffness of the tyre walls. For example, low tyre pressure and stiff tyre walls result in a slightly higher contact pressure underneath the tyre walls compared with the remainder of the contact area.

The use of the exact shape of the wheel/pavement contact area and the actual distribution of pressure over this area does not appear to be critical to the analysis of stresses and deformations in the pavement and subgrade. For this reason, the perimeter of the contact area is usually idealized to a circle, while the area enclosed is assumed

equal to the contact area. The pressure from the tyre is then assumed to be uniformly distributed over this area.

The pavement layers

The analysis of layered pavement systems is usually confined to those containing two or three layers. This is due to the difficulty in analysing and obtaining numerical solutions for higher order multi-layer systems. For a similar reason each layer is considered uniform in thickness.

A flexible road is normally an example of at least a three-layered system; this also applies to many rigid pavements. In three-layer theoretical approaches it is customary to take the whole surfacing as the uppermost layer, the roadbase as the intermediate layer, and the subgrade as the lower layer which extends downward to infinity. A problem arises, however, when there is a subbase between the roadbase and the subgrade. The difficulty is then in deciding within which of the idealized layers the subbase should be incorporated and what properties are representative of that combined layer. In this case, the roadbase properties are normally considered to be representative of the combination unless the subbase's properties are so obviously similar to those of the subgrade as to be naturally combined with it.

Many analyses consider the road to be a two-layered system and as a result even greater difficulties arise when choosing the elastic properties for two layers which are representative of the pavement and subgrade. The idealization of the pavement and subgrade to a two-

layered system has the advantage that such a system can be more easily analysed than a three-layered system.

Lateral dimensions of the pavement

The majority of the theories relating vehicle loads with the stresses and deformations in roads, for simplicity, assume that the road consists of a number of layers, all infinite in the horizontal direction, and overlying a subgrade of infinite thickness. Some others, however, assume the presence of a finite horizontal limitation to the extent of the pavement; this may be either a pavement edge or corner. These discontinuities in the pavement can form a closed pavement shape such as a rectangle or circle. Structural analyses of circular areas have been made but their application to actual pavement analysis is questionable.

Which structural analysis to apply to a particular pavement has been largely dependent upon the type of pavement being considered. Because of the absence of joints, sharply defined edges and flexural rigidity in flexible pavements, those analyses which consider the pavement to be infinite in extent horizontally have found application mainly in flexible pavements. This simplification has allowed other effects to be incorporated into the theoretical analysis which are especially pertinent to flexible pavements, e.g. transverse compression of the pavement. In contrast, those theories which have included edge effects, etc., are especially useful for rigid pavement analysis since the concrete slabs are usually cast in the form of rectangles. Because in

such cases the stresses and deformations generated are critical when the contact area is near an edge or corner, it is essential that the boundary effects are incorporated into the analysis.

A form of discontinuity which is similar to an edge is that of a crack in the pavement. Cracks are essentially a post-construction problem and a finite crack is, analytically, very difficult to handle. For these reasons little attention is usually given to them in most analyses.

With concrete slabs there is the additional problem of whether or not they obtain substantial support from adjacent slabs. This problem is compounded by the introduction of dowel bars which result in a decrease in the stresses and deformation of the loaded slab. Because of the difficulty of determining the efficiency with which particular dowel bars transfer stresses, this problem is idealized in most analyses by simply ignoring it; where it is taken into account it is through the introduction of empirical factors which enable the results to be modified in a suitable manner.

The behaviour of the pavement

In the specification of the pavement/subgrade system to be analysed, the elastic nature of the pavement and subgrade is probably the most important consideration. A balance has to be struck between the idealization of the system and the ability of such a system to be analysed.

Some pavements, especially those with bituminous layers, have

been shown to be viscoelastic to some extent. Even so the magnitude of the problem which would be created by the inclusion of a time variable into the analysis has largely led investigators to avoid this complication by assuming that the pavement and subgrade behave elastically.

The question as to whether the pavement is linearly elastic has also been given attention. The general conclusion is that at low levels of stress and high rates of loading most pavements and subgrades show a sufficient proportionality of stress to strain to enable the theory of elasticity to be used to predict stresses, strains and displacements. At higher levels of stress i.e. where failure of the pavement is approached, this is not so, as the pavement components do not exhibit linear elasticity. Since however, proper design does not allow undue deformation of the pavement to occur, it is unlikely that these higher regions of stress arise in the highway in practice. Therefore, a highway is usually considered to behave in a linear-elastic manner under the dynamic loading of moving vehicles.

The dynamic influence of a moving vehicle highlights the fact that the magnitude of the deformations within a pavement is related to the speed of a vehicle i.e. there is a decrease in the deformation of each layer as the speed of traffic increases. This effect can be included in a purely static elastic analysis, which most analyses are, by making use of values of dynamic elastic moduli which correspond with the design speed of the road. The main difficulty here,

however, is in developing satisfactory methods for determining the dynamic elastic moduli of the pavement and foundation materials. Until satisfactory methods are developed use must be made of the static elastic moduli in the purely static elastic analyses.

Finally, along with the requirement of elasticity, it is usual to consider each idealized layer as a homogeneous and isotropic material. These are basic assumptions which are necessary in order to make the problem mathematically tractable. Since, however, an idealized 'layer' may be composed of more than one actual layer, it could be seen that the former of these requirements may be impossible to satisfy in practice. Similarly, the action of construction traffic can result in reorientation of the pavement materials in a particular direction and so violate the isotropic requirements.

The behaviour of the foundation

The idealizations involved with respect to the subgrade are equally as important as those of the pavement layers, even so, greater simplifications are normally found in relation to the subgrade than occur in the pavement representation.

While the subgrade can usually be considered to distribute the stresses applied to it by compression and granular interaction, the use of simple elastic properties in analyses infers that it also possesses tensile strength. Except for the small amount provided by cohesion, and/or by the artificial (tensile) strength due to the pre-compressive effect of the pavement weight, there is little tensile strength present.

Thus there is a little justification for the use of elastic properties. The subgrade is usually considered to have tensile stiffness as otherwise the theoretical analysis becomes extremely difficult.

Whether the subgrade should also be considered as a homogeneous isotropic solid or as some simplification of this idealization is very much a case of convenience. The use of the simplification provided by the Winkler foundation is usually accepted as it enables more accurate idealizations in say the pavement to be incorporated in the analysis which would otherwise prove difficult to handle with the added complication of the homogeneous isotropic elastic solid foundation.

Another argument in favour of using a simplifying assumption, such as that provided by Winkler with regard to the subgrade is that on balance it may be just as near to the actual state of affairs as the three-dimensional elastic solid representation. For instance, if the concept of an isotropic elastic solid was to be used, then the presumption would be of similar values of elastic constants whether the point in question was in tension or compression. As has been noted before this is most unlikely to be the case and so the advantage of using the refinement of an elastic solid is questionable when the obvious basic violation is present anyway. Furthermore, the applied load is distributed within the subgrade to only a small degree by flexure, the main part being taken by direct compression in a direction transverse to the plane of the pavement. In view of this, the idealization of the pavement to a set of springs, as in the Winkler assumption, is not unreasonable, bearing in

mind its distinct advantages when attempting to obtain analytical solutions.

An added point which works against the use of the elastic solid concept of the subgrade is that related to the difficulty in obtaining satisfactory elastic properties for the subgrade. No method of obtaining suitable values is yet available. In contrast, the determination of the modulus of subgrade reaction - this is the 'elastic' property used to describe the Winkler foundation - by the plate bearing method has found acceptance by engineers and there is considerable experience in using the results of this test. It also has the advantage that the test may be performed on the actual 'in place' subgrade, thus avoiding the change in properties of the subgrade material which results from its removal from the roadway to the laboratory for testing. (This is not the case with the triaxial compression test which can be used to approximately determine the properties required for the elastic solid idealization.)

Karl Terzaghi (12) has presented a comprehensive study of the evaluation of moduli of subgrade reaction which shows that the determination and use of these coefficients in relation to the Winkler foundation involves two assumptions which are of particular importance. These are, firstly that the relationship between the applied pressure at the surface of the subgrade and the resulting surface displacement at that point is independent of the magnitude of the applied pressure and secondly, that this relationship is not affected by the presence of

pavement or bearing plate edges. Terzaghi found however that if a loading test is performed on a subgrade of any kind the settlement increases with increased pressure - in fact, he showed that the first assumption is approximately valid only for values of pressure which are smaller than about one-half of the ultimate bearing capacity of the subgrade. According to the second assumption the subgrade reaction at, for example, the base of a centrally loaded perfectly rigid slab, (as is the presumed state of the plate in the plate bearing test), has the same value everywhere. In reality, the pressure at the rim of the surface of contact is either greater or smaller than that at the centre depending on the elastic properties of the subgrade. In summary, Terzaghi therefore felt that with problems involving the modulus of subgrade reaction the limits of validity of the first assumption should always be taken into consideration when applying the results to such work. He also considered that, in connection with practical problems, the errors resulting from the second assumption could in many cases be disregarded.

Pavement/subgrade continuity

The interface between the pavement and the subgrade is unlikely to be either of such a roughness to provide for a complete transfer of stresses between the two layers, or to be smooth enough to allow only the transfer of stresses normal to the interface. The difficulty in determining the actual degree of partial transfer of stress in any instance is very great and the usual procedure in mathematical analyses has therefore been to utilize a simplification which considers the interface contact to be either completely smooth or completely rough. Thus,

for example, the Winkler concept considers the contact to be completely smooth.

Associated with the above is the possibility that an upward movement of the pavement at a little distance from the loading position may be accompanied by a loss of contact between the subgrade and the pavement at that point. This can occur with respect to rigid pavements although it must be also stated that the pre-compression of the subgrade, which results from the pavement weight, may be sufficient to exceed any subsequent upward movement due to wheel-loads and so contact may not be lost.

If loss of contact does occur then the result is the complete absence of stress transfer at that point. This creates a non-linear problem in which the relationships between stresses and deformations are entirely different to those when continuity is assumed to be preserved. Nearly all of the analyses ignore this possibility, however, and assume that the subgrade remains attached to the pavement at the interface, even though the pavement deflection may be upward. Some researchers have attempted to overcome this difficulty by first of all analysing the problem in the usual manner and then, on noting the points where upward movement take place, repeating the analysis with no subgrade support at these points. By carrying out this procedure repeatedly a more correct solution can be approached, but it is a very tedious approach.

Related to the possibility of loss of interface contact due to upward movement of the pavement is the difficulty in obtaining uniform support for the pavement since local loss of support due to pumping or

settlement of the subgrade is always a distinct possibility. While a number of investigators, notably Richart and Zia (13) and Sparkes (14) have attempted to treat this problem specifically by using various simplifications, they are generally omitted in pavement analyses on the grounds that, since they are primarily related to post-construction problems, it is better to design the road construction to avoid the possibility of their occurrence.

The variation of transverse stresses and deformation through the plate

The classical theory of elasticity as developed for plates has been available to engineers for many years and is used a great deal in the analysis of the pavement/subgrade system. It is treated exhaustively in many textbooks notable among which is that of Timoshenko and Woinowsky-Krieger (15). This theory contains a number of assumptions which are principally concerned with the transverse variation of stress and deformation through the thickness of a plate. In fact, the only type of plate which completely satisfies the assumptions made are those which are referred to in the literature as 'thin' plates.

Research workers have recently been giving more attention to these classical assumptions and have found that substantial inaccuracies are possible in certain problems. Two of the assumptions which are of particular importance are:

1. That the component of stress normal to the middle surface is small compared with other components of stress.
2. That plane cross-sections normal to the undeformed middle-

surface remain plane and normal to the deformed middle-surface.

These two assumptions are equivalent to neglecting the effects of transverse direct compression and transverse shear deformation, respectively. Plates for which these two assumptions are not justified, because of the inaccuracies which would result, are generally known as 'thick' plates. A theory of elasticity which is referred to as a thick plate theory strictly refers to one which only includes the effect of transverse shear deformation. However the majority of writers use this expression to describe a theory which includes both transverse shear deformation and transverse normal compression. The latter connotation is used in this thesis unless otherwise stated.

In the application of the thick or thin plate theory to the analysis of the pavement/subgrade system the pavement is considered to be a plate resting on a foundation. Whether the application of a thick plate theory would produce substantial improvements over the classical thin plate theory in the analysis of the system is very much dependent upon the actual geometry and elastic properties of the layers involved. Thus transverse compression of the pavement (plate) is an important influence on the distribution of stress and deformation within flexible pavements but probably not in rigid pavements. Transverse shear deformation is likely to be greater in plates which are supported on a foundation as compared with those which have other means of support, e.g. those with simply supported edges; this is because of the increased distribution of applied load over the plate through shear rather than flexure. In fact, the effect increases with increased stiffness of the foundation.

The presence of plate (pavement) discontinuities provided by pavement edges and corners can result in inaccuracies due to the neglect of transverse shear deformation especially when, as is the case in actual highways, the wheel-load is applied close to the edge. This is emphasized when the increased ability to accurately specify the boundary conditions at the edges of the plate (pavement), made possible by including the effect of transverse shear deformation, is considered.

Thus the use of the thick plate theory rather than the thin plate theory, i.e. including the effects of transverse normal compression and shear deformation, may result in a substantial increase in accuracy in determining the stresses and deformation of the pavement and subgrade.

Established Analyses of the Pavement/Subgrade System

The Introduction has given the approaches to and the requirements of pavement design methods. In the preceding section are listed and discussed the relevant idealizations of the pavement/subgrade system. The purpose of this section is to summarize the theoretical methods of analysis so that in association with the previous section and the background provided by the Introduction, the principal deficiencies in the present state of pavement analysis can be brought to light.

The analyses considered are discussed in chronological order as they span a period of activity from the 1920's to the present day. For convenience, they are referred to by the name of their authors.

Westergaard, H.M.

As has been explained before, the two-layer analysis of a slab resting on a foundation, presented by Westergaard (4) in 1926, provides the basis of the methods used to-day for the design of rigid pavements and for this reason is discussed in some detail. This analysis is performed for each of the three loading positions shown in Figure 2. These are referred to as the interior, edge and corner loading positions and are a large distance from any other slab corners or edges. The solutions obtained are in the form of simple formulae for the maximum tensile stress and maximum deflection of the slab at each of the positions considered. No direct analysis is made of the stress distribution within the foundation.

The basic assumptions in this analysis are:

1. The slab is treated as a thin, elastic, homogeneous, isotropic, solid plate.
2. The foundation is considered to be of the Winkler type.
3. The interface between the slab and the foundation is considered to be smooth.
4. The wheel-load is represented by a pressure of uniform intensity which is spread over a circular area.
5. Full contact is preserved between the slab and the foundation at all times.

The approaches to the three analyses are now briefly explained.

Interior loading position. The slab which is considered to be a circular plate of infinite extent horizontally, is first analysed using the thin plate theory. With slabs of the proportions as found in pavements this theory leads to a satisfactory determination of deflections at all points and of stresses at all points except in the immediate neighbourhood of a concentrated load such as the idealized circular wheel-load. The theory, in fact, produces infinite values of stress as the radius of the contact area decreases to zero.

To avoid this inaccuracy, Westergaard altered the formulae provided by the classical theory by replacing in these formulae the actual radius, c , of the contact area by an equivalent radius, b . This resulted in correct values of stress being computed from these formulae at points over and around the contact area. The relationship between the actual radius, c , the equivalent radius, b , and the thickness of the slab, h , which would give the correct stresses was determined by comparing the stresses from the classical theory with those based on an analysis performed by A. Nadai (16) which considered the concentrated load to be at the centre of a form of thick circular slab of small radius. Westergaard, in effect, inserted this circular slab into the centre of the large thin slab. The radius of this inner slab was arbitrarily chosen to be $5h$. By comparing the stresses given by the thin plate theory with those of the more accurate theory the relationship between c , b and h was found to be

$$\begin{aligned} b &= \sqrt{(1.6c^2 + h^2)} - 0.675h & \text{for } c \leq 1.724h \\ \text{and } b &= c & \text{for } c > 1.724h \end{aligned} \tag{1}$$

This indicates that for $c > 1.724h$ the thin plate gives substantially the same values of stress as the more accurate theory based on Nadai's analysis.

To facilitate the mathematical treatment, Westergaard introduced the term 'radius of relative stiffness' denoted by the symbol λ and expressed by the relationship:

$$\lambda^4 = \frac{Eh^3}{12(1-\mu^2)k}$$

where E is the modulus of elasticity of the slab, μ is the Poisson's ratio for the slab, and k is the modulus of subgrade reaction of the foundation. This quantity, λ , can also be considered as a measure of the relative stiffness of the slab flexure to the subgrade support.

The ordinary thin plate theory gave the following expression for the critical tensile stress, σ_i , under the centre of the contact area:

$$\sigma_i = \frac{3(1+\mu)\bar{P}}{2\pi h^2} \left(\log_e \frac{\lambda}{c} + 0.6159 \right) \quad (3)$$

where \bar{P} is the total wheel-load. The correct stress at the centre of the contact area was obtained by replacing c by the expression for b in equation (3).

The deflection, d_i , at the centre of the load was computed using the thin plate theory and is as follows:

$$d_i = \frac{\bar{P}}{8k\lambda^2} \quad (4)$$

Edge loading position. When dealing with the wheel-load at the edge, Westergaard assumed that an equivalent radius, b , might be introduced

in place of the true radius, c , in a manner similar to that for the preceding case and by the same formula. This assumption was justified on the ground that the distribution of energy due to vertical shearing stresses was similar for both cases. The correct stresses were obtained by introducing the equivalent radius, b , in place of c in the following formula for the maximum tensile stress, σ_e , along the bottom edge of the slab under the centre of the contact area:

$$\sigma_e = 0.529(1 + 0.54\mu)\frac{\bar{P}}{h^2}(4\log_e\frac{\lambda}{b} + 0.359) \quad (5)$$

From the classical theory, Westergaard found that the deflection, d_e , at the point of application of a concentrated force \bar{P} at the edge was approximately equal to

$$d_e = \frac{1}{\sqrt{6}}(1 + 0.4\mu)\frac{\bar{P}}{k\lambda^2} \quad (6)$$

Corner loading position. For this case, Westergaard considered a wheel acting close to the right-angled corner of a large panel of the slab. The critical failure stress in this instance is a tension at the top of the slab, at a critical section which is some distance from the corner. The centre of the circular load is then at a distance c_1 from the corner, where $c_1 = c\sqrt{2}$. Westergaard attempted to improve on previous critical stress formulae which assumed that the load was concentrated at the corner, i.e. $c_1 = c = 0$, and that there was no subgrade support between the corner and the critical section.

Westergaard obtained an improved approximation by employing the thin plate theory to arrive at an approximate expression for the

deflection, d , in the neighbourhood of the corner. Knowing that the reaction of the subgrade at any point to be equal to kd , when k is the modulus of subgrade reaction, Westergaard showed how the total bending moment M_1 at the section $x' = x_1$, where x' is the co-ordinate direction along the bisector of the square corner, due to the combined influence of the applied load and the reaction of the subgrade, could be obtained. He assumed that this bending moment was uniformly distributed over the width $2x_1$ of the cross-section of the slab perpendicular to the direction bisector, x' , of the corner; thus the bending moment per unit width became $M = M_1/2x_1$. The numerically greatest value of M was then found to occur approximately at the distance $x_1 = 2\sqrt{(c_1\lambda)}$. Division of this value of M by the section modulus per unit width, $h^2/6$, led Westergaard to the corresponding greatest tensile stress, σ_c . Thus

$$\sigma_c = \frac{3\bar{P}}{h^2} [1 - (c_1/\lambda)^{0.6}] \quad (7)$$

The associated deflection, d_c , at the corner was then found to be

$$d_c = (1.1 - 0.88c_1/\lambda) \frac{P}{k\lambda^2} \quad (8)$$

As can be seen from this brief account of his analysis, the simplicity of the solutions proposed by Westergaard lend themselves to the usage which engineers have made of them in rigid pavement design. A main advantage of the theory was that, for the first time, it attempted to allow for the effect of an edge or corner upon the stress distribution and deflection of a pavement slab.

Nowadays, Westergaard's approach is regarded as being far from a pure application of the thin plate theory. In the interior case approximate corrections are required in order that the thin plate theory may give finite stresses under the centre of the load. Additional approximations are also necessary in the edge loading case in order to allow for the boundary effect of the slab edge. In addition, many assumptions are necessary in the corner loading case in order to obtain the critical stress.

The Westergaard theory becomes increasingly inaccurate as the stiffness of the upper layer approaches that of the support. Thus, Hagstrom, Chambers and Tons (17) suggest that a limiting stiffness ratio of $E/k \geq 100$ should be chosen as a criterion for the plate-type behaviour of a pavement and the satisfactory application of Westergaard's theory. Modifications to his original 1926 equations were, in fact, made by Westergaard in 1933 (18), 1939 (19), and 1947 (20). These modifications were concerned primarily with interior loads and so are not discussed further here.

Murphy, G.

The main contribution of the two-layer analysis made by Murphy (21) is that the plate i.e. the pavement, is considered to be supported by only that portion of the subgrade with which it is actually in contact. This is in contrast with the majority of analyses in which the foundation is assumed to remain in contact with the layer above when upward movement of the slab takes place. The other point of major

interest in this analysis was that the plate was considered to be rectangular in shape.

In his analysis Murphy assumed the slab to be thin and the foundation to be of the Winkler type when both were in contact. His approach was basically to obtain an expression for the deflection of the plate (slab) and to compute the stresses within it from an equation based on this expression. This approach was an extension of the technique employed by Happel (22) in his analysis of a symmetrically loaded rectangular plate permanently in contact with the foundation.

Nadai's (16) expression for the energy change due to the application of a load on a plate was used by Murphy to relate the plate deflection with the normal load. The deflection was assumed by Murphy to be expressible in terms of a double hyperbolic series in which the arguments were selected to satisfy certain boundary conditions due to the presence of plate edges. These boundary conditions were expressed in terms of bending moments and shear forces, but could also be related to deflection. In order that the unknown deflection would satisfy these conditions use was made of the thin plate expressions which related vertical shear with deflection and bending moment with deflection.

The deflection series chosen by Murphy only approximately satisfied the above essential boundary conditions; furthermore, he showed that this difficulty was independent of the number of series terms considered. The deflection series was substituted into the energy-change expression and made to satisfy the requirements of the

thin plate theory of elasticity by minimizing the total energy of the system. The result was a system of simultaneous equations which could be solved for the unknown coefficients of the deflection series.

The ability of the plate and foundation to separate at a point on the interface when the plate at that point moves upward was retained in Murphy's theoretical analysis. The difficulty which then arose, however, was that before the simultaneous equations could be generated and solved it was necessary that the area of contact between the plate and foundation should be known. If this was not so, Murphy suggested that a method of overcoming this difficulty was to analyse the system initially assuming full contact and, on noting the deflection surface, to reanalyse the system with an adjusted area of contact. Repeated application of this approach would then eventually result in the correct solution.

In summary, it may be said that Murphy's consideration of a finite rectangular plate is only made possible by approximately satisfying the theoretical requirements of the plate boundary conditions. His consideration of the problem of loss of contact between the plate and slab during loading is numerically difficult to solve for the plate deflections as the problem is, in fact, non-linear in nature and requires the use of an iterative method of solution.

Hogg, A.H.H.

In 1938 Hogg (23) considered a symmetrically loaded thin plate (pavement) of infinite extent, resting on the horizontal smooth

surface of a semi-infinite elastic solid (subgrade), and obtained expressions for the curvature at the centre of the circular area over which the load was uniformly distributed. His analysis differed from that of Westergaard's for the interior load, principally in the manner in which the foundation was assumed to act on the underside of the plate. Westergaard assumed that the pressure applied to the underside of the slab was equal to kw where w was the deflection at that point and k was the modulus of subgrade reaction of the foundation. Hogg on the other hand made use of the general solution due to K. Terazawa (24) of a point load applied to the surface of a semi-infinite elastic solid and expressed in terms of Bessel functions. The expressions for surface deflection and normal direct stress obtained by Terazawa were substituted by Hogg into an equation relating the applied normal stress and the deflection which was obtained by using the thin plate theory of elasticity. He then solved the expression for the plate curvature under a circular load and expressed the result in terms of Bessel functions.

In 1944, Hogg presented a paper (25) which analysed a two layer system composed of a thin elastic slab of infinite extent resting on the upper smooth surface of a uniform layer of elastic material which, in turn, rested on a perfectly rough rigid horizontal surface. The analysis which he previously reported (23) is, in fact, a special case of this present problem. He obtained an exact solution for this general two-layer case in the form of an infinite integral and calculated

approximate values by numerical integration. Hogg later presented the results of this theoretical work in a more useful form (26) and considered how far they agreed with the result of experiment. He found fairly satisfactory agreement with such results as were available at that time if the properties of the subgrade were represented by an equivalent elastic layer.

The solution provided by Hogg can be considered to be relatively simple in form and to provide one of the first of the theoretical attempts involving consideration of the subgrade as an elastic layer. In order to include this effect he had, however, to keep the remainder of the system as simple as possible. Thus it is that he had to include the concept of an infinite horizontal slab and subgrade, the application of thin plate theory, and the smooth interface between slab and subgrade.

Burmister, D.M.

In 1943, Burmister (11) introduced a theory of stresses and displacement in two-layered pavement systems based on the assumption that the materials of each layer were three-dimensional elastic solids. His analysis then provided an exact solution to the three-dimensional problem for a given surface loading. (The equations he developed were rather cumbersome to work with in practice, however, and thus, computer solutions have since been developed for a large range of applications.) Burmister considered that the layers were infinite in extent horizontally and, as such, his theory was not intended to apply to corner or edge loadings on concrete pavements but was principally intended for airport

runways or, perhaps, the centre of a large pavement slab. Although some workers have developed design procedures for flexible roads which are based on Burmister's work, they have found relatively little acceptance up to the present time.

Burmister considered a two-layer system in his first paper (11); each layer was assumed to be a homogeneous isotropic elastic solid, and the interface between the layers was either allowed to have no slippage or no friction. Because of the complexity of the computation, the value of Poisson's ratio was assumed to be equal to 0.5 for the materials in both layers. The solution of the problem was required to satisfy certain boundary conditions, i.e. the surface of the upper layer had to be free from normal and shearing stresses outside the limit of the loading area and the stresses and displacements at infinite-depth in the subgrade layer had to equal zero. It was also assumed that the two layers were continuously in contact and acted together as an elastic medium of composite nature.

In developing the theory of the two-layer system, Burmister employed the stress and displacement equations of elasticity for the three-dimensional problem which were originally derived by Love (27) to satisfy the equations of equilibrium and compatibility of the theory of elasticity. Burmister took a stress function expressed in terms of Bessel functions for each of the layers and found that they satisfied the compatibility conditions and equilibrium equations. The arbitrary constants contained in these stress functions were then evaluated to

satisfy the conditions at the interface for both the no slip and no friction conditions and for a general surface loading distribution expressed in terms of Bessel functions.

The stress and displacement equations in both layers were next determined by Burmister from the equations of elasticity relating stresses and displacements to the stress functions. He then obtained an equation for the settlement of the upper layer under the centre of a circular bearing area of a uniformly distributed load and carried out some numerical computations using this equation.

L. Fox (28) of the National Physical Laboratory later extended Burmister's work by computing the stresses within the pavement and subgrade for various combinations of parameters. In this analysis Fox employed two methods of computation. The first, which was similar to Burmister's, dealt with both perfectly rough and perfectly smooth interface conditions; it enabled accurate results to be obtained at points on the vertical axis of symmetry for the stresses in the lower layer. The second method, based on relaxation methods applied to finite difference forms of the differential equations of elasticity, enabled Fox to obtain a general, though less accurate, picture of the stress distribution throughout the pavement and subgrade for a perfectly rough interface.

Burmister (29) later extended his theory of stresses and displacements to cover the more general case of three layers, with full continuity across the interfaces between the layers. On this occasion he only derived a settlement equation for points on the upper surface of

the bottom layer with a general loading distribution expressed in terms of Bessel functions applied to the top layer; no numerical results were, however, given. In order to remedy these deficiencies, Acum and Fox (30) deduced associated equations for the stresses on the vertical axis of symmetry. The loading distribution which they considered was that of a load which was uniformly distributed over a circular area, the centre of which lay on the vertical axis of symmetry. They then computed the stresses for various combinations of parameters, the variables being the radius of the loading area, the thicknesses of the two top layers and the elastic properties of the three layers. These results were presented by Acum and Fox in the form of tables.

To make Acum and Fox's data more easily usable A.C. Whiffin and N.W. Lister (31) recently presented a paper based on a close analysis of Acum and Fox's computation. Presenting their data in graphical form, Whiffin and Lister showed the effect of changes in elastic moduli and thickness of the layers upon the stresses on the vertical axis of symmetry. They also gave attention to the information available on the dynamic elastic modulus of road-making materials and suggested that the use of dynamic elastic moduli rather than static elastic moduli was necessary to any useful application of theoretical approaches to the structural analysis of actual pavement/subgrade systems.

Hank and Scriver (32) have also concerned themselves with making Burmister's theories more useful. For both the two-layer and three-layer theories, they deduced formulae for the stresses at the

upper interface from Burmister's work, and gave numerical values for various degrees of relative stiffness of the layers. Laboratory measured strengths of roadbase materials were also compared with the stresses in the top layer computed from the two-layer theory so as to determine the required depth of pavement. In addition, Hank and Scriver employed the three-layer theory to study the effects of thin subbases directly underneath concrete slabs.

Pickett and Ai (33) have also used Burmister's two-layer theory. They felt that the expressions for stresses which were obtained by Burmister and other workers using his theory, were too involved and required too much computational work to evaluate. They set out, therefore, to obtain, with the aid of a few simplifying assumptions and semi-empirical methods, much simpler expressions for the subgrade stresses under rigid-type pavements. The rigorous solution of Burmister was replaced by a solution based on the theory of thin plates. The thin plate solution was in turn modified to, in effect, take into account the neglected effects of shear in the pavement on deflection and horizontal shear at the interface between the subgrade and pavement. They then developed equations which gave results which were in agreement, over a wide range of conditions, with those obtained by means of the more-rigorous theory developed by Burmister.

Investigators have taken great interest in Burmister's work, even though it has the major disadvantage that it takes no account of pavement edges or corners. For this reason, its use has mainly been

confined to flexible pavements. The explanation for this interest is perhaps that Burmister's approach provides an exact solution, with each layer being considered as an elastic solid and no use being made of any plate theories. In addition, the pavement/subgrade system is analysed as a whole and not, as in most other theories, where the plate has been considered to be acted upon by an applied load and a subgrade reaction.

Pickett, G. and McCormick, F.J.

In 1951 Pickett and McCormick presented a paper (34) which was concerned with the analysis of both circular and rectangular plates with free edges, under a general distribution of loading using thin plate theory. The supporting foundation was assumed to be a homogeneous elastic solid of uniform thickness and to extend a great distance beyond the plate boundaries. In this paper, the pressure and deflection of the circular plate, expressed as double Fourier series, were equated, respectively, to the pressure and deflection of the surface of the elastic solid, expressed as Fourier-Bessel transforms. However, although circular plates are more easily analysed than rectangular plates and, for this reason, receive a great deal of attention, they do not readily fit into the consideration of actual pavements and are only useful in considering the inter-effect of pavement properties. For this reason they are not given further detailed attention in this thesis.

Pickett and McCormick were not successful in obtaining a solution to the rectangular plate problem by using the methods already employed in their analysis of circular plates. Instead, they obtained an approximate solution by replacing the thin plate differential equations

of elasticity and boundary conditions by their equivalent expressions in finite difference form. For this purpose they divided the area of the plate into squares, the finite difference technique being applied to the centre deflections of these squares. Although the plate equations were written in finite difference form, no approximations were made in regard to the elastic solid foundation, except to assume that the plate reaction would be uniformly distributed over that portion of the foundation surface directly in contact with the given square. Pickett and McCormick deduced a parametric equation which related the deflection at the centre of any square on the surface of an elastic solid resting on a rigid base with the forces at the centre of any one square due to the reactive forces over that square of the plate. Substitution of the finite difference form of the differential equations of the plate into the parametric equation resulted in a system of difference equations which could be solved for the deflections at the centres of each square in terms of the loads at the centre of every square.

In hindsight, it can be seen that the main attribute of this work and, indeed, that of Fox (28) is that the technique of replacing the governing differential equations by an equivalent finite difference form provides a method of obtaining approximate solutions to problems which otherwise might prove impossible to handle.

Livesley, R.K.

In his paper, R.K. Livesley (35) considered some of the approximations necessary for a mathematical treatment of the general problem of a loaded thin elastic plate resting on an elastic foundation,

and discussed in detail possible dynamic and static problems. Besides engaging in a purely general discussion of the problems involved in pavement analysis, Livesley also analysed the case of a pavement subjected to dynamic loading. The system which he considered consisted of a load which was uniformly distributed over a rectangular area and moved with constant velocity across an infinite thin plate resting on a Winkler foundation. He showed that there appeared to exist a certain critical vehicle velocity beyond which the deflection of a pavement became infinite; he also showed that this critical velocity was well beyond any which was likely to occur on a road or on an airport runway. The conclusion, that the plate deflection increases as the speed increases, is at first surprising, but Livesley points out that the plate was considered as an undamped elastic system whereas in most physical cases the effect of damping would be quite noticeable and would certainly in practice tend to reduce the deflection.

In order to consider the dynamic effects of loads, Livesley found it necessary to simplify the problem to a large degree. The result has been that the inaccuracies due to this simplification may well outweigh any advantage accruing from including dynamic effects. The problem increases enormously in complexity and calls for many assumptions on such things as the pavement and subgrade inertia.

Pister, K.S. and Westmann, R.A.

The majority of analyses of plates resting on elastic foundations are based upon thin plate theory which neglects the effects of transverse shear deformation and transverse normal compression.

In recent years, however, the thick plate theory, which includes these effects has been given more attention by a number of investigators. Thus, for example, Pister and Westmann (36) analysed, in 1962, an infinite plate which rested on a semi-infinite elastic foundation and, in this analysis, used the thick plate theory developed through the work of Reissner (37). The effect of the foundation on the slab was taken into account by using a previously mentioned formula developed by Terazawa (24) which relates the interface displacement and pressure. The applied load was considered to be a uniformly distributed pressure over the area of a circle.

Pister and Westmann compared numerical results from the thick plate theory with those of the classical thin plate theory and also with those of Burmister's exact three-dimensional theory. They showed that the discrepancy between the thick and thin plate theories increased as the ratio of the modulus, k , of the foundation to that of the upper layer increased. They also showed that thick plate theory gave satisfactory agreement with the elastic theory, even in the range of high foundation to plate modulus ratios (up to 10) where it might be anticipated that plate theory was inadequate. The graphical results which they presented indicated that as the ratio of the thickness of a slab to the radius of the loading area was increased (up to 1 to 2) the thick plate theory showed a definite improvement over the classical theory. As a result, Pister and Westmann concluded that the improvement of the thick plate theory over the thin plate theory for the axisymmetric bending of plates on an elastic half space was governed by the ratios of

foundation modulus to slab modulus and slab thickness to radius of loading area.

The application of thick plate theory to finite plates has been given very little attention by highway research workers. Nevertheless a distinct advantage of the thick plate theory in such cases might be in its ability to more accurately describe the boundary conditions at the edges of plates. When points near the edges of plates are of major interest, e.g. in the edge and corner loading cases of the Westergaard analysis, there is the very serious possibility that the application of thick plate theory is advantageous.

As flexible pavements have only a low flexural strength, they distribute applied wheel-loads to the foundation mainly by shearing and compression of the pavement. Thus any theory which might be useful in flexible pavement analysis should be based on the thick plate theory which includes the effects of transverse shear and transverse compression.

Hudson, W.R. and Matlock, H.

Numerical methods of analysis and computation are most often used as approximations of a governing equation by substitution of the finite difference forms for the derivatives or by the approximation of a continuous problem with a discrete nodal system. Examples in which these occur are in the previously described work of L. Fox (28) and Pickett and McCormick (34). A second method is to model the slab physically by a system of finite elements whose behaviour can be described with algebraic equations. In 1966, Hudson and Matlock (38)

applied this latter finite element technique to the analysis of discontinuous pavement slabs with freely variable foundation support such as a subgrade with holes in it. Their approach enables a variety of loads including transverse loads and in-plane forces, to be considered when analysing the pavement. The method is not limited by discontinuities and is suited to the analysis of finite slabs of various shapes.

The physical model used by Hudson and Matlock consisted of bars, elastic blocks, torsion bars and elastic springs. The bars were used as infinitely stiff connections between joints while the elastic blocks represented elastic joints at which bending occurred between the bars. The torsion bars represented the torsional stiffness of the plate, and the elastic support springs at each joint provided the foundation support which was considered to be of the Winkler type. Discontinuities and freely discontinuous changes in load, bending stiffness, torsional stiffness, subgrade support and other parameters were easily understood and represented by the physical model used by Hudson and Matlock.

The algebraic equations describing the behaviour of this physical model are derived by free body analysis of the finite model. This consisted of considering a particular member of the model and replacing the other members connected to it by equivalent forces. The equations describing the behaviour of the model were solved by iterative methods and because of the large amount of computation required in solving these equations use was made of an electronic computer to solve for the deflected shape of the plate. From this deflected shape the

bending moments and stresses were easily determined.

On the whole it can be said that numerical methods are extremely useful in formulating approximate solutions to problems having complicated parameters such as plate shape, applied loads and loss of subgrade support. A disadvantage is the large amount of computation required in obtaining solutions, especially when the plate is considered as being thick and if a large concentration of elements or nodal points is required in order to follow rapid changes in stresses and displacements which occur for example when wheel loads are applied at the edges of slabs.

This brief description of the above analyses of the pavement/subgrade system illustrates the diversity of approaches which are possible when attempting such an analysis. The governing factor in all of them seems to be that, in order to obtain solutions to a system containing an idealization of special interest, the remainder of the idealizations have to be made as simple as possible. Thus, for example, those analyses which place emphasis on the road materials neglect the geometry of the system, and visa-versa. As a result of this factor, no method yet described has a well-balanced and sufficiently general set of idealizations to give a single satisfactory analysis over a wide range of parameters. A simple indication of this disadvantage of the available analyses is the difficulty in applying the same analysis to both rigid and flexible pavements.

Summary and Discussion

A pavement is a structure consisting of superimposed layers of selected and processed materials whose primary function is to distribute concentrated vehicle wheel-loads to the supporting subgrade in such a way that the reduced pressure transmitted does not exceed the supporting capacity of the subgrade while, at the same time, ensuring that the structural failure of the pavement itself does not occur. Some of the main causes of structural failure are excessive stresses due to traffic, excessive stresses due to other factors such as temperature or moisture changes, stripping of the surface and deterioration of the subgrade after construction. An ideal method of design when trying to avoid pavement failure due to excessive traffic stresses should take account of wheel contact pressure distributions, multiple wheel configurations, dynamic and impact effects, the cumulative effect of wheel-loads, the true distribution of stress throughout the pavement and subgrade, and traffic intensity. Methods of pavement design do, in fact, attempt to take into account as many of these factors as possible. The methods commonly used to do so cover a wide range of approaches and vary from those based solely on personal judgement to those based purely on theoretical methods of pavement stress analysis. While the emphasis at the moment is on the use of empirically developed procedures, there appears to be a growing interest in using a purely theoretical stress analysis of the pavement and subgrade as the basis of a rational design method.

In developing such a theoretical analysis workers have found it necessary to idealize the pavement/subgrade system into a mathematically tractable form. The main points with which these idealizations appear to be concerned are the wheel/pavement contact area and pressure distribution, the pavement layers, the lateral dimensions of the pavement, the behaviour of the pavement with respect to its flexural stiffness, its stiffness against transverse compression and its stiffness against shear deformation, the behaviour of the foundation and the pavement/subgrade continuity.

The analyses which have been carried out have tended to concentrate upon one or two particular points and keep the remainder of the idealizations as simple as possible in order to facilitate the solution of the particular problem at hand. The idealizations which have, in fact, been made by relevant workers can be summarized in relation to the points listed above:

1. The load distributions which are of particular interest to highway engineers are those which represent a tyre in contact with a road surface. All analyses consider the contact area to be equivalent to that of a uniformly distributed pressure applied over the area of a circle. The reason is that the difference between this and the actual contact distribution is negligible in terms of its effect on stresses and deformation.

2. Pavements are made up of many layers of different materials but in order to make analytical problems soluble, the usual technique is to idealize the pavement/subgrade system to two or three

layers. The majority of analyses consider only two layers; three-layer analyses, because of their cumbersome nature have only been found of use in examining the effects of various pavement parameters on the stresses and deformation.

3. The lateral dimensions of the pavement are a major factor in the definition of the problem. Numerous solutions are available for the determination of stresses and deformations in infinite pavement slabs, while circular slabs have also been comprehensively treated. A small number of workers have considered the slab to be rectangular in shape. The analysis of infinite plates appears only to be of use for flexible pavements because of the negligible boundary effects, while that of finite rectangular plates can be applied to both flexible and rigid pavements.

4. In the past, it was common for investigators to evaluate pavements on the basis that they were either 'rigid' or 'flexible' according to whether flexural stiffness was accounted for in the stress and deformation analysis of the pavement/subgrade system. However, this dichotomy is now becoming less apparent as investigators realize that materials of low elastic moduli may possess significant flexural stiffness and also a worthwhile tensile strength.

Now pavements, irrespective of whether they are rigid or flexible, which are analysed to include both flexural and transverse direct compressive stiffness are referred to by many workers as elastic layers. The effect of transverse compression is of particular importance in pavements in which materials with low elastic moduli

are used, i.e. in flexible pavements.

The effect of transverse shear deformation is most significant in the analysis of plates (pavements) of large thickness. Thick plate theory refers to the theory which includes the effect of transverse shear deformation in analysing the distribution of stress and deformation throughout the plate. While the majority of analyses make use of thin plate theory it should be borne in mind that in the behaviour of what may be thought of as 'thin' plates, the transverse shear effect can be of considerable importance when the plates are supported continuously over one surface and loaded at edges or corners. While some researchers have included the effect of transverse shear deformation in their analyses, this has only been for infinite plates.

5. The two most common idealizations applied to the behaviour of a subgrade are either that it is a continuous elastic solid, as used by Burmister or that it acts as a set of discrete springs. This latter representation, which is known as the Winkler foundation, is used by Westergaard and many other workers. The Winkler foundation is simple in concept and use, and because of the complicated action of soils, it may well be just as reasonable a representation as the elastic solid assumption.

6. Most analyses assume that the foundation and pavement are in permanent contact for all modes of deformation. Consequently, they assume that the foundation possesses both tensile and compressive stiffness; the extent to which this is a valid assumption depends upon whether the weight of the pavement is sufficient to pre-stiffen

the foundation. This problem of loss of contact between the pavement and foundation has been considered, but there are great difficulties in solving this due to the non-linearity of the problem.

The above brief resume' of the present state of pavement structural analysis is not intended to cover all the points made previously but rather to help in pointing out and emphasizing the deficiencies of the established analyses in their application to pavement structural design. With the development of modern methods of numerical analysis and computation and with the advent of the electronic computer, analysts are now able to give increasing emphasis to better representation of the pavement/subgrade system. Nevertheless there still appears to be a need for an analysis which describes a thick rectangular plate (pavement) resting on a Winkler foundation (subgrade). This could well lead to an improvement in the analytical idealization of the road structure for pavement design purposes.

Considering the plate to be rectangular would enable rigid pavements to be analysed as well as flexible pavements and the use of the thick plate theory would enable transverse shear deformation and transverse compression to be included in the analysis. The former could well be important in the consideration of thick flexible or rigid pavements, or near loaded pavement edges or corners. The latter would be especially important in the consideration of flexible pavements.

In any such analysis the wheel/pavement contact should take the form of a uniformly distributed load over a circular area; this seems to have been found satisfactory by many previous workers. The

consideration of more than two layers in any analysis would appear to make the problem much more difficult and so any method aimed at being the basis of a design method should probably only consider two layers. With regard to the foundation, the use of the Winkler assumption is simple, the relevant subgrade property is easily determined and the use of the other alternative, the elastic solid assumption, has not yet been shown to be any more accurate than the Winkler assumption. Thus the use of the Winkler assumption might be quite reasonable in any two-layer analysis. Finally, while the possible loss of contact between the pavement and the subgrade due to the upward movement of the slab could prove important it should be kept in mind that the inclusion of this possibility into an analysis would create a problem which would most probably prove very difficult to solve because of its non-linear nature.

Hence, the problem which appears to deserve further consideration is that of a uniformly-distributed circular load which is applied at any point on the surface of a thick rectangular plate resting on a Winkler foundation. Full contact between the plate and the foundation should be assumed for the main analysis, but some consideration should, separately, be given to the problem of loss of contact between the pavement and the subgrade.

PROPOSED RESEARCH PROGRAM

There are five principal stages in the development of a theoretical analysis of a real structure. The development begins by obtaining an appreciation of the complete range of factors which contribute to the action of the structure. In the second stage, an appraisal is made of possible structural idealizations and a particular representation of the structure is chosen. The next stage is the formation of a mathematical model of this idealized structure, based on the theory of elasticity and expressed in terms of differential equations. Fourthly, the model is solved for the stresses and deformations in the structure by employing the methods of numerical analysis. Finally, the analysis is examined with the help of an experimental investigation.

The analysis of a pavement/subgrade system is no exception to this method of approach. The first two stages have been considered in the previous chapter of this thesis and as a result it is possible to propose for analysis an idealized pavement/subgrade system which is considered to be of practical interest. This system may be described as follows:

A general transverse load distribution applied to the upper surface of a thick rectangular plate which rests, with full

continuity, on the surface of a
Winkler foundation.

In this system a transverse load in the form of a uniformly distributed circular load applied at any point over the plate is of special interest. The problem of loss of contact between the plate and foundation also deserves special consideration.

The numerical solution of the mathematical model has almost always been the first consideration in previous analyses of the pavement/subgrade system and has been assisted by the analysis of a very much simplified system. Today, with the development of modern methods of numerical analysis and the advent of the electronic computer, more consideration can be given to the idealization of the system. Thus the intention in this research program is to concentrate upon the development of a mathematical model of the pavement/subgrade system and then to examine methods of solving this model.

The proposed sequence of work is based on the last three stages of the general approach to the analysis of structures and is as follows:

- a. The formation of a mathematical model of the above pavement/subgrade system.
- b. The consideration of possible methods of numerical analysis of this model.
- c. The mathematical representation of the applied load intensity distribution which is of special interest.

d. The numerical computation of stresses and deformations in the plate resulting from the application of the load distribution of special interest or any other load intensity distribution.

e. The examination of the idealized pavement/subgrade analysis with the assistance of laboratory experiments.

STRUCTURAL ANALYSIS OF THE HIGHWAY PAVEMENT

Introduction

The classical theory of thin elastic plates, which previous workers have developed and used to a high degree, leads to a differential equation of the fourth order for the deflection and to two boundary conditions at each plate edge. Nevertheless, there can in reality be prescribed three rather than two boundary conditions at each edge, whether that plate edge is simply supported, clamped or free as in the plate/foundation system of the present structural analysis. The two boundary conditions, which are associated with the thin plate theory, are a contracted form of these three boundary conditions. Kirchhoff (39) has shown that in the case of a free edge, the ability to reduce three apparently independent stress-resultant boundary conditions, i.e. bending moment, shear force and twisting moment, to two equivalent boundary conditions is dependent on the fact that the boundary conditions on the twisting moment and shear force are reducible to an equivalent single boundary condition. This is because the distortion of the plate due to transverse shearing forces is neglected when establishing the relations between the stresses and the deflection of the plate. The historical background to this reduction in the number of boundary conditions is given by Timoshenko (40).

The intention in this chapter is to develop a structural analysis of the highway pavement based on a theory which includes the effects of transverse shear deformation and transverse normal compression. A plate theory which includes the effect of transverse shearing deformation has been developed by E. Reissner (41,37). Later, he also extended this theory to include the effect of transverse compression (42,43). These works are fundamental to the understanding of the behaviour of thick plates and are briefly described and the previous relevant applications summarized in the sub-sections which follow.

Reissner's theory in elasticity

The linear theory of elastostatic bending of plates, as developed by E. Reissner (42,43) constitutes a definite improvement over the classical theory in that the effect of transverse normal and shearing stresses is retained in the stress-displacement relations. On this basis the question of appropriate plate boundary conditions is clarified and at the same time, the quantitative improvement of the solution of problems involving the edge zones of plates and/or localized surface loading is possible. For the analysis of 'thick' slabs, i.e., those where the thickness is not small when compared to the lateral dimensions, this is especially true.

Reissner (42) treated the problem of thick slabs by means of Castigliano's Principle of Least Work, where the strain energy due to transverse shear deformation and normal transverse compression was included in the total energy of the system. The minimization of the total energy was carried out by using the established techniques of variational calculus (44) and employing Lagrangian multipliers (44) in order to include the effect of equilibrium. This led to a theory which accounted for the effect of transverse shear deformation and transverse normal compression. Green (45) subsequently, rederived this same theory from the general equations of elasticity.

Later, Reissner (43) formulated a new approach in which both the equations of equilibrium and the stress/displacement relationships were both developed from the minimization of the total potential energy of the system. This method gave no preferential treatment to either of the two systems of differential equations and, also, eliminated the need to employ Lagrangian multipliers which was basic to the earlier work.

In 1951 Mindlin (46) developed a theory for vibrating plates, including the effects of shear deformation and rotatory inertia, which was analogous to that of Reissner's, by proceeding from the equations of elasticity.

Previous relevant applications of Reissner's theory

Since its introduction Reissner's theorem in elasticity has been applied to problems of plate flexure by several investigators.

Naghdi and Rowley (47) solved two problems involving axially symmetric bending of an infinite plate on a Winkler foundation. The reaction of the foundation was considered as a normal force applied to the bottom surface of the plate, with the deflection of the lower face of the plate, to which the reaction was proportional, being approximated to that of a weighted average of the deflections across the thickness of the plate. They found that serious errors in the classical theory of plates could result in cases where discontinuity is present, either in the plate configuration or due to the surface loading. Naghdi (48) also considered the problem of both plain bending and pure twisting of an infinite plate with an elliptical hole. The solution, which he obtained was approximate in character and was used to furnish results in the form of stress-concentration factors.

Frederick (49), employing the same approximations as Naghdi and Rowley, initially considered some problems in the bending of circular plates resting on a Winkler foundation. Later he applied the basic equations of Naghdi and Rowley to certain specific problems in the bending of rectangular plates

supported by a Winkler foundation (50). A Fourier series solution was obtained for a simply supported plate resting on a Winkler type foundation when the applied load took the form of a general load intensity distribution. The solution to the problem of a rectangular plate resting on a foundation and with two opposite edges simply supported, a line load applied parallel to these edges and with any combination of boundary conditions on the other two edges consistent with the Reissner theory, was also found to be expressible in a Fourier series form. Finally, Frederick extended the basic differential equations to include the effects of surface shear stresses on the top and bottom of the plate. He then applied these equations to the bending of a plate under uniform surface shear stresses where two opposite edges were clamped and also of infinite length.

The thickness/length parameter at which the effects of shear deformation and normal pressure become important can also be determined from the results illustrated in Frederick's paper. He felt that this secondary effect would be important when considering plates of a low modulus of elasticity which rest on a relatively stiff elastic foundation.

Pister and Westmann (36), in a paper which has been briefly discussed previously in this thesis, modified Reissner's original theorem (37) to represent a particular variation of the transverse co-ordinate z , and derived the following relationship:

$$w(x,y,z) = w(x,y) + zw'(x,y) + \frac{1}{2} z^2 w''(x,y) \quad (9)$$

where $w(x,y)$ is the transverse displacement of the middle surface, w' and w'' are undetermined contributions to the transverse normal strain and x and y are the orthogonal in-plane co-ordinate directions. Reissner's theory (37), presented in 1945, assumed that the transverse displacement of the plate did not vary over its thickness, i.e., that $w(x,y,z)$ equals $w(x,y)$. This was, however, avoided in later work (42,43) by the introduction of a weighted average displacement.

The significance of additional terms retained by Pister and Westmann in the expression for transverse displacement was illustrated in their discussion of the problem of axisymmetric bending of an infinite plate resting on an elastic half-space. The classical thin plate theory, the Reissner plate theory, (with the effect of transverse normal strain neglected) and the modified (Pister and Westmann) theory, were compared, where possible, with the equivalent three-dimensional analysis. For the case studied, they showed that terms associated with transverse shear deformation overcorrected both the transverse displacement and the interface pressure and, thus, must be corrected by adding terms associated with transverse normal strain. It appeared that for axisymmetric bending of plates on an elastic half-space, the Reissner theory (37), as set forward in 1945, did not always lead to an improvement over the results obtained from the classical thin plate theory. Likewise,

Figure 3. An infinitesimal cubic element of an elastic solid

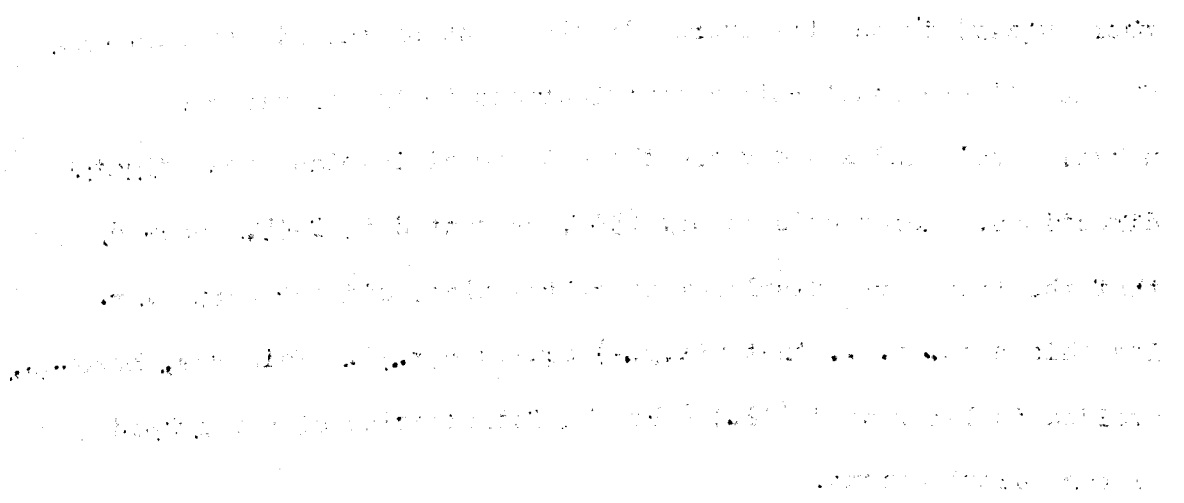
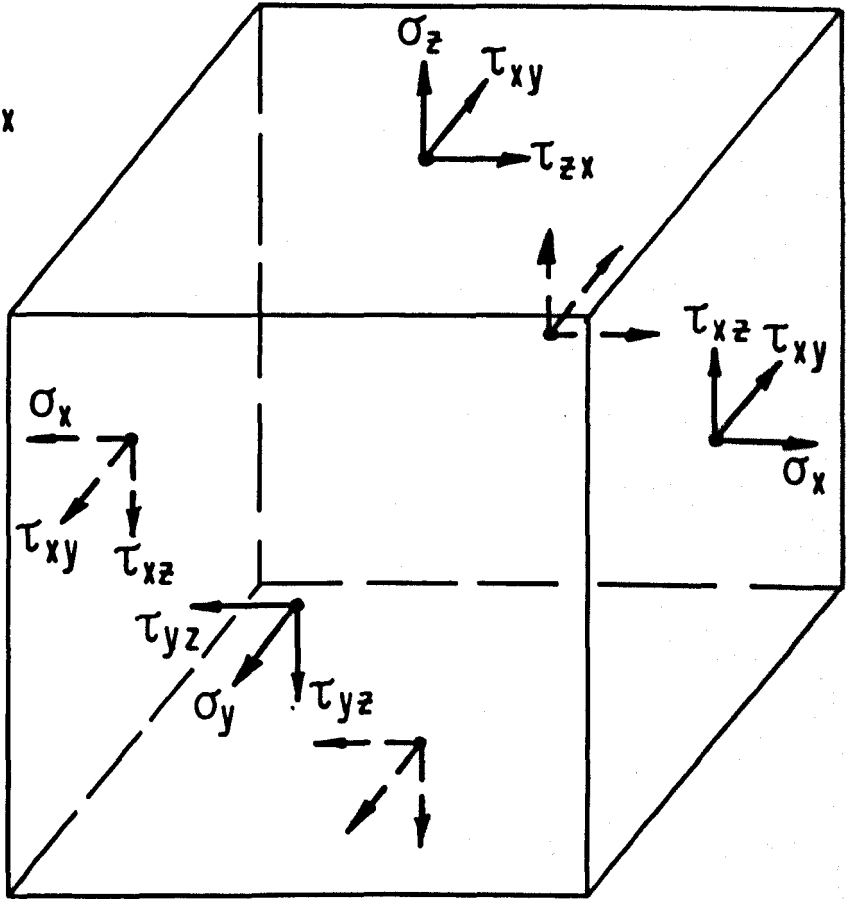
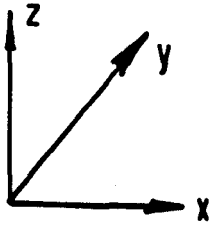


Figure 3. An infinitesimal cubic element of an elastic solid showing the notation for the components of stress acting on its sides and the positive directions of these stresses relative to the sides of the element.

The diagram illustrates the notation for the components of stress acting on the sides of the element. The positive directions of these stresses relative to the sides of the element are indicated by the arrows. The normal stress components are denoted by σ_{xx} , σ_{yy} , and σ_{zz} , and the shear stress components are denoted by τ_{xy} , τ_{yx} , τ_{xz} , and τ_{zx} .



the use of a higher order approximate theory did not necessarily lead to a more exact solution unless the theory was selected on the basis of the specific physical problem being considered.

Coull (51) carried out a direct stress analysis of a swept cantilever plate without the usual need for intermediate deflection calculations and, because of the inclusion of transverse shear deformation, was able to use three boundary conditions on each edge. In his analysis, the partial differential equations of elasticity were reduced to a set of ordinary linear differential equations by representing the load and stress-resultants in a power series form in the chordwise direction.

A Thick Plate Theorem in Elasticity

Reissner's theorem in elasticity (43) was used in the present investigation in order to include for the effect of transverse shear deformation and normal pressure. The latest form of this theorem, presented in 1950, is, therefore, now given in outline.

Energy considerations

In the deformation of an elastic solid, a function $W(\sigma_x, \sigma_y, \dots, \tau_{zx})$, known as the complementary energy density, is considered which, at every point, satisfies the six stress-displacement relations which are expressed in terms of the function W , the direct stresses σ_x , σ_y and σ_z , the shear stresses τ_{xy} , τ_{yz}

and τ_{zx} and the corresponding strains $\epsilon_x, \epsilon_y, \epsilon_z, \gamma_{xy}, \gamma_{yz}$ and γ_{zx} . These six stress-displacement relationships are:

$$\begin{aligned} \epsilon_x &= \frac{\partial W}{\partial \sigma_x}, \quad \epsilon_y = \frac{\partial W}{\partial \sigma_y}, \quad \epsilon_z = \frac{\partial W}{\partial \sigma_z} \\ \gamma_{xy} &= \frac{\partial W}{\partial \tau_{xy}}, \quad \gamma_{yz} = \frac{\partial W}{\partial \tau_{yz}}, \quad \gamma_{zx} = \frac{\partial W}{\partial \tau_{zx}} \end{aligned} \quad (10)$$

where the stress components ($\sigma_x, \sigma_y, \dots, \tau_{zx}$) are understood in the conventional sense, shown by Figure 3, in which stresses are shown as positive, and the strain components are defined by:

$$\begin{aligned} \epsilon_x &= \frac{\partial u}{\partial x}, \quad \epsilon_y = \frac{\partial v}{\partial y}, \quad \epsilon_z = \frac{\partial w}{\partial z} \\ \gamma_{xy} &= \frac{\partial u}{\partial y} + \frac{\partial v}{\partial x}, \quad \gamma_{yz} = \frac{\partial v}{\partial z} + \frac{\partial w}{\partial y}, \quad \gamma_{zx} = \frac{\partial w}{\partial x} + \frac{\partial u}{\partial z} \end{aligned} \quad (11)$$

where u, v and w are the displacements of a point in the x, y and z directions respectively.

It has been shown (44) that in the case of linear elasticity:

$$2W = \epsilon_x \sigma_x + \epsilon_y \sigma_y + \epsilon_z \sigma_z + \gamma_{xy} \tau_{xy} + \gamma_{yz} \tau_{yz} + \gamma_{zx} \tau_{zx} \quad (12)$$

A function F is now introduced by Reissner and it is defined in terms of the twelve arguments $\sigma_x, \sigma_y, \sigma_z, \tau_{xy}, \tau_{yz}, \tau_{zx}, \epsilon_x, \epsilon_y, \epsilon_z, \gamma_{xy}, \gamma_{yz}$ and γ_{zx} by the equation

$$F = \sigma_x \epsilon_x + \sigma_y \epsilon_y + \sigma_z \epsilon_z + \tau_{xy} \gamma_{xy} + \tau_{yz} \gamma_{yz} + \tau_{zx} \gamma_{zx} - W \quad (13)$$

This function is referred to as the strain energy density.

If the potential energy density of the external forces is denoted by P_e , then a function P is defined by:

$$P = \iiint_V F \, dV + \iint_S P_e \, dS \quad (14)$$

where F and P_e are summed over the volume V and surface S , respectively, of the elastic solid. The function P is called the total potential energy of the system.

Requirements of the theorem

Differential equations which must be satisfied at every interior point are the three equations of equilibrium:

$$\begin{aligned} \frac{\partial \sigma_x}{\partial x} + \frac{\partial \tau_{xy}}{\partial y} + \frac{\partial \tau_{zx}}{\partial z} &= 0 \\ \frac{\partial \tau_{xy}}{\partial x} + \frac{\partial \sigma_y}{\partial y} + \frac{\partial \tau_{yz}}{\partial z} &= 0 \\ \frac{\partial \tau_{zx}}{\partial x} + \frac{\partial \tau_{yz}}{\partial y} + \frac{\partial \sigma_z}{\partial z} &= 0 \end{aligned} \quad (15)$$

and the equations (10) which govern compatibility of displacement and inherently include the equations of elasticity.

Considering an element of area, with normal direction \underline{n} at the boundary of a solid body, the components p_x , p_y and p_z of the stresses acting on that area, in the directions x , y and z are given by:

$$\begin{aligned} p_x &= \sigma_x \cos(\underline{n}, x) + \tau_{xy} \cos(\underline{n}, y) + \tau_{zx} \cos(\underline{n}, z) \\ p_y &= \tau_{xy} \cos(\underline{n}, x) + \sigma_y \cos(\underline{n}, y) + \tau_{yz} \cos(\underline{n}, z) \\ p_z &= \tau_{zx} \cos(\underline{n}, x) + \tau_{yz} \cos(\underline{n}, y) + \sigma_z \cos(\underline{n}, z) \end{aligned} \quad (16)$$

where $\cos(\underline{n}, x)$, $\cos(\underline{n}, y)$ and $\cos(\underline{n}, z)$ are the direction cosines between the normal \underline{n} and the x, y and z axes, respectively.

The solution to any problem in solid mechanics must satisfy all the differential equations of elasticity at all points in the interior and at all points on the boundary, as well as the prescribed boundary conditions. Now, at a point on a boundary, in each of the three reference directions, either the stress p_x , p_y or p_z is prescribed, or the associated displacement of the point, u , v or w , is specified. (This is, in effect, the definition of a 'boundary' as considered in this thesis). Thus, a point on the surface of a solid body which is supported on an elastic restraint is not considered as a boundary point but rather as an interior point where neither the stress nor the displacement is explicitly specified.

Proof of the theorem

For a body to be in equilibrium both internally and externally, to be deformed in a compatible state, and to everywhere satisfy the prescribed boundary conditions, the total potential energy P of the system must have a stationary value. In order that P (mathematically a functional) should have a stationary value with

respect to each stress, strain and displacement component, the variation of P with respect to each of those functions should be zero. The variation of P is understood in the sense of the calculus of variations (44) and is signified by δP , that is:

$$\delta P = \delta \left\{ \iiint_V F \, dV + \iint_S P_e \, dS \right\} = 0 \quad (17)$$

The surface integral portion in equation (17) comprises a region S_1 , where stresses are prescribed, and a region S_2 , where displacements are prescribed. Then, as no variation of potential energy can take place at points where surface displacements are prescribed, equation (17) can be rewritten in the form:

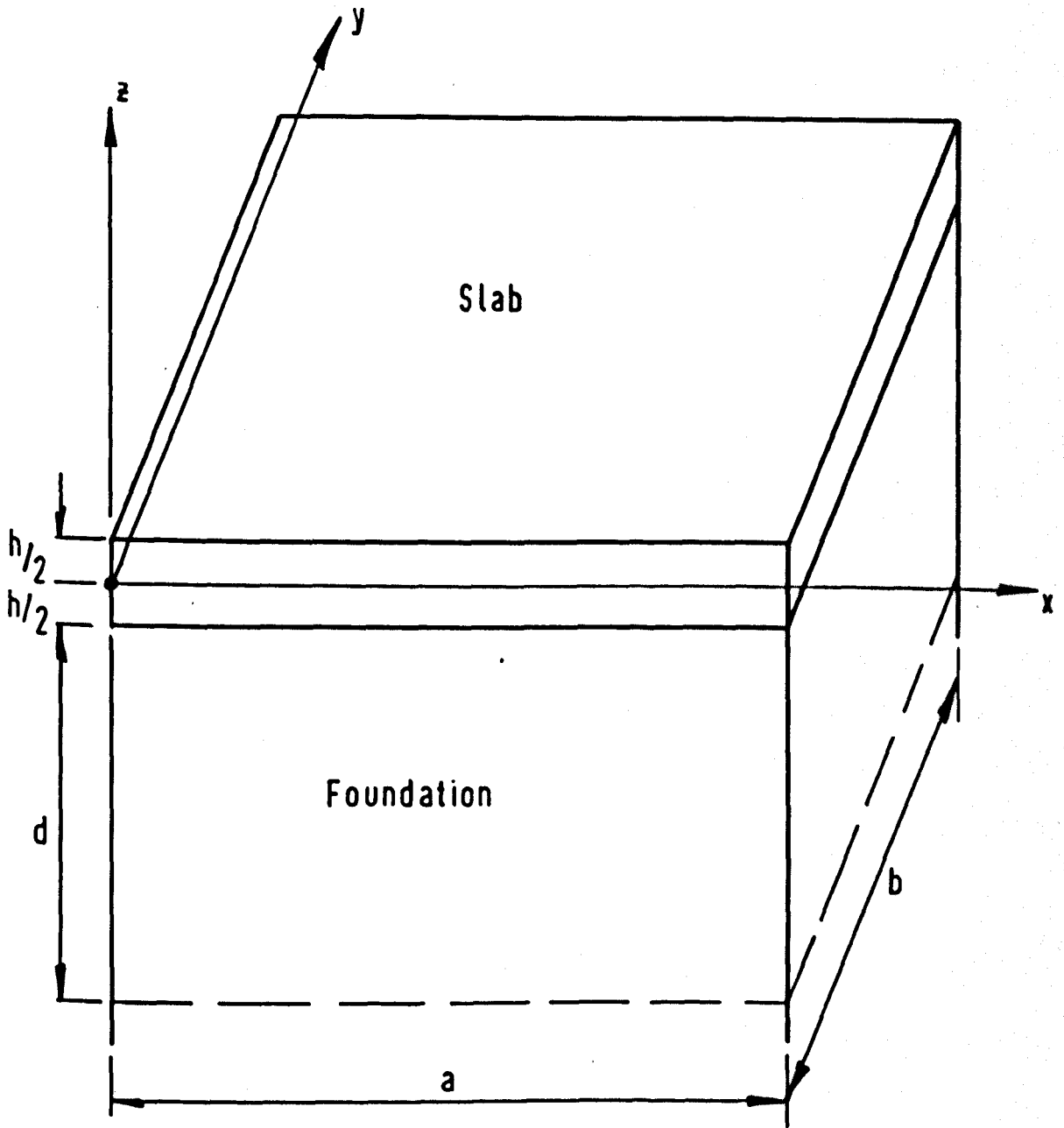
$$\delta \left\{ \iiint_V F \, dV - \iint_{S_1} (\bar{p}_x u + \bar{p}_y v + \bar{p}_z w) dS \right\} = 0 \quad (18)$$

where the bar above the stresses indicates that they are prescribed and hence invariant, i.e.

$$P_x = \bar{p}_x, P_y = \bar{p}_y \text{ and } P_z = \bar{p}_z \quad (19)$$

Reissner has demonstrated the proof of this theorem by expanding equation (18) with the form,

$$\begin{aligned} & \iiint_V \left[\left(\frac{\partial u}{\partial x} - \frac{\partial w}{\partial \alpha} \right) \delta \sigma_x + \left(\frac{\partial v}{\partial y} - \frac{\partial w}{\partial \beta} \right) \delta \sigma_y + \left(\frac{\partial w}{\partial z} - \frac{\partial w}{\partial \alpha} \right) \delta \sigma_z \right. \\ & + \left(\frac{\partial u}{\partial y} + \frac{\partial v}{\partial x} - \frac{\partial w}{\partial \tau_{xy}} \right) \delta \tau_{xy} + \left(\frac{\partial v}{\partial z} + \frac{\partial w}{\partial y} - \frac{\partial w}{\partial \tau_{yz}} \right) \delta \tau_{yz} \\ & \left. + \left(\frac{\partial w}{\partial x} + \frac{\partial u}{\partial z} - \frac{\partial w}{\partial \tau_{zx}} \right) \delta \tau_{zx} - \left(\frac{\partial \sigma_x}{\partial x} + \frac{\partial \tau_{xy}}{\partial y} + \frac{\partial \tau_{zx}}{\partial z} \right) \delta u \right. \end{aligned}$$



$$-\left(\frac{\partial \tau_{xy}}{\partial x} + \frac{\partial \sigma_y}{\partial y} + \frac{\partial \tau_{yz}}{\partial z}\right) \delta v - \left(\frac{\partial \tau_{zx}}{\partial x} + \frac{\partial \tau_{yz}}{\partial y} + \frac{\partial \sigma_z}{\partial z}\right) \delta w \Big] dV$$

$$+ \iint_{S_1} [(p_x - \bar{p}_x) \delta u + (p_y - \bar{p}_y) \delta v + (p_z - \bar{p}_z) \delta w] dS = 0 \quad (20)$$

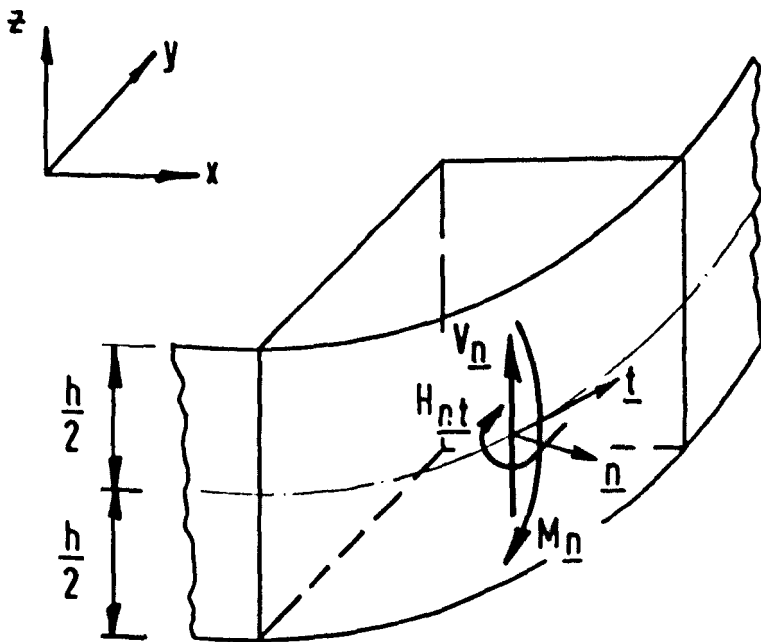
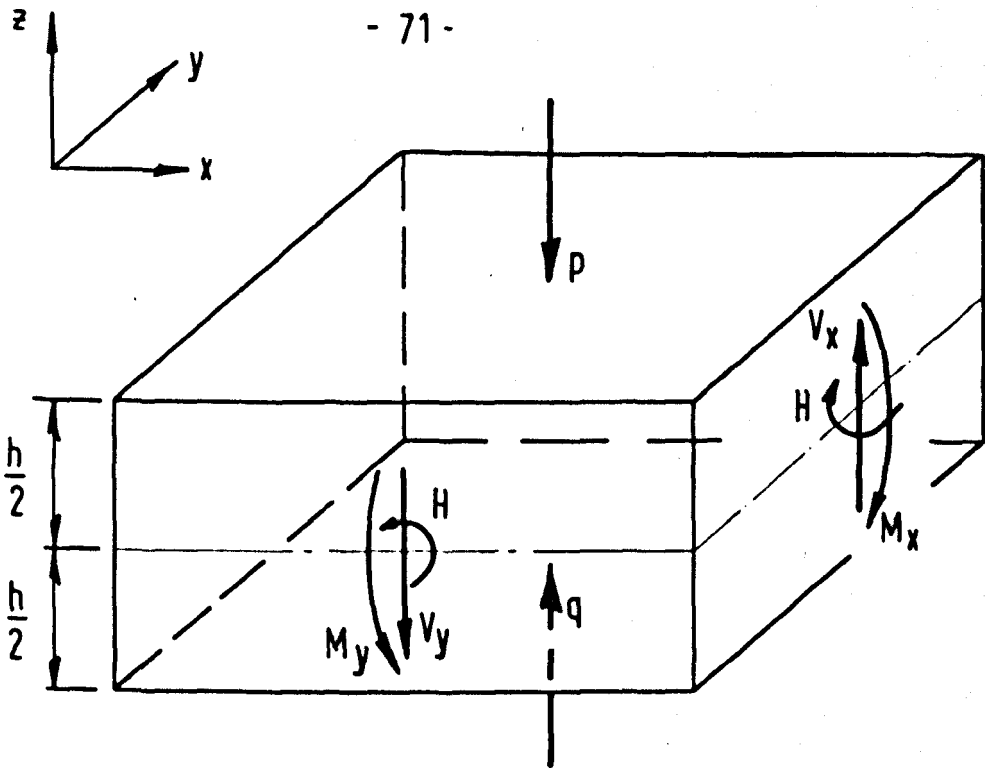
where the bracketed expressions are known as the Euler equations and must vanish separately in order to satisfy the variational equation, equation (17). These bracketed expressions are clearly the differential equations of elasticity, equations (10) and (15), and the stress boundary conditions, equations (19), each of which is associated with an alternative displacement boundary condition. Thus the variational equation (18) is shown to be equivalent to the complete system of the differential equation of elasticity, equations (10, 11 and 15), and the boundary conditions, equations (19), irrespective of whether they are specified in terms of stresses or displacements.

Specifications and Assumptions of the Structural Analysis

The structural system considered in this thesis consists of a thick, homogeneous, isotropic and linearly elastic slab resting on a linearly elastic foundation; this is shown in Figure 4. This figure indicates the geometry of the structure, its dimensions and the co-ordinate system being used. It is emphasised that the system is treated as one structural unit although it consists of two elements, the slab and the foundation.

Figure 5. An infinitesimal element at the interior of a plate showing the notation and also the orientation of the stress resultants and applied normal surface stresses.

Figure 6. An infinitesimal element at the curvilinear boundary of a plate showing the orientation of the stress resultants.



Stress/stress resultant relationships

The stress resultants in the plate shown in Figure 4 consist of the bending moments M_x and M_y , the twisting moment, H , and the shearing forces V_x and V_y ; the orientations of these are shown in Figure 5. Assumptions must be made on the internal stress distributions in each element of the plate, in terms of their stress resultants in order to reduce the problem to a two-dimensional form.

Considering, firstly the slab, as is customary in plate flexural theory the stress σ_x , σ_y and τ_{xy} are considered to be distributed linearly over the thickness of the slab, as follows:

$$\sigma_x = \frac{M_x}{h^2/6} \cdot \frac{z}{h/2} \quad , \quad \sigma_y = \frac{M_y}{h^2/6} \cdot \frac{z}{h/2}$$

and
$$\tau_{xy} = \frac{H}{h^2/6} \cdot \frac{z}{h/2} \tag{21}$$

The equations of internal equilibrium of the slab can then be written in terms of its stress resultants at a point as:

$$\frac{\partial M_x}{\partial x} + \frac{\partial H}{\partial y} - V_x = 0$$

$$\frac{\partial M_y}{\partial y} + \frac{\partial H}{\partial x} - V_y = 0 \tag{22}$$

$$(q-p) + \frac{\partial V_x}{\partial x} + \frac{\partial V_y}{\partial y} = 0$$

where p and q are the direct stress normal to its upper and lower surfaces, respectively, as shown in Figure 5.

Substitution of the first and third of equations (21), and the first of equations (22) into the first of equations (15) yields the differential equation for τ_{zx} as:

$$\frac{\partial \tau_{zx}}{\partial z} = - \frac{12}{h^3} z \cdot V_x$$

Integrating this equation and using the boundary conditions $\tau_{zx} = 0$ at $z = \pm h/2$, gives

$$\tau_{zx} = \frac{3}{2h} \cdot V_x \left[1 - \left(\frac{z}{h/2} \right)^2 \right] \quad (23)$$

and, similarly,

$$\tau_{yz} = \frac{3}{2h} \cdot V_y \left[1 - \left(\frac{z}{h/2} \right)^2 \right]$$

The substitution of equations (23) into the third of equations (15), and the elimination of the shearing forces V_x and V_y by using the third of equations (22), yields the differential equation for σ_z as:

$$\frac{\partial \sigma_z}{\partial z} = (q-p) \frac{3}{2h} \left[1 - \left(\frac{z}{h/2} \right)^2 \right]$$

Integrating this equation and using the boundary conditions $\sigma_z = -p$ at $z = h/2$, and $\sigma_z = -q$ at $z = -h/2$, gives

$$\sigma_z = - \frac{(q+p)}{2} + (q-p) \frac{3}{4} \left[\frac{z}{h/2} - \frac{1}{3} \left(\frac{z}{h/2} \right)^3 \right] \quad (24)$$

Consider, secondly, the foundation. Here the well-known Winkler assumption is adopted. Thus, the vertical stress, σ_z , is assumed to be directly proportional to the deflection, w_1 , of the

upper surface of the foundation , and all other stress components are considered as being equal to zero. Thus

$$\sigma_z (= -q = kw_1) \neq 0 \quad (25)$$

and $\sigma_x = \sigma_y = \tau_{xy} = \tau_{yz} = \tau_{zx} = 0$

Strain/average displacement relationships

In order to maintain the two-dimensional nature of the flexural behaviour of the slab the concept, used by Reissner, of weighted average displacements is also adopted here. These weighted average displacements, α_o , β_o and w_o , are defined as:

$$\begin{aligned} \alpha_o &= \frac{12}{h^3} \int_{-h/2}^{h/2} uz \, dz \\ \beta_o &= \frac{12}{h^3} \int_{-h/2}^{h/2} vz \, dz \\ w_o &= \frac{3}{2h} \int_{-h/2}^{h/2} w \left[1 - \left(\frac{z}{h/2} \right)^2 \right] dz \end{aligned} \quad (26)$$

Approximations for the displacement, v, u and w, can be obtained by introducing into the above equations the approximations,

$$u = \alpha_o^*(x,y)z, \quad v = \beta_o^*(x,y)z \quad \text{and} \quad w = w_o^*(x,y) \quad (27)$$

resulting in

$$\alpha_o^* = \alpha_o, \quad \beta_o^* = \beta_o \quad \text{and} \quad w_o^* = w_o$$

Thus, the starred quantities can be solved for, and using equations

(27) the actual displacements obtained. The approximation $w = w_0^{**}(x,y)$ is equivalent to the variation of transverse deformation through the thickness of the plate being neglected, as in Reissner's paper presented in 1945.

As far as the foundation/slab interface is concerned, its deflection is denoted by:

$$w_1 = w(x,y,-h/2) \quad (28)$$

where w is not equal to w_0 due to the transverse compression in the slab.

Boundary conditions

Finally the boundary conditions on the system must be considered.

As the slab is being treated as thick, ie. the transverse shear deformation is being taken into account, three independent boundary conditions must be prescribed at points on the outer edges of the slab. Using a curvi-linear boundary with normal direction \underline{n} and tangential direction \underline{t} , (Figure 6) the general boundary conditions are

$$\begin{aligned} M_{\underline{n}} &= \bar{M}_{\underline{n}} \quad \text{or } \alpha_0 \text{ prescribed} \\ H_{\underline{nt}} &= \bar{H}_{\underline{nt}} \quad \text{or } \beta_0 \text{ prescribed} \\ V_{\underline{n}} &= \bar{V}_{\underline{n}} \quad \text{or } w_0 \text{ prescribed} \end{aligned} \quad (29)$$

where the bar above the symbols indicates prescribed stress resultants. Here the problem being analysed is that of a slab with free edges and thus the two conditions of the classical theory,

$$\bar{M}_{\underline{n}} = 0 \text{ and } \bar{V}_{\underline{n}} + \frac{\partial H_{\underline{nt}}}{\partial \underline{t}} = 0 \quad (30)$$

are replaced by

$$\bar{M}_{\underline{n}} = H_{\underline{nt}} = \bar{V}_{\underline{n}} = 0 \quad (31)$$

at all points along the slab edges. It is, therefore, no longer necessary to transform the twisting moment, $H_{\underline{nt}}$, into an equivalent vertical shear as in the classical theory of thin plates.

On the upper surface of the slab the prescribed boundary conditions are all in terms of the specified loading normal to the upper surface of the slab and are thus described by

$$\bar{p}_z = -P(x,y), \quad \bar{p}_x = \bar{p}_y = 0 \quad (32)$$

the corresponding displacement is

$$w_u = w(x,y, h/2) \quad (33)$$

As far as the remaining boundaries are concerned, the conditions along the foundation sides do not enter the problem due to the Winkler foundation assumption, and along the bottom surface of the foundation,

$$w_{lf} = w(x,y, - (d+ h/2)) \quad (34)$$

Analysis of the Pavement with Full Interface Contact Preserved

In the application developed in this section the problem relates to that of a thick finite slab resting on a Winkler type foundation, complete contact between the slab and the foundation being preserved under all conditions of flexure. Returning to the general form of the variational theorem, equation (18), this must now be written in the form required for this application. Defining the strain energy density for the slab as F_p and for the foundation as F_f , the variational theorem then becomes

$$\delta \left\{ \int_{-h/2}^{h/2} F_p d\mathbf{s} + \int_{-(d+h/2)}^{-h/2} F_f dz - \bar{p}_g w \right\} dx dy = 0 \quad (35)$$

Using the relationship expressed by equations (13) and separating the external force component into $(\bar{p}_g w)_u$ and $(\bar{p}_g w)_{lf}$ for the upper surface of the slab and the bottom surface of the foundation respectively, equation (35) may be written as

$$\delta \left\{ \int_{-h/2}^{h/2} (\sigma_{ij_p} \epsilon_{ij_p} - W_p) d\mathbf{s} + \int_{-(d+h/2)}^{-h/2} (\sigma_{ij_f} \epsilon_{ij_f} - W_f) dz - (\bar{p}_g w)_u - (\bar{p}_g w)_{lf} \right\} dz dy = 0 \quad (36)$$

Expanding equation (36), substituting for ϵ_{ij} using equations (11), substituting for ϵ_x , γ_{xy} etc., in W using the stress-strain relationships of linear elasticity, $\epsilon_x = [\sigma_x - \mu(\sigma_y + \sigma_z)]/E$, $\gamma_{xy} = 2(1+\mu)\tau_{xy}/E$, etc., results in

$$\begin{aligned}
 & \int_{-h/2}^{h/2} \left[\left(\sigma_x \frac{\partial u}{\partial x} + \sigma_y \frac{\partial v}{\partial y} + \sigma_z \frac{\partial w}{\partial z} + \tau_{xy} \left(\frac{\partial u}{\partial y} + \frac{\partial v}{\partial x} \right) + \tau_{yz} \left(\frac{\partial v}{\partial z} + \frac{\partial w}{\partial y} \right) \right. \right. \\
 & \left. \left. + \tau_{zx} \left(\frac{\partial w}{\partial x} + \frac{\partial u}{\partial z} \right) \right) - \frac{1}{2E} \left(\sigma_x^2 + \sigma_y^2 + \sigma_z^2 - 2\mu(\sigma_x \sigma_y + \sigma_y \sigma_z \right. \right. \\
 & \left. \left. + \sigma_z \sigma_x) + 2(1+\mu)(\tau_{xy}^2 + \tau_{yz}^2 + \tau_{zx}^2) \right) \right] dz + \int_{-(d+h/2)}^{-h/2} \left[\left(\sigma_z \frac{\partial w}{\partial z} \right) \right. \\
 & \left. - \frac{1}{2E_f} \left(\sigma_z^2 \right) \right] dz \Big] dx dy - \iiint \left[-pw_u - qw_{1f} \right] dx dy \Big\} = 0 \quad (37)
 \end{aligned}$$

Each term in equation (37) is now integrated with respect to z , in order to obtain a two-dimensional system. Using the stress/stress-resultant and displacement/average displacement equations (21), (23), (24) and (26) the following relationships are obtained for the slab:

$$\int_{-h/2}^{h/2} \sigma_x \frac{\partial u}{\partial x} dz = M_x \frac{\partial \alpha_o}{\partial x}$$

$$\int_{-h/2}^{h/2} \sigma_y \frac{\partial v}{\partial y} dz = M_y \frac{\partial \beta_o}{\partial y}$$

$$\int_{-h/2}^{h/2} \sigma_z \frac{\partial w}{\partial z} dz = -pw_u + qw_1 - (q-p) w_o$$

$$\int_{-h/2}^{h/2} \tau_{xy} \left(\frac{\partial u}{\partial y} + \frac{\partial v}{\partial x} \right) dz = H \left(\frac{\partial \alpha_o}{\partial y} + \frac{\partial \beta_o}{\partial x} \right) \quad (38)$$

$$\int_{-h/2}^{h/2} \tau_{yz} \left(\frac{\partial v}{\partial z} + \frac{\partial w}{\partial y} \right) dz = V_y \left(\beta_o + \frac{\partial w_o}{\partial y} \right)$$

$$\int_{-h/2}^{h/2} \tau_{zx} \left(\frac{\partial w}{\partial x} + \frac{\partial u}{\partial z} \right) dz = V_x \left(\alpha_o + \frac{\partial w_o}{\partial x} \right)$$

Furthermore

$$\int_{-h/2}^{h/2} \sigma_z^2 dz = \frac{12}{h^3} M_x^2$$

$$\int_{-h/2}^{h/2} \sigma_y^2 dz = \frac{12}{h^3} M_y^2$$

$$\int_{-h/2}^{h/2} \sigma_z^2 dz = \frac{h}{70} (26p^2 + 26q^2 + 18pq)$$

$$\int_{-h/2}^{h/2} -2\mu \sigma_x \sigma_y dz = -\frac{24}{h^3} \mu M_x M_y$$

$$\int_{-h/2}^{h/2} -2\mu \sigma_y \sigma_z dz = -\frac{12}{5h} \mu (q-p) M_y$$

$$\int_{-h/2}^{h/2} -2\mu \sigma_z \sigma_x dz = -\frac{12}{5h} \mu (q-p) M_x \quad (39)$$

$$\int_{-h/2}^{h/2} 2(1+\mu)\tau_{xy}^2 dz = \frac{24}{h^3} (1+\mu) H^2$$

$$\int_{-h/2}^{h/2} 2(1+\mu)\tau_{yz}^2 dz = \frac{12}{5h} (1+\mu) V_y^2$$

$$\int_{-h/2}^{h/2} 2(1+\mu)\tau_{zx}^2 dz = \frac{12}{5h} (1+\mu) V_x^2$$

For the foundation

$$\int_{-(d+h/2)}^{-h/2} \sigma_z \frac{\partial w}{\partial z} dz = -Qw_1 + qw_{1f}$$

(40)

and
$$\int_{-(d+h/2)}^{h/2} \sigma_z^2 dz = dq^2$$

Substituting the integrals of equations (38), (39) and (40) into equation (37), introducing $-kw_1$ for q , and replacing E_f by $k \cdot d$ as w_{1f} is specified as zero at the lower face boundary of the system, yields the variational equation in terms of stress-resultants and the average displacement.

Thus

$$\delta \left\{ \iiint \left[\left(M_x \frac{\partial \alpha_o}{\partial x} + M_y \frac{\partial \beta_o}{\partial y} + (kw_1 + p)w_o + H \left(\frac{\partial \alpha_o}{\partial y} + \frac{\partial \beta_o}{\partial x} \right) + V_x \left(\alpha_o + \frac{\partial w_o}{\partial x} \right) \right. \right. \right. \\ \left. \left. \left. + V_y \left(\beta_o + \frac{\partial w_o}{\partial y} \right) - \frac{kw_1^2}{2} \right) - \frac{1}{2E} \left(\frac{12}{h^3} (M_x^2 + M_y^2 - 2\mu M_x M_y \right. \right. \right. \\ \left. \left. \left. + 2(1+\mu)H^2 \right) + \frac{12}{5h} (1+\mu) (V_x^2 + V_y^2) + \frac{12}{5h} \mu (kw_1 + p)(M_x \right. \right.$$

$$+M_y) + \frac{h}{70} (26p^2 + 26k^2 w_1^2 - 18pkw_1) \Big] dx dy \Big\} = 0 \quad (41)$$

The variations are now carried out on all terms which can vary, the techniques being similar to that of differentiation (44), to give

$$\begin{aligned} & \iiint \left[\left(\delta M_x \frac{\partial \alpha_o}{\partial x} + M_x \frac{\partial \delta \alpha_o}{\partial x} + \delta M_y \frac{\partial \beta_o}{\partial y} + M_y \frac{\partial \delta \beta_o}{\partial y} + kw_o \delta w_1 \right. \right. \\ & + (kw_1 + p) \delta w_o + \delta H \left(\frac{\partial \alpha_o}{\partial y} + \frac{\partial \beta_o}{\partial x} \right) + H \left(\frac{\partial \delta \alpha_o}{\partial y} + \frac{\partial \delta \beta_o}{\partial x} \right) \\ & + \delta V_x \left(\alpha_o + \frac{\partial w_o}{\partial x} \right) + V_x \left(\delta \alpha_o + \frac{\partial \delta w_o}{\partial x} \right) + \delta V_y \left(\beta_o + \frac{\partial w_o}{\partial y} \right) + V_y \left(\delta \beta_o \right. \\ & \left. + \frac{\partial \delta w_o}{\partial y} \right) - kw_1 \delta w_1 \Big) - \frac{1}{2E} \left(\frac{12}{h^3} (2M_x \delta M_x + 2M_y \delta M_y - 2\mu M_x \delta M_y \right. \\ & - 2\mu M_y \delta M_x + 4(1+\mu)H\delta H) + \frac{12}{5h} (1+\mu) (2V_x \delta V_x + 2V_y \delta V_y) \\ & \left. + \frac{12\mu}{5h} (kw_1 + p) (\delta M_x + \delta M_y) + \frac{12}{5h} \mu (M_x + M_y) k \delta w_1 \right. \\ & \left. + \frac{h}{70} (52k^2 w_1^2 - 18kp) \delta w_1 \right) \Big] dx dy = 0 \quad (42) \end{aligned}$$

Elimination of the partial derivatives of displacement variations by integration by parts, e.g.

$$\iint M_x \frac{\partial \alpha_o}{\partial x} dx dy = \int (M_x \delta \alpha_o) \Big|_{dy}^{x\text{-limits}} - \iint \frac{\partial M_x}{\partial x} \delta \alpha_o dx dy \quad (43)$$

and re-arrangement of terms, leads to

$$\iiint \left[\frac{\partial \alpha_o}{\partial x} - \frac{12}{Eh^3} (M_x - \mu M_y) - \frac{6\mu}{5Eh} (kw_1 + p) \right] \delta M_x$$

$$\begin{aligned}
 & + \left[\frac{\partial \beta_0}{\partial y} - \frac{12}{Eh^3} (M_y - \mu M_x) - \frac{6\mu}{5Eh} (kw_1 + p) \right] \delta M_y \\
 & + \left[\frac{\partial \alpha_0}{\partial y} + \frac{\partial \beta_0}{\partial x} - \frac{24(1+\mu)}{Eh^3} H \right] \delta H \\
 & + \left[\alpha_0 + \frac{\partial w_0}{\partial x} - \frac{12(1+\mu)}{5Eh} v_x \right] \delta v_x \\
 & + \left[\beta_0 + \frac{\partial w_0}{\partial y} - \frac{12(1+\mu)}{5Eh} v_y \right] \delta v_y \\
 & + \left[-\frac{\partial M_x}{\partial x} - \frac{\partial H}{\partial y} + v_x \right] \delta \alpha_0 \\
 & + \left[-\frac{\partial M_y}{\partial y} - \frac{\partial H}{\partial x} + v_y \right] \delta \beta_0 \\
 & + \left[(kw_1 + p) - \frac{\partial v_x}{\partial x} - \frac{\partial v_y}{\partial y} \right] \delta w_0 \\
 & + \left[kw_0 - kw_1 - \frac{6\mu k}{5Eh} (M_x + M_y) - \frac{h}{70E} (26k^2 w_1 - 9kp) \right] \delta w_1 \, dx \, dy \\
 & + \int \left[M_x \delta \alpha_0 + H \delta \beta_0 + v_x \delta w_0 \right]_{x\text{-limits}} dy + \int \left[H \delta \alpha_0 + M_y \delta \beta_0 + v_y \delta w_0 \right]_{y\text{-limits}} dx \\
 & = 0
 \end{aligned} \tag{44}$$

where the suffix 'x-limits' indicates that $\left[M_x \delta \alpha_0 + H \delta \beta_0 + v_x \delta w_0 \right]$ applies only to the plate edges which are perpendicular to the x-axis of the co-ordinate system. The suffix 'y-limit' has a corresponding meaning.

The contents of each bracket in equation (44) must vanish separately if, in order to satisfy the variational equation (17), the variation of the total potential energy is to vanish. Therefore, using the relationship $E = 2(1+\mu)G$ the following equations must be satisfied:

$$\frac{\partial \alpha_0}{\partial x} - \frac{12}{Eh^3} (M_x - \mu M_y) - \frac{6\mu}{5Eh} (kw_1 + p) = 0 \tag{45}$$

$$\frac{\partial \beta_0}{\partial y} - \frac{12}{Eh^3} (M_y - \mu M_x) - \frac{6\mu}{5Eh} (kw_1 + p) = 0 \tag{46}$$

$$\frac{\partial \alpha_0}{\partial y} + \frac{\partial \beta_0}{\partial x} - \frac{12}{Gh^3} H = 0 \quad (47)$$

$$\alpha_0 + \frac{\partial w_0}{\partial x} - \frac{6}{5Gh} V_x = 0 \quad (48)$$

$$\beta_0 + \frac{\partial w_0}{\partial y} - \frac{6}{5Gh} V_y = 0 \quad (49)$$

$$\frac{\partial M_x}{\partial x} + \frac{\partial H}{\partial y} - V_x = 0 \quad (50)$$

$$\frac{\partial M_y}{\partial y} + \frac{\partial H}{\partial x} - V_y = 0 \quad (51)$$

$$\frac{\partial V_x}{\partial x} + \frac{\partial V_y}{\partial y} - (kw_1 + p) = 0 \quad (52)$$

$$w_0 - w_1 - \frac{6\mu}{5Eh} (M_x + M_y) - \frac{h}{70E} (26kw_1 - 9p) = 0 \quad (53)$$

$$[M_x \delta \alpha_0 + H \delta \beta_0 + V_x \delta w_0]_{x\text{-limits}} = 0 \quad (54)$$

$$[M_y \delta \beta_0 + H \delta \alpha_0 + V_y \delta w_0]_{y\text{-limits}} = 0 \quad (55)$$

Equations (45) to (49) inclusive, along with equations (53), are the stress-displacement equations for the complete system, while equations (50), (51) and (52) are the equations of equilibrium. Equations (54) and (55) represent the natural boundary conditions along the edges perpendicular to the x and y axes respectively and are clearly satisfied by those of the particular problem being analysed, i.e. equations (31).

Equations (45 to 53) reduce to the customary equations of the plate theory by neglecting equations (53), replacing w_0 and w_1 by one

expression for the plate deflection and neglecting all terms which contain $1/\lambda^6$.

As the first step in the solution, w_1 , the deflection of the slab/foundation interface, is eliminated from the set of equations. This is done simply by substituting the expression for w_1 from equation (53) into the three other equations where it occurs i.e. equations (45), (46) and (52). Using the simplifying notation expressed by

$$\begin{aligned}
 g &= 1 + \frac{26hk}{70E} & T &= \frac{6\mu}{5Eh} \\
 C &= 1 + \frac{9hk}{70Eg} & e &= \frac{12}{Eh^3} \\
 \underline{m} &= \frac{12}{Gh^3} & r &= \frac{6}{5Gh} \\
 U &= \underline{e} - \frac{T^2k}{g} & \bar{V} &= \mu\underline{e} + \frac{T^2k}{g} \\
 s &= \bar{V}/U & f &= (1+\bar{V}/U) \\
 t &= (U - \bar{V}^2/U)
 \end{aligned} \tag{56}$$

equations (45) to (53) can be expressed as

$$\frac{\partial \alpha_o}{\partial x} - s \frac{\partial \beta_o}{\partial y} + tM_x + \frac{Tkf}{g} w_o = -TCfp \tag{57}$$

$$-\frac{\partial \beta_o}{\partial y} - s \frac{\partial \alpha_o}{\partial x} + tM_y + \frac{Tkf}{g} w_o = -TCfp \tag{58}$$

$$-\frac{\partial \alpha_o}{\partial y} - \frac{\partial \beta_o}{\partial x} + \underline{m} H = 0 \tag{59}$$

$$\alpha_o + \frac{\partial w_o}{\partial x} - rV_x = 0 \tag{60}$$

$$\beta_0 + \frac{\partial w_0}{\partial y} - r V_y = 0 \quad (61)$$

$$- \frac{\partial M_x}{\partial x} - \frac{\partial H}{\partial y} + V_x = 0 \quad (62)$$

$$- \frac{\partial M_y}{\partial y} - \frac{\partial H}{\partial x} + V_y = 0 \quad (63)$$

$$- \frac{\partial V_x}{\partial x} - \frac{\partial V_y}{\partial y} + \frac{k}{g} w_0 - \frac{kT}{g} (M_x + M_y) = -Cp \quad (64)$$

The solution of this set of eight equations is considered in detail elsewhere (52) but as the weighted average $\bar{\alpha}$ notations α_0 and β_0 are not used to specify the boundary conditions of the problem and are also of little interest in themselves, they are eliminated to produce the alternative set of six equations which is used hereafter.

From equations (60) and (61):

$$\alpha_0 = rV_x - \frac{\partial w_0}{\partial x}, \quad \beta_0 = rV_y - \frac{\partial w_0}{\partial y} \quad (65)$$

Substituting these expressions for α_0 and β_0 into the remaining equations, results in:

$$-r \frac{\partial V_x}{\partial x} - sr \frac{\partial V_y}{\partial y} + \frac{\partial^2 w_0}{\partial x^2} + s \frac{\partial^2 w_0}{\partial y^2} + \frac{Tkf}{g} w_0 + t M_x = -TCfp \quad (66)$$

$$-r \frac{\partial V_y}{\partial y} - sr \frac{\partial V_x}{\partial x} + \frac{\partial^2 w_0}{\partial y^2} + s \frac{\partial^2 w_0}{\partial x^2} + \frac{Tkf}{g} w_0 + t M_y = -TCfp \quad (67)$$

$$-r \frac{\partial V_x}{\partial y} - r \frac{\partial V_y}{\partial x} + 2 \frac{\partial^2 w_0}{\partial x \partial y} + \underline{m} H = 0 \quad (68)$$

$$- \frac{\partial M_x}{\partial x} - \frac{\partial H}{\partial y} + V_x = 0 \quad (69)$$

$$- \frac{\partial M_y}{\partial y} - \frac{\partial H}{\partial x} + V_y = 0 \quad (70)$$

$$-\frac{\partial V_x}{\partial x} - \frac{\partial V_y}{\partial y} + \frac{k}{g} \frac{\partial T}{\partial z} - \frac{kT}{g} (M_x + M_y) = -Cp \quad (71)$$

This system of six partial differential equations along with the boundary conditions

$$\begin{aligned} M_x = V_x = H = 0 \text{ at } x = 0 \text{ and } x = a \\ \text{and } M_y = V_y = H = 0 \text{ at } y = 0 \text{ and } y = b \end{aligned} \quad (72)$$

completely specify the boundary value problem.

Further reduction of the number of differential equations is inconvenient as, firstly, the introduction of higher differentials is always accompanied by loss in accuracy when attempting to obtain values for those terms which have been eliminated, secondly, all the remaining unknowns are of interest and, thirdly, the boundary conditions are specified in terms of five of these independent variables.

The solution of this problem, expressed in terms of the above equations (66 to 72) will be considered later but, before doing so, another boundary value problem is examined.

Analysis of the Pavement Including Possible Loss of Interface Contact

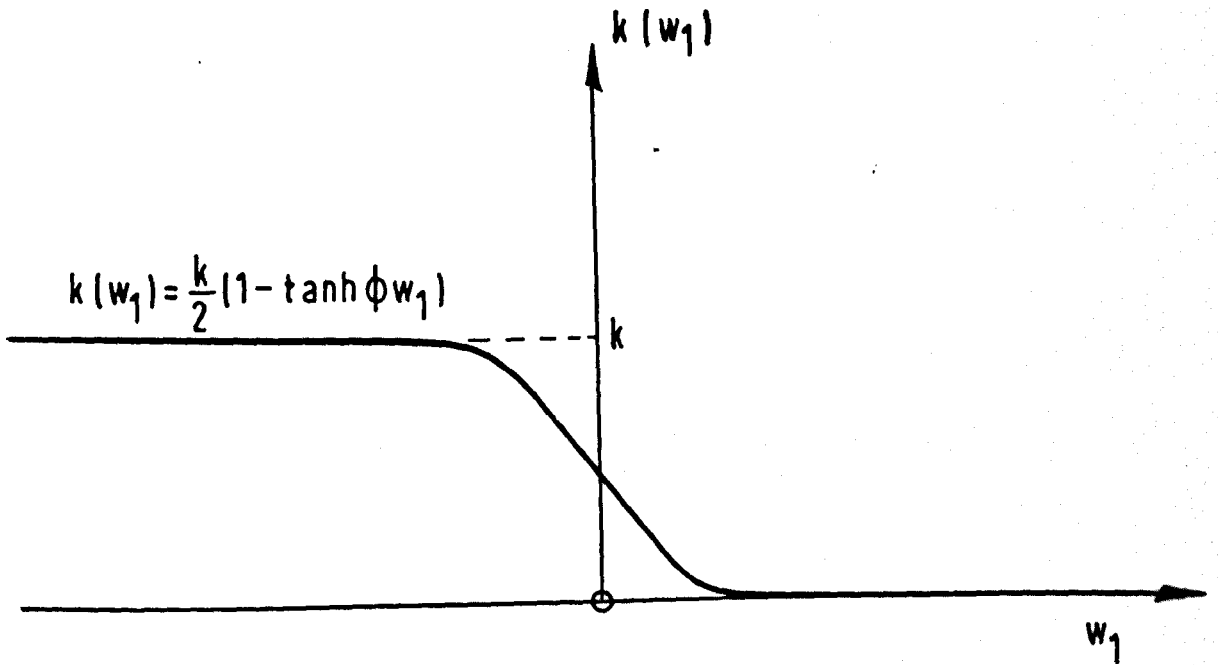
In the previous case, every point on the surface of the foundation is assumed to remain in contact with the bottom face of the slab, independently of whether the foundation at that point is in compression or tension. For the majority of cases this is acceptable for two reasons. Firstly, the weight of the slab has a 'prestressing' effect on the foundation, thus giving the foundation some apparent

tensile stiffness. Secondly, the region of the slab which is of real interest i.e. where the maximum stresses and deflections occur, is also an area where the foundation is in compression.

In situations where these arguments are not valid, it is useful to develop a mathematical model which describes the case of a system in which the foundation has no tensile stiffness. Most attempts, e.g. that of Murphy (21), at treating this problem involve an iterative procedure based on appreciation of the physical behaviour of the system. For example the system can first be analysed as if full contact is preserved in all modes of deformation. At points on the interface where tensile stresses are induced in the foundation, the slab is released. The analysis is then repeated, taking these releases into account, and further regions of tensile interface normal stress are obtained. These also are then released and a further analysis is carried out. The procedure is repeated until convergence of the solution occurs.

The treatment which follows, however, does not require such an iterative routine. The technique is based on a mathematical formulation of the foundation property which is described by specifying that the modulus of subgrade reaction, $k(w_1)$, should be a function of the deflection of the lower surface of the foundation, w_1 , such that

$$\begin{aligned} k(w_1) &= 0 \text{ when } w_1 > 0 \\ k(w_1) &= k \text{ when } w_1 < 0 \\ 0 \leq k(w_1) &\leq k \text{ when } w_1 = 0 \end{aligned} \tag{73}$$



Such a function is

$$k(w_1) = k \left[\frac{1 - \tanh \phi w_1}{2} \right] \quad (74)$$

which has the graphical form shown in Figure 7. ϕ is an arbitrary large positive number, an increase of which results in $k(w_1)$ more rapidly attaining a constant value as the modulus of w_1 increases or decreases from zero.

Substituting this function in place of k in equation

(41) results in:

$$\begin{aligned} & \delta \left\{ \iint \left[\left(M_x \frac{\partial \alpha_o}{\partial x} + M_y \frac{\partial \beta_o}{\partial y} + \left(\frac{k}{2} (1 - \tanh \phi w_1) w_1 + p \right) w_o + H \left(\frac{\partial \alpha_o}{\partial y} + \frac{\partial \beta_o}{\partial x} \right) \right. \right. \right. \\ & + V_x \left(\alpha_o + \frac{\partial w_o}{\partial x} \right) + V_y \left(\beta_o + \frac{\partial w_o}{\partial y} \right) - \frac{k}{4} (1 - \tanh \phi w_1) w_1^2 \left. \right. \\ & - \frac{1}{2E} \left(\frac{12}{h^3} (M_x^2 + M_y^2 + 2\mu M_x M_y + 2(1+\mu)H^2) \right. \\ & + \frac{12}{5h} (1+\mu) (V_x^2 + V_y^2) + \frac{12\mu}{5h} \left(\frac{k}{2} (1 - \tanh \phi w_1) w_1 + p \right) (M_x + M_y) \\ & \left. \left. \left. + \frac{h}{140} (52p^2 + 13k^2 (1 - \tanh \phi w_1)^2 w_1^2 - 18pk(1 - \tanh \phi w_1)) \right) \right] dx dy \right\} \\ & = 0 \quad (75) \end{aligned}$$

The labour of carrying out the variations and determining the Euler equations can be considerably reduced by the use of the general form of Euler equation, obtained from the consideration of the variation of a functional. (Many textbooks are available on this subject, for example, that by Fung (53).) If the variational equation is expressed as:

$$\delta \left\{ \iint K(x, y, u_1, u_2, u_3, \dots, u_i) dx dy \right\} = 0 \quad (76)$$

where u_1, u_2, \dots, u_i are the dependent functions and x, y are the independent variables, the Euler equation representing the variation of K with respect to u_i is

$$\frac{\partial K}{\partial u_i} - \frac{\partial}{\partial x} \cdot \frac{\partial K}{\partial u_{i_x}} - \frac{\partial}{\partial y} \cdot \frac{\partial K}{\partial u_{i_y}} = 0 \quad (77)$$

where $u_{i_x} = \frac{\partial u_i}{\partial x}$ and $u_{i_y} = \frac{\partial u_i}{\partial y}$

Consider the variation of equation (75) with respect to α_o . Rewriting equation (77) in terms of α_o , where [] indicates all the terms within the square brackets of equation (75):

$$\frac{\partial []}{\partial \alpha_o} - \frac{\partial}{\partial x} \cdot \frac{\partial []}{\partial \alpha_{o_x}} - \frac{\partial}{\partial y} \cdot \frac{\partial []}{\partial \alpha_{o_y}} = 0 \quad (78)$$

Then since

$$\frac{\partial []}{\partial \alpha_o} = V_x, \quad \frac{\partial []}{\partial \alpha_{o_x}} = M_x, \quad \frac{\partial []}{\partial \alpha_{o_y}} = H,$$

the resulting Euler equation is

$$V_x - \frac{\partial M_x}{\partial x} - \frac{\partial H}{\partial y} = 0 \quad (79)$$

The remaining Euler equations are obtained in a similar manner.

Thus, the Euler equations associated with the variations of $M_x, M_y,$

$H, V_x, V_y, \alpha_o, \beta_o, w_o$ and w_1 are

$$\frac{\partial \alpha_o}{\partial x} - \frac{12}{Eh^3} (M_x - \mu M_y) - \frac{6\mu}{5Eh} (p + \frac{k}{2} w_1 w) = 0 \quad (80)$$

$$\frac{\partial \beta_0}{\partial y} - \frac{12}{Eh^3} (M_y - \mu M_x) - \frac{6\mu}{5Eh} (p + \frac{k}{2} w_1 \underline{W}) = 0 \quad (81)$$

$$\frac{\partial \alpha_0}{\partial y} + \frac{\partial \beta_0}{\partial x} - \frac{12}{Gh^3} H = 0 \quad (82)$$

$$\alpha_0 + \frac{\partial w_0}{\partial x} - \frac{6}{5Gh} V_x = 0 \quad (83)$$

$$\beta_0 + \frac{\partial w_0}{\partial y} - \frac{6}{5Gh} V_y = 0 \quad (84)$$

$$V_x - \frac{\partial M_x}{\partial x} - \frac{\partial H}{\partial y} = 0 \quad (85)$$

$$V_y - \frac{\partial M_y}{\partial y} - \frac{\partial H}{\partial x} = 0 \quad (86)$$

$$(\frac{k}{2} w_1 \underline{W} + p) - \frac{\partial V_x}{\partial x} - \frac{\partial V_y}{\partial y} = 0 \quad (87)$$

$$\begin{aligned} & (w_0 + \frac{2Ph}{70E} - 6\mu(M_x + M_y)) (\underline{W} - \phi w_1 \operatorname{sech}^2 \phi w_1) \\ & - w_1 (1 - w_1 + w_1 \underline{W} + \phi w_1 \operatorname{sech}^2 \phi w_1) \\ & + \frac{26hk}{140E} w_1 (\underline{W}^2 - \phi w_1 \underline{W} \operatorname{sech}^2 \phi w_1) = 0 \end{aligned} \quad (88)$$

where $\underline{W} = 1 - \tanh \phi w_1 \quad (89)$

The accompanying natural boundary conditions are determined (53) from the general boundary conditions

$$\frac{\partial K}{\partial u_{i,x}} = 0 \quad \text{at the boundaries perpendicular to the x-axis} \quad (90)$$

and $\frac{\partial K}{\partial u_{i,y}} = 0 \quad \text{at the boundaries perpendicular to the y-axis.} \quad (91)$

For u_i equal to α_0 the condition $M_x = 0$ at $x = 0$ and $x = a$ is obtained from equation (90). The remaining conditions are obtained by considering each function in turn, resulting in the following complete set of boundary conditions which are those of the specified problem:

$$\begin{aligned} M_x = V_x = H = 0 \quad \text{on } x = 0 \text{ and } x = a \\ M_y = V_y = H = 0 \quad \text{on } y = 0 \text{ and } y = b \end{aligned} \quad (92)$$

Thus the case of a thick finite slab resting on, but unattached to, a Winkler foundation is specified in terms of the system of non-linear partial differential equations (80 to 88) and the boundary conditions, equations (92).

Discussion

In this chapter two mathematical models, each in the form of a system of partial differential equations and a set of boundary conditions, have been developed for the structural analysis of an idealized pavement/subgrade system in the form of a thick rectangular plate resting on a Winkler foundation. The models differ only in the manner in which the interface conditions between the plate (pavement) and foundation (subgrade) are specified.

In the first model, when the load intensity distribution is applied, the upper surface of the foundation remains in contact with the plate at every point on the interface, including these points at which the plate movement is upward. This is not a requirement of the

second model where the top surface of the foundation and the plate separate at points on the interface when, at these points, the plate deflects upward.

The second model may possibly be a more accurate representation of the actual state in, say, a rigid pavement. However, the non-linear nature of the associated partial differential equations is such that a numerical solution to this second model cannot be anything but extremely difficult to obtain. For this reason only the numerical solution to the first model, expressed in terms of equations (66 to 72), is considered in the next chapter.

SOLUTION TO THE DIFFERENTIAL EQUATIONS OF THE STRUCTURAL ANALYSIS

The analysis of a thick rectangular plate resting on a Winkler-type foundation and subjected to any arbitrary normal loading, is a typical example of a boundary value problem. It has been shown that this problem reduces to finding the solution to a system of simultaneous, linear, nonhomogeneous, partial differential equations with constant coefficients, which at the same time, satisfies a given set of boundary conditions. Finding a suitable mathematical technique for this task is most usefully approached by examining the possible methods, eliminating those which are clearly unsuitable, and then developing those which are promising.

Only in the simplest cases can a solution to a set of simultaneous partial differential equations be found in an exact, explicit form. Approximate methods are, therefore, of particular importance in the present problem. Two types of approximate method of solving sets of partial differential equations can be distinguished.

1. Methods by which approximate values, in tabular form, of the required solution can be found at various points over the physical region for which the problem is defined.

2. Methods by which the approximate solution is derived from an analytical form, e.g. by means of truncated series.

In the first category are the so-called numerical methods, which include finite difference and finite element techniques. Polynomial

and other series solutions fall into the second category where the exact solution is in the form of infinite series and the approximate solution would then be the sum of an arbitrary finite number of the terms of such series. In the present work however, it is considered that the future use of the solution, possibly as a basis for a design method, may find its greatest application if it is expressed in an analytical form. Hence, the numerical analysis has been concentrated in this area.

Two well-developed forms of polynomial expansions are power series and Chebyshev polynomials, while in the field of non-polynomial expansions, Fourier series is perhaps the best known. Text books by Agnew (54), Lanczos (55) and Churchill (56) provide a good basis for the study of power series, Fourier series and Chebyshev polynomials, respectively. In order to determine whether any of these three series can be utilized to furnish a solution to the mathematical model each of them is examined in this chapter, in turn.

General Approach to the Solution of the Equations

One way of solving boundary value problems is, first, to seek the general solution of the system of differential equations and then to determine the remaining constants associated with the solution so that the boundary conditions are satisfied. This method can, however, be unnecessarily tedious and more expeditious methods

therefore use the boundary conditions at the start of the process of obtaining solutions. In this manner a multitude of apparent 'solutions' are eliminated and a restricted range of possible solutions can be concentrated upon.

This is the approach which is used here. Thus, those functions which are subject directly to boundary conditions are first made to satisfy these conditions. Next, the functions are substituted into the system of differential equations and the unique solution sought. In order that this non-trivial solution may be obtained, the expansion used to describe each function must form a complete set of terms even though, at a later stage, some of these terms may prove to be non-contributory. (A set may be said to be complete if every piecewise continuous function can be approximated to any arbitrary degree by a linear combination of terms of the set). The form of the dependent functions which is mathematically most tractable is one which is similar to that of the independent function, i.e., the function describing the load on the slab.

Application of Power Series.

The most elementary example of a complete two-dimensional system of functions is given by the powers

$$\begin{array}{cccccc} 1, & y, & y^2, & \cdot & \cdot & \\ x, & xy, & xy^2, & \cdot & \cdot & \end{array}$$

$$\begin{array}{cccccc}
 x^2, & x^2y, & x^2y^2, & . & . \\
 . & . & . & . & . \\
 . & . & . & . & . \\
 . & . & . & . & .
 \end{array}$$

These form the basis of a power series used to represent a function, $f(x,y)$, that is,

$$\begin{aligned}
 f(x,y) = c_{00} + c_{01}y + c_{02}y^2 + \dots = \sum_{i=0}^{\infty} \sum_{j=0}^{\infty} c_{ij}x^i y^j \\
 c_{10}x + c_{11}xy + c_{12}xy^2 + \dots \\
 c_{20}x^2 + c_{21}x^2y + c_{22}x^2y^2 + \dots \\
 . \quad . \quad . \\
 . \quad . \quad .
 \end{aligned} \tag{93}$$

where c_{ij} is the ij th power series coefficient, and is a constant.

Relevant properties of power series

A possible limitation on the use of power series is that to each series there corresponds a positive number, R_1 , in the x -direction and R_2 in the y -direction, called the radius of convergence of the power series, such that the series converges where $|x| \leq R_1$ and $|y| \leq R_2$ and the series diverges when $|x| > R_1$ or $|y| > R_2$. It is impossible to examine the convergence of a series without first determining its coefficients and so the convergence of those series used to describe the dependent variables in the present investigation will be considered in a later chapter after applying the analysis to a

specific example of the plate/foundation system.

Power series have many uses in pure and applied mathematics and in particular they are often used in the solution of differential equations. The two following theorems are necessary for such applications.

Theorem 1:

If $\sum_{i=0}^{\infty} \sum_{j=0}^{\infty} c_{ij} x^i y^j$ converges

when $|x| \leq R_1$ and $|y| \leq R_2$ and $f(x,y) = \sum_{i=0}^{\infty} \sum_{j=0}^{\infty} c_{ij} x^i y^j$

then $f(x,y)$ is differentiable when $|x| \leq R_1$ and $|y| \leq R_2$ and the derivative may be obtained by termwise partial differentiation, e.g.

$$\frac{\partial f(x,y)}{\partial x} = \sum_{i=0}^{\infty} \sum_{j=0}^{\infty} i c_{ij} x^{i-1} y^j = \sum_{i=-1}^{\infty} \sum_{j=0}^{\infty} (i+1) c_{i+1,j} x^i y^j$$

The latter representation depends upon the fact that an integer (positive or negative) can be added to the index of the summation whenever it appears after the symbol \sum , provided that this is compensated for by subtracting the same integer^e from the index on the summation sign.

Theorem 2: Another requirement is that if $R_1 > 0$ and $R_2 > 0$, and also if $f_1(x,y) = \sum_{i=0}^{\infty} \sum_{j=0}^{\infty} c_{ij} x^i y^j$ and $f_2(x,y) = \sum_{i=0}^{\infty} \sum_{j=0}^{\infty} d_{ij} x^i y^j$, then $f_1(x,y) = f_2(x,y)$ when $|x| \leq R_1$ and $|y| \leq R_2$ if and, only if, $c_{00} = d_{00}$, $c_{01} = d_{01}$!

and, in general, if $c_{ij} = d_{ij}$

Proofs of these theorems can be obtained from most textbooks dealing with series.

These theorems, along with the ability of a power series to represent a function, enable the solution of the boundary value problem to be attempted.

The solution of the boundary value problem

The first consideration in the numerical analysis is the satisfaction of the boundary conditions by the dependent functions. The requirement that a function should be zero at, say, $x=0$ and $x=a$ is most easily attained by the introduction of a multiplier $(ax-x^2)$ which results in an ij th term of the form $c_{ij}x^i y^j (ax-x^2)$. This does not appear to impose any unwanted restrictions upon the derivatives of such a function. This technique is similar to one used by Coull (51).

Considerations similar to that described above apply to the y -direction. Thus, in the present work in order to satisfy the boundary conditions represented by equations (72) the dependent functions can be represented by

$$M_x = \sum_{i=0}^{\infty} \sum_{j=0}^{\infty} M_{x_{ij}} x^i y^j (ax-x^2)$$
$$V_x = \sum_{i=0}^{\infty} \sum_{j=0}^{\infty} V_{x_{ij}} x^i y^j (ax-x^2)$$

$$\begin{aligned}
 M_y &= \sum_{i=0}^{\infty} \sum_{j=0}^{\infty} M_{y_{ij}} x^i y^j (by-y^2) \\
 V_y &= \sum_{i=0}^{\infty} \sum_{j=0}^{\infty} V_{y_{ij}} x^i y^j (by-y^2) \\
 w_o &= \sum_{i=0}^{\infty} \sum_{j=0}^{\infty} w_{o_{ij}} x^i y^j \\
 H &= \sum_{i=0}^{\infty} \sum_{j=0}^{\infty} H_{ij} x^i y^j (ax-x^2)(by-y^2)
 \end{aligned} \tag{94}$$

while the load intensity distribution, p , applied to the slab maybe described by a loading function which is assumed to be expressable in the form

$$p = \sum_{i=0}^{\infty} \sum_{j=0}^{\infty} p_{ij} x^i y^j \tag{95}$$

These series expressed by equations (94) and (95) can now be substituted into the system of partial differential equations, equations (66 to 71). For example, consider equation (69):

$$-\frac{\partial M_x}{\partial x} - \frac{\partial H}{\partial y} + V_x = 0 \tag{69}$$

Theorem 1 on the assumption of the initial convergence of the dependent functions enables the series to be substituted, thus:

$$\begin{aligned}
 &- \sum_{i=0}^{\infty} \sum_{j=0}^{\infty} M_{x_{ij}} \left[a(i+1)x^i - (i+2)x^{i+1} \right] y^j \\
 &- \sum_{i=0}^{\infty} \sum_{j=0}^{\infty} H_{ij} x^i (ax-x^2) \left[b(j+1)y^j - (j+2)y^{j+1} \right] \\
 &+ \sum_{i=0}^{\infty} \sum_{j=0}^{\infty} V_{x_{ij}} x^i (ax-x^2) y^j = 0
 \end{aligned}$$

Theorem 2 enables relationships between the coefficients to be obtained by summing the coefficients of the function, $x^i y^j$, thereby resulting in the ij th equation

$$-(i+1) \left(aM_{x_{ij}} - M_{x_{i-1,j}} \right) - (j+1) \left(abH_{i-1,j} - bH_{i-2,j} - aH_{i-1,j-1} + H_{i-2,j-1} \right) + \left(aV_{x_{i-1,j}} - V_{x_{i-2,j}} \right) = 0$$

By applying the same techniques to the remainder of the partial differential equations, (66 to 71), the following system of six general algebraic simultaneous equations maybe produced, which interrelate all the coefficients of the various series:

$$-r(i+1) \left(aV_{x_{ij}} - V_{x_{i-1,j}} \right) - sr(j+1) \left(bV_{y_{ij}} - V_{y_{i,j-1}} \right) + (i+1)(i+2)w_{o_{i+2,j}} + s(j+1)(j+2)w_{o_{i,j+2}} + t \left(aM_{x_{i-1,j}} - M_{x_{i-2,j}} \right) + \frac{Tkf}{g} w_{o_{ij}} = -TCfp_{ij} \quad (96)$$

where: $i=0,1,2 \dots \infty; j = 0,1,2 \dots \infty$

$$-r(j+1) \left(bV_{y_{ij}} - V_{y_{i,j-1}} \right) - sr(i+1) \left(aV_{x_{ij}} - V_{x_{i-1,j}} \right) + (j+1)(j+2)w_{o_{i,j+2}} + s(i+1)(i+2)w_{o_{i+2,j}} + t \left(bM_{y_{i,j-1}} - M_{y_{i,j-2}} \right) + \frac{Tkf}{g} w_{o_{ij}} = -TCfp_{ij} \quad (97)$$

where: $i=0,1,2 \dots \infty; j = 0,1,2 \dots \infty$

$$\begin{aligned}
 & -r(j+1) \left(aV_{x_{i-1,j+1}} - V_{x_{i-2,j+1}} \right) - r(i+1) \left(bV_{y_{i+1,j-1}} - V_{y_{i+1,j-2}} \right) \\
 & + 2(i+1)(j+1)W_{o_{i+1,j+1}} + \frac{m}{\epsilon} \left(abH_{i-1,j-1} - aH_{i-1,j-2} - bH_{i-2,j-1} \right. \\
 & \left. + H_{i-2,j-2} \right) = 0 \quad (98)
 \end{aligned}$$

where: $i=0,1,2 \dots \infty; j=0,1,2 \dots \infty$

$$\begin{aligned}
 & -r(i+1) \left(aM_{x_{ij}} - M_{x_{i-1,j}} \right) - (j+1) \left(abH_{i-1,j} - bH_{i-2,j} \right. \\
 & \left. - aH_{i-1,j-1} + H_{i-2,j-1} \right) + \left(aV_{x_{i-1,j}} - V_{x_{i-2,j}} \right) = 0 \quad (99)
 \end{aligned}$$

where: $i=0,1,2 \dots \infty; i=0,1,2 \dots \infty$

$$\begin{aligned}
 & -(j+1) \left(bM_{y_{ij}} - M_{y_{i,j-1}} \right) - (i+1) \left(abH_{i,j-1} - aH_{i,j-2} \right. \\
 & \left. - bH_{i-1,j-1} + H_{i-1,j-2} \right) + \left(bV_{y_{i,j-1}} - V_{y_{i,j-2}} \right) = 0 \quad (100)
 \end{aligned}$$

where: $i=0,1,2 \dots \infty; i = 0,1,2 \dots \infty$

$$\begin{aligned}
 & -(i+1) \left(aV_{x_{ij}} - V_{x_{i-1,j}} \right) - (j+1) \left(bV_{y_{ij}} - V_{y_{i,j-1}} \right) \\
 & + \frac{k}{\epsilon} w_{o_{ij}} - \frac{kT}{\epsilon} \left(aM_{x_{i-1,j}} - M_{x_{i-2,j}} + bM_{y_{i,j-1}} - M_{y_{i,j-2}} \right) \\
 & = -Cp_{ij} \quad (101)
 \end{aligned}$$

where: $i=0,1,2 \dots \infty; j=0,1,2 \dots \infty$

Only a limited number of terms are, in fact, used to approximately represent the loading function, i.e.,

$$p = \sum_{i=0}^m \sum_{j=0}^n p_{ij} x^i y^j \quad (102)$$

although the solution is still the solution of an infinity of equations in an infinity of unknowns. The practical possibility of a solution can then only be considered if the dependent series are also truncated. However, attempting to satisfy all equations in which the allowable coefficients appear results in an overdetermined system. Therefore, only an approximate solution, in which the coefficient of the truncated series are required to satisfy a limited number of the equations, and not the complete set, can be obtained.

The choice as to which equations should be disregarded is largely arbitrary, however, certain reasonable requirements should be maintained. These are: 1. that any equation containing a loading function coefficient should not be neglected; 2. that the lengths of the various series should be of similar order; and 3. that the number of equations created from each i th equation should also be similar. Hence, it would appear that the ranges of each general equation and of each dependent function should be the same and at least equal to the loading function.

A minor difficulty arises in that the last term of the series representing the twist^{ing} moment, H_{mn} , is not defined by any equation. In order to overcome this difficulty and still preserve an orderly system, the upper limit of the twist^{ing} moment series is defined by $H_{m-1,n-1}$ and the range of equation (98) is taken as $i:0$ to $m-1$, $j:0$ to $n-1$. Using this system, the ranges of the series and

simultaneous equations are then as shown in Table 1 and Table 2, respectively.

Series	Range of i	Range of j
p	o to m	o to n
w_o	o to m	o to n
H	o to m-1	o to n-1
M_x	o to m	o to n
M_y	o to m	o to n
V_x	o to m	o to n
V_y	o to m	o to n

Table 1. Ranges of series

Equations	Range of i	Range of j
(96)	o to m	o to n
(97)	o to m	o to n
(98)	o to m-1	o to n-1
(99)	o to m	o to n
(100)	o to m	o to n
(101)	o to m	o to n

Table 2. Ranges of equations.

The solution to the boundary value problem is thus reduced to the solution of a number of simultaneous algebraic equations, Q , in a similar number of unknown power series coefficients, where

$$Q = 6mn + 5m + 5n + 5 \quad (103)$$

Application of Chebyshev Polynomials

Of all the forms of expansion, the Chebyshev polynomial series provides the maximum convergence inasmuch as it requires the smallest number of terms to achieve an approximation of a function which does not deviate from its true value by more than an arbitrary small amount, at any point of the given basic range $[-1,+1]$ of the independent variable.

Fundamental properties of Chebyshev polynomials

The Chebyshev polynomials $T_i(\eta)$, where η is the independent variable and i indicates that $T_i(\eta)$ is the i th term of a Chebyshev polynomial series, possess a very valuable property in that they are expressible in terms of elementary trigonometric functions. They are, in effect, merely the simple trigonometric functions $\cos i\theta$ but expressed in the variable $\eta = \cos \theta$. This fundamental relation, which translates the many useful properties of Fourier series into the area of power expansions, is the most important property of the Chebyshev polynomials.

The shifted Chebyshev polynomial $T_i^{*'}(\eta)$ is of special interest. This is simply a Chebyshev polynomial with a range of

definition $[0,1]$. The renormalization of the $T_i(\eta)$ to the new range is easily arrived at by putting $\cos \theta = 2\eta - 1$ in place of $\cos \theta = \eta$. The shifted Chebyshev polynomials are thus defined by

$$T_i^*(\eta) = \cos i\theta = \cos [i \cos^{-1}(2\eta - 1)] \quad (104)$$

The new polynomials, $T_i^*(\eta)$, have coefficients which are entirely different to those of the standard Chebyshev form $T_i(\eta)$. In their polynomial expansions of the function, $f(\eta)$ they are represented by the series

$$f(\eta) = \sum_{i=0}^{\infty} c_i T_i^*(\eta) \quad (105)$$

Since this expansion is, in fact, a reinterpretation of a cosine series, the shifted Chebyshev polynomials form a complete set in the interval $[0,1]$. Theorems 3 to 6 are now developed relating to shifted Chebyshev polynomials.

Theorem 3. The connection between shifted Chebyshev polynomials and trigonometric functions can be used to obtain a recursive relationship between polynomials. Taking the trigonometric formula

$$\cos(s+t)\theta + \cos(s-t)\theta = 2 \cos s\theta \cos t\theta$$

and employing the notation of $T_s^*(\eta)$ and $T_t^*(\eta)$ the following recursive formula is obtained:

$$T_{s+t}^*(\eta) + T_{s-t}^*(\eta) = 2T_s^*(\eta)T_t^*(\eta) \quad (106)$$

Theorem 4. The orthogonality condition in Fourier series which applies to a discrete set of points, (θ_α) ,

$$\sum_{\alpha=0}^{n-1} \cos s\theta_\alpha \cos t\theta_\alpha = \begin{cases} n & (s=t=0) \\ n/2 & (s=t \neq 0) \\ 0 & (s \neq t) \end{cases}$$

is easily expressed in the following polynomial form

$$\sum_{\alpha=0}^{n-1} T_s^*(\eta) T_t^*(\eta) = \begin{cases} n & (s=t=0) \\ n/2 & (s=t \neq 0) \\ 0 & (s \neq t) \end{cases} \quad (107)$$

where $2\eta_\alpha - 1 = \cos \theta_\alpha$.

Theorem 5. Similarly, the orthogonality condition applying to a continuous surface

$$\int_0^\pi \cos(s\theta) \cos(t\theta) d\theta = \begin{cases} \pi & (s=t=0) \\ \pi/2 & (s=t \neq 0) \\ 0 & (s \neq t) \end{cases}$$

can be expressed in the following polynomial form:

$$\int_0^1 \frac{T_s^*(\eta) T_t^*(\eta)}{\sqrt{(\eta^2 - \eta)}} d\eta = \begin{cases} \pi & (s=t=0) \\ \pi/2 & (s=t \neq 0) \\ 0 & (s \neq t) \end{cases} \quad (108)$$

Theorem 6. When the need arises to differentiate shifted Chebyshev polynomials, the best approach to the development of a technique for this purpose is to study their integration.

A useful relationship which provides the basis for the integration of shifted Chebyshev polynomials is

$$\frac{T_{i+1}^*(\eta)}{i+1} - \frac{T_{i-1}^*(\eta)}{i-1} = 4 \int T_i^*(\eta) d\eta \quad (i > 1) \quad (109)$$

This can be arrived at by taking the trigonometric form of $T_{i+1}^*(\eta) - T_{i-1}^*(\eta)$, differentiating, employing again the cosine relationship, integrating throughout, and rearranging,

Also:

$$T_1^*(\eta) d\eta = \text{constant} + \frac{T_1^*(\eta)}{8} \quad (110)$$

and $T_0^*(\eta) d\eta = \text{constant} + \frac{T_1^*(\eta)}{2}$

Equations (110) can both be verified (54) by consideration of the power expansion form of the shifted Chebyshev polynomials.

Assuming that a function $f(\eta)$ is expressable in a shifted Chebyshev polynomial form;

$$f(\eta) = \frac{1}{2} A_0 + A_1 T_1^*(\eta) + A_2 T_2^*(\eta) + A_3 T_3^*(\eta) + \dots$$

and assuming a similar expansion for the derivative $f'(\eta)$ of this function

$$f'(\eta) = \frac{1}{2} a_0 + a_1 T_1^*(\eta) + a_2 T_2^*(\eta) + a_3 T_3^*(\eta) + \dots$$

where the halves are introduced for convenience, then on integrating $f'(\eta)$ and applying equations (109) and (110):

$$f(\eta) = \int f'(\eta) d\eta = \text{constant} + a_0 \frac{T_1^*(\eta)}{2} + a_1 \frac{T_2^*(\eta)}{8} + \sum_{i=2}^{\infty} \frac{a_i}{4} \left[\frac{T_{i+1}^*(\eta)}{i+1} - \frac{T_{i-1}^*(\eta)}{i-1} \right]$$

or $f(\eta) = \sum_{i=0}^{\infty} A_i T_i^*(\eta) \quad (111)$

where the symbol ' indicates that the first term is associated with a factor of one half and, in general,

$$A_i = \frac{a_{i-1} - a_{i+1}}{4i} \quad (i > 0) \quad (112)$$

A_0 is determined by the lower limit of integration. The problem of differentiation is the inverse of the above. Given a set $A_0, A_1, A_2 \dots$, the required coefficients $a_0, a_1, a_2 \dots$, can be found using:

$$a_{i-1} = a_{i+1} + 4iA_i \quad (113)$$

which is a rearrangement of equation (112). If A_m is the coefficient of the highest order which is not negligible, taking $a_m = a_{m+1} = a_{m+2} = \dots = 0$ and then finding $a_{n-1}, a_{n-2}, \dots, a_0$ by successive application of equation (113) results in the differentiated series.

Differentiation, orthogonality and the recursive nature of shifted Chebyshev polynomials have all been considered in Theorems 6, 4 and 5, and 3, respectively. These are essential to the application of such polynomials to any boundary value problem and now can be used to attack the present problem, represented by the system of partial differential equations (66 to 71) and by the boundary conditions, equations (72).

The solution to the boundary value problem.

Since the range of definition of the shifted Chebyshev series is $[0,1]$, then computation is simplest if the rectangular

plate ($0 \leq x \leq a$, $0 \leq y \leq b$) is transformed into an equivalent unit square plate by the use of the transformations $\eta = x/a$ and $\xi = y/b$.

Noting that

$$\frac{\partial}{\partial x} = \frac{1}{a} \frac{\partial}{\partial \eta} \quad \text{and} \quad \frac{\partial}{\partial y} = \frac{1}{b} \frac{\partial}{\partial \xi} \quad (114)$$

a transformed system of partial differential equations can also be obtained.

The assumption is also made that the applied normal loading, p , may be written in the form

$$p = \sum_{i=0}^{\infty} \sum_{j=0}^{\infty} ' p_{ij} T_i^* (\eta) T_j^* (\xi) \quad (115)$$

and the weighted average deflection, w_o , in the form

$$w_o = \sum_{i=0}^{\infty} \sum_{j=0}^{\infty} ' w_{o_{ij}} T_i^* (\eta) T_j^* (\xi) \quad (116)$$

where the symbol ' indicates that p_{i0} , p_{0j} , $w_{o_{i0}}$ and $w_{o_{0j}}$, are each associated with one-half, and p_{00} and $w_{o_{00}}$ are each associated with one-quarter so that the technique of differentiation can be easily applied.

In order that the given boundary conditions should be satisfied, e.g. $M_x = 0$ at $\eta = 0$ and $\eta = 1$, the series multiplier $(\eta - \eta^2)$ may be employed in its shifted Chebyshev polynomial form;

$$\left[T_0^*(\eta) - T_2^*(\eta) \right] / 8$$

This latter expression is obtained by using the shifted Chebyshev form of simple power terms. Taking M_x as an example, and multiplying the basic series by the series multiplier in order to make it satisfy the required boundary conditions,

$$M_x = \sum_{i=0}^{\infty} \sum_{j=0}^{\infty} M_{x_{ij}} T_i^*(\eta) T_j^*(\xi) \left[T_0^*(\eta) - T_2^*(\eta) \right] / 8$$

or, applying the recursive relationships expressed by equation (106),

$$M_x = \sum_{i=0}^{\infty} \sum_{j=0}^{\infty} \frac{M_{x_{ij}}}{16} \left[2 T_i^*(\eta) - T_{i+2}^*(\eta) - T_{i-2}^*(\eta) \right] T_j^*(\xi) \quad (117)$$

Similarly, for the other dependent functions:

$$M_y = \sum_{i=0}^{\infty} \sum_{j=0}^{\infty} \frac{M_{y_{ij}}}{16} T_i^*(\eta) \left[2 T_j^*(\xi) - T_{j+2}^*(\xi) - T_{j-2}^*(\xi) \right] \quad (118)$$

$$V_x = \sum_{i=0}^{\infty} \sum_{j=0}^{\infty} \frac{V_{x_{ij}}}{16} \left[2 T_i^*(\eta) - T_{i+2}^*(\eta) - T_{i-2}^*(\eta) \right] T_j^*(\xi) \quad (119)$$

$$V_y = \sum_{i=0}^{\infty} \sum_{j=0}^{\infty} \frac{V_{y_{ij}}}{16} T_i^*(\eta) \left[2 T_j^*(\xi) - T_{j+2}^*(\xi) - T_{j-2}^*(\xi) \right] \quad (120)$$

$$H = \sum_{i=0}^{\infty} \sum_{j=0}^{\infty} \frac{H_{ij}}{(16)^2} \left[2 T_i^*(\eta) - T_{i+2}^*(\eta) - T_{i-2}^*(\eta) \right] \left[2 T_j^*(\xi) - T_{j+2}^*(\xi) - T_{j-2}^*(\xi) \right] \quad (121)$$

Returning to the system of partial differential equations (66 to 71) -

and considering equation (71) as an example - the equation transformed to the new co-ordinate system, by means of equations (114), takes the form

$$-\frac{1}{a} \frac{\partial V_x}{\partial \eta} - \frac{1}{b} \frac{\partial V_y}{\partial \xi} + \frac{k}{g} w_0 - \frac{kT}{g} (M_x + M_y) = - C_p \quad (122)$$

Substituting equations (115 to 120) results in

$$\begin{aligned} & -\frac{1}{a} \sum_{i=0}^{\infty} \sum_{j=0}^{\infty} V_{x_{ij}}^{\eta} \left[2 T_i^*(\eta) - T_{i+2}^*(\eta) - T_{i-2}^*(\eta) \right] T_j^*(\xi) \\ & -\frac{1}{b} \sum_{i=0}^{\infty} \sum_{j=0}^{\infty} V_{y_{ij}}^{\xi} T_i^*(\eta) \left[2 T_j^*(\xi) - T_{j+2}^*(\xi) - T_{j-2}^*(\xi) \right] \\ & + \frac{k}{g} \sum_{i=0}^{\infty} \sum_{j=0}^{\infty} w_{0_{ij}} T_i^*(\eta) T_j^*(\xi) - \frac{kT}{g} \sum_{i=0}^{\infty} \sum_{j=0}^{\infty} \frac{M_{x_{ij}}}{16} \left[2 T_i^*(\eta) \right. \\ & \left. - T_{i+2}^*(\eta) - T_{i-2}^*(\eta) \right] T_j^*(\xi) - \frac{kT}{g} \sum_{i=0}^{\infty} \sum_{j=0}^{\infty} \frac{M_{y_{ij}}}{16} T_i^*(\eta) \left[2 T_j^*(\xi) \right. \\ & \left. - T_{j+2}^*(\xi) - T_{j-2}^*(\xi) \right] = - C_p \sum_{i=0}^{\infty} \sum_{j=0}^{\infty} p_{ij} T_i^*(\eta) T_j^*(\xi) \quad (123) \end{aligned}$$

where from equation (113),

$$V_{x_{i-1,j}}^{\eta} = V_{x_{i+1,j}}^{\eta} + 4i V_{x_{ij}}^{\eta}$$

and

$$V_{y_{i,j-1}}^{\xi} = V_{y_{i,j+1}}^{\xi} + 4j V_{y_{ij}}^{\xi}$$

and the superscripts η and ξ denote the coefficients of the derived series obtained by differentiating the original series with respect

to the η and ξ directions respectively. Similarly, higher order derivatives are denoted by a corresponding number of superscripts.

Multiplying through by $\frac{T_s^*(\eta)}{\sqrt{(\eta^2 - \eta)}} \cdot \frac{T_t^*(\xi)}{\sqrt{(\xi^2 - \xi)}}$

and integrating, in dimensionless co-ordinates, between the limits 0 and 1 in each case, enables the continuous orthogonality conditions expressed by equations (108) to be applied. Thus, for example:

$$\frac{1}{b} \sum_{i=0}^{\infty} \sum_{j=0}^{\infty} \frac{v_{ij}^{\xi}}{16} T_i^{*s}(\eta) T_{j+2}^{*t}(\xi)$$

becomes $\frac{1}{b} \sum_{i=0}^{\infty} \sum_{j=0}^{\infty} \frac{v_{ij}^{\xi}}{16} \int_0^1 \frac{T_i^{*s}(\eta) T_{j+2}^{*s}(\eta)}{\sqrt{(\eta^2 - \eta)}} d\eta \cdot \int_0^1 \frac{T_{j+2}^{*t}(\xi) T_t^{*t}(\xi)}{\sqrt{(\xi^2 - \xi)}} d\xi$

which equals $\frac{1}{b} \frac{v_{s,t-2}^{\xi}}{16} \left[1 \cdot \frac{\pi}{2} \cdot \frac{\pi}{2} \right]$ for $s \neq 0$ and $t \neq 0$,

or $\frac{1}{b} \frac{v_{s,t-2}^{\xi}}{16} \left[\frac{1}{2} \cdot \frac{\pi}{2} \cdot \pi \right]$ for $s \neq 0$ and $t = 0$,

or $\frac{1}{b} \frac{v_{s,t-2}^{\xi}}{16} \left[\frac{1}{2} \cdot \pi \cdot \frac{\pi}{2} \right]$ for $s = 0$ and $t \neq 0$,

or $\frac{1}{b} \frac{v_{s,t-2}^{\xi}}{16} \left[\frac{1}{4} \cdot \pi \cdot \pi \right]$ for $s = 0$ and $t = 0$

Returning to equation (123) and cancelling through by the constant in the square brackets which is common to all terms in the equation for a particular i and j , independent of whether $s = 0$ or > 0 or $t = 0$ or > 0 , results in the following ij th equations on replacing s by i and t by j for convenience:

$$-\frac{1}{a} \left[2V_{x_{ij}}^\eta - V_{x_{i-2,j}}^\eta - V_{x_{i+2,j}}^\eta \right] - \frac{1}{b} \left[2V_{y_{ij}}^\xi - V_{y_{i,j-2}}^\xi - V_{y_{i,j+2}}^\xi \right] + 16 \frac{k}{g} w_{o_{ij}}$$

$$-\frac{kT}{g} \left[2M_{x_{ij}} - M_{x_{i-2,j}} - M_{x_{i+2,j}} \right] - \frac{kT}{g} \left[2M_{y_{ij}} - M_{y_{i,j-2}} - M_{y_{i,j+2}} \right] = -16 C_{p_{ij}}$$

rewriting $\left[2V_{x_{ij}}^\eta - V_{x_{i-2,j}}^\eta - V_{x_{i+2,j}}^\eta \right]$ in the form $\left[\left(V_{x_{ij}}^\eta - V_{x_{i+2,j}}^\eta \right) - \left(V_{x_{i-2,j}}^\eta - V_{x_{ij}}^\eta \right) \right]$

and applying the differential relationship, equation (113), results in

$$\left[4(i+1)V_{x_{i+1,j}} - 4(i-1)V_{x_{i-1,j}} \right]$$

Thus the ij th equation, equation (123), can be rewritten as

$$\begin{aligned} & -\frac{4}{a} \left[(i+1)V_{x_{i+1,j}} - (i-1)V_{x_{i-1,j}} \right] - \frac{4}{b} \left[(j+1)V_{y_{i,j+1}} - (j-1)V_{y_{i,j-1}} \right] \\ & + 16 \frac{k}{g} w_{o_{ij}} - \frac{kT}{g} \left[2M_{x_{ij}} - M_{x_{i-2,j}} - M_{x_{i+2,j}} \right] - \frac{kT}{g} \left[2M_{y_{ij}} - M_{y_{i,j-2}} - M_{y_{i,j+2}} \right] \\ & = -16 C_{p_{ij}} \end{aligned} \tag{124}$$

where: $i = 0, 1, 2 \dots \infty$; $j = 0, 1, 2 \dots \infty$

The same considerations also apply to the remaining five partial differential equations, i.e. equations (66 to 70). The overall result, then, is the following set of six general simultaneous linear algebraic equations:

$$\begin{aligned} & -\frac{4r}{a} \left[(i+1)V_{x_{i+1,j}} - (i-1)V_{x_{i-1,j}} \right] - \frac{4sr}{b} \left[(j+1)V_{y_{i,j+1}} - (j-1)V_{y_{i,j-1}} \right] \\ & + \frac{16}{a^2} \cdot w_{o_{ij}}^\eta \end{aligned}$$

$$+\frac{16s}{b} \frac{\xi\xi}{w} o_{ij} + t \left[2M x_{ij}^{-M} x_{i-2,j}^{-M} x_{i+2,j}^{-M} \right] + \frac{TKf}{g} w o_{ij} = -TCf P_{ij} \quad (125)$$

$$-\frac{4x}{b} \left[(j+1)V y_{i,j+1} - (j-1)V y_{i,j-1} \right] - \frac{4sx}{a} \left[(i+1)V x_{i+1,j} - (i-1)V x_{i-1,j} \right] + \frac{16}{b^2} \frac{\xi\xi}{w} o_{ij}$$

$$+\frac{16s}{a} \frac{\eta\eta}{w} o_{ij} + t \left[2M y_{ij}^{-M} y_{i,j-2}^{-M} y_{i,j+2}^{-M} \right] + \frac{TKf}{g} w o_{ij} = -TCf P_{ij} \quad (126)$$

$$-\frac{4x}{b} \left[(i+1)V x_{i+1,j} - (i-1)V x_{i-1,j} \right] - \frac{4x}{a} \left[(j+1)V y_{i,j+1} - (j-1)V y_{i,j-1} \right] + \frac{32}{ab} w o_{ij} \xi\xi$$

$$+\frac{m}{16} \left[4H_{ij}^{-2H} x_{i-2,j}^{-2H} x_{i+2,j}^{-2H} y_{i,j-2}^{-2H} y_{i,j+2}^{-2H} \right] + 2^H x_{i,j+2}^{-2H} x_{i-2,j+2}^{-2H}$$

$$+H_{i+2,j+2}] = 0$$

$$-\frac{4}{a} \left[(i+1)M_{x_{i+1,j}} - (i-1)M_{x_{i-1,j}} \right] - \frac{1}{4b} \left[(j+1)(2H_{i,j+1} - H_{i-2,j+1} - H_{i+2,j+1}) \right]$$

$$- (j-1)(2H_{i,j-1} - H_{i+2,j-1} - H_{i-2,j-1}) + \left[2V_{x_{i,j}} - V_{x_{i-2,j}} - V_{x_{i+2,j}} \right] = 0 \quad (128)$$

$$-\frac{4}{b} \left[(j+1)M_{y_{i,j+1}} - (j-1)M_{y_{i,j-1}} \right] - \frac{1}{4a} \left[(i+1)(2H_{i+1,j} - H_{i+1,j-2} - H_{i+1,j+2}) \right]$$

$$- (i-1)(2H_{i-1,j} - H_{i-1,j-2} - H_{i-1,j+2}) + \left[2V_{y_{i,j}} - V_{y_{i,j-2}} - V_{y_{i,j+2}} \right] = 0 \quad (129)$$

$$\frac{4}{a} \left[(i+1)V_{x_{i+1,j}} - (i-1)V_{x_{i-1,j}} \right] - \frac{4}{b} \left[(j+1)V_{y_{i,j+1}} - (j-1)V_{y_{i,j-1}} \right] + \frac{16k}{g} w_{o_{ij}}$$

$$-\frac{kT}{g} \left[2M_{x_{i-2,j}} - M_{x_{i+2,j}} \right] - \frac{kT}{g} \left[2M_{y_{i,j}} - M_{y_{i,j-2}} - M_{y_{i,j+2}} \right] = -16Cp_{ij} \quad (130)$$

$$\text{where: } w_{ij}^{\eta\eta} = \left[2(i+2)w_{i+2,j}^{\eta\eta} - (i+1)w_{i+4,j}^{\eta\eta} + 16(i+1)(i+2)(i+3)w_{i+2,j}^{\eta\eta} \right] \frac{1}{(i+3)}$$

$$w_{ij}^{\xi\xi} = \frac{1}{(j+3)} \left[2(j+2)w_{i,j+2}^{\xi\xi} - (j+1)w_{i,j+4}^{\xi\xi} + 16(j+1)(j+2)(j+3)w_{i,j+2}^{\xi\xi} \right] \quad (131)$$

$$w_{ij}^{\eta\xi} = \left[w_{i,j+2}^{\eta\xi} + w_{i+2,j}^{\eta\xi} - w_{i+2,j+2}^{\eta\xi} + 16(i+1)(j+1)w_{i+1,j+1}^{\eta\xi} \right]$$

The expansion used to approximately represent the loading function must of necessity be limited to a finite number of terms, say, m terms in the η - dimension and n terms in the ξ -dimension. Thus

$$p = \sum_{i=0}^{m-1} \sum_{j=0}^{n-1} p_{ij} T_i^*(\eta) T_j^*(\xi) \quad (132)$$

In order that the system of general equations and dependent variables should be compatible with the limited number of terms contained in the loading function, the range of the dependent variables are all

$$i : 0 \text{ to } m - 1 \quad \text{and} \quad j : 0 \text{ to } n - 1 \quad (133)$$

and each of the general equations has the range

$$i : 0 \text{ to } m - 1 \quad \text{and} \quad j : 0 \text{ to } n - 1 \quad (134)$$

Because the expansions which are used to satisfy the boundary conditions are combinations of Chebyshev series all the terms are interdependent and as such, require the solution of all coefficients at one and the same time.

During the creation of the simultaneous algebraic equations the coefficients $w_{ofk}^{\eta\eta}$ etc. are replaced by combinations of the coefficients of the original terms, w_{ost} , by applying equation (131) to $w_{om-1,n-1}^{\eta\eta}$ and progressing down to $w_{oo}^{\eta\eta}$ taking $w_{o+1,j}^{\eta\eta} = w_{oo,j}^{\eta\eta} = w_{o-1,j}^{\eta\eta} = w_{o-2,j}^{\eta\eta} = \dots = 0$, where f, k, s and t are general subscripts. Similar considerations apply to $w_{oij}^{\xi\xi}$ and $w_{oij}^{\eta\xi}$.

Thus, from the system of six general equations, equations (125 to 130), are created $6mn$ simultaneous algebraic equations which can be solved for the $6mn$ dependent coefficients. The series, defined by equations (116) and (117 to 120), which describe the dependent variables in terms of non-dimensionless co-ordinates are easily expressed in terms of the original co-ordinate system by the substitution: $\eta = x/a$ and $\xi = y/b$.

Application of Fourier Series

Fourier series has found innumerable applications to the solution of boundary value problems, due principally to a powerful fundamental property possessed by this form of expansion.

A fundamental property of Fourier series

The most important theorem concerning Fourier series expansions is that every function, $f(x)$, which is piecewise smooth in the interval $-\pi \leq x \leq \pi$, and periodic with the period 2π , may be expanded in a Fourier series, i.e. a series of the following form:

$$s_i(x) = \frac{1}{2} a_0 + \sum_{i=1}^m (a_i \cos ix + b_i \sin ix) \quad (135)$$

which converges to $f(x)$ with increasing m , where the Fourier coefficients (a_0, a_i and b_i) are given by:

$$a_i = \frac{1}{\pi} \int_{-\pi}^{\pi} f(x) \cos ix \, dx \quad (i = 0, 1, 2 \dots m)$$
$$b_i = \frac{1}{\pi} \int_{-\pi}^{\pi} f(x) \sin ix \, dx \quad (i = 0, 1, 2 \dots m) \quad (136)$$

this theorem follows from the orthogonality and completeness of the trigonometric functions. It can be extended to cater for any arbitrary interval $s \leq x \leq t$. A further consequence is that the best approximation to a function, in the mean, is obtained by the Fourier polynomial.

Consideration of a Fourier series solution

The method of solution employed here is similar to that used in previous sections and consists of the selection of suitable functions which can be made to satisfy both the boundary conditions, expressed by equations (72), and the system of partial differential equations given by equations (66 to 71).

As the Fourier coefficients are completely determined by the differential equations, the trigonometric form of the selected functions should be such as to permit satisfaction of the boundary conditions. The conflicting requirements of the boundary conditions

can be stated as:

(a) The function should be zero at certain arbitrary points.

(b) The trigonometric functions should form a complete set, i.e. any function within the limitations set out above, should be describable by the series.

Such requirements are perhaps most easily met by defining the functions, $f(x)$, in the Fourier half interval $(0, \pi)$. To expand such a function all that need be done is to prolong it into the other half-interval $(-\pi, 0)$ and expand this function - now defined in the full Fourier interval $(-\pi, \pi)$ - by the usual Fourier series techniques. This is possible, as no matter how the function is extended into the interval $(-\pi, 0)$ it will still represent the desired function in $(0, \pi)$ as well as in $(2\pi, 3\pi)$, $(4\pi, 5\pi)$, etc. There are two accepted methods of prolonging the function into the half interval $(-\pi, 0)$, i.e. either as an even function or as an odd function. A function, $f(x)$, is said to be even if

$$f(-x) = f(x)$$

and odd if

$$f(-x) = -f(x)$$

An example of an even function is $\cos x$, since

$$\cos(-x) = \cos x$$

and $\sin x$ is an odd function, since

$$\sin (-x) = - \sin x$$

The expanded even-function form in the half-interval $(0, \pi)$ taken by $f(x)$ is

$$f(x) = \frac{1}{2} a_0 + \sum_{i=1}^{\infty} a_i \cos ix$$

where
$$a_i = \frac{2}{\pi} \int_0^{\pi} f(x) \cos ix \, dx \quad (i=1,2, \dots \infty)$$

and the odd function form is

$$f(x) = \sum_{i=1}^{\infty} b_i \sin ix$$

where
$$b_i = \frac{2}{\pi} \int_0^{\pi} f(x) \sin ix \, dx \quad (i=1,2, \dots \infty)$$

By applying a transformation, the following even and odd functions in the half range can be obtained from those above:

Even function

$$f(x) = \frac{1}{2} a_0 + \sum_{i=1}^{\infty} a_i \cos \frac{i\pi x}{a} \tag{137}$$

where
$$a_i = \frac{2}{a} \int_0^a f(x) \cos \frac{i\pi x}{a} \, dx \quad (i = 0,1,2, \dots \infty)$$

Odd function

$$f(x) = \sum_{i=1}^{\infty} b_i \sin \frac{i\pi x}{a} \tag{138}$$

where
$$b_i = \frac{2}{a} \int_0^a f(x) \sin \frac{i\pi x}{a} \, dx \quad (i = 1,2, \dots \infty)$$

Each of these two functions forms a complete set in the

interval $(0, a)$. In the case of the odd function $f(x)$ is zero at $x=0$ and $x=a$ in the interval $(0, a)$. The odd function satisfies the opposing requirements of the possible boundary conditions in that $f(x)$ is expected to be expandable and yet be zero on the boundaries $x=0$ and $x=a$.

The boundary value problem under consideration makes it necessary to be able to expand functions of two variables into half-range Fourier series with a half-range of $(0, a)$ in the x -direction and of $(0, b)$ in the y -direction. The form of the Fourier series terms is dependent upon whether the need is for an even or odd function in the x or y directions. For example, if a function, $f(x, y)$, is required to be odd in the x -direction and even in the y -direction, then the double half-range series will take the form

$$f(x, y) = \sum_{i=1}^{\infty} \sum_{j=0}^{\infty} f(x, y)_{ij} \sin \frac{i\pi x}{a} \cos \frac{j\pi y}{b} \quad (139)$$

The remaining three possible trigonometric terms are as follows:

$$\sin \frac{i\pi x}{a} \sin \frac{j\pi y}{b}, \cos \frac{i\pi x}{a} \cos \frac{j\pi y}{b}, \cos \frac{i\pi x}{a} \sin \frac{j\pi y}{b} \quad (140)$$

Restating the boundary conditions of the present analysis:

$$M_x = V_x = H = 0 \text{ at } x = 0 \text{ and } x = a \quad (141)$$

$$M_y = V_y = H = 0 \text{ at } y = 0 \text{ and } y = b$$

then the form taken by the stress resultants and deflection expansions are as follows:

$$M_x = \sum_{i=1}^{\infty} \sum_{j=0}^{\infty} M_{x_{ij}} \sin \frac{i\pi x}{a} \cos \frac{j\pi y}{b} \quad (142)$$

$$M_y = \sum_{i=0}^{\infty} \sum_{j=1}^{\infty} M_{y_{ij}} \cos \frac{i\pi x}{a} \sin \frac{j\pi y}{b} \quad (143)$$

$$V_x = \sum_{i=1}^{\infty} \sum_{j=0}^{\infty} V_{x_{ij}} \sin \frac{i\pi x}{a} \cos \frac{j\pi y}{b} \quad (144)$$

$$V_y = \sum_{i=0}^{\infty} \sum_{j=1}^{\infty} V_{y_{ij}} \cos \frac{i\pi x}{a} \sin \frac{j\pi y}{b} \quad (145)$$

$$H = \sum_{i=1}^{\infty} \sum_{j=1}^{\infty} H_{ij} \sin \frac{i\pi x}{a} \sin \frac{j\pi y}{b} \quad (146)$$

$$w_o = \sum_{i=0}^{\infty} \sum_{j=0}^{\infty} w_{o_{ij}} \cos \frac{i\pi x}{a} \cos \frac{j\pi y}{b} \quad (147)$$

and the loading function

$$p = \sum_{i=0}^{\infty} \sum_{j=0}^{\infty} p_{ij} \cos \frac{i\pi x}{a} \cos \frac{j\pi y}{b} \quad (148)$$

The series can now be substituted into the system of partial differential equations and, by employing the orthogonality conditions, simultaneous algebraic equations relating to Fourier coefficients can be obtained. The most immediate and interesting result from these equations is that all the bending moment Fourier coefficients are found to be zero. This indication that the solution is trivial in nature, shows that the selection of these particular trigonometric forms of the dependent variables by inspection and elimination, is unsuccessful in obtaining a real solution.

Summary

The solution of the primary boundary value problem, represented by a system of partial differential equations (66 to 71) and a number of boundary conditions i.e. equations (72), has been considered. By assuming certain general forms of the variables, it has been possible to obtain a solution in terms of a system of interrelated algebraic simultaneous equations, when such variables have been expressed in terms of power series and Chebyshev polynomials. Because of the particular form of solution employed, this has not, however, been possible in the case of Fourier series representations.

Before proceeding with the solution of the principal boundary value problem under consideration a more detailed examination must be made of the function describing the load intensity distribution. This will take the form of the development and comparison of the loading functions as represented by power, Chebyshev or Fourier series.

FUNCTIONS DESCRIBING THE APPLIED TRANSVERSE WHEEL-LOAD

The solution to the system of the partial differential equations (66 to 71) is based upon the availability of suitable functions which describe the applied normal load. These loading functions, in terms of power, Chebyshev and Fourier series, are each now developed and compared.

In order that such functions may be obtained it is inevitable that, to some degree, the load intensity distribution must be initially specified. As the stress analysis of a highway pavement under applied wheel-loads is of prime interest, then, idealizing the contact area of a single wheel to that of a circle, the load intensity distribution, p , considered may be taken as that of a unit load spread uniformly over a circle of radius c and centre (x_0, y_0) , as shown in Figure 8. There is no applied load over the remainder of the area of definition of the function, which is taken as that area covered by the rectangular slab $(0 \leq x \leq a, 0 \leq y \leq b)$. Such a loading function can be used, by the method of superposition, to describe any combination of such wheel-loads, e.g. dual and/or tandem wheels.

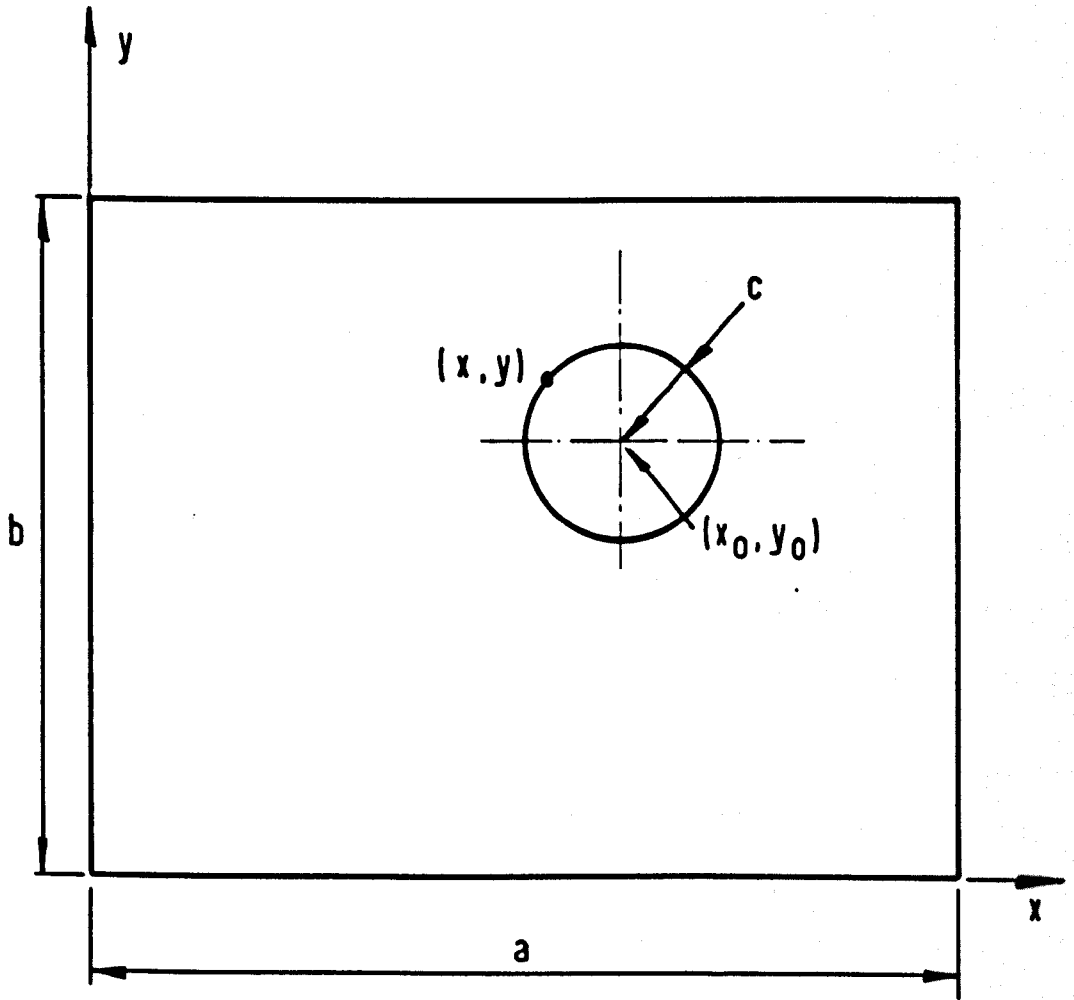
Methods of obtaining the loading functions of other wheel contact shapes are mentioned during the following development of the loading functions for the circular contact area.

The idealized load intensity distribution is represented by the loading functions which is applied to the surface of a plate. This distribution consists of a unit load spread uniformly over a circle of radius c , with centre (x_0, y_0) ; no load is applied to the remainder of the plate surface.

Figure 8. The idealized load intensity distribution represented by the loading functions which is applied to the surface of a plate. This distribution consists of a unit load spread uniformly over a circle of radius c , with centre (x_0, y_0) ; no load is applied to the remainder of the plate surface.

The idealized load intensity distribution is represented by the loading functions which is applied to the surface of a plate. This distribution consists of a unit load spread uniformly over a circle of radius c , with centre (x_0, y_0) ; no load is applied to the remainder of the plate surface.

The idealized load intensity distribution is represented by the loading functions which is applied to the surface of a plate. This distribution consists of a unit load spread uniformly over a circle of radius c , with centre (x_0, y_0) ; no load is applied to the remainder of the plate surface.



Development of the Loading Functions

Power series representation

There are, basically two types of load intensity distributions:

1. Those which are expressed exactly by a polynomial,

e.g.

$$p = \underline{a} + \underline{b}x + \underline{c}y \quad (149)$$

where a, b and c are constants.

- 2, Distributions which do not have an exact polynomial representation, e.g. one which contains a discontinuity.

The first type needs no further development here, as the load intensity distribution is explicitly represented by a truncated power series.

In order that, in the second case, a polynomial expansion can be used to approximate to the load intensity distribution, a criterion must first be decided upon which uses the degree of error between the approximating and actual load intensity to arrive at the 'best' approximation. The criterion, 'that the square of the error over the region of definition should be a minimum,' is employed in this case because, in comparison with other possible criteria, the series coefficients are simple to determine from the known values of the load intensity at points over

the region of definition.

Let it be assumed that $p(x,y)$ represents the loading function and let $x_d, y_d, (d = 1,2, \dots, N)$ be the sequence of data points at which the values of the load intensity, p_d , are known. If $x_d^i y_d^j, (i = 0,1,2, \dots, m; j = 0,1,2, \dots, n)$ are a sequence of powers defined for every x_d, y_d , then p_d can be approximated by a linear combination of $x_d^i y_d^j$, thus:

$$p_d \approx \sum_{i=0}^m \sum_{j=0}^n p_{ij} x_d^i y_d^j \quad (d = 1,2, \dots, N) \quad (150)$$

with the constant coefficients p_{ij} determined so that

$$L(p_{00}, p_{01}, p_{10}, \dots, p_{mn}) = \sum_{d=1}^N \left[p_d - \sum_{i=0}^m \sum_{j=0}^n p_{ij} x_d^i y_d^j \right]^2 - \sum_{d=1}^N R_d^2 \quad (151)$$

is minimized. This is the mathematical formulation of the above mentioned criterion. The quantity R_d , called the residual, is only zero in the case when the number of approximating functions is equal to the number of data points, i.e. $N = (m+1)(n+1)$. Normally, the number of approximating functions is much less than the number of data points, in which case the usual intention is to make the function as accurate as possible by making the square of the residual a minimum. The coefficients, p_{ij} , for such a minimum are calculated by taking the partial derivative of L with respect to p_{fk}

and setting it equal to zero, thereby making L a minimum with respect to the unknown coefficients:

$$\frac{\partial L}{\partial p_{fk}} = -2 \sum_{d=1}^N \left[p_d - \sum_{i=0}^m \sum_{j=0}^n p_{ij} x_d^i y_d^j \right] x_d^f y_d^k = 0 \quad (152)$$

where $f = 0, 1, 2, \dots, m$; $k = 0, 1, 2, \dots, n$.

Interchanging summations results in:

$$\sum_{i=0}^m \sum_{j=0}^n p_{ij} \left[\sum_{d=1}^N x_d^{i+f} y_d^{j+k} \right] = \sum_{d=1}^N p_d x_d^f y_d^k \quad (153)$$

where $f = 0, 1, 2, \dots, m$; $k = 0, 1, 2, \dots, n$.

Equation (153) is a system of $(m+1)(n+1)$ linear equations which are generally called the normal equations for the $(m+1)(n+1)$ unknown p_{ij} coefficients.

In the case of a unit load distributed over the area of a circle of radius c , such as is illustrated in Figure (8), whether or not the load intensity p_d at an arbitrarily chosen data point (x_d, y_d) is $1/\pi c^2$ depends on whether or not that point lies on or within the circle. The mathematical expression of this criterion is

$$\text{if } (x_d - x_0)^2 + (y_d - y_0)^2 - c^2 \leq 0 \quad (154)$$

then $p_d = 1/\pi c^2$, otherwise the load intensity is zero. Thus, a system of N data points is obtained which may be used in equations (153) to solve for the power series coefficients, p_{ij} .

may be considered as an approximation to $p(\eta, \xi)$. The error, \underline{E} , of this approximation is given by the infinite series

$$\underline{E} = \sum_{i=m}^{\infty} \sum_{j=0}^{n-1} p_{ij} T_i^*(\eta) T_j^*(\xi) + \sum_{i=0}^{\infty} \sum_{j=n}^{\infty} p_{ij} T_i^*(\eta) T_j^*(\xi) \quad (158)$$

If the convergence of the series is sufficiently rapid, an acceptable estimate of the error can be arrived at by keeping only the first terms:

$$\underline{E} = \frac{p_{m0}}{2} T_m^*(\eta) T_0^*(\xi) + \frac{p_{0n}}{2} T_0^*(\eta) T_n^*(\xi) \quad (159)$$

This indicates that the error is of an oscillatory nature since shifted Chebyshev polynomials are themselves oscillatory. If the estimate is sufficiently close, then the problem of obtaining the coefficient p_{ij} of the expansion given by equation (157) is now transformed into an interpolation problem. The vanishing of \underline{E} at the zeros of $T_m^*(\eta)$ and $T_n^*(\xi)$ can be interpreted as the loading function $p(\eta, \xi)$ and the approximation $p_{mn}(\eta, \xi)$ coinciding at the zeros of $T_m^*(\eta)$ and $T_n^*(\xi)$. Thus, the problem of producing a strongly convergent expansion of $p(\eta, \xi)$ in the polynomials $T_i^*(\eta) T_j^*(\xi)$ is, in practice, equivalent to $p(\eta, \xi)$ being interpolated by a polynomial of $(m-1)(n-1)$ st degree, the tabular points being chosen at the zeros of the first neglected polynomial, $T_m^*(\eta) T_n^*(\xi)$, i.e. the points (η_α, ξ_β) at which $T_m^*(\eta)$ and $T_n^*(\xi)$ are both zero.

Translating the algebraic conditions

$$T_m^*(\eta_\alpha) = 0 \text{ and } T_n^*(\xi_\beta) = 0 \quad (160)$$

where (η_α, ξ_β) are the zero tabular points, to the angular variables θ_α and ϕ_β by using equation (104), gives

$$\cos m\theta_\alpha = 0 \text{ and } \cos n\phi_\beta = 0 \text{ respectively,} \quad (161)$$

These then become

$$m\theta_\alpha = [\alpha + \frac{1}{2}]\pi \text{ and } n\phi_\beta = [\beta + \frac{1}{2}]\pi \quad (162)$$

where there are m and n zero points, respectively and

$$\alpha = 0, 1, 2, \dots, m-1, \beta = 0, 1, 2, \dots, n-1.$$

As $\cos \theta_\alpha = 2\eta_\alpha - 1$ and $\cos \phi_\beta = 2\xi_\beta - 1$, then

$$\eta_\alpha = \cos^2 \frac{\pi}{4m} (2\alpha + 1) + \frac{1}{2} \text{ and } \xi_\beta = \cos^2 \frac{\pi}{4n} (2\beta + 1) + \frac{1}{2} \quad (163)$$

The expressions for the data points (η_α, ξ_β) can thus be seen to be non-uniformly spread over the interval $(0 \leq \eta \leq 1, 0 \leq \xi \leq 1)$, and to be more highly concentrated at the end points of that interval.

Consider again the approximation of $p(\eta, \xi)$ to a finite number of terms. In order to determine the series coefficients, equation (157) is first multiplied throughout by $T_s^*(\eta) T_t^*(\xi_\beta)$ and the operator $\sum_{\alpha=0}^{m-1} \sum_{\beta=0}^{n-1}$ applied. Then

$$\begin{aligned} & \sum_{\alpha=0}^{m-1} \sum_{\beta=0}^{n-1} p_{mn}(\eta_\alpha, \xi_\beta) T_s^*(\eta_\alpha) T_t^*(\xi_\beta) \\ &= \sum_{i=0}^{m-1} \sum_{j=0}^{n-1} p_{ij} \left[\sum_{\alpha=0}^{m-1} T_i^*(\eta_\alpha) T_s^*(\eta_\alpha) \right] \left[\sum_{\beta=0}^{n-1} T_j^*(\xi_\beta) T_t^*(\xi_\beta) \right] \end{aligned}$$

This enables the orthogonality condition, equation (107), for a discrete set of points, to be applied, thus:

$$\sum_{\alpha=0}^{m-1} \sum_{\beta=0}^{n-1} P_{mn}(\eta_{\alpha}, \xi_{\beta}) T_s^*(\eta_{\alpha}) T_t^*(\xi_{\beta}) = \sum_{i=0}^{m-1} \sum_{j=0}^{n-1} P_{ij} \delta_{is} \cdot \frac{m}{2} \cdot \delta_{jt} \cdot \frac{n}{2}$$

where δ_{is} is the Kronecker delta defined as

$$\delta_{is} = 0 \quad \text{if } i \neq s$$

$$\text{and } \delta_{is} = 1 \quad \text{if } i = s$$

and δ_{jt} is the Kronecker delta defined as (164)

$$\delta_{jt} = 0 \quad \text{if } j \neq t$$

$$\delta_{jt} = 1 \quad \text{if } j = t$$

Consider the term $i = s, j = t$

$$P_{st} = \frac{4}{mn} \sum_{\alpha=0}^{m-1} \sum_{\beta=0}^{n-1} P_{mn}(\eta_{\alpha}, \xi_{\beta}) T_s^*(\eta_{\alpha}) T_t^*(\xi_{\beta})$$

Replacing $P_{mn}(\eta, \xi)$ by $p(\eta, \xi)$, since $P_{mn}(\eta, \xi)$ is intended to be an approximation to $p(\eta, \xi)$, and replacing s by i and t by j for convenience, results in

$$P_{ij} = \frac{4}{mn} \sum_{\alpha=0}^{m-1} \sum_{\beta=0}^{n-1} p(\eta_{\alpha}, \xi_{\beta}) T_i^*(\eta_{\alpha}) T_j^*(\xi_{\beta}) \quad (165)$$

where $i = 0, 1, 2 \dots m-1$; $j = 0, 1, 2 \dots n-1$

Thus the coefficients can be determined knowing the value of the load intensity distribution $p(\eta, \xi)$ at each tabular point $(\eta_{\alpha}, \xi_{\beta})$.

$$\int_0^a \int_0^b \dots = \int_0^1 \int_0^1 \dots$$

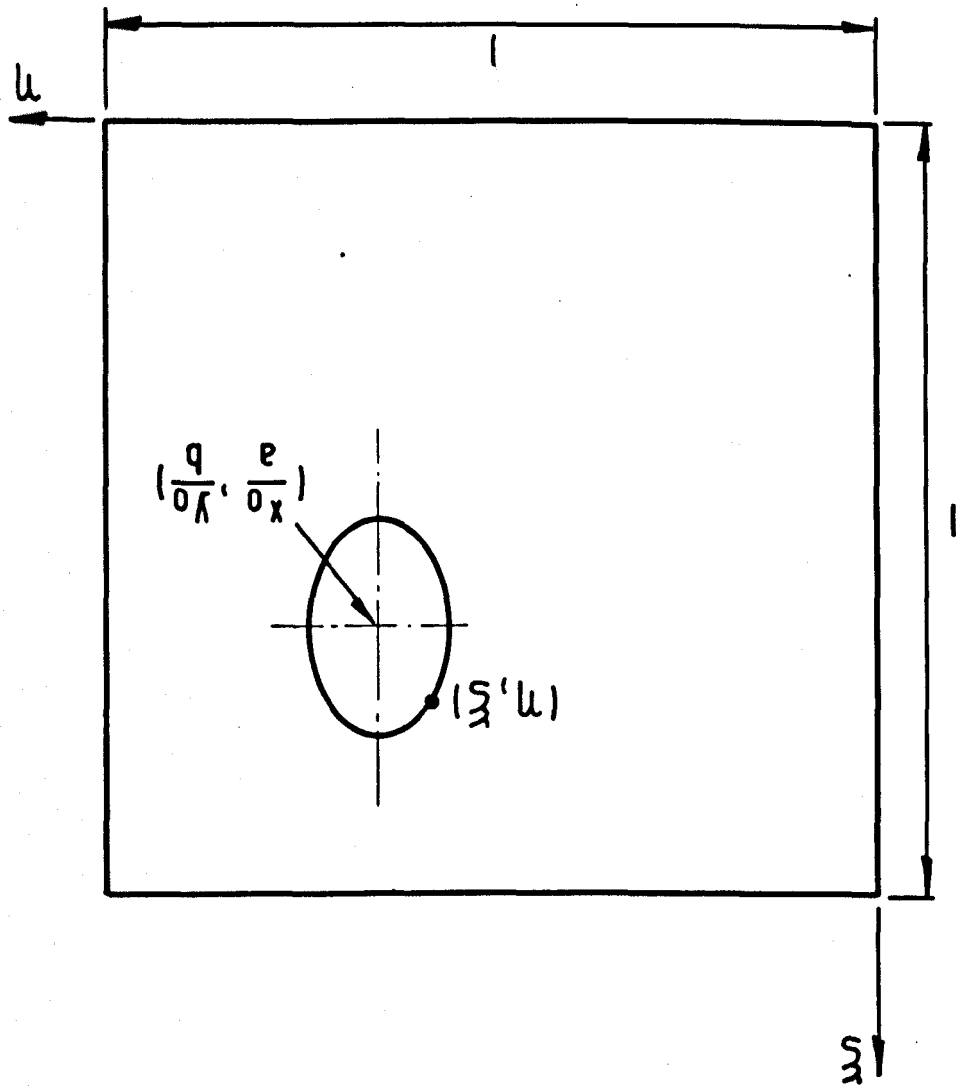
Figure 9. The form of the representation given in Figure 8 re-expressed in terms of a dimensionless co-ordinate system (η, ξ) for use in the shifted Chebyshev polynomial representation of the idealized wheel-load. The circular area over which the unit load is applied is transformed into an equivalent elliptical area, and the plate area $(0 \leq x \leq a, 0 \leq y \leq b)$ is transformed into an equivalent square $(0 \leq \eta \leq 1, 0 \leq \xi \leq 1)$.

$$\int_0^a \int_0^b \dots = \int_0^1 \int_0^1 \dots$$

...

...

...



For the case of a unit load spread uniformly over the area of a circle of radius c (Figure 8), the transforms $\eta = x/a, \xi = y/b$ enable the criterion given by equations (154) to be expressed in terms of a dimensionless co-ordinate system, where as is shown in Figure 9 the circle is transformed into an equivalent ellipse. The criterion for a point lying within or on the circle then becomes

$$(a\eta_{\alpha} - x_0)^2 + (b\xi_{\beta} - y_0)^2 - c^2 \leq 0 \quad (166)$$

Again, as in the power series representation, other contact shapes can be considered by using the appropriate criterion.

Thus the first step in obtaining the loading function is to derive the co-ordinates $(\eta_{\alpha}, \xi_{\beta})$ of the tabular points from equation (163) and the value of the load intensity at each of these points from equation (166). These figures may then be substituted into equation (165) and the coefficients of the series obtained. Thus, the shifted Chebyshev polynomial series which approximately represents the load intensity distribution is finally determined.

Fourier series representation

Referring to Figure 8, it can be seen that the load intensity distribution, $p(x,y)$, is considered to be a unit load uniformly distributed over the area of a circle of radius, c , and with centre (x_0, y_0) . The function, $p(x,y)$ is defined at every point within the rectangular region $(0 \leq x \leq a, 0 \leq y \leq b)$ thus, determining the half-range Fourier intervals $(0-a, 0-b)$.

The loading function may be expanded in terms of a half-range Fourier series in two dimensions, thus:

$$p(x,y) = \sum_{i=0}^{\infty} \sum_{j=0}^{\infty} p_{ij} \cos \frac{i\pi x}{a} \cos \frac{j\pi y}{b} \quad (167)$$

First the relevant orthogonality condition is noted for the x-dimension :

$$\int_0^a \cos \frac{\bar{\alpha}\pi x}{a} \cos \frac{i\pi x}{a} dx = \frac{a}{2} \cdot \delta_{\bar{\alpha}i} \quad (168)$$

where $\delta_{\bar{\alpha}i}$ is the Kronecker delta defined as

$$\delta_{\bar{\alpha}i} = \begin{cases} 0 & \text{if } \bar{\alpha} \neq i \\ 1 & \text{if } \bar{\alpha} = i \end{cases}$$

These conditions are valid for all non-negative integral values of $\bar{\alpha}$ and i which are not both zero. For the condition where $\bar{\alpha} = i = 0$, then

$$\int_0^a \cos 0x \cos 0x dx = a \quad (169)$$

Similar conditions apply to the y-dimension.

Now, returning to the Fourier series expansion, as given by equation (167) and multiplying through by $\cos \frac{\bar{\alpha}\pi x}{a} \cos \frac{\beta\pi y}{b}$, then integrating over the region 0 to a and 0 to b, and applying the orthogonality conditions, results in

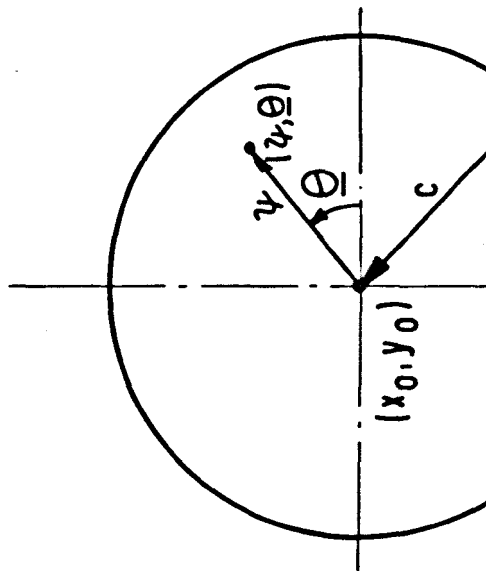
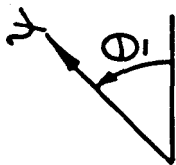
(10)

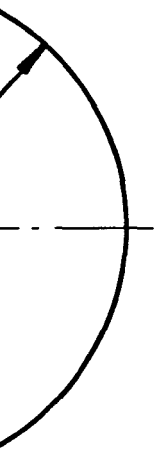


Figure 10. The polar co-ordinate system which is introduced to facilitate the representation of the load intensity distribution by Fourier series. The origin of this polar co-ordinate system (ϕ, θ) lies at the centre of the idealized circular wheel-load with original Cartesian co-ordinates of (x_0, y_0) and a radius c .

(11)

1000





$$p_{ij} = \frac{4}{ab} \int_0^a \int_0^b p(x,y) \cos \frac{i\pi x}{a} \cos \frac{j\pi y}{b} dx dy \quad (170)$$

where $i = 1, 2, 3, \dots, \infty$; $j = 1, 2, 3, \dots, \infty$

Multiplying the expansion given in equations (167) by

$\cos \frac{i\pi x}{a} \cos 0y$, integrating and applying the above conditions gives

$$p_{i0} = \frac{2}{ab} \int_0^a \int_0^b p(x,y) \cos \frac{i\pi x}{a} dx dy \quad (171)$$

where $i = 1, 2, 3, \dots, \infty$

In a similar manner

$$p_{0j} = \frac{2}{ab} \int_0^a \int_0^b p(x,y) \cos \frac{j\pi y}{b} dx dy \quad (172)$$

where $j = 1, 2, 3, \dots, \infty$

By multiplying the expansion by $\cos 0x \cos 0y$ and integrating, the following is obtained:

$$p_{00} = \frac{1}{ab} \int_0^a \int_0^b p(x,y) dx dy \quad (173)$$

Introducing the polar co-ordinates (ϕ, θ) defined in Figure 10 in place of the Cartesian co-ordinates and noting that $p(x,y)$ is zero at every point outside the circle of radius c , then the new form of equation (170) is

$$p_{ij} = \frac{4}{ab} \cdot \frac{1}{\pi c^2} \int_0^c \int_0^{2\pi} \cos \frac{i\pi(x_0 + \phi \cos \theta)}{a} \cos \frac{j\pi(y_0 + \phi \sin \theta)}{b} \phi d\phi d\theta$$

Let $\frac{j\pi x_0}{a} = \alpha_i$, $\frac{j\pi\phi}{a} = \beta_i$,

$\frac{j\pi y_0}{b} = \alpha_j$, and $\frac{j\pi\phi}{b} = \beta_j$

then $p_{ij} = \frac{4}{ab} \cdot \frac{1}{\pi c^2} \int_0^c \int_0^{2\pi} \cos(\alpha_i + \beta_i \cos\theta) \cos(\alpha_j + \beta_j \sin\theta) \phi \, d\phi \, d\theta$

Expanding and then multiplying the trigonometric terms results in

$$p_{ij} = \frac{4}{ab} \cdot \frac{1}{\pi c^2} \left[\cos \alpha_i \cos \alpha_j \int_0^c \int_0^{2\pi} \cos(\beta_i \cos\theta) \cos(\beta_j \sin\theta) \phi \, d\phi \, d\theta \right. \\ - \cos \alpha_i \sin \alpha_j \int_0^c \int_0^{2\pi} \cos(\beta_i \cos\theta) \sin(\beta_j \sin\theta) \phi \, d\phi \, d\theta \\ - \sin \alpha_i \cos \alpha_j \int_0^c \int_0^{2\pi} \sin(\beta_i \cos\theta) \cos(\beta_j \sin\theta) \phi \, d\phi \, d\theta \\ \left. + \sin \alpha_i \sin \alpha_j \int_0^c \int_0^{2\pi} \sin(\beta_i \cos\theta) \sin(\beta_j \sin\theta) \phi \, d\phi \, d\theta \right]$$

Now, considering

$$f(\theta) = \cos(\beta_i \cos\theta) \cos(\beta_j \sin\theta)$$

it can be seen that $f(\theta)$ is periodic with π . Moreover,

$$\cos(\beta_i \cos(\pi - z_p)) \cos(\beta_j \sin(\pi - z_p))$$

$$= \cos(\beta_i \cos(\pi + z_p)) \cos(\beta_j \sin(\pi + z_p))$$

for any value of z_p . Thus

$$\int_0^{\pi/2} f(\underline{\theta}) d\underline{\theta} = \int_{\pi}^{3\pi/2} f(\underline{\theta}) d\underline{\theta} \text{ by periodicity,}$$

$$\int_{\pi/2}^{\pi} f(\underline{\theta}) d\underline{\theta} = \int_{3\pi/2}^{2\pi} f(\underline{\theta}) d\underline{\theta} \text{ by periodicity,}$$

and $\int_{\pi/2}^{\pi} f(\underline{\theta}) d\underline{\theta} = \int_{\pi}^{3\pi/2} f(\underline{\theta}) d\underline{\theta}$ by the above cosine relationship

Therefore $\int_0^{2\pi} f(\underline{\theta}) d\underline{\theta} = 4 \int_0^{\pi/2} f(\underline{\theta}) d\underline{\theta}$

Similar considerations result in

$$\int_0^{2\pi} g(\underline{\theta}) d\underline{\theta} = 0 \text{ where } g(\underline{\theta}) = \cos(\beta_i \cos \underline{\theta}) \sin(\beta_j \sin \underline{\theta})$$

$$\int_0^{2\pi} h(\underline{\theta}) d\underline{\theta} = 0 \text{ when } h(\underline{\theta}) = \sin(\beta_i \cos \underline{\theta}) \cos(\beta_j \sin \underline{\theta})$$

$$\int_0^{2\pi} k(\underline{\theta}) d\underline{\theta} = 0 \text{ where } k(\underline{\theta}) = \sin(\beta_i \cos \underline{\theta}) \sin(\beta_i \sin \underline{\theta})$$

Therefore, applying these relationships to the previous expression for p_{ij} gives

- 140 -

$$P_{ij} = \frac{4}{ab} \cdot \frac{1}{\pi c^2} \cdot \cos \alpha_i \cos \alpha_j \int_0^c \int_0^{2\pi} \cos(\beta_i \cos \theta) \cos(\beta_j \sin \theta) \phi \, d\phi \, d\theta$$

$$= \frac{16}{ab\pi c^2} \cdot \cos \alpha_i \cos \alpha_j \int_0^c \phi \, d\phi \int_0^{\pi/2} \cos(\beta_j \sin \theta) \cosh(\sqrt{-1} \beta_i \cos \theta) \, d\theta$$

With the aid of the following relationship, which is taken from a standard table of integrals (57)

$$\int_0^{\pi/2} \cos(\beta_j \sin \theta) \cosh(\sqrt{-1} \beta_i \cos \theta) \, d\theta = \frac{\pi}{2} \cdot J_0[(\beta_j^2 + \beta_i^2)^{1/2}]$$

(where J_0 is the Bessel function of order zero), then

$$P_{ij} = \frac{16}{ab\pi c^2} \cdot \cos \alpha_i \cos \alpha_j \int_0^c \phi \cdot \frac{\pi}{2} \cdot J_0\left[\left(\frac{i^2}{a^2} + \frac{j^2}{b^2}\right)^{1/2} \cdot \pi\phi\right] \, d\phi$$

$$= \frac{8}{abc^2} \cdot \cos \alpha_i \cos \alpha_j \int_0^c \frac{\pi\phi \left(\frac{i^2}{a^2} + \frac{j^2}{b^2}\right)^{1/2} \cdot J_0\left[\left(\frac{i^2}{a^2} + \frac{j^2}{b^2}\right)^{1/2} \cdot \pi\phi\right] \, d\left[\left(\frac{i^2}{a^2} + \frac{j^2}{b^2}\right)^{1/2} \cdot \pi\phi\right]}{\left[\pi \left(\frac{i^2}{a^2} + \frac{j^2}{b^2}\right)^{1/2}\right]^2}$$

Using an integral quoted by Watson (58), p.132

$$P_{ij} = \frac{8}{abc^2} \cos \alpha_i \cos \alpha_j, \frac{1}{\gamma_{ij}^2} [\phi \gamma_{ij} J_1(\gamma_{ij} \phi)]_0^c$$

where $\gamma_{ij} = \pi \left(\frac{i^2}{a^2} + \frac{j^2}{b^2}\right)^{1/2}$ and $J_1(\gamma_{ij} \phi)$ is the Bessel function of order one with argument $\gamma_{ij} \phi$

Hence
$$P_{ij} = \frac{8}{abc \gamma_{ij}} \cos \frac{i\pi x_0}{a} \cos \frac{j\pi y_0}{b} \cdot J_1(\gamma_{ij} c) \quad (174)$$

where $i = 1, 2, 3, \dots, \infty$; $j = 1, 2, 3, \dots, \infty$

By the same approach, the following are obtained

$$p_{i,0} = \frac{4}{bc\pi i} \cos \frac{i\pi x_0}{a} \cdot J_1 \left(\frac{\pi c i}{a} \right) \quad (175)$$

where $i = 1, 2, 3, \dots \infty$

$$\text{and } p_{0,j} = \frac{4}{ac\pi j} \cos \frac{j\pi y_0}{b} \cdot J_1 \left(\frac{\pi c j}{b} \right) \quad (176)$$

where $j = 1, 2, 3, \dots \infty$

In the case of p_{00}

$$p_{00} = \frac{1}{ab} \int_0^a \int_0^b p(x,y) dx dy = \frac{1}{ab} \cdot \frac{1}{\pi c^2} \int_0^c \int_0^{2\pi} \psi d\psi d\theta$$

Integrating, the above becomes

$$p_{00} = \frac{1}{ab} \quad (177)$$

When the load intensity is represented by only a limited number of terms, $i = 0, 1, 2, \dots m$; $j = 0, 1, 2, \dots n$, then the complete expansion takes the form

$$p(x,y) = \sum_{i=0}^m \sum_{j=0}^n p_{ij} \cos \frac{i\pi x}{a} \cos \frac{j\pi y}{b} \quad (178)$$

$$\text{where } p_{ij} = \frac{8}{abc\gamma_{ij}} \cos \frac{i\pi x_0}{a} \cos \frac{j\pi y_0}{b} \cdot J_1(\gamma_{ij}c) \quad (174)$$

for $i = 1, 2, 3, \dots m$; $j = 1, 2, 3, \dots n$

$$p_{i0} = \frac{4}{bc\pi i} \cos \frac{i\pi x_0}{a} \cdot J_1 \left(\frac{\pi c i}{a} \right) \quad (175)$$

for $i = 1, 2, 3, \dots m$

$$p_{0j} = \frac{4}{\pi c \pi j} \cos \frac{j \pi y_0}{b} \cdot J_1 \left(\frac{\pi c j}{b} \right) \quad (176)$$

for $j = 1, 2, 3, \dots, n$

and, finally,

$$p_{00} = \frac{1}{ab} \quad (177)$$

(It may be noted that a similar analysis which uses odd trigonometric terms has been developed by Woinowsky - Krieger (59), who with Timoshenko (15) also considered rectangular loading areas.)

Numerical Computation of the Loading Functions

Because of the extremely large amount of computation involved in obtaining the loading function, the use of an electronic digital computer is obviously essential for this study.

The programs which are developed are described below by means of flow diagrams and copies of the actual programs are given in Appendix B. In explaining the details of the programs use is made of the symbol comment n where n is any integer. Thus, in the text which follows, the symbol comment 5 accompanies the description of the block which follows a similar label in the program itself.

Before considering the programs associated with each of the three forms of loading function, a brief account is given of the computer installation available at the University of Leeds.

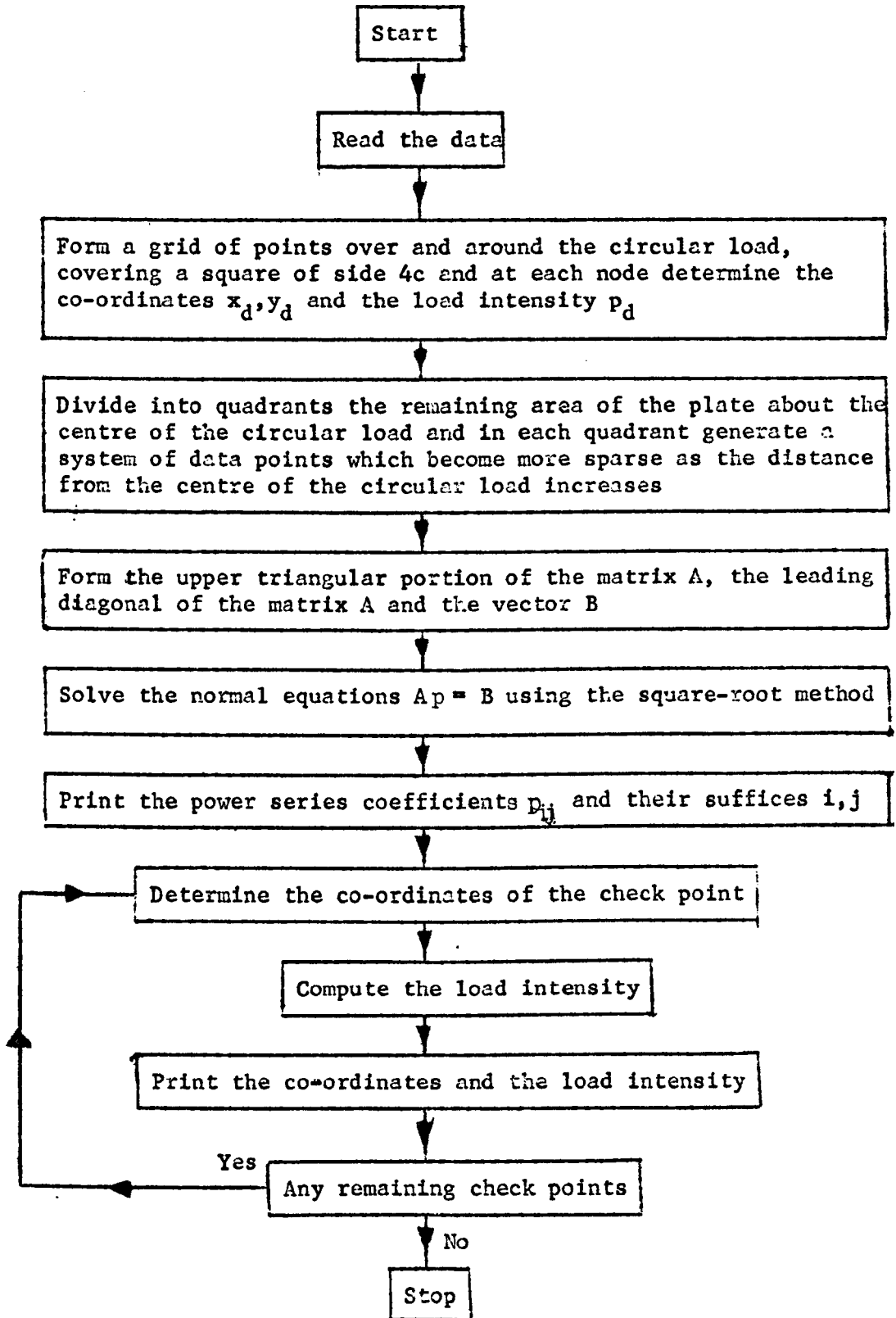
The KDF-9 computer

The facility for computation which is available at the Leeds University Computing Laboratory is based upon a medium-sized digital computer, i.e. the English Electric Leo-Marconi KDF-9. One language through which instructions and information are presented to the computer is ALGOL 60(60,61) and the programs presented in this thesis are written in this language. This is convenient since programs written in ALGOL 60 can be run on many computers.

In order that a computer can execute the instructions contained in the program they must be translated from Algol into the machine language. This translation is attained with the aid of either the Whetstone or Kidsgrove compiler which are both machine programs permanently available to the computer. The Whetstone compiler is used during the development stage due to its more rapid translation speed while the Kidsgrove computer is used during the running of actual problems on account of its much faster execution speed.

A machine language version of each program is established to avoid constant retranslation when many separate execution runs are to be made.

Algol programs which are under development, and problem data for running, are presented to the computer, through a reader, in the form of punched-hole paper tape. The main store of the



computer which contains the program instructions and the space required for computation has had for most of the period of this research program a capacity of 16K(16 x 1024) words. Recently, the capacity has been increased to 32K but only the same store, approximately 16K, is still available to any one program.

Results obtained are first stored in the computer on magnetic tape and there, at a later and more convenient time, are output in the form of punched - hole paper tape or 'line printed' sheets of paper.

Limits of the truncated series

So far, the upper limits of the expansions representing the load intensity distribution have been expressed in terms of m and n . Since, however, there is no reason to emphasise either co-ordinate direction, m will be assumed equal to n for the numerical computations discussed here.

Power series program

The following explanation of the program entitled 'Wheel-Load Expressed as a Power Series' should be considered in conjunction with the flow diagram, shown in Figure 11 which illustrates the general sequence of operations.

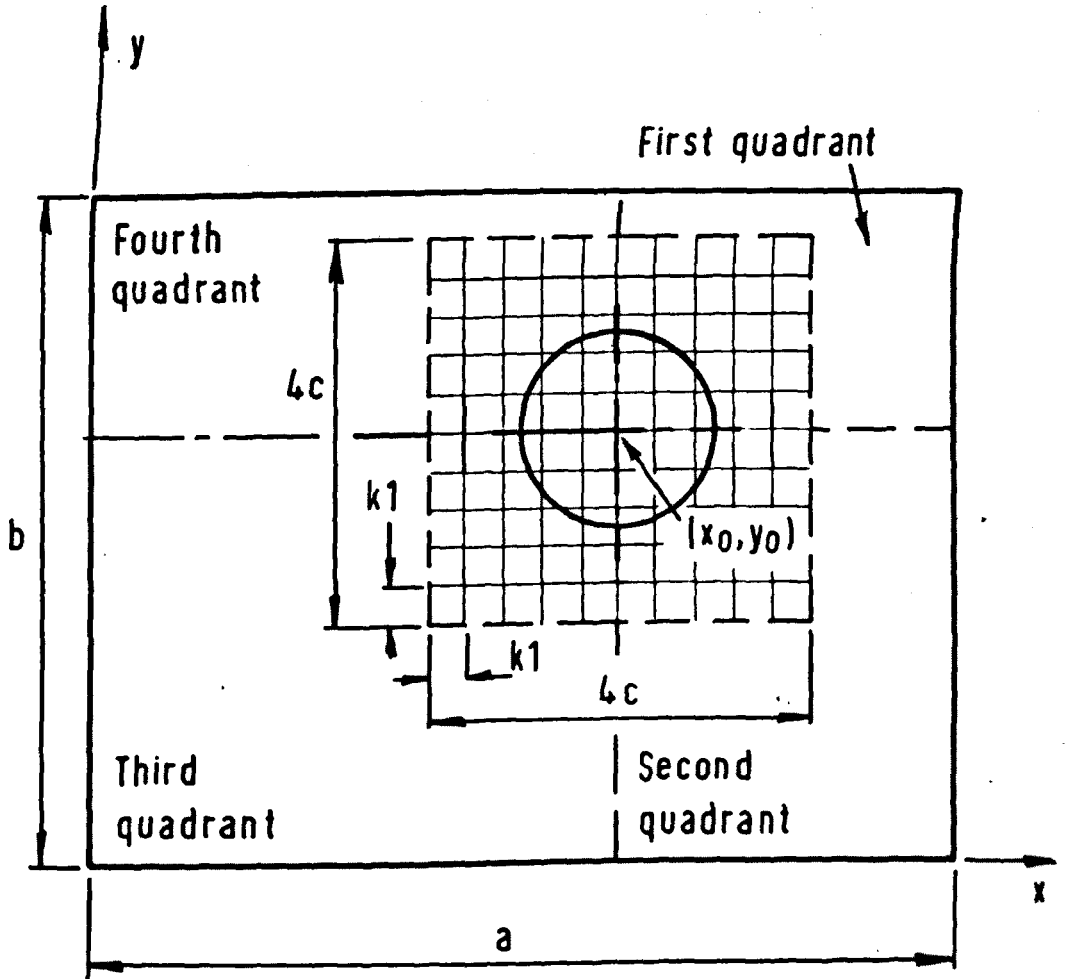
The computation starts by first reading the data [comment 1 and 14]. This consists of: a title enclosed between brackets,

i.e. <TITLE>, the length of the plate in the x-direction (a), the width of the plate in the y-direction (b), the co-ordinates of the centre of the circular load (x_0, y_0), the radius of the circular load (c), the data grid elemental side length (kl), the multiplier (cl), the maximum index considered in the power expansion (n), a number chosen to exceed the number of data points likely to be created (number), the number of grid divisions in each co-ordinate direction (pp in the x-direction, qq in the y-direction), the number of extra check points which are of special interest (tt) and, finally, the co-ordinates of each of those extra check points (xx,yy). Hence the data takes the form:

```
<TITLE>
a,b,x0;y0;c;kl;cl;n;number;pp;qq;tt;
xx1;yy1;
xx2;yy2;
. .
. .
. .
. .
xxtt;yytt;
```

The preparation and storing of the N data points now begins. These consist of the co-ordinates of each data point (x_d, y_d) and the intended value of the load intensity at that point (p_d). Referring to Figure 12, the first set of data points collected are those at

Figure 12. The division of the idealized load intensity distribution of Figure 8 into (a) a uniformly spaced set of data points within a square of side $4c$ centred about x_0, y_0 , and (b) over the remainder of the plate a set of data points which become more sparse as their distance from x_0, y_0 increases. This is in order to generate data points for use in the power series representation of the idealized wheel-load.



the nodal points of a grid, (elemental side length kl), set over a square area of side $4c$ which is placed symmetrically about the centre of the circular load [comment 2]. Whether a data point value is 0 or $1/\pi c^2$ is determined from the criterion set out in equation (154).

The second set of data points to be stored are those which lie outside this grid area but are still inside the limits of the plate, This remaining area is divided into quadrants by a pair of perpendicular axes, centred at the centre of the circular load and parallel to the co-ordinate directions, see Figure 12. As these data points cannot lie on the load, they all have zero intensity. The quadrants are dealt with in clockwise order, the quadrant containing the corner $x=a, y=b$ being considered first [comment 3]. Data points are obtained by moving along the line $y=y_0$ from the outer edge of the grid area towards the edge $x=a$. The distance between each successive data point is a multiple, c_1 , of the distance between the previous two data points, the first distance between successive data points, being $kl.c_1$. This procedure for selecting data points is stopped at the last possible data point within the plate and finally one extra data point is placed on the edge, $x=a$, of the plate. This technique is repeated to cover the area of the quadrant with the spacing in the y -direction between successive lines of the data points, parallel to the

x-direction, being governed by the multiplier c_1 . The remaining three quadrants are handled in a similar manner and, finally, N data points are obtained [comment 4,5, and 6].

The multiplier c_1 is chosen to be greater than unity so that as the distance increases away from the centre of the load, data points become more sparse. This is necessary because the computer size limits the number of possible data points and hence, since the area around the load is of major interest, the data points are concentrated there.

Having generated the system of N data points, the normal equations can now be set-up and solved. The normal equations,

$$\sum_{i=0}^n \sum_{j=0}^n p_{ij} \left[\sum_{d=1}^N x_d^{i+f} y_d^{j+k} \right] = \sum_{d=1}^N p_d x_d^f y_d^k \quad (153)$$

where $f = 0,1,2, \dots, n$; $k = 0,1,2, \dots, n$,

are e in number, where $e = (n+1)(n+1)$. Rewriting these equations in matrix form

$$A p = B \quad (179)$$

where A is the matrix of elements a_{st} of value

$$a_{st} = \sum_{d=1}^N x_d^{i+f} y_d^{j+k} \quad \begin{matrix} s = 0,1,2, \dots, e \\ t = 0,1,2, \dots, e \end{matrix} \quad (180)$$

$$\text{with the row position } s: s = (n+1)f + k + 1 \quad (181)$$

$$\text{and the column position } t: t = (n+1)i + j + 1$$

The column vector of constants B is defined by

$$b_s = \sum_{d=1}^N p_d x_d^f y_d^k \quad s = 0,1,2, \dots, e \quad (182)$$

and p is the column vector of unknown power series coefficients, where the coefficients p_{ij} has a column position t.

Consider the matrix A, where

$$A = \begin{bmatrix} a_{0,0} & a_{0,1} & \cdot & \cdot & \cdot & a_{0,e} \\ a_{1,0} & a_{1,1} & \cdot & \cdot & \cdot & a_{1,e} \\ \cdot & \cdot & \cdot & \cdot & \cdot & \cdot \\ \cdot & \cdot & \cdot & \cdot & \cdot & \cdot \\ \cdot & \cdot & \cdot & \cdot & \cdot & \cdot \\ a_{e,0} & a_{e,1} & \cdot & \cdot & \cdot & a_{e,e} \end{bmatrix}$$

to be made-up of the following three parts:

1. The upper triangular portion:

$$\begin{array}{ccccccc} a_{0,1} & a_{0,2} & \cdot & \cdot & \cdot & \cdot & a_{0,e} \\ & a_{1,2} & \cdot & \cdot & \cdot & \cdot & a_{1,e} \\ & & \cdot & \cdot & \cdot & \cdot & \cdot \\ & & & \cdot & \cdot & \cdot & \cdot \\ & & & & \cdot & \cdot & \cdot \\ & & & & & \cdot & \cdot \\ & & & & & & a_{e-1,e} \end{array}$$

The computer now proceeds to solve the system of normal equations. The matrix is symmetric and is also called positive definite, as the quadratic form $p^T A p$ is positive for any real vector p , where p^T is the transpose of p . This is proved in the following manner:

$$p^T A p = \sum_{s=0}^e \sum_{t=0}^e p_s p_t a_{st} \quad (184)$$

but $a_{st} = \sum_{d=1}^N f(x,y)_s f(x,y)_t$ from equation (180)

$$\begin{aligned} \text{Therefore } p^T A p &= \sum_{s=0}^e \sum_{t=0}^e p_s p_t \sum_{d=1}^N f(x,y)_s f(x,y)_t \\ &= \sum_{d=1}^N \left[\sum_{s=0}^e p_s f(x,y)_s \right] \left[\sum_{t=0}^e p_t f(x,y)_t \right] \\ &= \sum_{d=1}^N \left[\sum_{s=0}^e p_s f(x,y)_s \right]^2 > 0 \end{aligned} \quad (185)$$

The method of solving the normal equations is based upon the square-root method (62) which is one of the most effect techniques for fully utilizing the symmetrical nature of the matrix A . Because of this symmetry, A can be expressed as the product of an upper triangular matrix G and its transpose G^T , so that $A = G^T G$. The elements of G are computed from those of A using the following recurrence formulae:

$$\begin{aligned}
 g_{11} &= (a_{11})^{1/2} \\
 g_{1t} &= a_{1t}/g_{11} \quad t = 2,3, \dots e \\
 g_{ss} &= \left[a_{ss} - \sum_{v=1}^{s-1} g_{vs}^2 \right]^{1/2} \quad s = 2,3, \dots e \\
 g_{st} &= \left[a_{st} - \sum_{v=1}^{s-1} g_{vs} g_{vt} \right] / g_{ss} \quad \begin{array}{l} s = 2,3, \dots e \\ t = 2,3, \dots e \end{array}
 \end{aligned} \tag{186}$$

except $g_{st} = 0$ where $s > t$

Each row of A is considered in turn and, therefore, in the program the computed values of g_{st} replace those of a_{st} [comment 7].

The solution is now undertaken in two stages. First of all a vector F of the same order as p and B is introduced so that $Gp = F$ and $B = G^T F$. Using the latter relationship, the elements of F are computed from

$$\begin{aligned}
 f_1 &= b_1/g_{11} \\
 f_s &= \left[b_s - \sum_{v=1}^{s-1} g_{vs} f_v \right] / g_{ss} \quad s = 2,3, \dots e
 \end{aligned} \tag{187}$$

and the computed values replace those in B [comment 8].

The second stage involves the back substitution process using the relationship $Gp = F$. The terms of p, the unknown power series coefficients, are computed from the formulae

$$p_e = f_e/g_{ee}$$

and
$$p_t = \left[f_t - \sum_{v=e}^{t+1} g_{tv} p_v \right] / g_{tt} \quad t = e-1, e-2, \dots, 1 \quad (188)$$

and then temporarily placed in B [comment 9]. They are afterwards placed in their own vector p.

The coefficients of the power series expansion of the load intensity distribution are then output on the line printer, along with their i,j suffices [comment 12].

As the qualitative check on the accuracy of the power expansion, the value of the load intensity at each of several points over the area of the plate are next computed from equation (155) and output along with the co-ordinates of these points [comment 13]. The points fall into two groups; firstly, a grid system of points distributed over the plate with pp divisions in the x-direction and qq divisions in the y-direction and, secondly, a number tt of points of particular interest with co-ordinates (xx, yy).

The final form of the output sheet is as follows:

I	J	COEFF
.	.	.
.	.	.
2	3	-1.0562 ₁₀ ⁻²
.	.	.

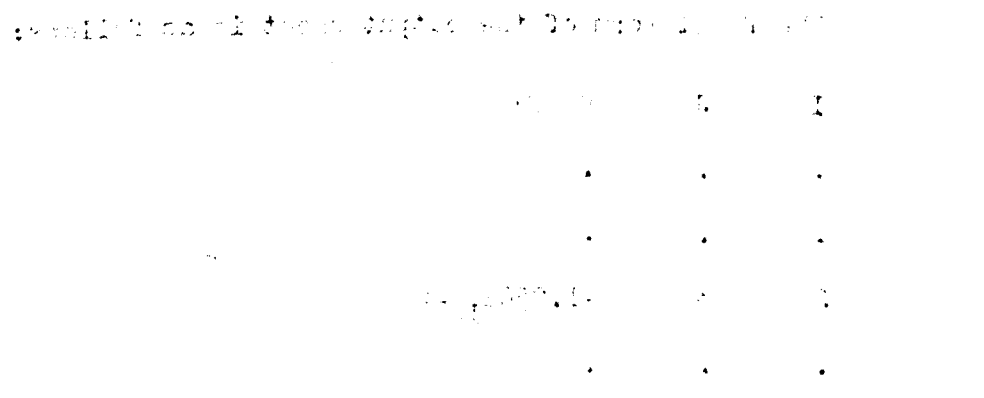
$$f(x) = \sum_{n=0}^N a_n T_n(x) \quad (13)$$

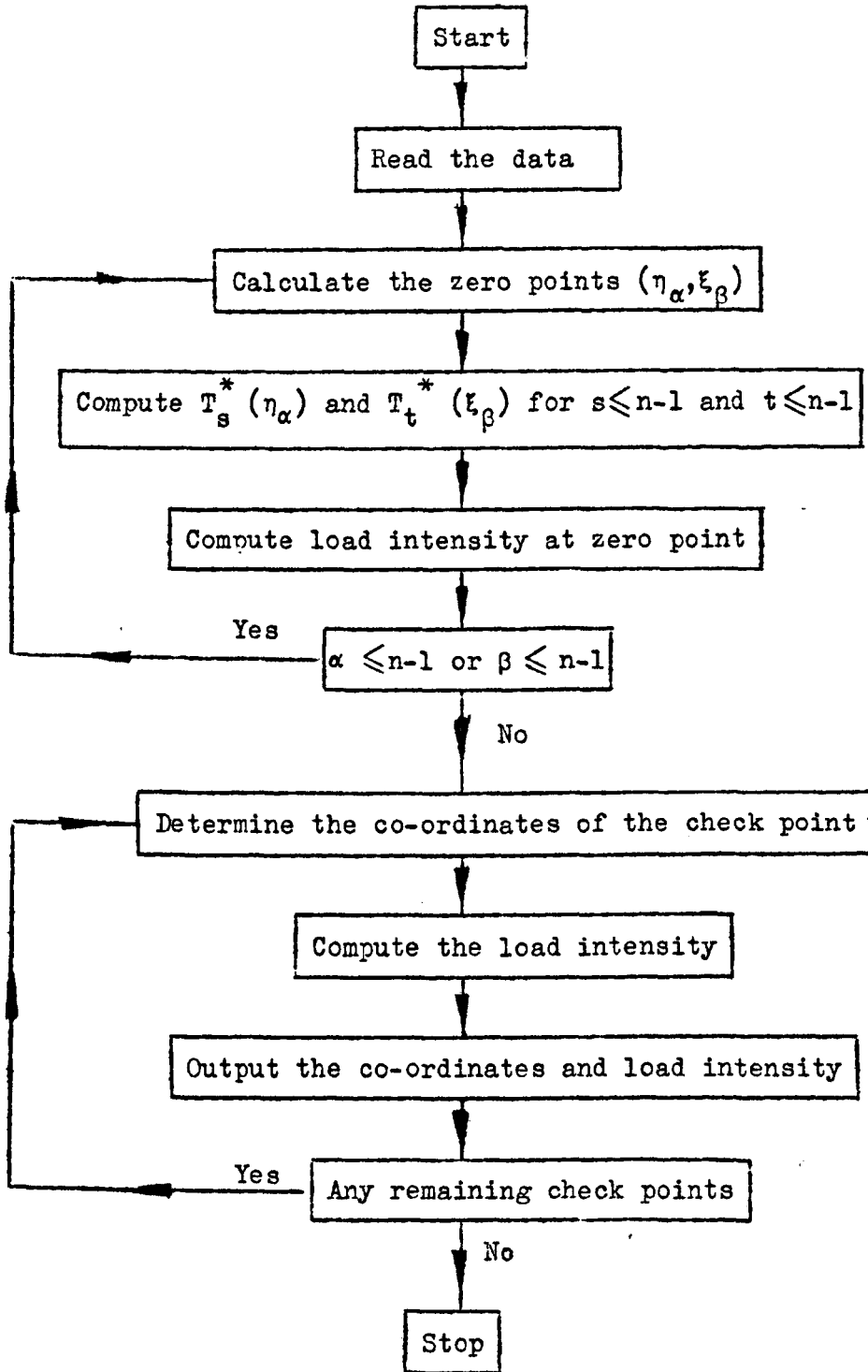
where $T_n(x)$ is the Chebyshev polynomial of the first kind of order n .

The coefficients a_n are determined by the method of least squares.

The resulting series is then used to describe the load intensity.

Figure 13. Flow diagram illustrating the major stages of computation in obtaining a shifted Chebyshev series function to describe a load intensity distribution in the form of an idealized circular wheel-load.





X	Y	LOAD
.	.	.
.	.	.
10	5	0.57103
.	.	.

Chebyshev polynomial program

The program developed to represent the load intensity distribution in terms of shifted Chebyshev polynomials and entitled 'Wheel-Load Expressed as a Chebyshev Series' is based on the flow diagram appearing in Figure 13. This diagram indicates that the computer first accepts the data, which is in the following form [comment 1 and 8]:

<TITLE>
a;b;x₀;y₀;c;n;pp;qq;tt;

xx₁;yy₁;

xx₂;yy₂;

. .

. .

xx_{tt};yy_{tt};->

(It should be noted that the symbols used above have the same connotation as before, in the power series program.)

The co-ordinates of the tabular points (η_α, ξ_β) are next computed along with values of the shifted Chebyshev arguments $T_s^*(\eta_\alpha)$ and $T_t^*(\xi_\beta)$ for each tabular point and each value of s and t [comment 3]. Equations (163) and the relationships

$$\begin{aligned} T_0^*(X) &= 1, T_1^*(X) = 2X - 1 \\ T_{i+1}^*(X) &= (4X-2) T_i^*(X) - T_{i-1}^*(X) \end{aligned} \quad (189)$$

are made use of in this connection. The first two relationships of equation (189) are obtained from considering the polynomial form of shifted Chebyshev polynomials and the latter relationship is derived from equation (106). The value of the load intensity at each of the tabular points is calculated using equation (166) [comment 4].

From equation (165) the shifted Chebyshev coefficients can now be computed [comment 5], with the contribution from each α, β term being determined separately [comment 2]. These coefficients are then finally output along with their suffices [comment 6].

Again, as a check on the accuracy of the polynomial expansion, the load intensities at several points over the plate are computed from the expansion using equation (157) [comment 7]. The check points are chosen in a similar manner to that which has been described for those in the power series program. The output sheet is also similar in form to that of the power series program.

Fourier series program

The flow diagram shown in Figure 14 illustrates the order

the (ρ_{ij}) are the elements of the matrix ρ and
 are the vectors ρ_{ij} of the matrix ρ . The matrix ρ is
 a square matrix of order n and its elements are (ρ_{ij}) and (ρ_{ji})
 with $\rho_{ij} = \rho_{ji}$ and $\rho_{ii} = 1$.

(14)

$$F = \sum_{i=1}^n (\rho_{ij} \cdot f_j) \cdot \cos(\theta_j)$$

$$f_j = \sum_{i=1}^n (\rho_{ij} \cdot f_i) \cdot \cos(\theta_i)$$

The matrix ρ is the matrix of the elements ρ_{ij} and
 the vectors ρ_{ij} are the vectors of the elements ρ_{ij} .
 The matrix ρ is a square matrix of order n and its
 elements are (ρ_{ij}) and (ρ_{ji}) with $\rho_{ij} = \rho_{ji}$ and
 $\rho_{ii} = 1$.

Figure 14. Flow diagram illustrating the major stages of

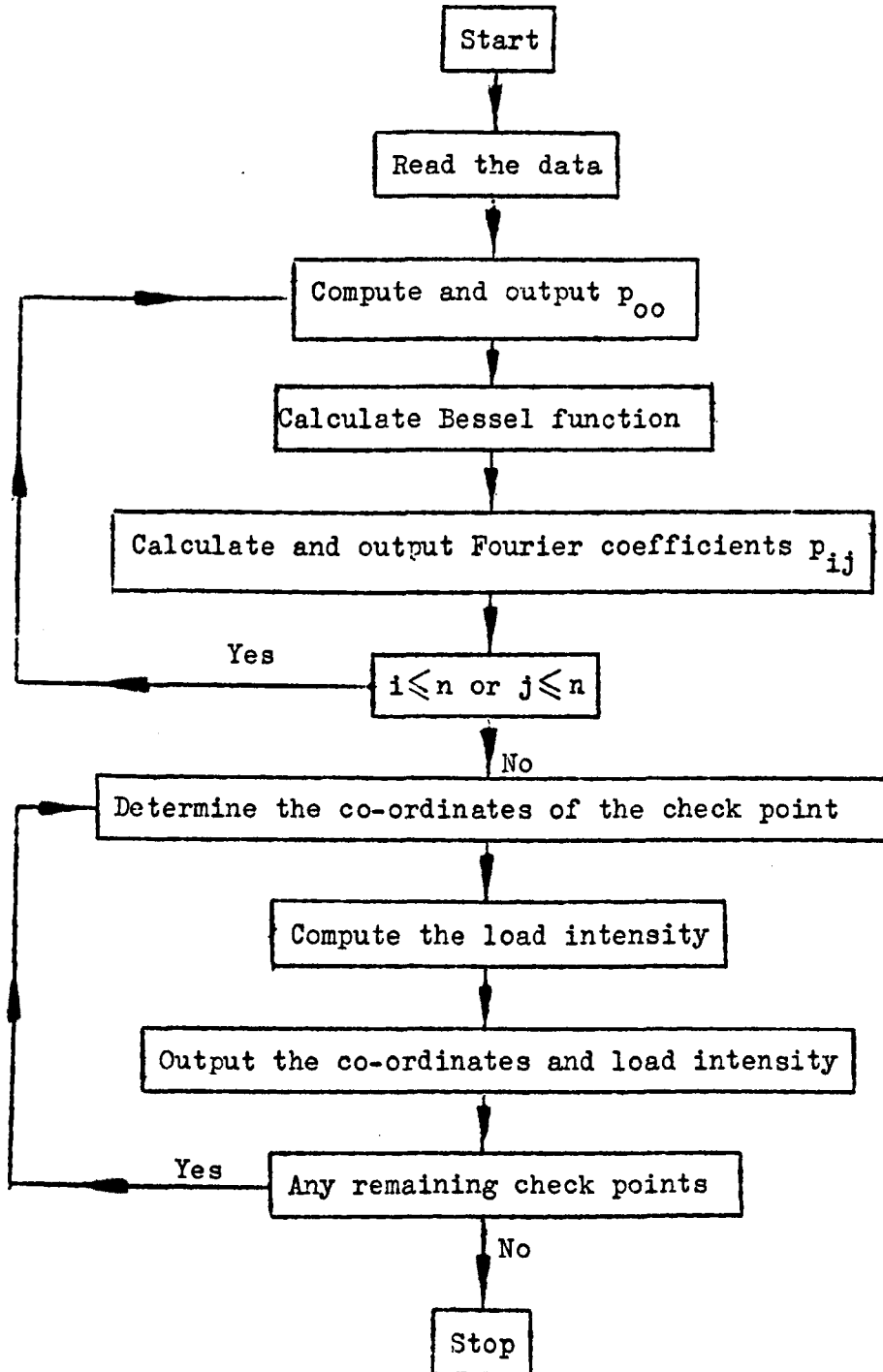
computation in obtaining a Fourier series function
 to describe a load intensity distribution in the
 form of an idealized circular wheel-load.

The matrix ρ is the matrix of the elements ρ_{ij} and
 the vectors ρ_{ij} are the vectors of the elements ρ_{ij} .

The matrix ρ is a square matrix of order n and its
 elements are (ρ_{ij}) and (ρ_{ji}) with $\rho_{ij} = \rho_{ji}$ and
 $\rho_{ii} = 1$. The matrix ρ is the matrix of the
 elements ρ_{ij} and the vectors ρ_{ij} are the vectors
 of the elements ρ_{ij} . The matrix ρ is a square
 matrix of order n and its elements are (ρ_{ij}) and
 (ρ_{ji}) with $\rho_{ij} = \rho_{ji}$ and $\rho_{ii} = 1$.

continued on next page

The matrix ρ is the matrix of the elements ρ_{ij} and the vectors ρ_{ij} are the vectors of the elements ρ_{ij} .



of computation of this program which is entitled 'Wheel-Load Expressed as a Fourier Series'.

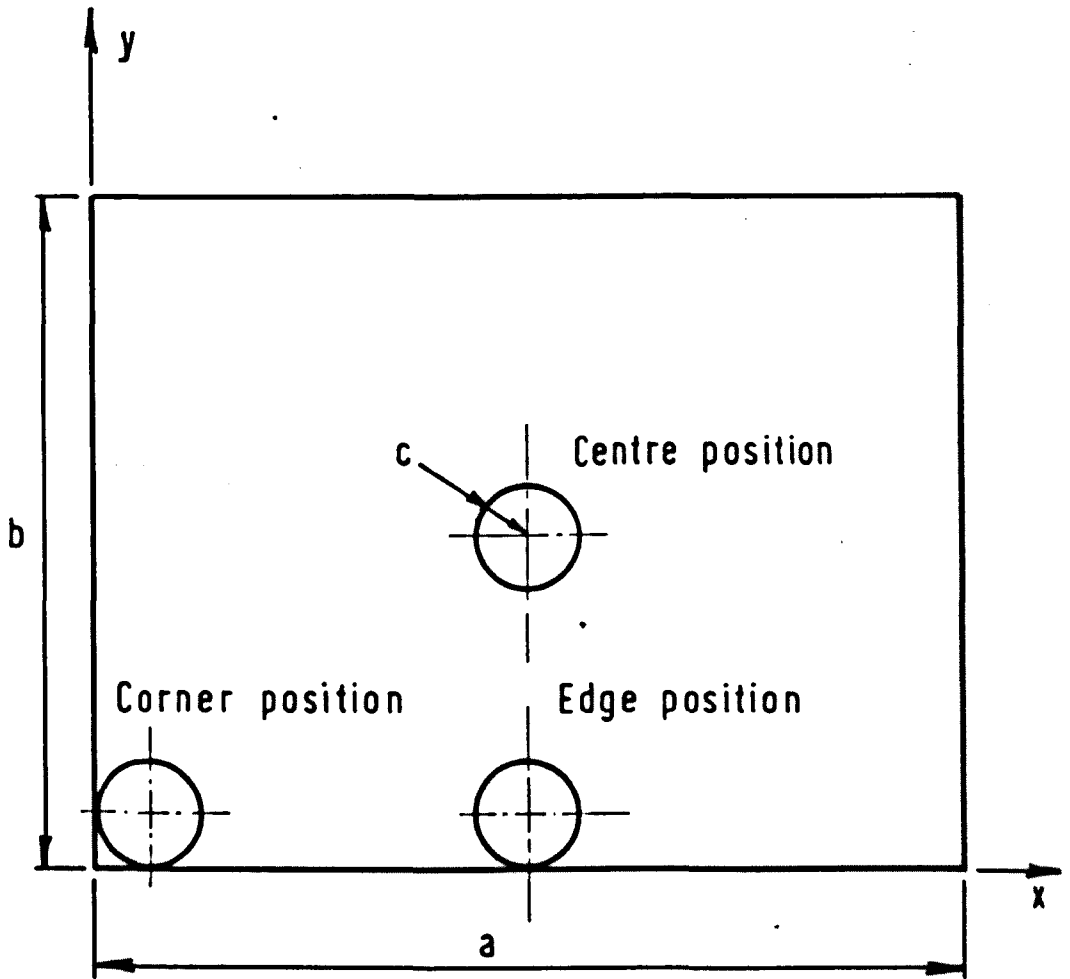
This diagram illustrates how, as a first step, the data - which have exactly the same form as that for the Chebyshev polynomial program - are read [comment 1 and 3]. The coefficient p_{00} is next computed from equation (177) and output together with its suffices [comment 4]. Then the coefficients, $p_{i,0}$, associated with equation (175) are calculated [comment 3] and output [comment 5]. The Bessel function of order one is obtained (56) from

$$J_1(x) = \sum_{R=1}^{\infty} \frac{(-1)^R}{R!(R+1)!} \left(\frac{x}{2}\right)^{1+2R} \quad (190)$$

where the number of terms considered is decided from the criterion that the difference between values computed from R and R+1 terms, expressed as a fraction of that computed from R terms, is less than $1.0 \cdot 10^{-12}$ [comment 2]. More exacting requirements can be introduced by replacing this limit in the program. The coefficients represented by equation (176) and equation (174) are dealt with in a similar manner to p_{i0} [comment 6].

By applying equation (178) a number of check points are then examined in an identical manner to those described in the previous two programs. The final output sheet is also similar to those in the previous programs.

Figure 15. Three positions at which the idealized circular wheel-load is applied to the surface of the plate in order to compare the manner in which power, Chebyshev and Fourier series are able to represent this idealized load intensity distribution



Comparison of the Loading Function Representations

The loading cases chosen as a basis of comparison

In order that the three representations of the loading function can be compared it is necessary to choose as a basis of such a qualitative comparison a particular set of loading arrangements. In highway engineering there are three cases which are normally used as a basis of comparison in theoretical and experimental work; these are the centre, edge and corner loading cases shown in Figure 15. For this reason, and also because they provide a reasonable variety of loading configurations based upon a circular load, the three cases are used in this thesis to compare the three series representations.

Particular values for the dimensions shown in Figure 15 which are approximately representative of the proportions found in highway pavements, are;

a = 20 units of length, b = 10 units of length and

c = 0.5 units of length

The ancillary data used in the computation are as follows:

$k_1 = 0.08$ units of length, $c_1 = 1.15$, $n = 4$,

number = 2,000, $pp = 10$ and $qq = 5$,

along with a number of extra check points about the circular load.

The load intensity within the circular wheel-load thus equals $4/\pi$.

Examining the representations individually.

In order to compare the surfaces describing the power,

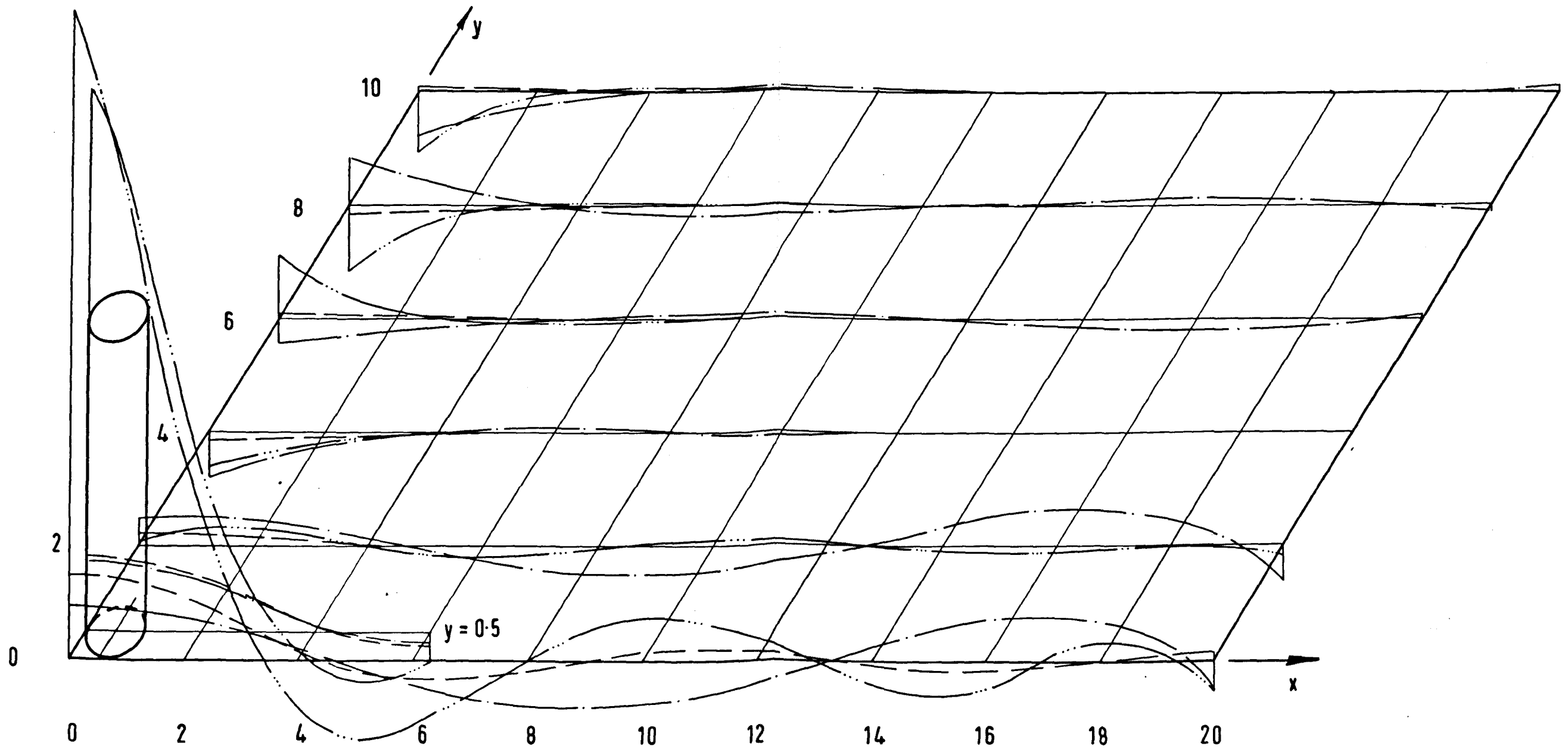
... of the ...

... of the ...

Figure 16. Three surfaces describing the load intensity distribution, as represented by power, Chebyshev and Fourier, series, superimposed on the actual load

intensity distribution of the idealized wheel-load in the corner position.

... of the ...



Legend: Actual load intensity distribution 
Power series surface 
Chebyshev series surface 
Fourier series surface 
Load intensity within circle = $1/\pi$ weight units/length units²

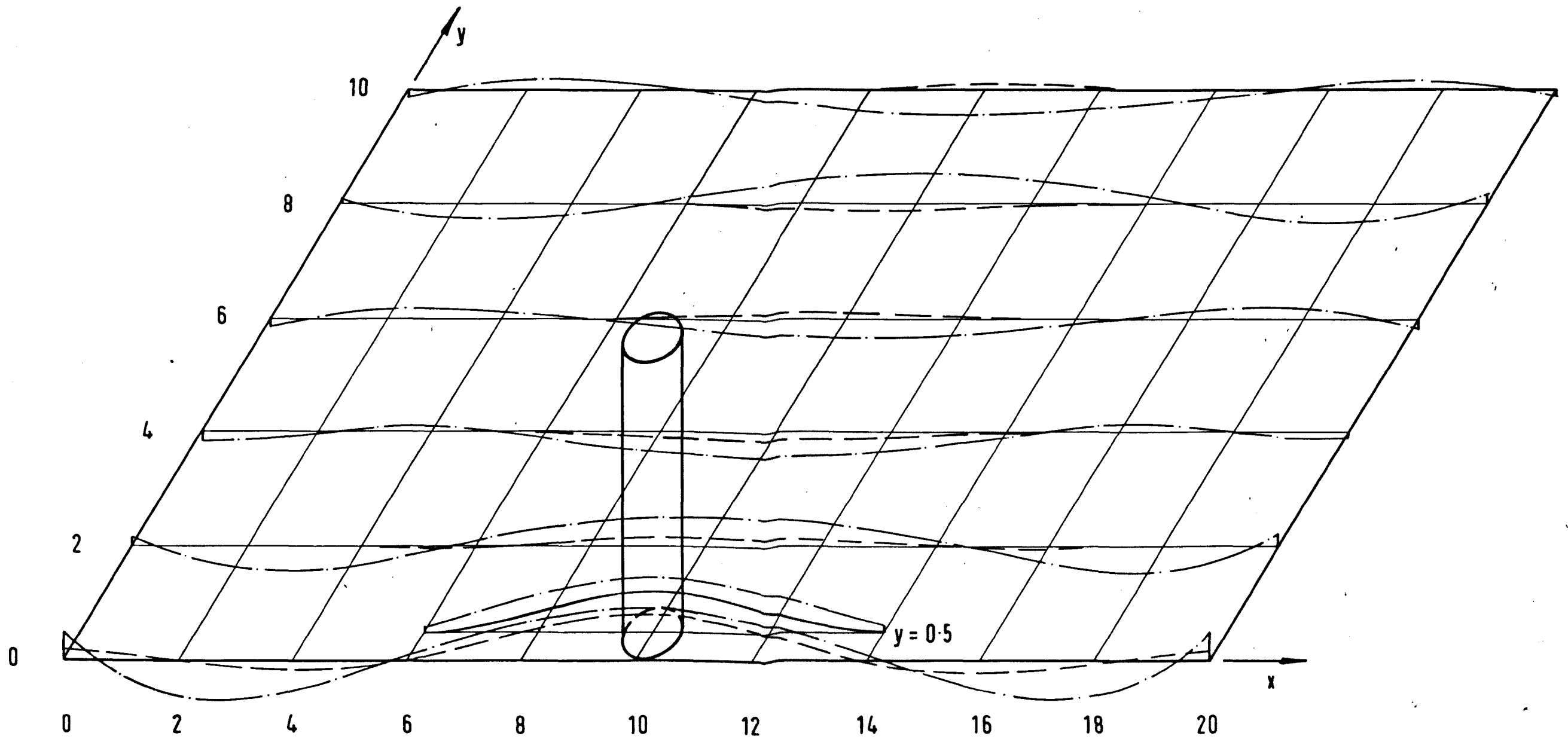
Chebyshev and Fourier series representations of a particular load intensity distribution, they are superimposed upon that loading configuration and shown in diagrammatic form. Thus Figures 16, 17 and 18 show the surfaces for the corner, edge and centre cases, respectively.

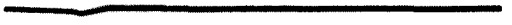
Studying first the surfaces resulting from the power series expansions it can be seen that there are several points in each of the three loading arrangements where the surface moves away from the datum plane. The reason for this is a lack of constraint on the power series at those points due to the increased sparseness of data points at such distances from the loading area. While increasing the number of data points, in this region improves the surface at those points it also results in a poorer representation around the circular load, which is the point of major interest.

As the power series argument is non-oscillatory in nature it increases indefinitely in magnitude as the independent variables grow large. The resulting inability of the expansion to represent the given load intensity distribution for large values of the independent variables is important. For this reason, there may be advantages in placing the origin of the co-ordinate system at the centre of the circular load, which is the main region of interest, instead of at some distance from it as in the present analysis.

In order to check on this possibility, the centre loading

Figure 17. Two surfaces describing the load intensity distribution, as represented by power and Fourier series, superimposed on the actual load intensity distribution of the idealized wheel-load in the edge position.



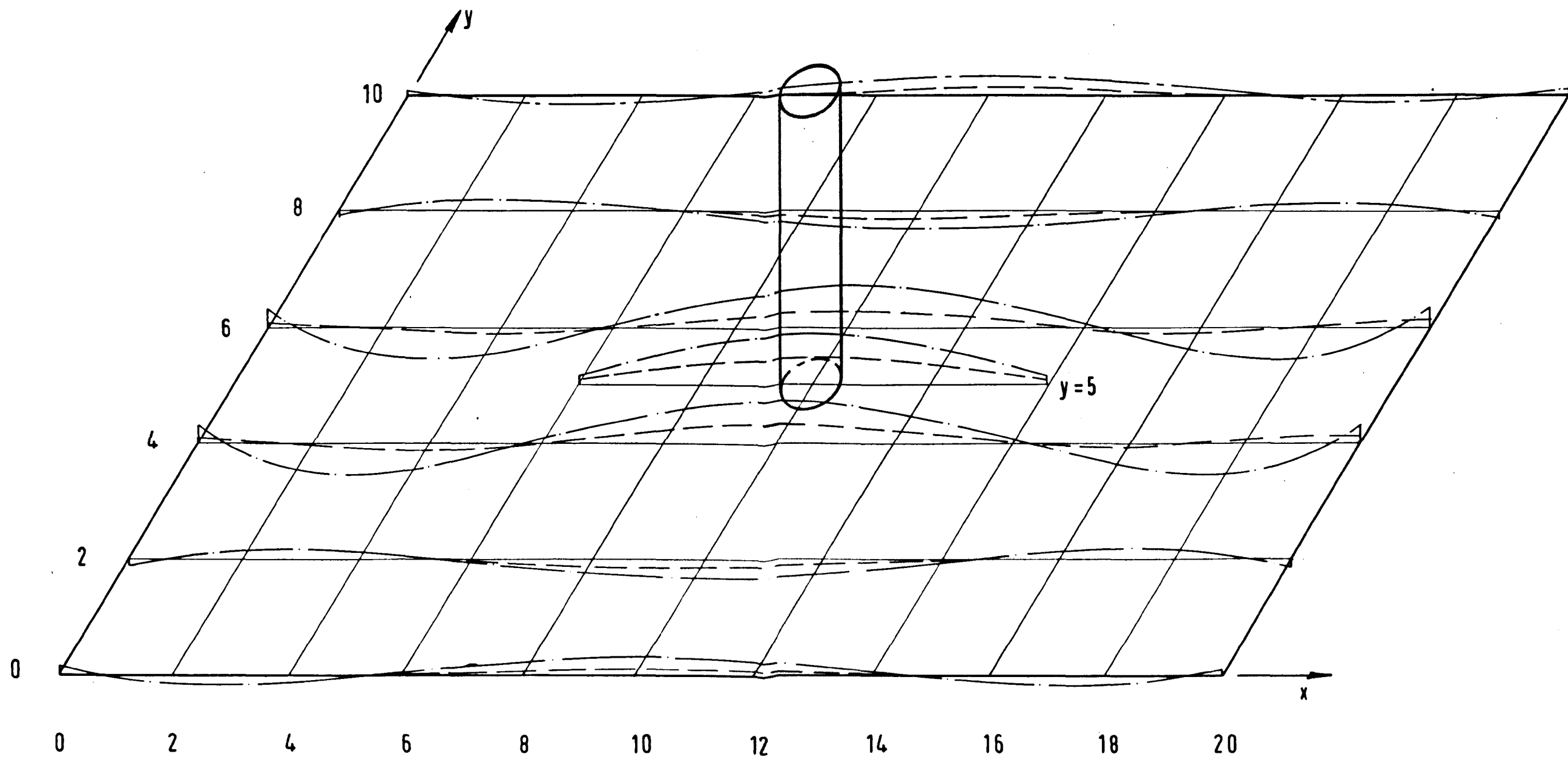
Legend: Actual load intensity distribution: 
Power series surface: 
Fourier series surface: 
Load intensity within circle = $1/\pi$ weight units / length units²

case was further examined. Thus, Figure 19 shows the profile obtained for the load intensity distribution on the vertical plane parallel to the x-axis and passing through the centre of the circular load. Here, for $n = 4$, the surface resulting from the origin being at the centre of the circular load is compared with that resulting from the origin being at the left-hand edge of the plate, and, as may be seen, the two surfaces are identical. Therefore, for the distance which any part of the plate is likely to be from the origin, there is no advantage in having the origin at any point other than the corner of the plate. The reason is that, relative to infinity, the maximum values of the independent variables are still close to zero no matter where the origin is on the plate.

In the Chebyshev expansions, and where $n = 4$, no surface function appears in any of the three cases, since there is no tabular point (η_α, ξ_β) that is a zero point and lies within the loading circle. This results in a load intensity distribution of zero being described by the expansion for all points over the area of the plate. This difficulty can be overcome by increasing the number of terms in the series thereby increasing the total number of zero points with the consequent increase in the likelihood of a zero point lying within the loading circle.

Increasing the value of n from 4 to 6 results in a non-zero surface being formed for the corner case but not for the other two cases. The reason for this difference is related to the form of

Figure 18. Two surfaces describing the load intensity distribution, as represented by power and Fourier series, superimposed on the actual load intensity distribution of the idealized wheel-load in the centre position.



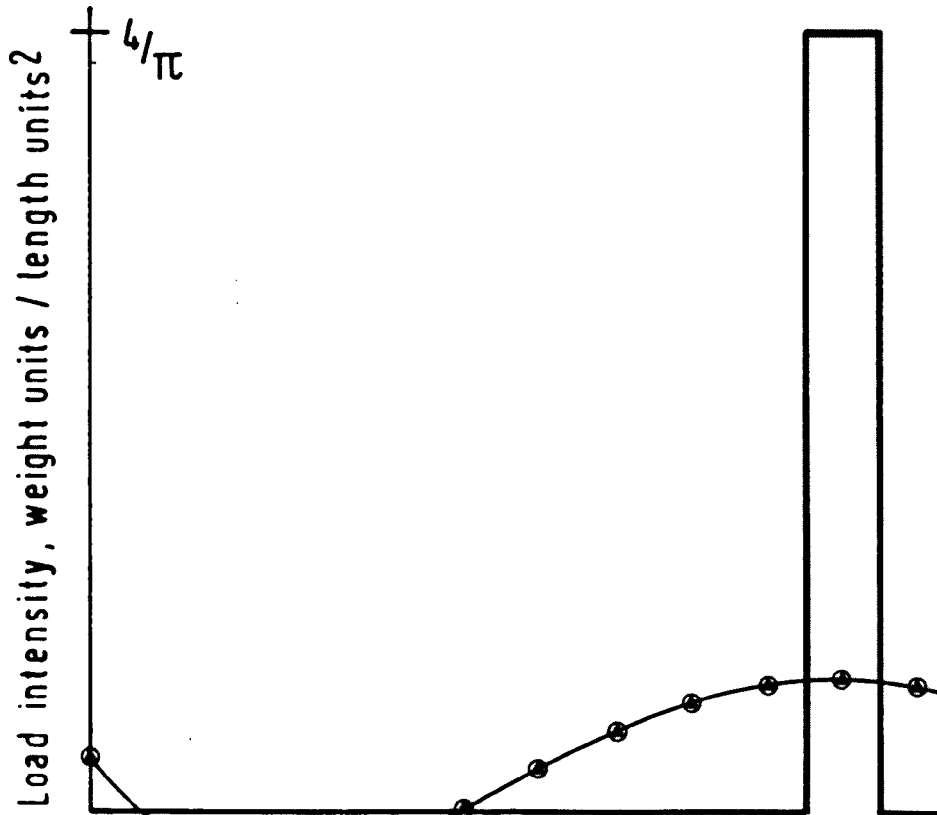
Legend: Actual load intensity distribution 
Power series surface 
Fourier series surface 
Load intensity within circle = $1/\pi$ weight units/length units²

equation (163) - it determines the zero points - which results in a predominance of zero points near the origin of the co-ordinate system. In the corner loading case as compared with the centre and edge cases, this increases the possibility of obtaining a zero point which lies within the loading circle.

No such difficulties arise with the Fourier series expansion as this is arrived at by the consideration of a continuous surface and not a set of discrete tabular points as in the Chebyshev expansion. In each of the three loading cases illustrated in Figures 16, 17 and 18 the Fourier Series representation can be seen to represent, to a similar degree, each region of the load intensity distribution even though it does not respond very much to the load intensity distribution within the circular load.

Comparing the representations

None of the three expansions is capable of representing accurately the discontinuities of the load intensity distribution at the circular edge. This capability can be improved, however by including more terms in each of the truncated series, although it is theoretically impossible for a power series to describe accurately a discontinuity. To illustrate this consider Figure 20 which shows the one-dimensional surface for the plane parallel to the x-axis passing through the centre of the load in the centre loading case, for various values of n in the truncated power series expansion. In



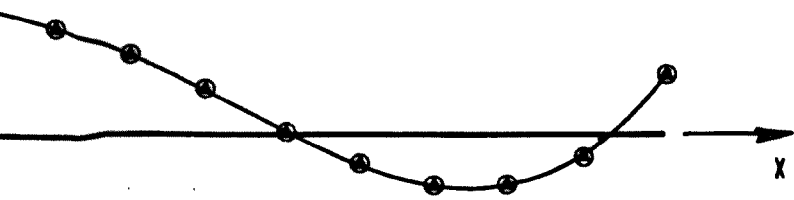
Offset co-ordinates

0 2 4 6 8 10

Central co-ordinates

-10 -8 -6 -4 -2 0

Legend: Origin at left-hand edge of plate:
 Origin at centre of circular load:
 Actual load intensity distribution:



12 14 16 18 20

2 4 6 8 10

○

▲

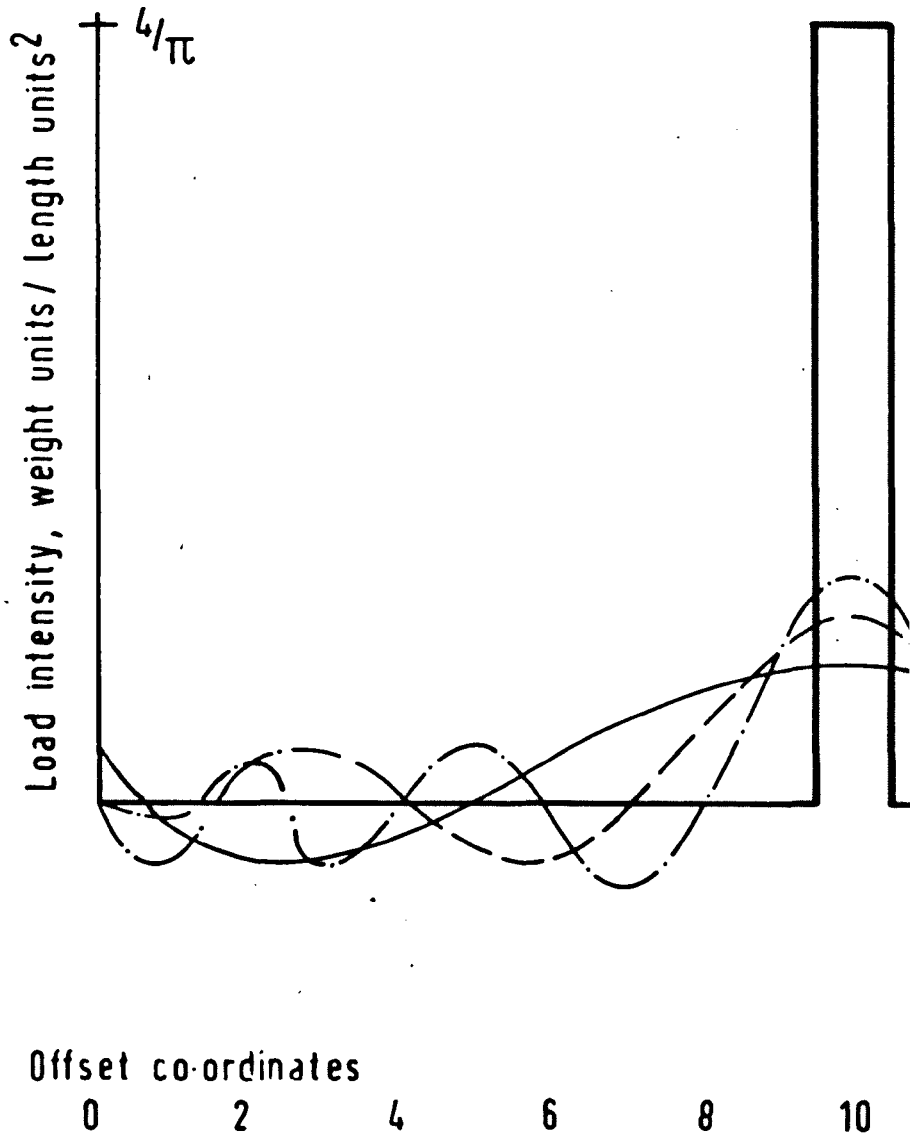


this figure, it can be seen that, for a limited increase in the number of terms, the discontinuities of the circular load are represented to a much greater degree of accuracy. Similar results apply to the Fourier and Chebyshev expansions.

Where there is zero load intensity i.e. over the remainder of the plate, the surfaces are often wave-like in form. If, however, the value of n in all three series expansions is increased then this profile will appear to decrease in the sense that the number of ripples will increase and eventually effectively merge.

Even allowing for the increased value of n to 6, the Chebyshev expansion responds, in the corner case, far more readily to the non-zero load intensity distribution within the circle than do the other two expansions. Only one zero point falls within the circular load i.e. at the co-ordinates (0.72, 0.36), and at this point the surface has a value of 1.8 instead of the actual intensity value of 1.27. This greater response may be attributed to the criterion used to minimize the difference between the computed surface and the actual load intensity distribution.

The Chebyshev polynomial expansion relies upon the criterion that the maximum error occurring at any one zero point over the plate should be a minimum, whereas the Fourier and power series each uses the criterion that the square of the total error over the plate should be a minimum. Since the major part of the load

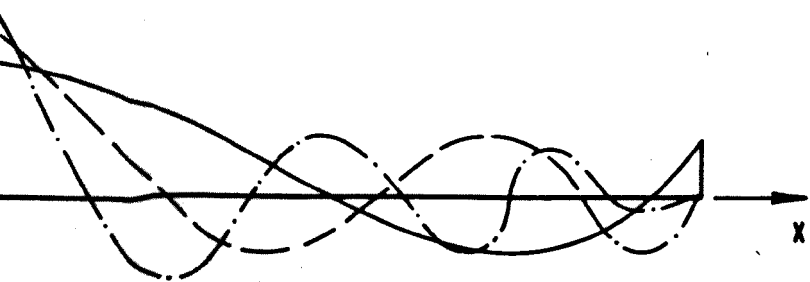


Legend: Actual load intensity distribution:

$n = 4:$

$n = 8:$

$n = 12:$



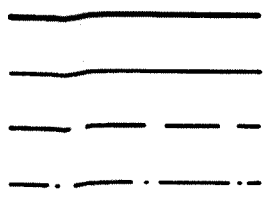
12

14

16

18

20



intensity distribution is zero, then the expansion based on the square of the error being a minimum tends to follow the datum plane even near the loading circle and, as can be seen from Figures 16, 17 and 18, responds to the non-zero intensity to a limited degree. On the other hand, the Chebyshev expansion at the zero point (0.72, 0.36) attains the actual load intensity distribution to a closer degree than either of the other series as it is here that - compared with the datum surface, which would be accurately represented by a Chebyshev expansion with all coefficients zero - the error is very likely to be the limiting maximum error for the whole plate.

The reason why the load intensity continues to increase from the centre of the load to the nearest corner of the plate is that the load intensity is undefined between the tabular point (0.72, 0.36) and the corner of the plate. This difficulty can, however, be overcome by increasing the number of terms in the series.

A major advantage of the Fourier series, over the other two series, is that it has no bias in accuracy with respect to any region of the load intensity distribution. This is because of the equal ripple wave form of its cosine argument. The Chebyshev polynomial expansion, on the other hand, has a concentration of zero points near both the origin and the corner of the plate which is furthest from the origin and, therefore, it represents to a better degree the load intensity distribution in these regions.

It may be noted that the power series expansion is theoretically only perfectly accurate at the origin although this point has been shown not to be relevant to the size of plate considered here.

Discussion

In this chapter, the power, Chebyshev and Fourier series representations of the applied loads, with particular reference to circular wheel-loads, have been formulated, programmed and compared on a qualitative basis. None of these representations was, however, found to describe accurately the discontinuous load intensity distribution for the size of truncated series which was considered.

While the Chebyshev polynomial expansion was found to have serious drawbacks with respect to its ability to represent to any degree some loading configurations, it was shown that the difficulty could be overcome by increasing the number of terms in the polynomial expansion. While this was then shown to be comparatively successful in representing the load intensity distribution, the computer space necessary for solving the associated general simultaneous algebraic equations (125 to 130) is prohibitive on account of the available computer facility.

The Fourier series expansion utilized is based on a continuous surface and not, as in the case of the other two forms of expansion, on a set of discrete data points. For this reason it was possible to show that the Fourier series follows the datum

plane over the unloaded portion of the plate to a far better degree than does either the power series or the Chebyshev series which are both undefined in areas between the data and tabular points.

The power series expansion for the case of discontinuous load distributions was shown not to be subject to abrupt surface undulations around the load because of the greater concentration of data points in that region. The remainder of the plate does not have the same concentration of data points because the region around the circular load is of major interest and the computer time limitations did not enable more data points to be considered.

Better computer facilities would have enabled larger truncated power series expansions to be considered. Increases in the number of terms in a truncated series have been shown to improve the representation of the load intensity distribution even when such increases are small.

COMPUTATION OF THE PAVEMENT STRESSES AND DEFORMATIONS

The pavement stresses and deformations are now computed from the analysis of the principal boundary value problem in which contact between the slab and foundation is preserved during all modes of interface displacement. The limitations in representing the load intensity distribution in terms of Chebyshev polynomials and the inability of the chosen Fourier series representations to furnish a non-trivial solution to the boundary value problem indicate the need to concentrate on the further development of the power series solution.

As has been indicated previously the number of terms required by the series p in order to describe the continuous surface which best simulates an arbitrary load intensity distribution may be quite high. Similar requirements may also apply to a load intensity distribution which is represented explicitly in terms of co-ordinate powers. Consequently, the number of simultaneous equations generated from the general ij th equations, equations (96 to 101), may also be large. In order to solve these equations a computer is again necessary.

In order to obtain a solution it is now essential to consider the set of equations in the general matrix form

$$\underline{A} \underline{x} = \underline{b} \quad (191)$$

where \underline{x} is the vector of unknown series-coefficients, \underline{b} is the vector

of constants and A is the matrix of parameters which are functions of the properties and dimensions of the slab and foundation and also of the values of i and j of equations (96 to 101) which are relevant to each term. The vector b consists of either zeros or known functions of the coefficients of p and the major part of its elements are zero. The matrix A is extremely sparse and is non-symmetric.

The determination of the stresses and deformations in a slab under the applied load falls conveniently into three parts. Firstly, there is the setting-up of the matrix A and the vector b; secondly, the solution of this system of equations; and, thirdly, the computation of stresses, strains and deflections from the vector x and the loading series p . Furthermore, in order that the maximum amount of computer space and time is retained for the major portion of the computation, which is the solution of the simultaneous equations, programming is split into three separate parts, each of which performs one of the above three functions. The following is a brief description of the three programs and of their relevant mathematical theory. (A copy of each of these three programs appears in Appendix C).

Setting-up the Algebraic Form of the Differential Equations

The arrangement of the simultaneous equations

The creation of the simultaneous equations (191) from the general equations (96 to 101) is based upon a system of reference numbers. These numbers refer to each general coefficient, e.g. $V_{x_{i-1,j}}$

in equation (96); and since there are fifty two general coefficients in the system of general equations, these numbers run from one to fifty two. The general coefficients to which these numbers refer are best indicated by rewriting equations (96 to 101) and replacing the coefficients by their relevant reference numbers:

$$r(i+1)(a[1]-[2])+sr(j+1)(b[3]-[4])-(i+1)(i+2)[5]-s(j+1)(j+2)[6] \\ -t(a[7]-[8])-\frac{Tkf}{g} [9] = TCp_{ij} \quad (192)$$

$$r(j+1)(b[10]-[11])+sr(i+1)(a[12]-[13])-(j+1)(j+2)[14]-s(i+1)(i+2)[15] \\ -t(b[16]-[17])-\frac{Tkf}{g} [18] = TCp_{ij} \quad (193)$$

$$-r(j+1)(a[19]-[20])-r(i+1)(b[21]-[22])+2(i+1)(j+1)[23] \\ +m(ab[24]-a[25]-b[26]+[27]) = 0 \quad (194)$$

$$(i+1)(a[28]-[29])+(j+1)(ab[30]-b[31]-a[32]+[33]) \\ -(a[34]-[35]) = 0 \quad (195)$$

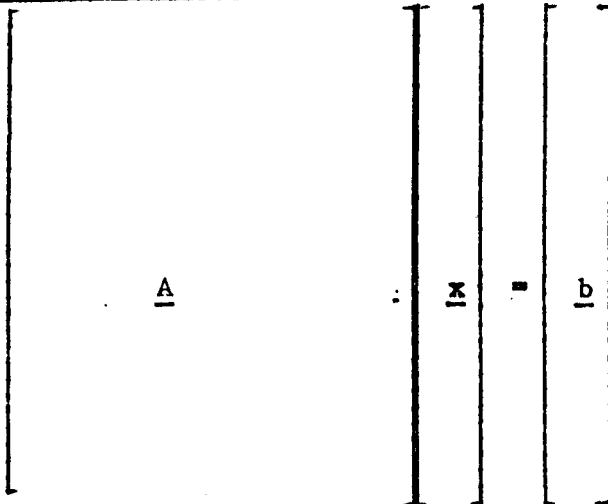
$$(j+1)(b[36]-[37])+(i+1)(ab[38]-a[39]-b[40]+[41]) \\ -(b[42]-[43]) = 0 \quad (196)$$

$$-(i+1)(a[44]-[45])-(j+1)(b[46]-[47])+\frac{k}{g} [48]-\frac{kT}{g} (a[49]-[50]) \\ -\frac{kT}{g} (b[51]-[52]) = -Cp_{ij} \quad (197)$$

The functions which multiply each general coefficient are referred to as multipliers and it is these multipliers which furnish the values in the matrix A. The form which this matrix takes is shown

<u>KK</u>	<u>HH</u>	Eqn
$B_1 = 0$	n	96
$B_2 = (n+1)^2$	n	97
$B_3 = 2(n+1)^2$	n-1	98
$B_4 = 2(n+1)^2 + n^2$	n	99
$B_5 = 3(n+1)^2 + n^2$	n	100
$B_6 = 4(n+1)^2 + n^2$	n	101

<u>Series</u>	<u>LL</u>	<u>MM</u>
V_x	n	$B_1 = 0$
V_y	n	$B_2 = (n+1)^2$
H	n-1	$B_3 = 2(n+1)^2$
M_x	n	$B_4 = 2(n+1)^2 + n^2$
M_y	n	$B_5 = 3(n+1)^2 + n^2$
w_o	n	$B_6 = 4(n+1)^2 + n^2$



in Figure 21. The matrix is divided horizontally into six sections; each section containing the equations generated from a particular general equation. Running down the matrix A, the number of equations KK occurring before a particular section is expressed in the column in terms of B_1, B_2, B_3, B_4, B_5 and B_6 which are functions of the maximum power n of the p series. In each section the simultaneous equations are arranged vertically in ij th order, i.e. 00, 01, ,10,11, , etc. Thus the position, r, which a simultaneous equation has vertically is given by

$$r = \underline{KK} + (\underline{HH}+1) i + j + 1$$

where HH is the maximum value of j for each section (see Figure 21).

The matrix is also divided vertically into six sections, each section of which contains the coefficients of one of the dependent series. These sections are arranged in the order shown, the only requirement being that the main diagonal elements of the H - series should also be the main diagonal elements of equation (98). Running across A from the left, the number of coefficients occurring before a particular section is indicated in the row MM in terms of B_1, B_2, B_3, B_4, B_5 and B_6 which are functions of the maximum power n of the p series. In each part, the dependent coefficients are arranged horizontally in order of their suffices taken in rows, e.g. V_x ,
OO
 $V_{x_{01}}$, . . . $V_{x_{0n}}$, $V_{x_{10}}$, $V_{x_{11}}$, . . . $V_{x_{1n}}$, etc. Thus, the position, u, along the horizontal which a coefficient with suffices s_m, t_m takes is given by

$$\underline{u} = \underline{MM} + (\underline{LL} + 1)s_m + t_m + 1$$

where \underline{LL} is the maximum value of s_m for each dependent series (see Figure 21). To create the multiplier associated with each dependent coefficient, the range of substitution of i and j in the general coefficient is equal to that of the relevant general ij th equation, with the limitation that no multiplier should be considered which is associated with a dependent coefficient lying outside the limits of the particular dependent truncated series.

<u>AA</u>	<u>BB</u>	<u>CC</u>	<u>DD</u>	<u>EE</u>	<u>FF</u>	<u>GG</u>	<u>HH</u>	<u>KK</u>	<u>LL</u>	<u>MM</u>	<u>NN</u>
1	0	n	0	n	0	0	n	B ₁	n	B ₁	+ra (i + 1)
2	1	n	0	n	-1	0	n	B ₁	n	B ₁	-r (i + 1)
3	0	n	0	n	0	0	n	B ₁	n	B ₂	srb (j + 1)
4	0	n	1	n	0	-1	n	B ₁	n	B ₂	-sr (j + 1)
5	0	n-2	0	n	2	0	n	B ₁	n	B ₆	-(i + 1)(i + 2)
6	0	n	0	n-2	0	2	n	B ₁	n	B ₆	-s (j + 1)(j + 2)
7	1	n	0	n	-1	0	n	B ₁	n	B ₄	-at
8	2	n	0	n	-2	0	n	B ₁	n	B ₄	t
9	0	n	0	n	0	0	n	B ₁	n	B ₆	Tkf/d
10	0	n	0	n	0	0	n	B ₂	n	B ₂	rb (j + 1)
11	0	n	1	n	0	-1	n	B ₂	n	B ₂	-r (j + 1)
12	0	n	0	n	0	0	n	B ₂	n	B ₁	sra (i + 1)
13	1	n	0	n	-1	0	n	B ₂	n	B ₁	-sr (i + 1)
14	0	n	0	n-2	0	2	n	B ₁	n	B ₆	-(j + 1)(j + 2)
15	0	n-2	0	n	2	0	n	B ₂	n	B ₆	-s(i + 1)(i + 2)
16	0	n	1	n	0	-1	n	B ₂	n	B ₅	-tb
17	0	n	2	n	0	-2	n	B ₂	n	B ₅	t
18	0	n	0	n	0	0	n	B ₂	n	B ₆	Tkf/d
19	1	n-1	0	n-1	-1	1	n-1	B ₃	n	B ₁	-ra (j + 1)
20	2	n-1	0	n-1	-2	1	n-1	B ₃	n	B ₁	r (j + 1)

Continued overleaf.

<u>AA</u>	<u>BB</u>	<u>CC</u>	<u>DD</u>	<u>EE</u>	<u>FF</u>	<u>GG</u>	<u>HH</u>	<u>KK</u>	<u>LL</u>	<u>MM</u>	<u>NN</u>
21	0	n-1	1	n-1	1	-1	n-1	B ₃	n	B ₂	-rb (i + 1)
22	0	n-1	2	n-1	1	-2	n-1	B ₃	n	B ₂	r (i + 1)
23	0	n-1	0	n-1	1	1	n-1	B ₃	n	B ₆	2 (i + 1)(j + 1)
24	1	n-1	1	n-1	-1	-1	n-1	B ₃	n-1	B ₃	abm
25	1	n-1	2	n-1	-1	-2	n-1	B ₃	n-1	B ₃	-am
26	2	n-1	1	n-1	-2	-1	n-1	B ₃	n-1	B ₃	-bm
27	2	n-1	2	n-1	-2	-2	n-1	B ₃	n-1	B ₃	n
28	0	n	0	n	0	0	n	B ₄	n	B ₄	a (i + 1)
29	1	n	0	n	-1	0	n	B ₄	n	B ₄	- (i + 1)
30	1	n	0	n-1	-1	0	n	B ₄	n-1	B ₃	ab (j + 1)
31	2	n	0	n-1	-2	0	n	B ₄	n-1	B ₃	-b (j + 1)
32	1	n	1	n	-1	-1	n	B ₄	n-1	B ₃	-a (j + 1)
33	2	n	1	n	-2	-1	n	B ₄	n-1	B ₃	(j + 1)
34	1	n	0	n	-1	0	n	B ₄	n	B ₁	-a
35	2	n	0	n	-2	0	n	B ₄	n	B ₁	l
36	0	n	0	n	0	0	n	B ₅	n	B ₅	b (j + 1)
37	0	n	1	n	0	-1	n	B ₅	n	B ₅	- (j + 1)
38	0	n-1	1	n	0	-1	n	B ₅	n-1	B ₃	ab (i + 1)
39	0	n-1	2	n	0	-2	n	B ₅	n-1	B ₃	-a (i + 1)
40	1	n	1	n	-1	-1	n	B ₅	n-1	B ₃	-b (i + 1)
41	1	n	2	n	-1	-2	n	B ₅	n-1	B ₃	(i + 1)
42	0	n	1	n	0	-1	n	B ₅	n	B ₂	-b
43	0	n	2	n	0	-2	n	B ₅	n	B ₂	l
44	0	n	0	n	0	0	n	B ₆	n	B ₁	-a (i + 1)
45	1	n	0	n	-1	0	n	B ₆	n	B ₁	(i + 1)
46	0	n	0	n	0	0	n	B ₆	n	B ₂	-b (j + 1)
47	0	n	1	n	0	-1	n	B ₆	n	B ₂	(j + 1)
48	0	n	0	n	0	0	n	B ₆	n	B ₆	k/d
49	1	n	0	n	-1	0	n	B ₆	n	B ₄	-a kT/d
50	2	n	0	n	-2	0	n	B ₆	n	B ₄	kT/d
51	0	n	1	n	0	-1	n	B ₆	n	B ₅	-bkT/d
52	0	n	2	n	0	-2	n	B ₆	n	B ₅	kT/d

Table 3. Information required for generating each non-zero matrix element of the algebraic equations of the power series solution.

Table 3 shows the information required for the creation of each non-zero element of the matrix A, i.e. each multiplier. The column AA lists the reference numbers, thus relating the other columns to the fifty two general coefficients. The columns, BB, CC, DD, and EE contain the range of substitution of the ij suffices of each general coefficient e.g. the range of substitution of i and j in $V_{x_{i-1,j}}$; these are minimum i, minimum j, maximum i, and maximum j, respectively. The columns FF and GG list the adjustments to each i and j required for each general coefficient in order to determine the suffix s_m, t_m e.g. - 1 and 0 in $V_{x_{i-1,j}}$. The next four columns list the values of HH, KK, LL and MM in that order. The last column NN contains the algebraic form of the multiplier associated with each general coefficient; some of these are functions of i and j.

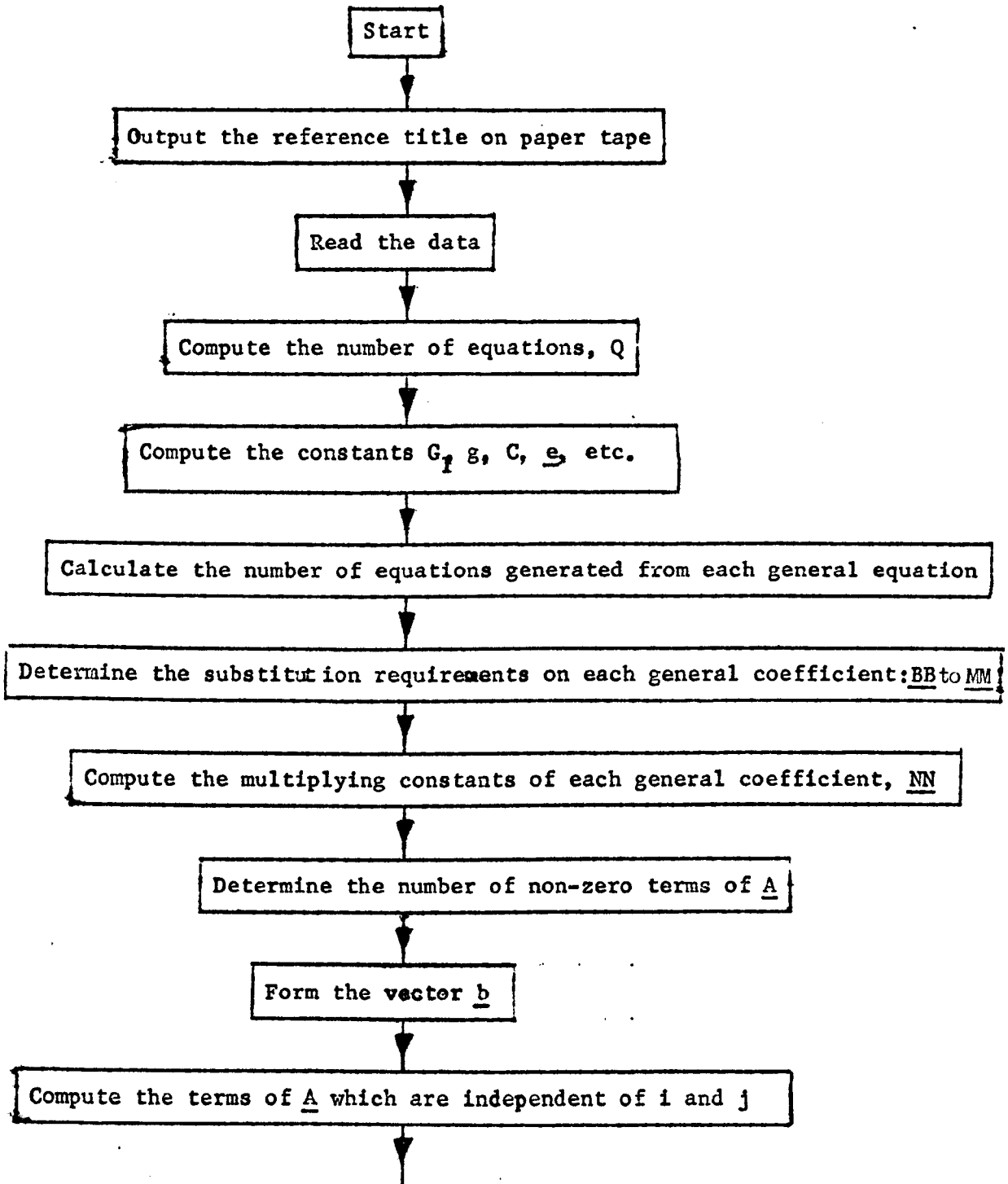
Thus the non-zero element $a_{\underline{r},\underline{u}}$ of the matrix A has a value of NN and a position obtained from

$$\underline{r} = \underline{KK} + (\underline{HH} + 1) i + j + 1 \tag{198}$$

$$\underline{u} = \underline{MM} + (\underline{LL} + 1) (i + \underline{FF}) + (j + \underline{GG}) + 1$$

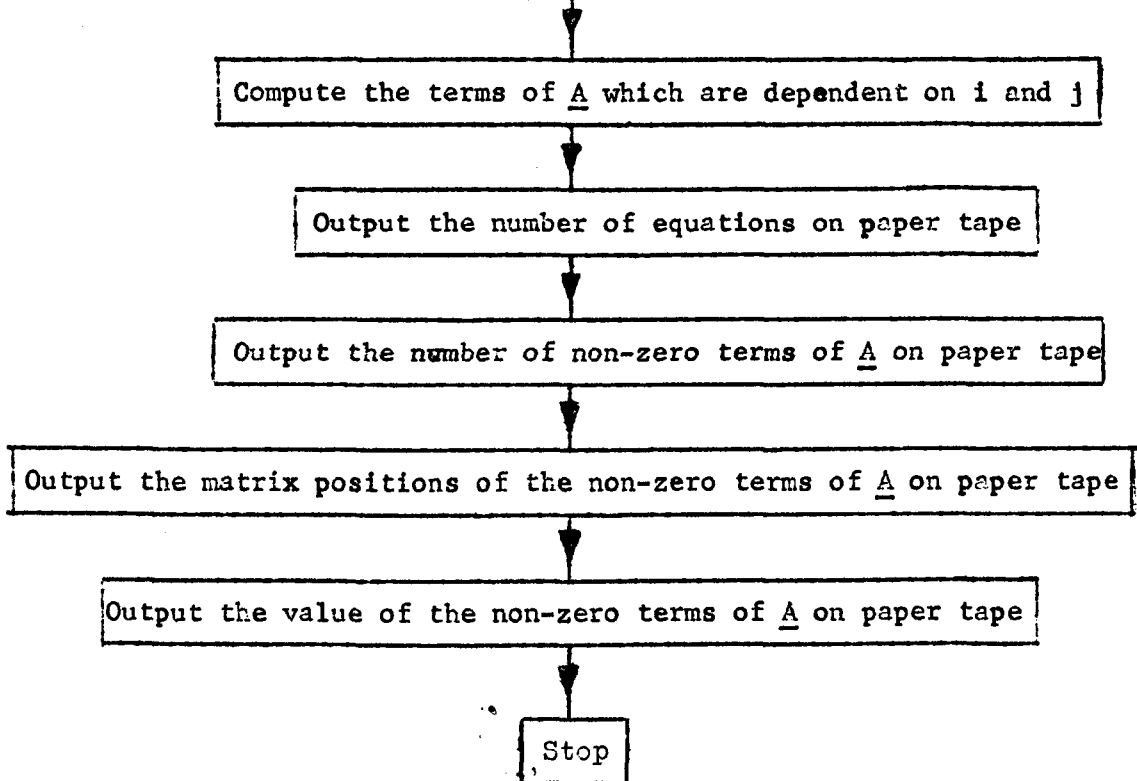
the most efficient manner of gathering the non-zero elements of the matrix is by considering all the multipliers associated with each general coefficient, the limits of substitution of i and j being taken from the columns BB, CC, DD and EE.

The elements of the vector of constants b are only non-zero in the case of the general equations (96, 97 and 101). The value of



continued overleaf:

Continued from previous page:



these elements are simple multiples of p_{ij} for a particular ij th equation.

The program

This description of the program entitled 'Setting-up the Equations' should be read in conjunction with the flow diagram appearing in Figure 22, this shows the general sequence of operations for which the program is written.

As may be seen from the figure, the problem data are first read; these consist of a title enclosed between brackets, <TITLE>, the length of the plate (a), the width of the plate (b), the maximum power occurring in the truncated power series describing the load intensity distribution (n), the thickness of the plate (h), Poisson's ratio for the plate (μ), the modulus of elasticity for the plate (E), the modulus of subgrade reaction of the foundation (k) and the matrix of coefficients of the power series describing the load intensity distribution, taken in rows; $p_{00}, p_{01}, \dots, p_{0n}, p_{10}, p_{11}, \dots, p_{1n}$, etc., [comment 1, 2 and 20]. Thus the data take the form;

```
<TITLE >
a,b;n,h; $\mu$ ;E;k;
P00;P01; . . . P0n;
P10;P11; . . . P1n;
. . . . .
. . . . .
Pn0;Pn1; . . . Pnn; →
```

In the case of an explicitly defined polynomial function describing the load intensity distribution, the truncated power series is the series which, at least, includes all the coefficients of the polynomial function, the remaining coefficients in the truncated series being equal to zero. This system enables the maximum number of terms to be used for the description of the dependent variables, and the same program to be used for both an explicitly and approximately described applied load.

Computation begins with the determination of the values defined by equation (56) and the six possible values KK and MM [comment 3 and 4]. The non-zero values of BB, CC and EE, DD, FF GG, HH and LL, KK and MM are then computed [comment 5, 6, 7, 8, 9, 10, 11, and 12, respectively]. The constant terms of NN are next calculated [comment 13] after which the number of non-zero multipliers in the matrix A is determined [comment 14].

The vector of constants b is calculated from the loading series using the general form of the right-hand side of equations (96 to 101) [comment 15]. Each non-zero multiplier of the matrix A is next computed, along with its elemental position (r, u) [comment 16]; those multipliers which are independent of i and j are considered first, followed by the dependent multipliers [comment 17 and 18].

The number of equations, the number of non-zero multipliers, the b vector and the non-zero multipliers along with their positions are finally output onto punch-hole paper tape [comment 19], and this is

preserved for use in the next program i.e. for the solution of the algebraic equations.

Solution of the Algebraic Equations

The consideration of methods of solution

As stated before the matrix A is extremely sparse and hence a method of solution which processes only the non-zero terms of A can save a great deal of computer storage space. Iterative methods of solution lend themselves to this idea, since only the non-zero terms contribute to the residual, $\underline{b} - \underline{A}\underline{x}$ and thus the zero coefficients need not be processed. The equation is satisfied when the residual is zero. After initially making an arbitrary approximation to the vector of unknowns x each subsequent estimation of x uses the previous residual to estimate the values of the unknowns, until after repeated estimations the residual reaches zero and the correct x is obtained.

In the majority of iterative methods, it is only after an infinite number of iterations have been carried out that the residual can possibly reach zero, although after a finite number of iterations a good approximation of the true value of x can be obtained. An exception to the iterative techniques which have this drawback is the method of conjugate gradients (63) which, theoretically, is able to obtain the correct solution after $Q+1$ iterations, where Q is the number of equations. This method also has the advantage that the elements of A can be processed in any order. Thus elements which are

formed from the same combination of parameters can be treated as a group even though they appear in different equations and thus can then be generated in an economical manner.

Because of these advantages which allow large systems of equations to be solved, this method of solution has been examined in detail to ascertain its potential for the present problem. However the method, when applied to this problem, was found not to converge to a solution after $Q+1$ iterations. This was still true after $2(Q+1)$ iterations and better initial approximations to \underline{x} did not help. Thus it appears that for this system of equations the method, as at present programmed, does not converge to the solution in a stable and rapid manner. For this reason the method is not considered further.

The direct methods of solution which can be relied upon to give a solution for \underline{x} are now examined, although the use of such methods is wasteful in computer space. The first difficulty which arises in their application to the present problem is that zeros appear on the leading diagonal of the matrix \underline{A} . This can be overcome by premultiplying each side of the system of equations by the transpose of \underline{A} ; thus

$$\underline{A}^T \underline{A} \underline{x} = \underline{A}^T \underline{b} \tag{199}$$

where \underline{A}^T is the transpose of \underline{A} . This system of equations not only has the same solution as $\underline{A} \underline{x} = \underline{b}$ but has no zeros on the leading diagonal; the only obvious requirement on \underline{A} is that at least one element

in each row of \underline{A} is non-zero. Another consequence of premultiplying by \underline{A}^T is that $\underline{A}^T \underline{A}$ is a symmetric matrix and so the square-root method of solution is suitable for solving the new system of equations.

Because $\underline{A}^T \underline{A}$ is non-positive definite it may turn out that the root expression in the square-root method contains a negative term. However, this does not produce basic difficulties since the arithmetic operations in the case of imaginary numbers are identical to those of real numbers. A tracer is introduced which simply notes whether the term is negative and, on taking the square-root, holds the imaginary number $(-1)^{1/2}$ separately so that all numbers which are subsequently acted upon by this diagonal term are altered accordingly. Then the solution for \underline{x} , which is made up of real numbers, may be obtained.

As there is also a possibility of a diagonal term being close to zero, the elements of \underline{A} and \underline{b} are scaled up by a factor of 1.0×10^{10} in order to avoid any chance of dividing, in the square-root method, by a number close to zero.

The program

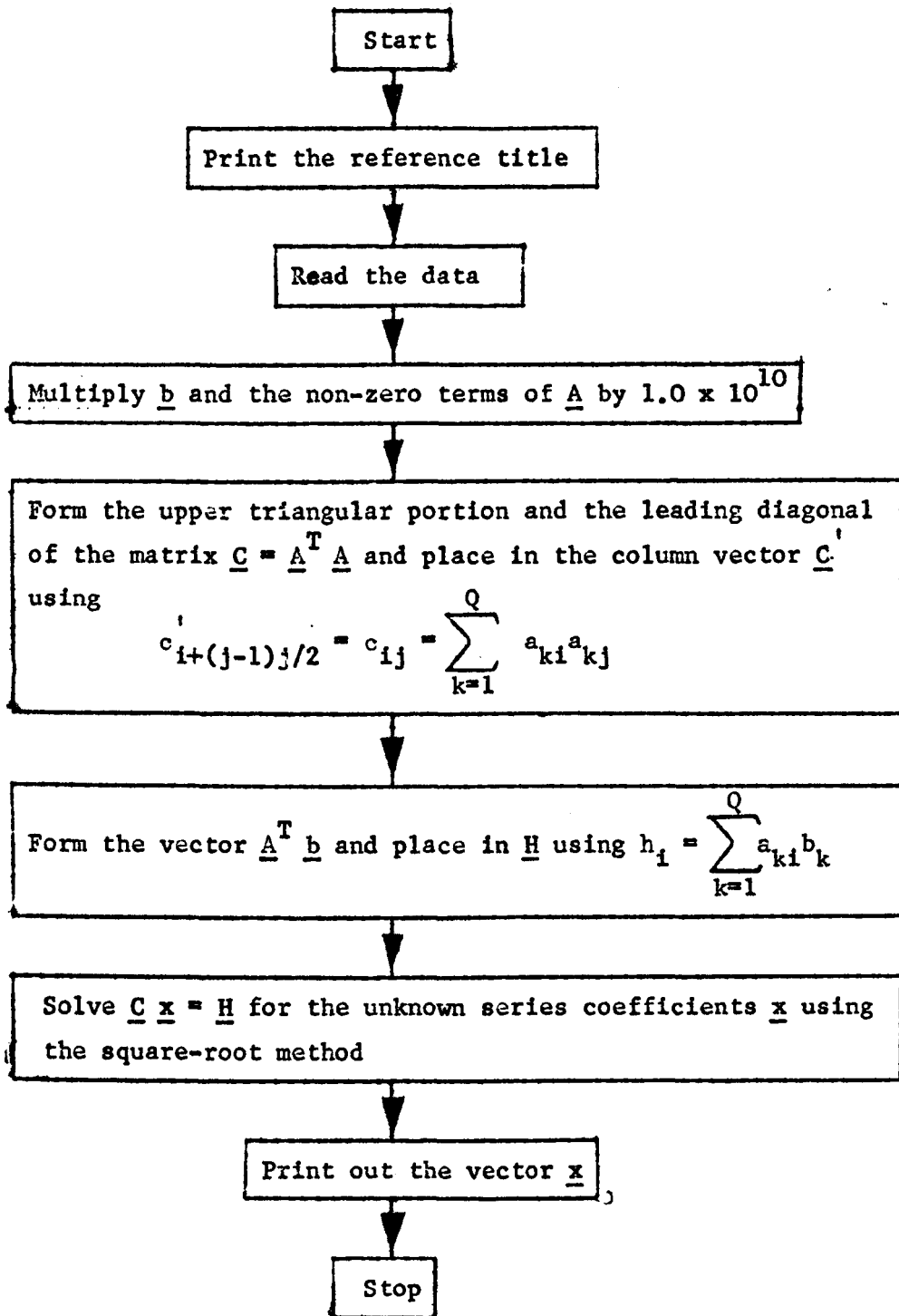
The output on paper tape from the previous program, 'Setting-up the Equations', is used as the data for the present program which is entitled 'Solving the Equations'; the flow diagram for this program appears in Figure 23.

The first stage of the computation involves the solution of the system of algebraic simultaneous equations generated from equations (96 to 101) in the power series solution of the mathematical model.

Figure 23. Flow diagram of the major stages of computation involved in solving the system of algebraic simultaneous equations generated from equations (96 to 101) in the power series solution of the mathematical model.

The second stage of the computation involves the solution of the system of algebraic simultaneous equations generated from equations (96 to 101) in the power series solution of the mathematical model.

The third stage of the computation involves the solution of the system of algebraic simultaneous equations generated from equations (96 to 101) in the power series solution of the mathematical model.



The program begins by reading in the data, which consists of a title between brackets<and>, the number of equations, the number of non-zero multipliers, the vector of constants \underline{b} , and the non-zero multipliers along with their matrix positions [comment 1 and 3]. The non-zero multipliers and the \underline{b} vector are all multiplied by 1.0×10^{10} on entry to the program.

The first stage in the computation is the premultiplication of \underline{A} by its transpose \underline{A}^T . Letting the new matrix $\underline{A}^T \underline{A}$ be represented by \underline{C} , then the element c_{ij} of the matrix \underline{C} is determined from

$$c_{ij} = \sum_{k=1}^Q a_{ik}^t a_{kj} \quad (200)$$

where Q is the number of equations, a_{kj} is an element of \underline{A} and a_{ik}^t is an element of \underline{A}^T . Since $a_{ik}^t = a_{ki}$ then

$$c_{ij} = \sum_{k=1}^Q a_{ki} a_{kj} \quad (201)$$

Noting that $a_{ki} a_{kj} = a_{kj} a_{ki}$ i.e., that $c_{ij} = c_{ji}$, then, since \underline{C} is symmetric, only the upper triangular portion and the leading diagonal need be stored. Since the non-zero multipliers of \underline{A} alone contribute to the elements of \underline{C} , only their contribution to \underline{C} need be considered. Because two elements of \underline{A} multiplied together, $a_{ki} a_{kj}$, only contribute to c_{ij} when their row counters, k , are equal, each row counter of the non-zero multipliers of \underline{A} is compared to every other;

then if they are equal, the two elements are multiplied together, $a_{ki} a_{kj}$, and added to the element c_{ij} which is originally zero.

In order to avoid multiplying two multipliers together twice - one contributing to the upper triangular portion and the other to the lower triangular portion of \underline{C} - only multipliers which have not been multiplied together previously are considered and if $j > i$ then c_{ij} is contributed to c_{ij} ; if $j \leq i$, then c_{ij} is added to c_{ji} .

Because the saving of computer space is so important and the lower triangular portion of \underline{C} contains only zeros, the upper triangular portion and the leading diagonal are placed column-wise in a column vector \underline{C}' such that the element c_{ij} has a position t_c in the column vector, where:

$$t_c = i + [(j-1)j/2] \quad (202)$$

The sequence of operations concerned with the formation of $\underline{A}^T \underline{A}$ in \underline{C}' is then carried out in a compact manner [comment 4]. After this the computer forms $\underline{A}^T \underline{b}$ in the column vector \underline{H} [comment 5]. The element h_i of \underline{H} is determined from

$$h_i = \sum_{k=1}^Q a_{ik}^t b_k$$

or, applying $a_{ki} = a_{ik}^t$,

$$h_i = \sum_{k=1}^Q a_{ki} b_k \quad (203)$$

The computer is then able to solve the system of equations

$$\underline{C} \underline{x} = \underline{H} \quad (204)$$

using the square-root method. This does not differ basically from its use previously in the solution of the normal equations, except that each term of \underline{C} must be sought in \underline{C}' and the possibility of \underline{C} being non-positive definite must be guarded against [comment 2].

After the solution for the vector of unknown power series coefficients is obtained the coefficients are then printed out. The order of printing is: V_x , V_y , H , M_x , M_y and w_o . The coefficients of a particular unknown are printed in row-wise order, i.e. $V_{x_{00}}$, $V_{x_{01}}$, $V_{x_{0n}}$, $V_{x_{10}}$, $V_{x_{11}}$, $V_{x_{1n}}$, etc. These coefficients along with the coefficients of the loading function are then available to determine the stresses, strains and deflections of the slab resting on an elastic foundation.

Determination of Stresses, Strains and Deflections.

Stresses, strains and deflections of interest.

Having solved for the dependent variables, the final stage in computation is the evaluation of any required results. In the horizontal plane of the upper surface of the slab, the maximum principal stress (σ_{max}), the minimum principal stress (σ_{min}), the maximum principal strain (ϵ_{max}), the minimum principal strain (ϵ_{min})

and the direction of the maximum principal stress and strain (ϕ_p), are all of interest. The upper surface of the slab, rather than the lower surface, is chosen simply on an arbitrary basis - the lower surface stresses and strains are of the same magnitude but the opposite sign. The interior stresses are not considered as they are less in magnitude and, therefore, less critical than those on the surface.

The dependent variable concerned with deflection is the weighted average displacement, w_o , which does not itself have any practical significance. It is not possible to compute the actual transverse displacement w from w_o , other than by assuming the form of the variation of w through the thickness of the slab. This is because the analysis of the three-dimensional slab has been transformed into a two-dimensional problem by assumptions on the variation of stresses in the transverse direction. The simplest assumption is to neglect altogether the effect of transverse compression on the transverse displacements, i.e.

$$w = w_o^*(x,y) \quad (205)$$

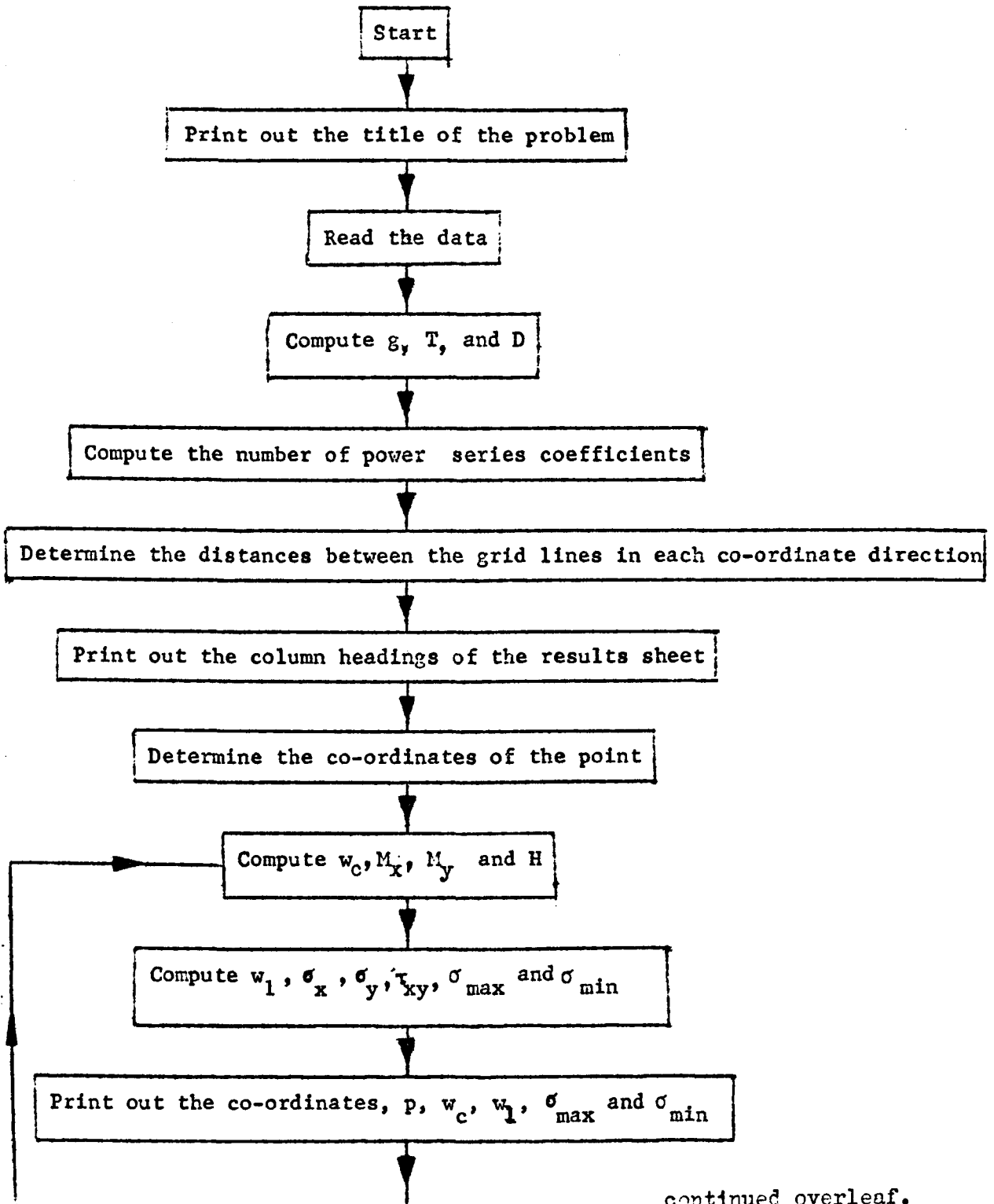
and then substituting into the first of equations (26) and integrating gives

$$w_o = w_o^*(x,y)$$

or $w_c = w = w_o \quad (206)$

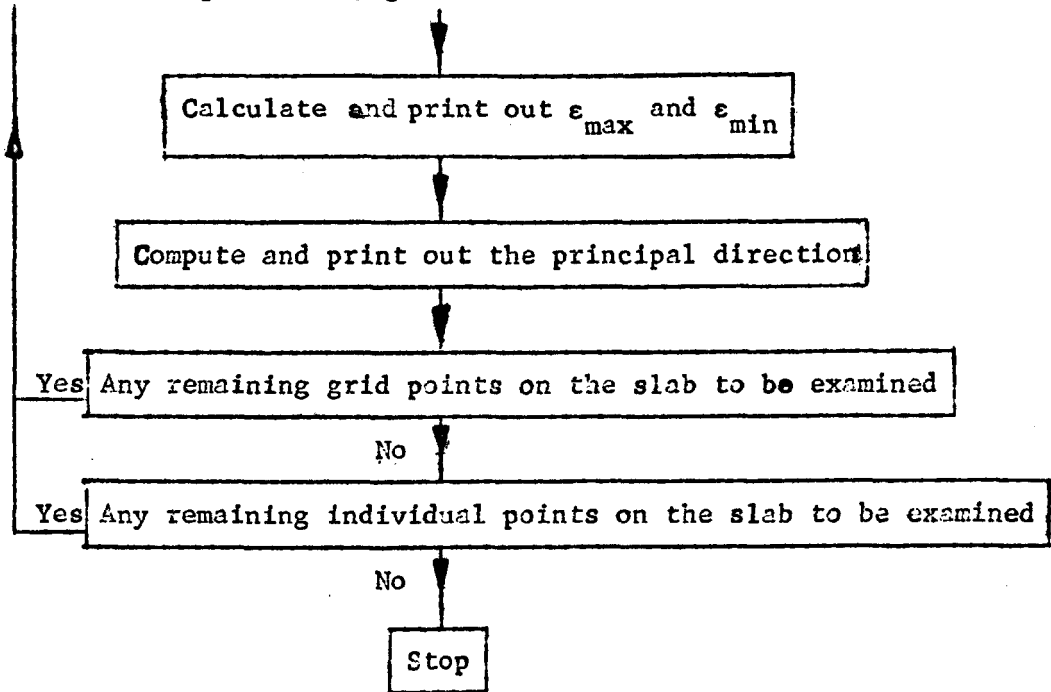
where w_c is the transverse displacement of the plate with the effect of transverse compression neglected. Thus, the displacement computed

Figure 24. Flow diagram of the major stages of the computation involved in calculating the stresses, strains and deflections in the plate from the power series describing the stress resultants, weighted average deflection and load intensity distribution.



continued overleaf.

continued from previous page:



from the w_0 series is the transverse displacement of the slab, with transverse compression, neglected, and is referred to as the 'plate deflection', w_0 .

A possibility still remains of observing the effect of transverse compression on the deflection by considering the deflection of the lower surface of the slab. The deflection of this surface, after neglecting transverse compression, is simply the plate deflection. The deflection with this effect included however is w_1 ($\neq w_0$) and, this can be determined from w_0 by re-arranging equation (53) into the form

$$w_1 = \frac{1}{g} [w_0 - T(M_x + M_y) + D.p] \quad (207)$$

where $g = (1 + \frac{26kh}{70E})$, $T = \frac{6\mu}{5Eh}$ and $D = \frac{9h}{70E}$

The load intensity, and the above stresses, strains and deflections are of interest at many points over the surface of the slab. The program which computes these values at any point on the surface of the slab is now described.

The program

The program which is now to be described is entitled 'Determination of Stresses, Strains and Deflections'. The flow diagram of this computation is shown in Figure 24.

The program begins by accepting the data. First is a title enclosed between brackets <and> Secondly the dimensions and elastic properties of the plate: the length (a), the width (b), the

thickness (h), Poisson's ratio (μ), and the modulus of elasticity (E) are read. Thirdly the highest power of the truncated power series describing the load intensity distribution (n) is input. Fourthly, the number of grid divisions in the x-direction and y-direction (pp and qq respectively), which are understood in the same sense as before, are read. Fifthly, the number of extra points on the slab of special interest (tt) completes this section of the data to be read [comment 1].

The data then continue with the coefficients of the truncated series, taken in rows, in the following order: p , w_0 , M_x , M_y and H [comment 9]. Finally, the co-ordinates of the extra points of interest (xx , yy) are read [comment 10]. Thus the data take the form

<TITLE>

a;b;h; μ ;E;k;n;pp;qq;tt;

P_{00} ; P_{01} ; . . . P_{0n} ;

P_{10} ; P_{11} ; . . . P_{1n} ;

.

P_{n0} ; P_{n1} ; . . . P_{nn} ;

similarly w_0

" M_x

" M_y

" H

xx_1 ; yy_1 ;

$xx_2; yy_2;$

. .
. .

$xx_{tt}; yy_{tt}; \rightarrow$

At each co-ordinate point of interest the load intensity (p), plate deflection (w_c), x-direction bending moment (M_x), y-direction bending moment (M_y) and twisting moment (H) are computed from the power series expansions [comment 2]. The slab-foundation interface deflection (w_1) is then computed [comment 3], after which the direct stresses σ_x , σ_y and shearing stresses τ_{xy} are calculated from equations (21) [comment 4] and the principal stresses from

$$\sigma_{\max} = \frac{\sigma_x + \sigma_y}{2} + \frac{1}{2} [(\sigma_x - \sigma_y)^2 + 4\tau_{xy}^2]^{1/2} \quad (208)$$

$$\sigma_{\min} = \frac{\sigma_x + \sigma_y}{2} - \frac{1}{2} [(\sigma_x - \sigma_y)^2 + 4\tau_{xy}^2]^{1/2}$$

These principal stresses are printed out along with the co-ordinates of the point, the load intensity, plate deflection, interface deflection and the principal strains [comment 5]. The principal strains are computed from

$$\epsilon_{\max} = \frac{\sigma_{\max} - \mu\sigma_{\min}}{E} \quad (209)$$

$$\epsilon_{\min} = \frac{\sigma_{\min} - \mu\sigma_{\max}}{E}$$

The principal direction (ϕ_p) is finally computed [comment 6] and printed out using

EXPERIMENTAL MODEL-HALF INCH PLATE THICKNESS

CO-ORDS		LOAD INTENSITY	PLATE DEFLECTION	INTERFACE DEFLECTION	MAXIMUM STRESS
X	Y				
0.0	0.0	2.50000×10^{-1}	-3.25421×10^{-2}	-3.24407×10^{-2}	0.00000
0.0	12.0	4.35200×10^{-7}	1.02499×10^1	1.02235×10^1	0.00000
24.0	0.0	8.95943×10^{-9}	1.64690×10^2	1.64267×10^2	0.00000
24.0	12.0	2.53580×10^{-7}	3.30826×10^4	3.29976×10^4	0.00000
0.0	0.0	2.50000×10^{-1}	-3.25421×10^{-2}	-3.24407×10^{-2}	0.00000
0.0	0.8	2.05994×10^{-1}	-2.87781×10^{-2}	-2.86554×10^{-2}	0.00000
.
.
0.8	0.0	2.27287×10^{-1}	-3.06553×10^{-2}	-3.05256×10^{-2}	0.00000
0.8	0.8	1.87279×10^{-1}	-2.72826×10^{-2}	-2.71303×10^{-2}	-3.29015×10^{-2}
.
.
.
24.0	12.0	2.53580×10^{-7}	3.30826×10^4	3.29976×10^4	0.00000

MINIMUM STRESS	MAXIMUM STRAIN	MINIMUM STRAIN	PRINCIPAL DIRECTION
0.00000	0.00000	0.00000	
0.00000	0.00000	0.00000	
0.00000	0.00000	0.00000	
0.00000	0.00000	0.00000	
0.00000	0.00000	0.00000	
-7.43474 _x -1	3.41752 _x -4	-8.21518 _x -4	0.00000
.	.	.	.
.	.	.	.
-7.57633 _x -1	3.48260 _x -4	-8.37164 _x -4	-9.00000 _x 1
1 -1.17512 _x 0	1.76614 _x -4	-1.14724 _x -3	-4.79364 _x 1
.	.	.	.
.	.	.	.
.	.	.	.
0.00000	0.00000	0.00000	

$$2\phi_p^* = \tan^{-1} [2\tau_{xy}/(\sigma_x - \sigma_y)] \quad (210)$$

where if $\tau_{xy} = 0$, then $\phi_p = 0$;
if $(\sigma_x - \sigma_y) = 0$, then there is no one principal direction,
if $(\sigma_x - \sigma_y) > 0$, then $\phi_p = -\phi_p^*$;
and if $(\sigma_x - \sigma_y) < 0$, then $\phi_p = -\phi_p^* - 90$,

where ϕ_p is measured in degrees from the x-axis in a clockwise direction.

The points for which these values are determined fall into two groups. Firstly, they fall within a grid system of points over the plate with pp divisions in the x-direction and qq divisions in the y-direction [comment 7]. Also, there are a number of points of particular interest, with co-ordinates (xx,yy), which form the second group [comment 8]. The final form of the printed output is shown in Figure 25.

Discussion

In this chapter, programs have been described, which upon insertion of the dimensions and elastic properties of the slab and foundation, and the truncated power series describing the load intensity distribution over the surface of the slab, determine the stresses, strains and deflections at any point on the slab.

The programming has been designed to make the most efficient use of the available computer space which, in the case of the installation

of the University of Leeds, is 17,000 words. Splitting the programming into three parts has increased considerably the number of algebraic simultaneous equations which can be solved by a computer. This maximum number of simultaneous equations, with the Leeds installation, is generated when the limit, n , of the truncated power series describing the load intensity distribution, is four.

A LIMITED EXPERIMENTAL APPLICATION OF THE STRUCTURAL ANALYSIS

The examination of a proposed theoretical analysis of an idealized structural system by experiment is intended usually to determine the degree of accuracy with which the analysis computes the stresses and deformations in that system and hence to decide the limitations of the analysis.

In the present investigation certain requirements, namely the available computer space and computer time, limited the extent to which the analysis of the idealized pavement/subgrade (plate/foundation) system could be examined. Thus, in order to examine the analysis, even to only a limited degree, the experimental investigation had to be so designed so as to minimise the effect of those external restrictions; at the same time it had to represent as closely as possible the idealized pavement/subgrade system. As a result, only experimental deflection values were obtained for comparison with the results of the analysis. (The reason for this is made clear later in this chapter).

The use of a laboratory model enabled a close control to be kept over the environmental conditions and the representation of the boundary conditions. Due to limitations of the available computer facilities, however, it was considered that no useful purpose could be served in carrying out an exhaustive program of experimental work and so the number of laboratory models was kept to the minimum consistent with obtaining the maximum useful information.

The experimental apparatus for loading and measuring the deflection of the plate/foundation system, shown in Figure 26, consists of the following components:

1. A rigid base plate supported by a foundation.

2. A loading equipment consisting of a vertical column and a horizontal beam.

3. A measuring device consisting of a vertical column and a horizontal beam.

4. A dial indicator for measuring the deflection of the plate/foundation system.

5. A load cell for measuring the load applied to the plate/foundation system.

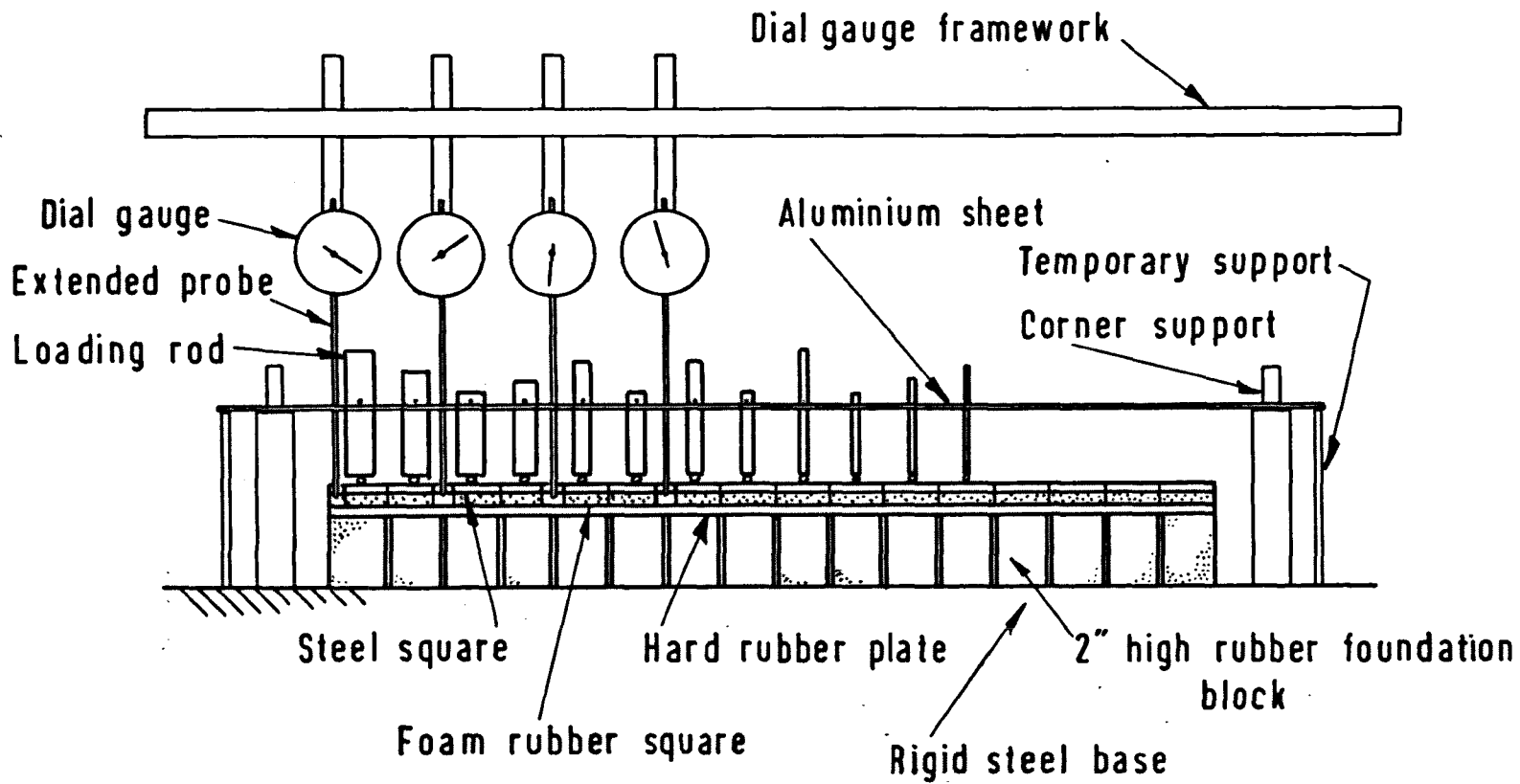
6. A data acquisition system for recording the load and deflection data.

Figure 26. Experimental apparatus for loading and measuring

the deflection of the plate/foundation system, shown in Figure 26, with the loading equipment in the rest position.

The experimental apparatus is shown in Figure 26. The loading equipment consists of a vertical column and a horizontal beam. The measuring device consists of a vertical column and a horizontal beam. The dial indicator is used to measure the deflection of the plate/foundation system. The load cell is used to measure the load applied to the plate/foundation system. The data acquisition system is used to record the load and deflection data.

The experimental apparatus is shown in Figure 26. The loading equipment consists of a vertical column and a horizontal beam. The measuring device consists of a vertical column and a horizontal beam. The dial indicator is used to measure the deflection of the plate/foundation system. The load cell is used to measure the load applied to the plate/foundation system. The data acquisition system is used to record the load and deflection data.



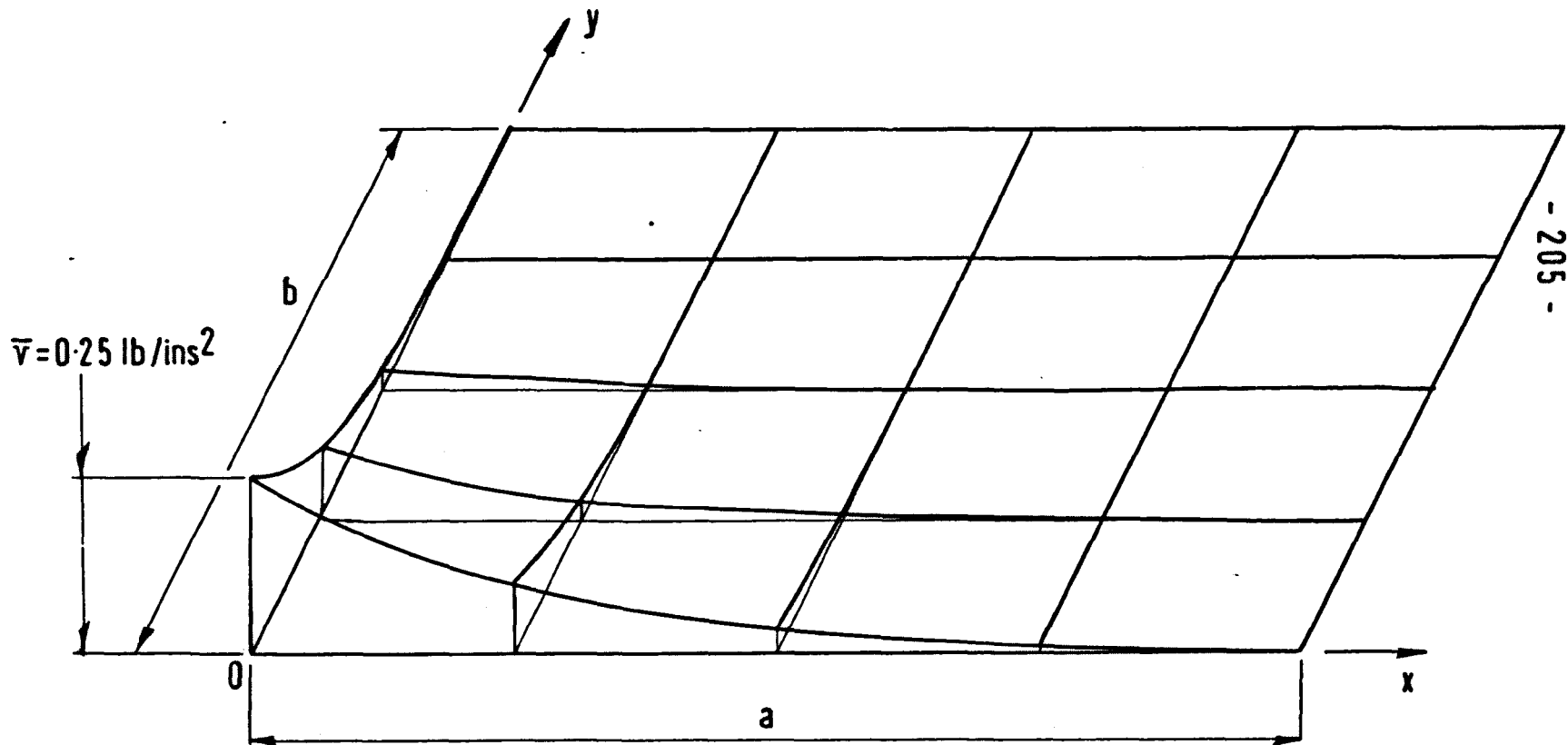
Design of the Experimental Investigation

The computational restrictions took two forms. Firstly, there was the difficulty of a truncated power series in describing the load intensity distribution and, secondly, there was the problem of the limited number of algebraic simultaneous equations which could be solved. This first difficulty was eliminated by considering a continuous load intensity distribution which was described explicitly by a limited number of terms; the second could only be minimized by the choice of the plate and foundation properties and by the distribution of the continuous load. These requirements did not cause any violation of the assumptions upon which the analysis was based and thus the basic intention of this investigation which was to examine the proposed structural analysis was still preserved even though a discontinuous load intensity distribution was not used. The general test arrangement is shown in Fig. 26.

Description of the model configuration

The lateral dimensions of the rectangular plate used were such that the ratio of length to width approximated to that of a concrete road slab, the length being 24 inches and the width 12 inches.

Two plates of different thicknesses and one type of foundation were considered. The thicknesses selected were $1/4$ inch and $1/2$ inch; again these choices were guided from knowledge of typical highway pavement proportions.



The thickness of the foundation which rested on a rigid steel base plate was 2 inches. This thickness was considered to be a compromise between an excessive thickness which might result in the buckling of the 'springs' in the Winkler type foundation and the minimum thickness required for the foundation to act as a set of springs in the Winkler manner.

Applied load intensity distribution

The load intensity distribution described by a limited number of terms, was designed to resemble that of a wheel-load on the corner of the pavement. It consisted of a load intensity, \bar{v} , at the corner (0,0) which decreased rapidly to zero away from that corner without becoming negative. The function which described this load intensity distribution, p , is:

$$p = \bar{v}(1 - 1.25 \times 10^{-1}x + 5.2083 \times 10^{-3}x^2 - 7.2338 \times 10^{-5}x^3) \\ \times (1 - 2.5 \times 10^{-1}y + 2.0833 \times 10^{-2}y^2 - 5.7870 \times 10^{-4}y^3)$$

A value of $\bar{v} = 0.25 \text{ lbs/in.}^2$ was selected in order to obtain measureable value of plate deflection without them becoming excessive. The resulting load intensity distribution is shown in Figure 27.

Plate and foundation materials

Theoretically, each dependent variable can only be represented exactly by an infinite series. This applies even when the load intensity distribution is described exactly by a series of limited

length. However any major error will not arise directly through truncating the dependent variable series, but rather it will be due to partial violation of the basic assumption upon which the use of multipliers to satisfy the boundary conditions rests. This is best appreciated by considering the ij th term of a particular series, which is acted upon by a multiplier e.g.

$$M_{x_{ij}} x^i y^j (ax - x^2)$$

or, rewriting,

$$M_{x_{ij}} (ax^{i+1}y^j - x^{i+2}y^j)$$

Each simultaneous algebraic equation is the sum of the coefficients of a particular argument, for example, $x^i y^j$. If the maximum argument considered in generating the equations is $x^m y^n$ and in the above example $m=i+1$ and $n=j$ then the equation arising from $x^{i+2}y^j$ will not be considered. Hence although $M_{x_{ij}}$ satisfies the simultaneous equation arising from $x^{i+1}y^j$, it does not satisfy the equation generated from the sum of the coefficients of $x^{i+2}y^j$. The assumption implied by using the multiplier technique to satisfy the boundary conditions is that m and n are sufficiently high, and the expansion converges sufficiently rapidly, for the effects on $M_{x_{ij}}$ of this unconsidered equation to be negligible.

Because of the low order of the truncated dependent variable series this assumption is not completely satisfied and so its adverse effects must be minimised in the design of the experimental investigation,

in particular by the choice of the properties of the plate and foundation. If each w_{0ij} in the power series expansion of w_0 is multiplied by an argument $x^i y^j$, then the errors in the coefficients of w_0 (and similarly the other dependent variables) arising through the non-satisfaction of certain algebraic simultaneous equations are magnified and the errors are functions of x and y .

In the experimental investigation described here, these errors were minimised in the plate region which was of major interest - in this case this was the area around the maximum load intensity - by concentrating this region of maximum stress and deformation as closely as possible in the origin. This meant that the magnifying effect of, for example, $x^i y^j$ on w_{0ij} was reduced until at the origin only the first term of the dependent variable series was significant and thus there was no magnification of the error in this coefficient. This led naturally to the maximum load intensity being placed at the corner which was the origin for x and y .

An added advantage of the above arrangement was that it allowed the edge effects of the plate to play a major part in the distribution of stresses and deformations in this region, thereby enabling to some extent the ability of the mathematical model to analyse the effect of these free edge boundary conditions to be utilized.

The elastic properties of the plate and foundation were

principally chosen also to bring the area of major deformation as near as possible to the origin. A plate of low flexural stiffness and a foundation of high support stiffness were chosen with this aim in mind. The plate material was a hard black rubber and the foundation material was an industrial latex foam rubber.

In order that the foundation would satisfy the Winkler assumption the 2-inch thickness of foam rubber was cut vertically into individual blocks, mostly $1\text{-}\frac{3}{8}$ inches x $1\text{-}\frac{3}{8}$ inches. At the outer edges of the foundation the size of block was increased slightly so that they could stand flush with the edges of the plate. Each block was assumed to act as a vertical 'spring'. This block was small enough for the major portion of its stiffness to be axial but not so small as to create the possibility of its buckling under load.

It might be noted that the actual thickness of the foundation is not a factor in the analysis and although this model foundation is not, of course, the same as an actual subgrade, it does satisfy the theoretical requirements in that at some depth, d , the deflection is zero. Here, this depth is 2 inches, in an actual pavement the depth would be infinite. The factor which enables the theory to apply to both cases is that the modulus of subgrade reaction k , is a function of the depth of the particular foundation being considered.

It is likely that transverse shear stresses due to the

stiff foundation, and transverse compression due to the low stiffness of the plate, would be influencing factors in the distribution of stresses and deformations. The models were not however, designed with this principally in mind because, although these stresses are of major interest, it was considered that they would be most difficult to examine and discuss because of the inaccuracies in the values of stresses and deformations likely to result from truncation of the power series expansions.

Upper and lower surfaces of the foundation

At the interface between the plate and foundation full continuity of transverse direct stresses on both upward and downward movement of the plate is preserved in the theoretical analysis. Although physical attachment of the plate to the foundation was required to completely satisfy this assumption, this presented experimental difficulties since more than one plate had to be tested. In order to attain the same end, without having to connect, for example by gluing^e, the plate and foundation together at the interface, the foundation was precompressed; this was achieved by the application of a uniformly distributed load over the area of the plate, the deflection of which exceeded any subsequent upward movement due to the test load.

To retain the foundation blocks in position they were glued to a rigid base. The thickness of the model foundation was considered

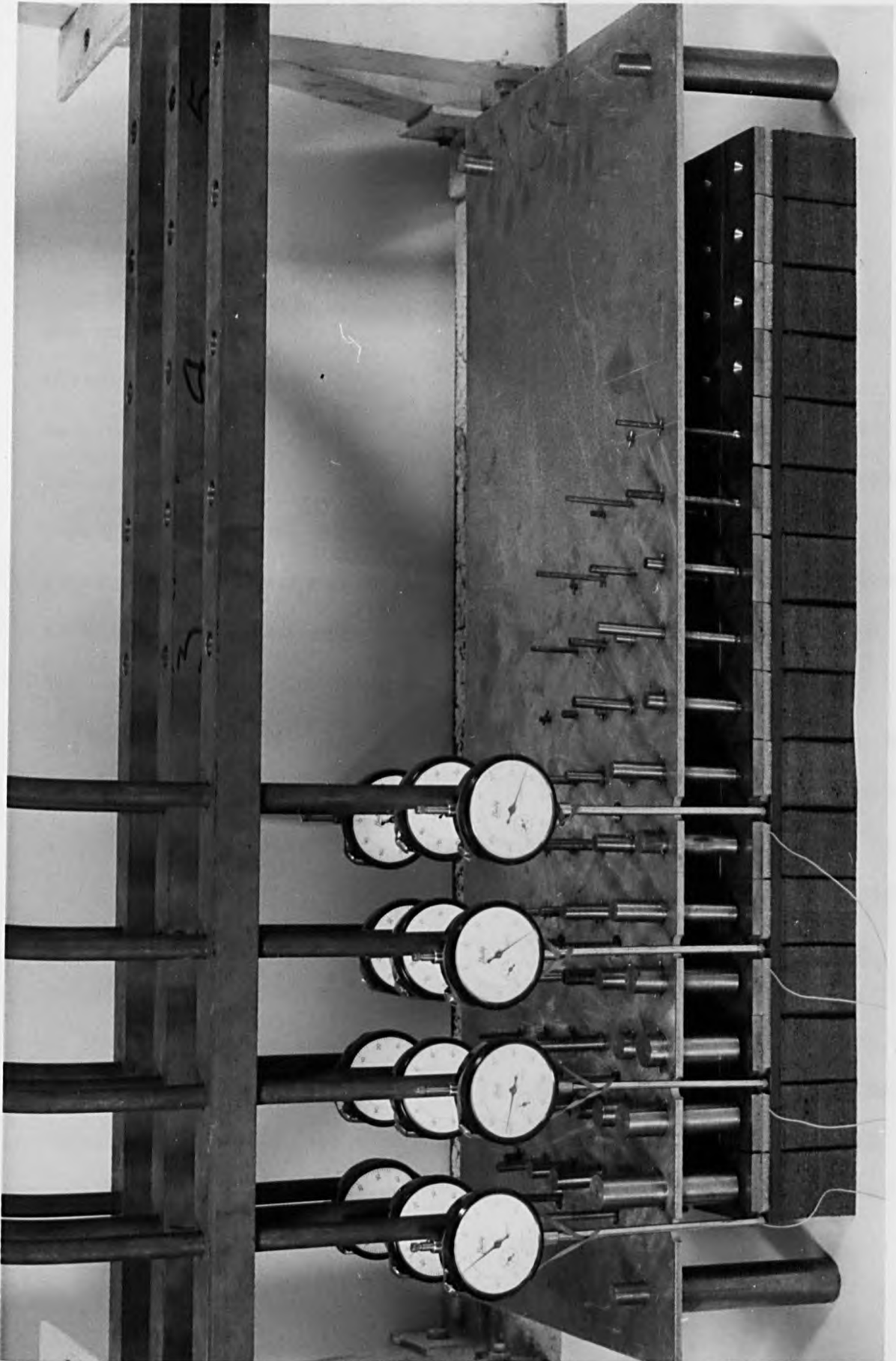
and the other side of the plate, the load is applied through the steel and foam rubber square pads. The load intensity is shown in the form of rods applied to the plate through the steel and foam rubber square pads. The load intensity is shown in the form of rods applied to the plate through the steel and foam rubber square pads. The load intensity is shown in the form of rods applied to the plate through the steel and foam rubber square pads.

Plate 1: The experimental apparatus used to test the model plate/

foundation system. Note that the load intensity and distribution in the form of rods is shown applied to the plate through the steel and foam rubber square pads.

The load intensity is shown in the form of rods applied to the plate through the steel and foam rubber square pads. The load intensity is shown in the form of rods applied to the plate through the steel and foam rubber square pads. The load intensity is shown in the form of rods applied to the plate through the steel and foam rubber square pads.

The load intensity is shown in the form of rods applied to the plate through the steel and foam rubber square pads. The load intensity is shown in the form of rods applied to the plate through the steel and foam rubber square pads.

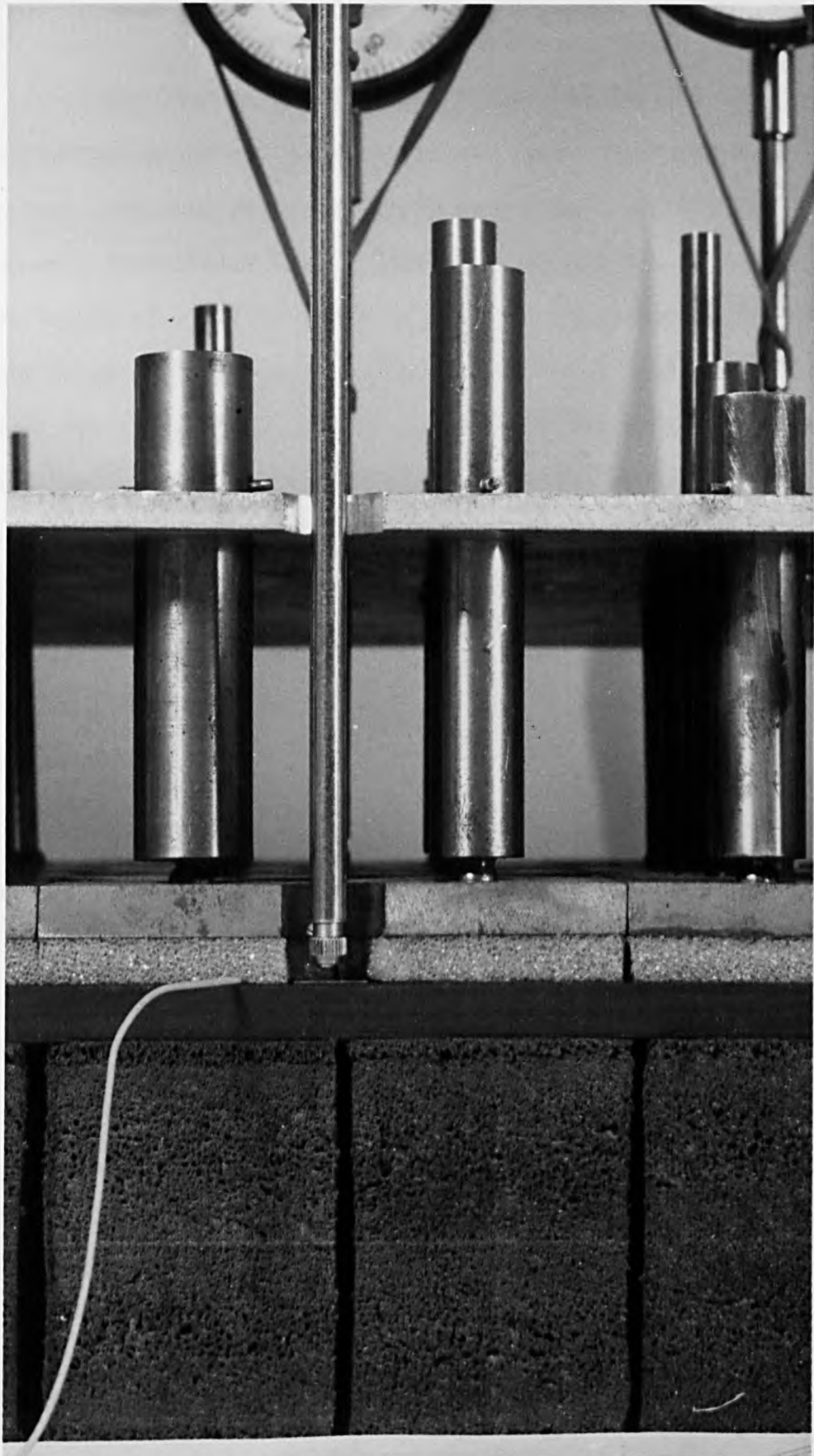


to be sufficient to avoid this arrangement having any undue effect on the distribution of deflections.

The test rig

The principal aim was to measure the deflections over the corner of interest and to compare them with those given by the theoretical analysis. Unfortunately, it proved impracticable to determine the experimental principal strains over the upper surface of the plate because none of the strain measuring equipment considered, including electrical resistance strain gauges, had the obvious requirements of both an effective stiffness which was lower or equal to that of the plate rubber and a sufficiently short gauge length.

Plates 1 and 2 show a general view and close up, respectively, of the load intensity distribution being applied to the 1/4-inch thick rubber plate. The load intensity distribution applied to this and the other plate had a maximum value of 0.25 lbs/in² at the origin and tended rapidly to zero as the distance from the origin increased. In order that the foundation could be precompressed sufficiently a uniformly distributed load was applied over the surface of the plate in the form of a 1/4 inch thick layer of steel. With the intention of preserving full contact between the steel layer and the deformed rubber plate, the steel layer was cut into squares of 1-1/2 inch side and a 1/4 inch thick piece of soft foam rubber of similar shape was glued to the lower face of each square. (see Figure 26).



The load intensity distribution was applied to the plate and foundation through these steel and foam rubber pads. First, the load over each square was represented by a statically equivalent uniformly distributed load. This was then applied at the centre of each square of steel as a point load; the square was sufficiently rigid to uniformly spread the load. The total load applied to each square was in the form of a steel circular rod of the required weight. The weight of each rod was transferred to the centre of each square through a steel ball of 1/4-inch diameter which was soldered to the base of the rod and seated in a conical depression in the centre of the pad, as shown in Plate 2. This avoided the creation of secondary stresses during rotation of the pad when it took up the deflected surface.

A practical difficulty arose in holding the rods in position and yet allowing them to move downwards during the deflection of the plate. This was overcome by having vertical guides down which each rod could move freely. These guides were in the form of slightly over-size holes in a 1/4-inch thick horizontal aluminium plate through which the rods then passed. The aluminium plate was positioned approximately 1.7 inches above the top of the steel squares and was supported at its corners which lay outside the area of the model plate and foundation, as is shown in Plate 1.

The load intensity had to be capable of being applied instantly at all points over the area of the plate. Thus, each steel

ball soldered to the base of a rod was initially placed a very short distance above the conical seating of the corresponding steel square. This was accomplished by placing a 1/16-inch diameter cross-piece through each rod so that the rod was supported clear of the model by the cross-piece resting on the top of the aluminium plate. (see Figure 26). The load was then applied by lowering the aluminium plate a distance of a 1/4-inch; this resulted in the balls coming to rest in the conical depressions and the weight of the rods being transferred from the aluminium plate to the squares of steel and thus to the rubber model (see Plate 2).

The ability to vary the size of the rods for different points on the plate was an essential requirement, due to the wide range of loads which it was intended to apply to the steel squares. For a large portion of the plate, the load applied to each square was extremely small and it was decided on practical grounds to ignore those which were less than one percent of the maximum value. These small loads would have been applied at points which were quite large distances from the origin and, consequently, would have had little effect on the deformation in the region around the origin. The diameter of the rods varied from 3/4 inch to 1/8 inch and their length from 1.90 inches to 3.66 inches.

Measurement of plate deflection

The intention was to measure the deflection of the plate

The dial gauge is used to measure the deflection of the plate at various points. The dial gauge is placed on the surface of the plate and the dial is read. The dial gauge is used to measure the deflection of the plate at various points. The dial gauge is placed on the surface of the plate and the dial is read. The dial gauge is used to measure the deflection of the plate at various points. The dial gauge is placed on the surface of the plate and the dial is read.

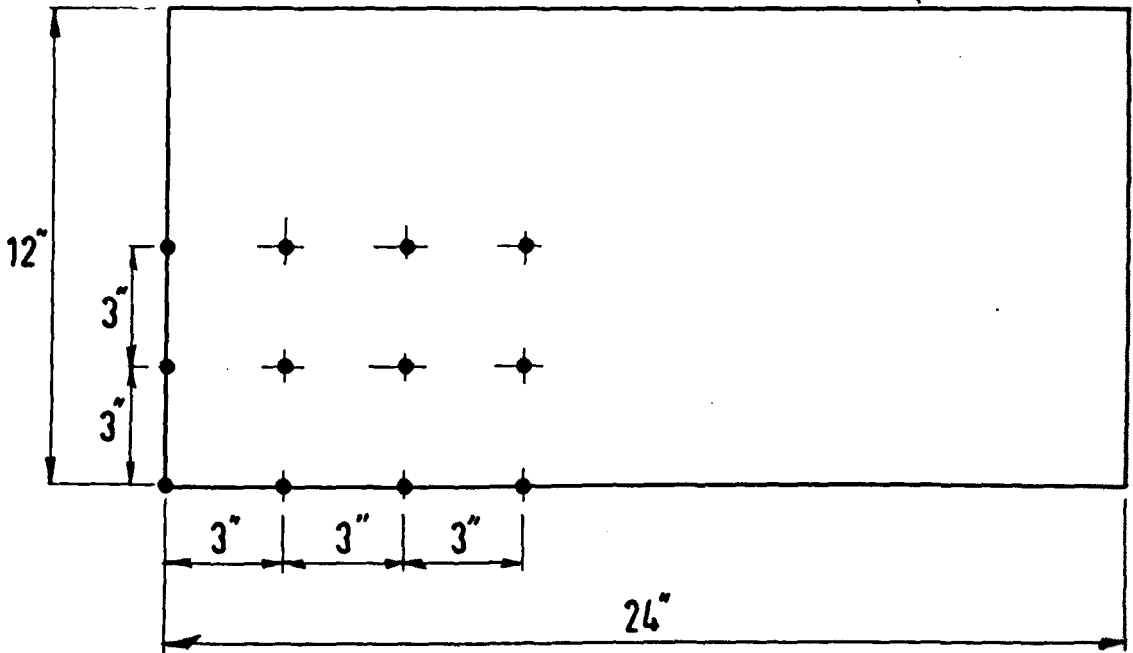
Figure 28. Dial gauge positions for the measurement of plate

deflection. The dial gauge is used to measure the deflection of the plate at various points. The dial gauge is placed on the surface of the plate and the dial is read. The dial gauge is used to measure the deflection of the plate at various points. The dial gauge is placed on the surface of the plate and the dial is read. The dial gauge is used to measure the deflection of the plate at various points. The dial gauge is placed on the surface of the plate and the dial is read.

The dial gauge is used to measure the deflection of the plate at various points.

The dial gauge is used to measure the deflection of the plate at various points.

Boundary of the model plate



Legend Dial gauge positions •

at a number of points over the area of special interest, i.e. the area around the origin in which the major deformation could be expected to take place. The theoretical analysis gives the actual deflection of the lower face of the plate and also the deflection which would result from neglecting the effect of transverse compression. Unfortunately, the practical difficulties of measuring any deflection other than the upper surface deflection of the plate are so large as to make such a task impracticable. Further, for a load intensity of 0.25 lbs /in.^2 which is the maximum occurring on the plate, a plate thickness of $1/2$ -inch and a modulus of elasticity of 750 lbs/in^2 , the transverse compression is only in the order of 1.7×10^{-4} inches which is barely the order of discrimination of the most sensitive dial gauges. Thus, for the purpose of the experimental results, the deflection of the upper face of the plate was considered as being representative of those of all corresponding points throughout the plate thickness.

In the course of the experimental study the deflection of the upper surface of the plate was measured by dial gauges which were placed in the positions shown in Figure 28. They were rigidly fixed to a framework above and the probes of extended length passed through holes drilled in the aluminium sheet. In order that the probe points could reach the model, holes were also drilled in the squares of steel and soft foam rubber; the effect of this

upon the deformation of the model was assumed to be negligible. To avoid erroneous readings which might have resulted from the probe of the dial gauge penetrating the rubber of the plate, a small pad of steel, 0.25 inches x 0.25 inches x 0.005 inches, was placed under each probe and glued to the upper surface of the rubber plate. In order, also, to prevent the pressure of the probe on the steel pad from materially affecting the deflection of the plate locally at the point of contact, the probe, when the deflection was being measured, was lowered until contact was only just made with the thin steel pad. This was facilitated by the help of an electrical circuit which consisted of a wire passing from the dial gauge support framework through, first, a small electric bulb and, second, a 6-volt battery, from which wires passed to each steel pad. The circuit was completed and the bulb lit when contact was made. Before and after the load was applied each probe was lowered in turn and the dial readings were noted.

Elastic Properties of the Plate and Foundation Materials

The properties required for the analysis were the modulus of elasticity and Poisson's ratio of each plate and the modulus of subgrade reaction of the foundation.

Elastic properties of the plates

Here, the principal difficulty in determining the elastic

Figure 29. Apparatus used to determine the elastic properties

of the plate by measuring the change in gauge length

due to the application of an in-plane tensile force to the specimen.

The apparatus consists of a specimen, a gauge, and a load cell.

The specimen is a rectangular plate of uniform thickness.

The gauge is a device that measures the change in length of the specimen.

The load cell is a device that measures the force applied to the specimen.

The apparatus is used to determine the elastic properties of the plate.

The elastic properties are determined by measuring the change in gauge length

due to the application of an in-plane tensile force to the specimen.

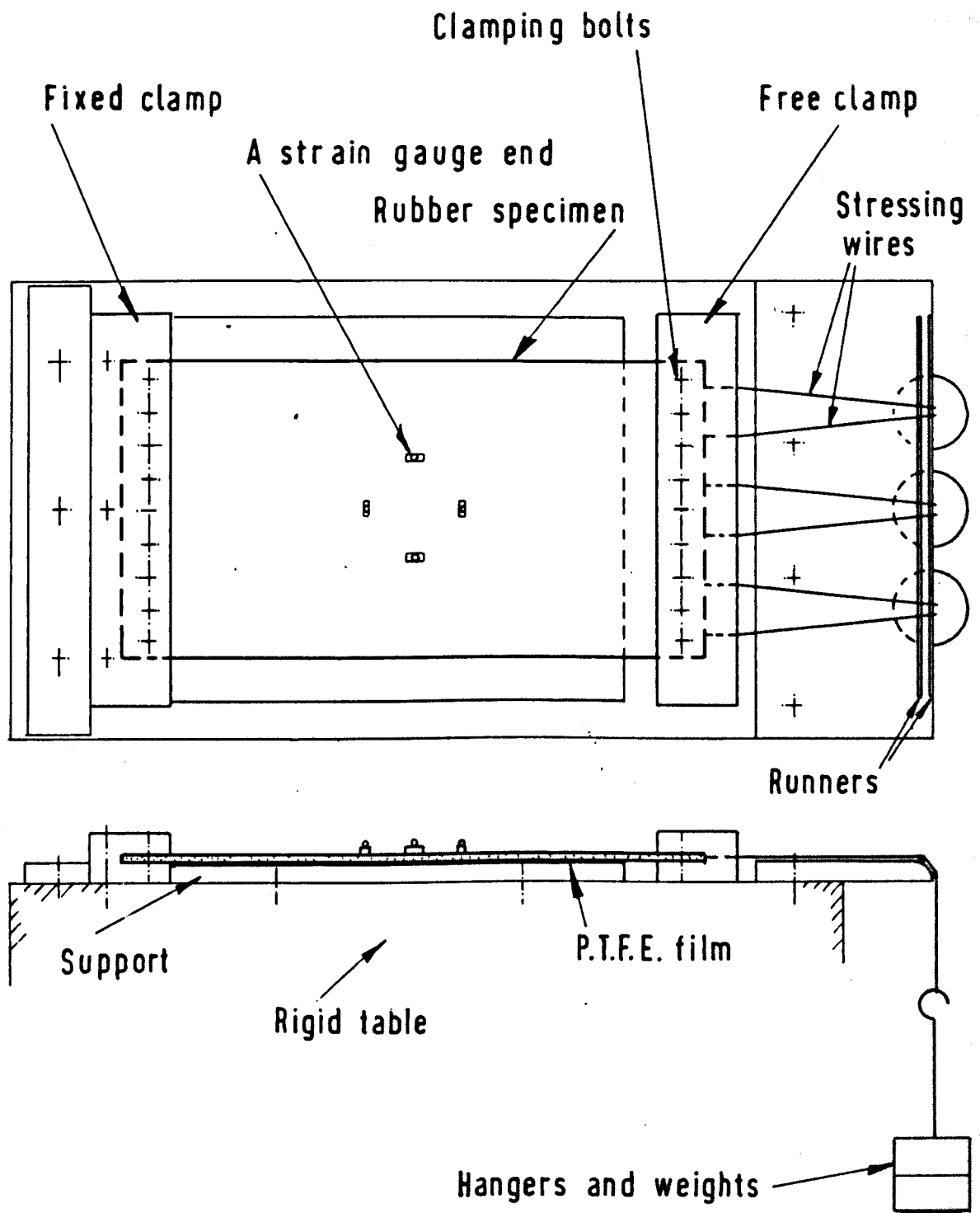
The apparatus consists of a specimen, a gauge, and a load cell.

The specimen is a rectangular plate of uniform thickness.

The gauge is a device that measures the change in length of the specimen.

The load cell is a device that measures the force applied to the specimen.

The apparatus is used to determine the elastic properties of the plate.



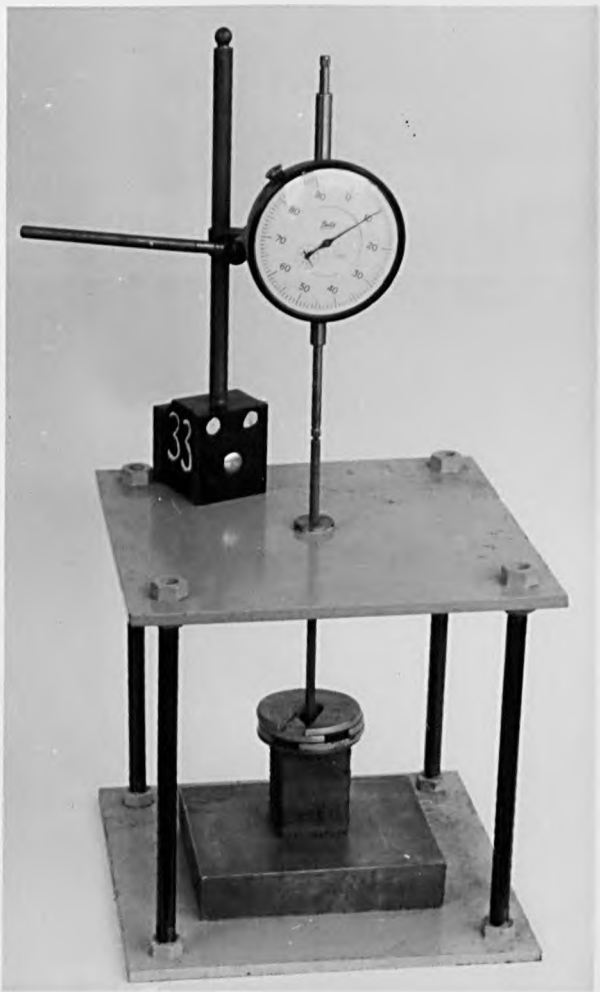
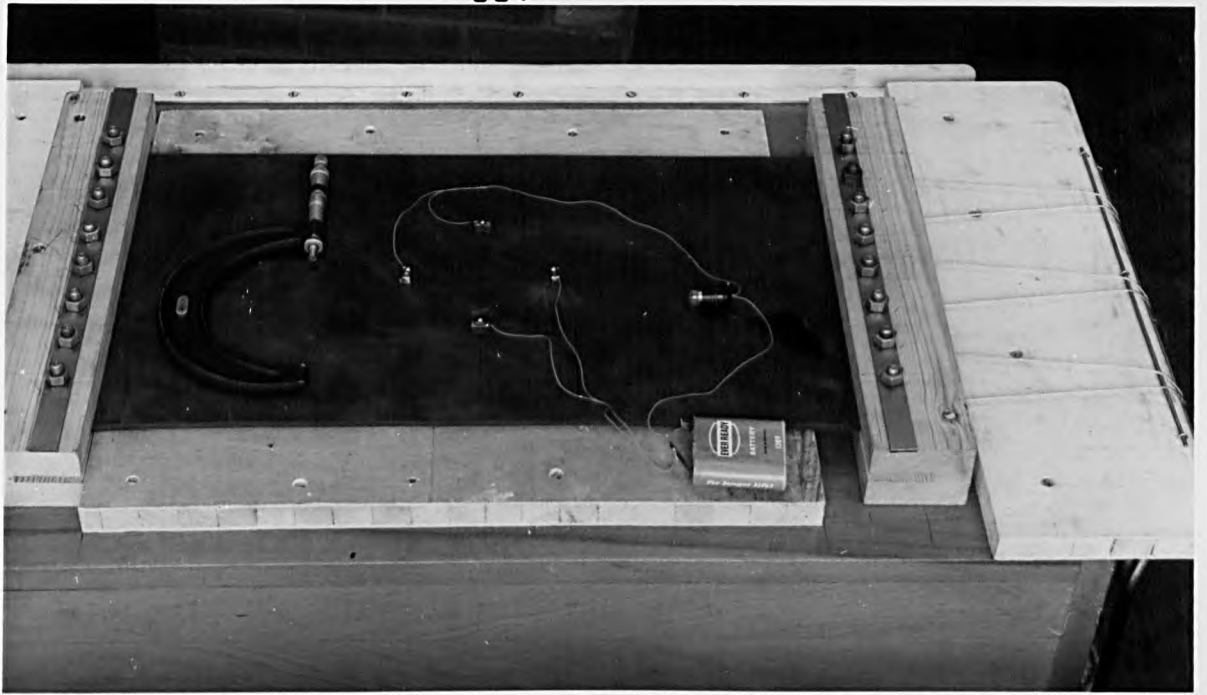
properties of a hard rubber is that the electrical strain gauges commercially available are many times stiffer than the rubber itself. Thus, the gauges would stiffen the test material at the points at which they were affixed. This would result in apparent properties which could be grossly incorrect.

Strain measurement is essential for the direct determination of Poisson's ratio and a mechanical method of measuring strain is considered as being the simplest and most reliable solution to the above difficulties. The material was stretched in one direction and the increases of longitudinal and transverse gauge lengths were measured mechanically. The experimental set-up is shown in Figure 29 and Plate 3.

After the model tests were carried out, each rubber plate was taken and placed in the testing apparatus to determine its elastic properties. Close fitting wooden clamps were placed over each end of the plate and were bolted-up to grip the rubber, see Figure 29. The clamped plate was then placed on a solid wooden table and one of the clamps screwed down to its top. Wires were attached to the other clamp at the level of the mid-plane of the specimens; see Figures 29. These wires were then passed over metal runners vertically down to three weight-hangers. To ensure that no bending stresses would be present a wooden spacer was placed between the table-top and the specimen. To reduce the friction between the specimen and the spacer

Plate 3. The apparatus used to determine the elastic properties of the plate. Shown are the electrical contact circuit and the 4-inch micrometer.

Plate 4. The apparatus used to determine the modulus of subgrade reaction of the foundation material by obtaining the load deflection curve of an individual block of the rubber foundation.



a sheet of P.T.F.E. was placed between them.

The longitudinal and transverse strain gauge lengths were placed about the centre of the upper surface of the rubber plate ; one parallel, and the other perpendicular, to the direction of the applied uni-directional tensile stress. The gauge lengths themselves were each chosen to be slightly less than 4 inches; this was considered to be the maximum length at which the boundary effects of the plate sides and its clamped ends would not affect the strain incurred over the gauge lengths. Each end of the gauge length was defined by a 1/8-inch diameter steel ball soldered to a 1/2-inch length of steel of 1/4-inch x 1/4-inch section which, in turn, was glued to the rubber plate; this is shown in Figure 29 and Plate 3.

The gauge length between the outside edges of each corresponding pair of steel balls was measured during the test by means of the micrometer shown in Plate 3. In the course of testing it was found that the micrometer ratchet was not sensitive enough to stop the closing movement of the micrometer when contact was just being made between the micrometer face and outer edge of the steel ball at each end of the gauge length. To overcome this source of inaccuracy an electrical circuit 'alarm' was introduced, similar to that used previously for measuring deflection in the model tests; see Plate 3.

In tensioning the specimen a number of small weights were

placed initially on the hangers to apply a pre-tension to the rubber plate and the first gauge readings were taken. Then additional weights were applied in increments, up to a maximum load of 105 lbs for the 1/2-inch plate and 60 lbs for the 1/4-inch plate; each increment was 15 lbs. After the application of each increment, the wooden spacer was vibrated slightly to release any frictional resistance before the gauge lengths were measured.

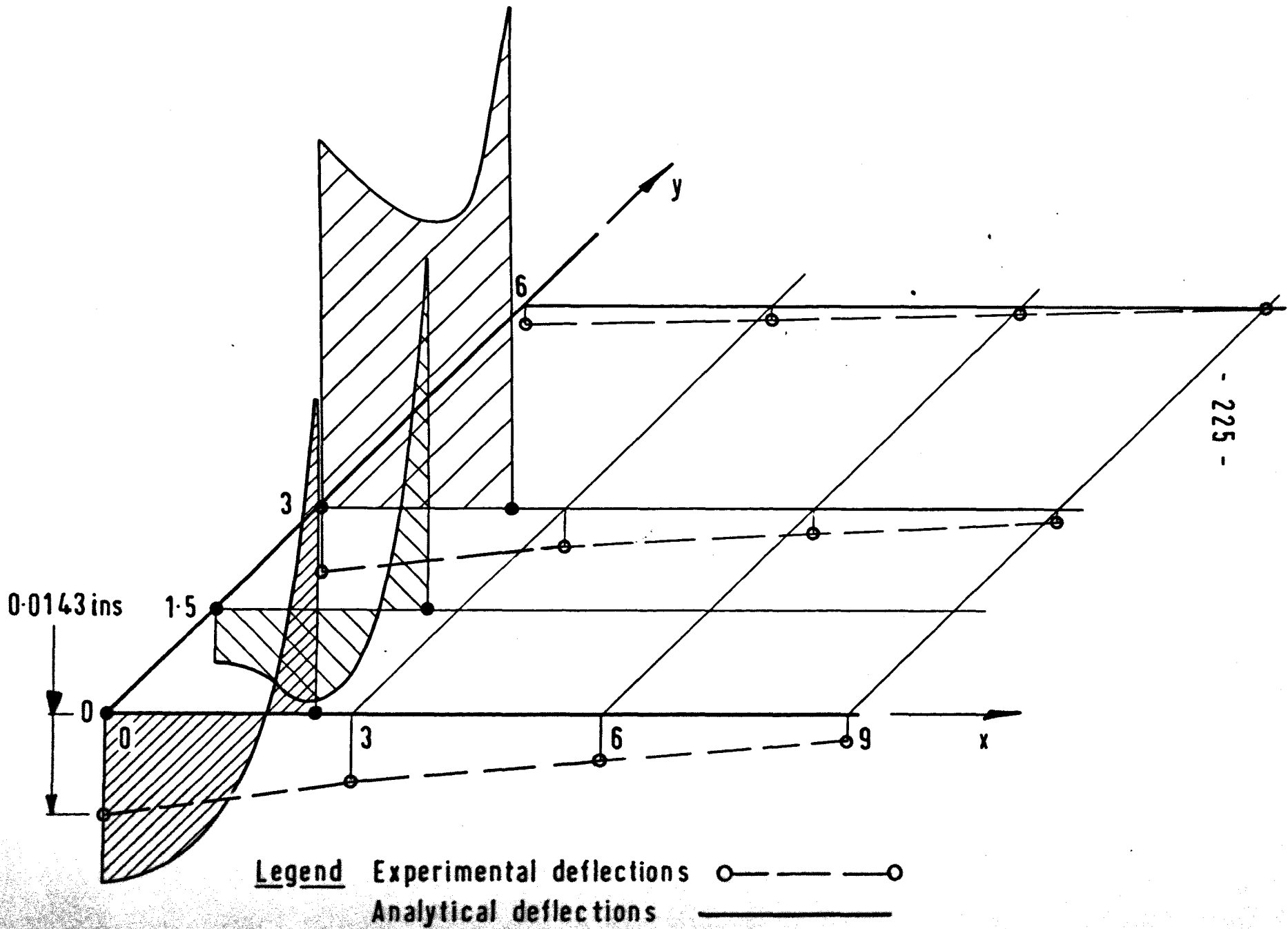
The stresses were computed using the original cross-sectional area of the specimen. When the standard stress/strain plots were drawn for each rubber plate, they were found to be linear. The values of modulus of elasticity obtained from these data for the 1/4-inch and 1/2-inch plates were 777 and 905 lbs/in.², respectively. The corresponding values of Poisson's ratio were 0.322 and 0.416, respectively. (The perhaps surprising difference in the elastic properties between the 1/4-inch and 1/2-inch rubber plates was confirmed by their International Rubber Hardness values; these were 58.0 and 68.0 degrees for the 1/4-inch and 1/2-inch plates, respectively.)

Elastic properties of the foundation

By definition, the modulus of subgrade reaction, k , is the pressure required to cause unit deflection of the surface of a foundation. There were two methods available for obtaining this k -value. The first was to test a single 1-3/8 inch x 1-3/8 inch x 2-inch block

in compression and then to plot the resulting load - deflection curve from which k could be calculated. The second method was to test the entire foundation in-situ in a similar manner. The former method had the advantage that it would be able to indicate the nature of the load-deflection curve. A disadvantage was that although each block was $1\frac{3}{8}$ inches x $1\frac{3}{8}$ inches in area, it actually 'supported' an area of $1\frac{1}{2}$ inches x $1\frac{1}{2}$ inches due to the $\frac{1}{8}$ -inch gap between adjacent blocks. Thus the apparent value of k obtained from testing a block could be expected to be incorrect if used to represent the foundation. (This could, of course, be overcome by considering the area, over which the load is applied, to be $1\frac{1}{2}$ inches x $1\frac{1}{2}$ inches when computing k). The alternative experimental method of determining k eliminates any doubt in the validity of the single block test when applied to the complete foundation. For this reason it was considered that more confidence may be placed in the value of k determined from an in-situ test. Nevertheless both methods were used to obtain comparative values of k.

First of all, a small testing frame was employed to determine the load-deflection curve for a single block; the set-up is clearly shown in Plate 4. The load/deflection plot which resulted from 0.2 lb. increments up to a maximum of 1.0 lb. was linear. Using the actual area of the block ($1\frac{3}{8}$ inches x $1\frac{3}{8}$ inches) the value of k was found to be $14.50 \text{ lbs/inch}^2/\text{inch}$; using the area supported by the block when part of the foundation ($1\frac{1}{2}$ inches x $1\frac{1}{2}$ inches),



the value of k obtained was 12.20 lbs./inch²/inch.

In the second method of obtaining the modulus of subgrade reaction a linear load/deflection relationship could be safely assumed and thus, the uniformly distributed load was applied in a single increment. The k-value obtained from this test was 12.56 lbs./inch²/inch.

As explained previously, more confidence may be placed in the k-value which is determined on the basis of loading the foundation in-situ. Thus of the three moduli of subgrade reaction values, the one which was selected as being most representative was the figure of 12.56 lbs./inch²/inch.

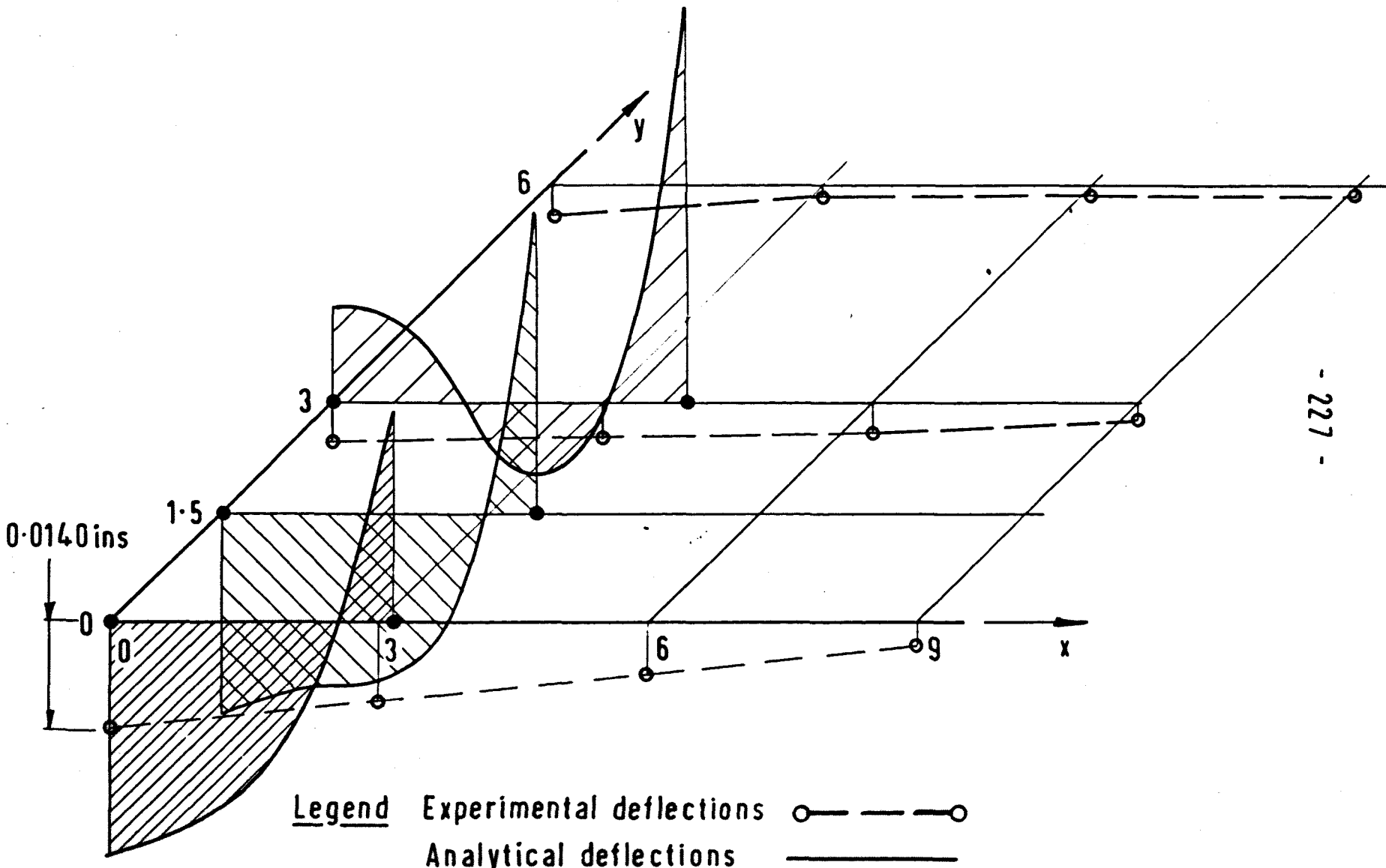
Obtaining the Analytical Results

The experimental deflections and analytical plate deflections, for n=4, are presented for both plate thicknesses in Figure 30 and 31, for the portion of the plate around the origin.

The analytical deflections were obtained from the three computer programs which are presented in Appendix C and which have already been described in detail.

The form of the input data for the 1/2-inch thick plate is given below and begins with that for the first program, entitled 'Setting-up the Simultaneous Algebraic Equations', thus

<EXPERIMENTAL MODEL-HALF INCH PLATE THICKNESS>



24;12;4;0.5;0.416;905;12.56;
0.25; -6; 25₁₀⁻²; 5.20833₁₀⁻³; -1.446759₁₀⁻⁴; 0;
-3.125₁₀⁻²; 7.8125₁₀⁻³; -6.5104156₁₀⁻⁴; 1.80844906₁₀⁻⁵; 0;
1.3020833₁₀⁻³; -3.2552081₁₀⁻⁴; 2.712673003₁₀⁻⁵; -7.535203945₁₀⁻⁷; 0;
-1.808449₁₀⁻⁵; 4.5211225₁₀⁻⁶; -3.7676014305₁₀⁻⁷; 1.0465561275₁₀⁻⁸; 0;
0;0;0;0;0; →

The paper tape output from this program was fed without alteration, into the second program entitled 'Solving the Simultaneous Algebraic Equations.' The output from this second program consisted of the coefficients of the independent variables and these were then used to punch the input tape for the final program entitled 'Determination of Stresses, Strains and Deflections', thus

<EXPERIMENTAL MODEL-HALF INCH PLATE THICKNESS>

24;12;0.5;0.416;905;12.56;4;1;1;99;

p coefficients in rows

w₀ coefficients in rows

M_x coefficients in rows

M_y coefficients in rows

H coefficients in rows

0;0;

0;0.75;

0;1.50;

.

.

co-ordinates of the remainder of the 99 points at which the analytical deflections are required

.
. →

The form of the analytical results produced on the final line-printed output sheet is shown in Figure 25. The deflection values thus obtained were then used to plot the analytical surface of deflection shown in Figure 31.

Discussion of Analytical and Experimental Results

The main points which come to light from a comparison of analytical and experimental results can be isolated and dealt with in turn.

1. As was expected, the plate deflection values-which can be seen in Figures 30 and 31 - increased rapidly with the distance away from the origin, thereby indicating that the radii of convergence R_1 and R_2 of the w_0 series are very small. The reason for this has already been explained in this chapter and so need not be repeated here. It does confirm however, that there is a considerable need to concentrate the region of deformation as closely as possible to the origin in order to obtain useful results for the purposes of the experimental application of this form of solution.

2. When the analytical and experimental corner deflections are compared it is seen that they are of the same order of magnitude

even though at short distances from the origin, e.g. 4.5 inches, the analytical plate deflections are many times larger than the corresponding experimental corner deflections.

3. It must be pointed out that the differences which do exist between the analytical and experimental deflections at the corner of the plate are to a large extent due to the experimental difficulties in applying the load intensity distribution in the exact theoretical manner and also in measuring the resulting deflections. In the test, the intensity applied at the origin was not 0.25 lbs./inch², as it should have been, but was 0.187 lbs./inch² due to the finite nature of the loading pads. With a plate of higher flexural stiffness, for example had it been of perspex, this discrepancy, would not have had any significant effect. The low stiffness of the plate material, which was chosen to meet other requirements which have already been explained, is indicated by the similarity of the deflection surfaces of the 1/4-inch and 1/2-inch plates. Consequently the experimental corner deflections of the plates have been due to an actual intensity of 0.187 lbs /inch² rather than the theoretical 0.25 lbs/inch² which was used in the analysis. As a uniformly distributed load of 0.187 lbs/inch² produces a theoretical deflection of 0.0149 inches and an intensity of 0.125 lbs /inch² produces one of 0.0199 inches, this conclusion would seem to be confirmed because the actual corner deflections of the 1/4-inch and 1/2-inch thick plates are 0.0143 inches and 0.0140 inches, respectively.

4. Two points which are illustrated by the results shown in Figure 25, which refers to the 1/2-inch model, should be noted. Firstly, the interface deflection at a given point is slightly less than that of the plate deflection; this is due to the presence of lateral plate support when transverse effects are included in the analysis. Secondly, the principal directions of the stresses are quite accurate even though the magnitudes of the principal stresses become excessive as the distance away from the origin increases.

5. Because of the unrealistic form of the two analytical plate deflection surfaces, (shown in Figures 30 and 31) it would be unwise to make any detailed recommendations on the applicability of the analysis to plate/foundation systems based on the comparison of these surfaces with experimentally measured deflections. Nevertheless, the results of this analysis are useful to further the understanding of the mathematical analysis.

6. An important fact which comes to light when examining the series coefficients of the independent variables is that the coefficients $M_{x_{oj}}$ and $M_{y_{io}}$ for any value of j and i , respectively, have values as large as $5.0 \cdot 10^{-7}$ even though, theoretically, they should be equal to zero, according to equations (99 and 100). The most likely explanation is that the system of simultaneous algebraic equations, generated from equations (96 to 101) for this particular problem, is ill-conditioned. It is probable that because of the low flexural stiffness of the plate there is very little redistribution

of the load and hence the load intensity at a point tends to pass through the plate, directly to the foundation. Thus, the major structural factor is the vertical equilibrium of the system and consequently the differential equation describing the vertical equilibrium of the system, equation (71) dominates the set of differential equations, equations (66 to 71). Hence, the simultaneous algebraic equations generated from equation (101), which is the i th form of equation (71), predominates over the remaining equations. This ill-conditioning is found to be confirmed when, on substituting the solutions back into the algebraic equations, those which are found to have negligible residuals are those generated from equation (101).

7. The very rapid increases in the theoretical values of plate deflection, (shown in Figures 30 and 31) have previously been explained as being due to the magnification, by the series arguments, of errors in the series coefficients. These errors are caused by the inability of the coefficients of the variables to satisfy all algebraic equations in which they occur. To some extent this explanation can be confirmed by comparing the plate deflection surface for a truncated power series limit of $n = 3$ to that with a limit of $n = 4$. For either plate thickness the result is that for $n = 3$ the deflection surface is found to remain finite at a much greater distance from the origin than for $n = 4$. For example, in the case of the 1/2-inch thick plate, the deflection at the point

whose co-ordinates are (6.0,0) is equal to - 0.023 inches, whereas the deflection at the same point for $n = 4$ is calculated to be 0.618 inches. If theoretically, a more accurate solution should arise when n is taken equal to 4 rather than 3, then the magnification caused by multiplying coefficients by $x^4 y^j$ and $x^i y^4$, in the case of $n = 4$, is likely to be the cause of the much more rapid divergence of the surface. This hypothesis is supported by the fact that at the origin where no magnification takes place, the solution for $n = 4$ gives a plate deflection which agrees more closely with the experimental corner deflection for both the 1/4-inch and 1/2-inch plates.

8. The effect of the coefficients of the independent variables not satisfying particular algebraic equations in which they occur and the manner in which this difficulty can be overcome by increasing the number of terms in the series, may be illustrated as follows. Consider the theoretical analysis (using the computer programs) of, say, the 1/4-inch thick plate and foundation to which a uniformly distributed intensity of 0.25 lbs/inch^2 is applied, and where the truncated loading series has a limit of $n = 4$. A uniform deflection of 0.0199 inches is theoretically produced by such an applied load intensity, while there are no bending moments, twisting moments or shear stresses induced in the plate. As a result all the coefficients of the independent variables should be zero except w_{00} .

In fact, however, the analysis produces coefficients which although small, are non-zero. The reason for this is that the neglected equations are those which would make the coefficients of the higher terms zero and these, in turn, - through the other equations - would make the coefficients of the lower terms of the series zero, thereby leaving only $w_{0\infty}$ to be non-zero. This disadvantage, which is emphasised in this example, is inherent in this method of solving the differential equations.

9. That this disadvantage can be overcome by increasing the number of terms in the series, i.e. by raising the limit of n , is also illustrated by these results. Relative to the series describing the load intensity distribution there are many more terms in the independent variables of this example than in that of the experimental analysis with its varying load intensity distribution. Although not graphically reproduced here, it was found that the deflection of the plate remained at a value of 0.0199 inches for a large portion of its area (including the origin), even though the terms of the deflection series were non-zero. The principal stresses were also found to remain close to zero.

10. This limited application of the analysis has shown that the disadvantages of the solution are associated with the truncation of the power series describing the dependent variables.

CONCLUSIONS

The major conclusions which may be drawn from the foregoing research program are:

1. A thick rectangular plate attached to a Winkler foundation and loaded transversely by a general load intensity distribution, (referred to as the first boundary value problem), can be described by a mathematical model consisting of nine linear partial differential equations of elasticity and three boundary conditions at each free edge of the plate. The prescribed dependent variable is the load intensity distribution, p , and the unknown dependent variables are the bending moments, M_x and M_y , the shear forces, V_x and V_y , the twisting moment, H , the weighted average rotations α_0 and β_0 , the weighted average deflection, w_0 , and the deflection of the lower face of the plate, w_1 .

2. A thick rectangular plate which merely rests on a Winkler foundation, (referred to as the second boundary value problem), where loss of contact between the pavement and subgrade is allowed during upward deformation of the pavement, can also be described by a mathematical model. This consists of nine non-linear partial differential equations of elasticity and a set of boundary conditions which are similar to those of the first boundary value problem.

3. In each of the two analyses the pavement and subgrade can be considered to be a complete system and not simply a pavement

acted upon by the subgrade stresses.

4. The direct stress within the subgrade is expressible in the correct Winkler manner, i.e. as a function of the deflection of the lower face of the pavement and not, as in other published thick plate analyses, as some approximation to this e.g. the weighted average deflection.

5. The nine partial differential equations of the first boundary value problem are reducible to an equivalent system of six higher order partial differential equations in the dependent variables, p , w_0 , M_x , M_y , V_x , V_y and H .

6. The solution of the second mathematical model appears to be extremely difficult because of the non-linear nature of the associated partial differential equations.

7. A solution to the first boundary value problem is obtainable in terms of a system of simultaneous algebraic equations where the dependent variables are represented by power series or Chebyshev polynomials.

8. A non-trivial solution is not found to be possible with the particular forms of Fourier series used to represent the dependent variables although they are chosen to satisfy the boundary conditions.

9. In both the power series and Chebyshev polynomial solutions of the first boundary value problem the use of multipliers

to satisfy the boundary conditions suffers from an important disadvantage. This is that there are a number of algebraic equations which are not considered and yet within which coefficients of the truncated series arise. Consequently there are conditions, represented by these neglected equations, which are not satisfied by the dependent variables.

10. None of the power, Chebyshev or Fourier series representations of the circular wheel-load distribution is found to accurately describe the discontinuous load intensity distribution for the length of truncated series which is considered.

11. Difficulties which arise in the ability of the truncated Chebyshev series to describe anything other than a zero load intensity in the case of the circular wheel-load can be overcome by increasing the length of the polynomial expansion.

12. When the truncated series is of the minimum sufficient length to produce a non-zero load intensity, the Chebyshev expansion produces a surface which represents the wheel-load intensity better than do those of power or Fourier series of similar length as far as the circular area of contact is concerned.

13. Because of the continuous nature of the function, the Fourier series expansion follows the plane of zero intensity over the unloaded portion of the plate to a better degree than the other two forms of expansion.

14. In each of the three circular wheel-load distributions, the power series expansion produces a wave-like surface except in the area around the circular load. This is due to the greater sparseness of load intensity data points in those areas as compared with around the circular load.

15. The ability of the truncated power series expansion to represent the circular wheel-load intensity distribution is seen to be much improved by only a small extension in its length.

16. For a circular wheel-load, the minimum computer space required for the solution of the general simultaneous equations associated with the Chebyshev expansion is prohibitive as far as the computer facility available in the University of Leeds is concerned.

17. In the programmed solution of the simultaneous algebraic equations arising from the power series solution of the primary boundary value problem, $n = 4$ is the limit of the truncated power series expansions of the dependent variables which can be accommodated by the programs if the available computer fast store is 17,000 words (as is the case with the University's installation).

18. The numerical and experimental tests indicate that, given better computing facilities, the method using power series expansions should lead to a more satisfactory analysis of the first boundary value problem.

RECOMMENDATIONS FOR FURTHER RESEARCH

While these suggestions for further research are principally concerned with improving the programmed solution of the primary boundary value problem, some suggestions are also made with respect to other relevant points of interest.

1. A further examination should be made of the power series solution using a computer of larger capacity. This should enable power series of greater length to be used.
2. Re-programming the power series solution using disc files should be considered. This should eliminate the major limitation on the lengths of the power series expansions. The new limitation of required computer time will not be as acute as it would be with magnetic tape decks.
3. A detailed analysis of iterative methods of solution, such as that of conjugate gradients, is indicated, as these lend themselves to sparse matrices of coefficients. Work has already begun on this subject and is proving very promising.
4. Programming the Chebyshev polynomial solution to the primary boundary value problem is required. This, together with any one of the above suggestions, should produce more useful results because of the orthogonal nature of the Chebyshev polynomials.
5. The representation of the dependent variables in the primary boundary value problem by other forms of Fourier series

expansion, perhaps of a more general nature, is worthy of investigation.

6. The solution to the second boundary value problem might profitably be undertaken by applying one of the limited number of methods available for the solution of non-linear partial differential equations.

7. The analysis of a pavement/subgrade system in which the subgrade is considered to be a semi-infinite three-dimensional elastic solid should be given attention.

8. An analysis should be made for a pavement/subgrade system in which the rectangular slab is considered to have partial support from adjacent slabs by means of, say, dowel bars, as this situation is common in practice.

9. The programming of the analysis for dual and tandem wheel configurations and elliptical wheel contact shapes applied to the surface of the plate should be undertaken.

10. The application of these suggested analyses to experimental large scale pavement/subgrade systems is clearly indicated should the analyses prove successful in determining the stresses and deformations in laboratory models.

SELECTED REFERENCES

1. Department of Scientific and Industrial Research. Road Research Laboratory. Harmondsworth. Soil Mechanics for Road Engineers. London. Her Majesty's Stationery Office. 1952.
2. Steele, D.J. Classification of highway subgrade materials. Highway Research Board. Proceedings 25:376-384 and 388-392. 1945.
3. Porter, O.J. The preparation of subgrades. Highway Research Board. Proceedings 18:324-331. 1938.
4. Westergaard, H.M. Stresses in concrete pavements computed by theoretical analysis. Public Roads. 7(2):25-35. 1926.
5. Westergaard, H.M. Analysis of stresses in concrete roads caused by variations of temperature. Public Roads. 8(3):54-60. 1927.
6. Thomlinson, J. Temperature variations and consequent stresses produced by daily and seasonal temperature cycles in concrete slabs. Concrete and Constructional Engineering. 35(6):298-307, 35(7):352-360. 1940.
7. U.S. War Department. Office of the Chief of Engineers. Design of runways, aprons and taxiways at Army Airforce Stations. Washington D.C. Engineering Manual, Chapter XX. 1943.
8. Kelley, E.F. Application of the results of research to the

- structural design of concrete pavements. Public Roads. 20(5): 83-104. 1939.
9. Spangler, M.G. Stresses in the corner region of concrete pavements. Ames, Iowa. Iowa Engineering Experimental Station, Iowa State College. Bulletin 157. 1942.
 10. Pickett, G. A study of stresses in the corner region of concrete pavement slabs under large corner loads. Concrete Pavement Design. Portland Cement Association. Chicago. pp. 77-86. 1951.
 11. Burmister, D.M. The theory of stresses and displacements in layered systems and applications to the design of airport runways. Highway Research Board. Proceedings 23: 126-144. 1943. Discussion 23:144-148. 1943.
 12. Terzaghi, K. Evaluation of coefficients of subgrade reaction. Geotechnique. 5:297-326. 1955.
 13. Richart, F.E. and Zia, P. Effects of local loss of support on foundation design. American Society of Civil Engineers. Journal of Soil Mechanics and Foundation Division. SMI, Paper No. 3056:1-27. 1962.
 14. Sparkes, F.N. Stresses in concrete road slabs. Structural Engineer. 17(2):98-116. 1939.

15. Timoshenko, S. and Woinowsky-Krieger, S. Theory of Plates and Shells. New York. McGraw-Hill. 1959.
16. Nadai, A. Die Elastischen Platten. Berlin. Julius Springer. 1925.
17. Hagstrom, J., Chambers, R.E. and Tons, E. Low modulus pavement on elastic foundation. Highway Research Record 71:172-192. 1964.
18. Westergaard, H.M. Analytical tools for judging results of structural tests of concrete pavements. Public Roads. 14(10):185-188. 1933.
19. Westergaard, H.M. Stresses in concrete runways of airports. Highway Research Board. Proceedings 19:197-202. 1939.
20. Westergaard, H.M. New formulas for stresses in concrete pavements of airfields. American Society of Civil Engineers. Proceedings 73(5):687-701. 1947.
21. Murphy, G. Stresses and deflections in loaded rectangular plates on elastic foundations. Ames, Iowa. Iowa Engineering Experimental Station, Iowa State College. Bulletin 135. 1937.
22. Happel, H. Uber das Gleichgewicht von elastischen platten unter einer einzellast. Mathematische Zeitschrift. 6:203-218. 1920.

23. Hogg, A.H.A. Equilibrium of a thin plate, symmetrically loaded, resting on an elastic foundation of infinite depth. The Philosophical Magazine. 7th series, 25:576-582. 1938.
24. Terazawa, K. On the elastic equilibrium of a semi-infinite solid. Tokyo. Imperial University of Tokyo. Journal of the College of Science. XXVII, Article 7. 1916.
25. Hogg, A.H.A. Equilibrium of a thin slab on an elastic foundation of finite depth. The Philosophical Magazine. 7th series, 35:265-276. 1944.
26. Hogg, A.H.A. Pavement slabs on a non-rigid foundation. Proceedings of the Second International Conference on Soil Mechanics and Foundation Engineering. Rotterdam. III:70-74. 1948.
27. Love, A.E.H. Treatise on the Mathematical Theory of Elasticity. Cambridge. University Press. 1923.
28. Fox, L. Computation of traffic stresses in a simple road structure. Department of Scientific and Industrial Research. Road Research Technical Paper 9. Her Majesty's Stationery Office, London. 1948.
29. Burmister, D.M. The general theory of stresses and displacements in layered systems, III. Journal of Applied Physics. 16(5): 296-302. 1945.

30. Acum, W.E.A. and Fox, L. Computation of load stresses in a three-layer elastic system. *Geotechnique*. 2(4):293-300. 1951.
31. Whiffin, A.C. and Lister, N.W. The application of elastic theory to flexible pavements. *Proceedings of the International Conference on the Structural Design of Asphalt Pavements*. Ann Arbor, Michigan. University of Michigan. pp. 499-521. 1962.
32. Hank, R.J. and Scrivner, F.H. Some numerical solutions of stresses in two and three-layered systems. *Highway Research Board. Proceedings* 28:457-468. 1948.
33. Pickett, G. and Ai, K.Y. Stresses in subgrade under rigid pavement. *Highway Research Board. Proceedings* 33:121-129. 1954.
34. Pickett, G. and McCormick, F.J. Circular and rectangular plates under lateral load and supported by an elastic solid foundation. *Proceedings of the First U.S. National Congress of Applied Mechanics*. Chicago, Illinois. Illinois Institute of Technology. pp.331-338. 1951.
35. Livesley, R.K. Some notes on the mathematical theory of a loaded elastic plate resting on an elastic foundation. *Quarterly Journal of Mechanics and Applied Mathematics*. 6:32-44. 1953.

36. Pister, K.S. and Westmann, R.A. Bending of plates on an elastic foundation. *Journal of Applied Mechanics*. 29(2): 369-374. 1962.
37. Reissner, E. The effect of transverse shear deformation on the bending of elastic plates. *Journal of Applied Mechanics*. 67:A69-A77. 1945.
38. Hudson, W.R. and Matlock, H. Analysis of discontinuous orthotropic pavement slabs subjected to combined loads. *Highway Research Record* 131:1-48. 1966.
39. Kirchhoff, G.R. *Vorlesungen uber mathematische Physik, Mechanik*, Leipzig. 1876.
40. Timoshenko, S. *History of Strength of Materials*. New York. McGraw-Hill. 1953.
41. Reissner, E. On the theory of bending of elastic plates. *Journal of Mathematics and Physics*. 23:184-191. 1944.
42. Reissner, E. On the bending of elastic plates. *Quarterly of Applied Mathematics*. 5(1):55-68. 1947.
43. Reissner, E. On a variational theorem in elasticity. *Journal of Mathematics and Physics*. 29:90-95. 1950.
44. Mikhlin, S.G. *Variational Methods in Mathematical Physics*. Oxford. Pergamon Press. 1964.

45. Green, A.E. On Reissner's theory of bending of elastic plates. Quarterly of Applied Mathematics. 7(2):223-228. 1949.
46. Mindlin, R.D. Influence of rotating inertia and shear on flexural motions of isotropic, elastic plates. Journal of Applied Mechanics. 18:31-38. 1951.
47. Nagdhi, P.M. and Rowley, J.C. On the bending of axially symmetric plates on elastic foundations. Proceedings of the First Midwestern Conference on Solid Mechanics. Urbana, Illinois. University of Illinois. pp. 119-123. 1953.
48. Naghdi, P.M. The effect of elliptic holes on the bending of thick plates. Journal of Applied Mechanics. 77:89-94. 1955.
49. Frederick, D. On some problems in bending of thick circular plates on an elastic foundation. Journal of Applied Mechanics. 78:195-200. 1956.
50. Frederick, D. Thick rectangular plates on an elastic foundation. American Society of Civil Engineers. Transactions 122:1069-1087. 1957.
51. Coull, A. The direct stress analysis of swept cantilever plates of low aspect ratio. Aircraft Engineering. 37(6):182-190. 1965.
52. Yettram, A.L., O'Flaherty, C.A. and Fleming, M.E. The analysis of pavements under arbitrary loading: an application of

- variational methods to thick rectangular plates on elastic foundation. Proceedings of the Second International Conference on the Structural Design of Asphalt Pavements. Ann Arbor, Michigan. University of Michigan. pp. 201-211. 1967.
53. Fung, Y.C. Foundations of Solid Mechanics. Englewood Cliffs, N.J. Prentice-Hall. 1965.
54. Agrew, R.P. Differential Equations. London. McGraw-Hill. 1960.
55. Lanczos, C. Applied Analysis. London. Pitman. 1957.
56. Churchill, R.V. Fourier Series and Boundary Value Problems. New York. McGraw-Hill. 1963.
57. Gradshteyn, I.S. and Ryzhik, I.M. Table of Integrals, Series and Products. New York and London. Academic Press. 1965.
58. Watson, G.N. A Treatise on the Theory of Bessel Functions. Cambridge. University Press. 1952.
59. Woinowsky-Kreiger, S. Uber die biegun g dunner rechteckiger platten durch kreislasten. Ingenieur-Archiv. 3:236-250. 1932.
60. Reeves, C.M. and Wells, M. A Course on Programming in ALGOL 60. London. Chapman and Hall. 1964.
61. Green, J.S. KDF-9 ALGOL Programming. English-Electric Leo-Marconi Mini-Manual. Kidsgrove. English-Electric Leo-Marconi. 1963.

62. Faddeev, D.K. and Faddeeva, V.N. Computational Methods of Linear Algebra. San Francisco and London, Freeman. 1963.
63. Ralston, A. and Wilf, H.S. Mathematical Methods for Digital Computers. London. Wiley. 1960.

ACKNOWLEDGEMENTS

The author is indebted to Professor R.H. Evans, C.B.E., D.Sc., D.es Sc., Ph.D., M.I.C.E., M.I.Mech.E., M.I. Struct.E., and to Professor C.A. O'Flaherty, B.E., M.S., Ph.D., A.M.I.C.E.I., M.Inst.H.E. and Mr. A.L. Yettram, B.A., B.A.I., under whose supervision this investigation was carried out, for their guidance and encouragement during the course of this research program.

Sincere thanks are extended to the technical staff of the Civil Engineering Laboratories for their assistance in the preparation of experimental equipment and to the staff of the University of Leeds Electronic Computing Laboratory for their advice in the writing of the programs.

APPENDIX A: NOMENCLATURE

Geometry

x, y, z	Cartesian co-ordinate system
a	Slab length in the x-direction
b	Slab width in the y-direction
h	Slab thickness in the z-direction
d	Arbitrary depth of foundation
V	Volume of complete system
S	Surface of complete system
S_1	Surface over which stresses are prescribed
S_2	Surface over which displacements are prescribed
\underline{n}	Direction normal to S
\underline{t}	Direction tangential to S

Elasticity

E	Modulus of elasticity for the material of the slab
E_f	Modulus of elasticity for the material of the foundation
G	Modulus of rigidity for the material of the slab
μ	Poisson's ratio for the material of the slab
k	Modulus of subgrade reaction, tension and compression, for the material of the foundation
$k(w_1)$	Modulus of subgrade reaction, compression only, for the material of the foundation
$\sigma_x, \sigma_y, \sigma_z$	Direct stresses in the x-, y- and z-directions

τ_{xy}, τ_{yz} , Shear stresses relative to the x-, y- and z-directions

τ_{zx}

$\sigma_{ij_p}, \sigma_{ij_f}$ Generalized form of stress in the slab and foundation
respectively

$\epsilon_x, \epsilon_y, \epsilon_z$ Direct strains in the x-, y- and z-directions

γ_{xy}, γ_{yz} , Shear strains relative to the x-, y- and z-directions

γ_{zx}

$\epsilon_{ij_p}, \epsilon_{ij_f}$ Generalized form of strain in the slab and the
foundation respectively

u, v, w Displacements in the x-, y- and z-directions

w_u Displacement of the upper surface of the slab in the
z-direction

w_l Displacement of the lower surface of the slab in the
z-direction

w_{lf} Displacement of the foundation at depth d, in the
z-direction

α_o, β_o Weighted average rotations in the x- and y-directions

w_o Weighted average displacement in the z-direction

α_o, β_o Weighted average rotations in the x- and y-directions with
the effect of transverse compression neglected.

w_o Weighted average displacement in the z-direction with the
effect of transverse compression neglected

M_x, M_y Bending moments per unit width in the slab in the x- and
y-directions

H	Twisting moment per unit width in the slab relative to the x-and y-directions
V_x, V_y	Shearing forces per unit width in x-and y-directions
F	Strain energy density
F_p	Strain energy density for the slab
F_f	Strain energy density for the foundation
W	Complementary energy density
W_p	Complementary energy density for the slab
W_f	Complementary energy density for the foundation
P	Total potential energy of the system
P_e	Potential energy density of the external forces
q	Direct stress in the z-direction in the foundation
$g, T, C, e,$	Intermediate symbols as defined in the text
$m, r, f, t,$	
U, V, s	
K	A general functional
u_i	General function associated with the functional K
\underline{W}	A function of the deflection of the upper face of the foundation, as defined in the text
\emptyset	Arbitrary large positive number
λ	Radius of relative stiffness
\bar{P}	Total wheel-load in the Westergaard analysis
$\sigma_i, \sigma_e, \sigma_c$	Maximum tensile stresses in the pavement slab for the interior, edge and corner loading positions of the Westergaard analysis

- d_i, d_e, d_c Maximum deflection of the pavement slab for the interior, edge and corner loading positions of the Westergaard analysis
- M_1, x_1, c_1 Intermediate symbols of the Westergaard analysis, as defined in the text
- $w(x, y, z)$ Deflection of the plate, according to the analysis of Pister and Westmann, which is expressed as a function of the transverse displacement contributions: $w(x, y), w'(x, y)$ and $w''(x, y)$.

Boundary

- P_x, P_y, P_z Surface stresses in the x-, y- and z-directions
- $\bar{P}_x, \bar{P}_y, \bar{P}_z$ Specified values of P_x, P_y, P_z
- P Applied normal load intensity distribution on the upper surface of the plate
- $\bar{\alpha}_0, \bar{\beta}_0$ Specified values of α_0, β_0 at the surface
- \bar{w}_0 Specified value of w_0 at the surface
- $M_{\underline{n}}$ Bending moment per unit width in the \underline{n} -direction
- $H_{\underline{nt}}$ Twisting moment per unit width relative to the \underline{n} - and \underline{t} -directions
- $V_{\underline{n}}$ Shearing forces per unit width in the \underline{n} -direction
- $M_{\underline{n}}$ Specified value of bending moment per unit width in the \underline{n} -direction
- $H_{\underline{nt}}$ Specified value of twisting moment per unit width relative to the \underline{n} - and \underline{t} - directions

- \bar{V}_n Specified value of shearing force, per unit width in the n -direction
- a, b, c General constants
- x_o, y_o Co-ordinates of the centre of the idealized circular area of wheel contact
- x_d, y_d Co-ordinates of a data point in the area over which the load intensity distribution is prescribed in the power series representation
- N Number of data points x_d, y_d ($d=1, 2, \dots, N$)
- L Functional equalling the sum of the squares of the residuals R_d at each data point x_d, y_d
- \underline{E} Error in truncating the Chebyshev series expansion of a load intensity distribution after mn terms
- $P_{mn}(\eta, \xi)$ Approximation to p at the point (η, ξ) by the truncated Chebyshev series of mn terms
- η_α, ξ_β Zero points of the Chebyshev arguments $T_m^*(\eta_\alpha)$ and $T_n^*(\xi_\beta)$ where α and β are integer subscripts for each zero point
- $\theta_\alpha, \phi_\beta$ Angular variable form of η_α, ξ_β
- $\bar{\alpha}, \bar{\beta}$ Integer subscripts
- ϕ, θ Polar co-ordinates with origin at the centre of the idealized circular wheel contact area
- $\alpha_i, \alpha_j, \beta_i, \beta_j$ Intermediate symbols, as defined in the text
- $f(\theta), g(\theta), h(\theta), k(\theta)$ Intermediate symbols, as defined in the text

γ_{ij}	Intermediate symbol, as defined in the text
e	Number of simultaneous normal equations in the power series representation of a load intensity distribution
A	Matrix of elements, a_{st} , of the normal equations
B	Vector of constants, b_s , of the normal equations
G,F	Intermediate matrices in the solution of the normal equations and defined in the text with elements g_{st} and f_t
X	General independent variable applicable to x and y
R	Number of terms considered in the convergence of the Bessel function of order one

Computation

$f(x,y)$,	General functions of the independent variables x and y
$f_1(x,y)$,	
$f_2(x,y)$	
i,j	Subscripts denoting the ijth term of a series
c_{ij} , d_{ij}	General coefficients of power series with subscripts i,j
m,n	Subscripts associated with the limit of the truncated series describing the load intensity distribution p
R_1, R_2	Radii of convergence of a series in the x- and y- directions respectively
$M_{x_{ij}}$, $M_{y_{ij}}$	ijth coefficients of the series representing the dependent variables $M_x, M_y, V_x, V_y, w_0, H$ and p respectively
$V_{x_{ij}}$, $V_{y_{ij}}$	

- w_{0ij}, H_{ij}
- P_{ij}
- s, t General integer subscripts
- Q Number of simultaneous algebraic equations from the power series solution to the boundary value problem
- η, ξ Dimensionless co-ordinate system related to x, y by the transforms $\eta = x/a$ and $\xi = y/b$
- $f(\eta)$ General function of the dimensionless variable η , expanded as a Chebyshev series
- $f'(\eta)$ Derivative of the function $f(\eta)$ expressed as a Chebyshev series
- A_i General Chebyshev series coefficient of the expansion of $f(\eta)$
- a_i General Chebyshev series coefficient of the expansion of $f'(\eta)$
- $w_{0ij}^{\eta\eta}, w_{0ij}^{\xi\xi}$, Symbols associated with the differentiated form of the Chebyshev expansion of w_0 , as defined in the text
- $w_{0ij}^{\eta\xi}$
- $s_1(x)$ General truncated Fourier series expansion, with series coefficients a_0, a_i and b_i , which converges to the function $f(x)$
- \underline{x} Vector of unknown power series coefficients of the dependent variables.

- A Matrix of coefficients of the simultaneous algebraic equations in the power series solution to the primary boundary value problem.
- b Vector of constants of the simultaneous algebraic equations
- B₁, B₂, B₃, Intermediate symbols, as defined in the text
- B₄, B₅, B₆
- r, u Row and column positions of an element a_{r, u} of the matrix A
- s_m, t_m Suffices of an unknown dependent series coefficient
- AA, BB, CC, DD, EE, FF, GG, HH, KK, LL, MM, NN Group symbols associated with the formation of the matrix of coefficients of the system of algebraic simultaneous equations of the power series solution
- C, C', H Intermediate matrices in the solution of the algebraic simultaneous equations, as defined in the text
- σ_{max}, σ_{min} Maximum and minimum principal stresses in the upper surface of the slab
- ε_{max}, ε_{min} Maximum and minimum principal strains in the upper surface of the slab
- ϕ_p Direction of the maximum principal stress and strain in the upper surface of the slab

ϕ_p^*

Intermediate symbol defined in the text

w_c

Displacement of the slab in the z -direction with the effects of transverse compression neglected

Experimental

\bar{v}

Maximum intensity of the load intensity distribution p applied to the experimental model

APPENDIX B: PROGRAMS TO DETERMINE THE FUNCTIONS
DESCRIBING THE APPLIED TRANSVERSE WHEEL-LOAD

The following three computer programs are written in order to calculate the coefficients of the power series, shifted Chebyshev series and Fourier series, each of which describes the load intensity distribution of an idealized circular wheel-load applied to any point on the surface of a rectangular slab. Each of these programs also calculates, from the resulting series, the value of the load intensity at points over the surface of the plate.

Wheel-Load Expressed as a Power Series

```
begin library AO,A6,A14;  
  integer n,N,ee,number,tt,i2,pp,qq;  
  real a,b,x0,y0,,k1,c1,p1;  
  
comment 1;  
  open(20);open(70);copytext(20,70,[_<>]);  
  a:=read(20);b:=read(20);x0:=read(20);y0:=read(20);  
  c:=read(20);k1:=read(20);c1:=read(20);n:=read(20);  
  number:=read(20);pp:=read(20);qq:=read(20);  
  tt:=read(20);
```

```
pi:=3.141592654;N:=0;ee:=(n+1)x(n+1);  
begin real array p[1:ee],store[1:number,1:3],  
  xx,yy[1:tt];  
  procedure DATMAKER;  
  begin real FF,x,y,p1,q1,m,w;  
    procedure dodgy(X,Y,FUNCTION);  
    value X,Y,FUNCTION; real X,Y,FUNCTION;  
    begin N:=N+1;  
      store[N,1]:=X;  
      store[N,2]:=Y;  
      store[N,3]:=FUNCTION;  
    end;
```

comment 2;

```
  for x:=x0-2xc+k1,  
  x+k1 while x<(x0+2xc-k1+0.0001) do  
  for y:=y0-2xc+k1,  
  y+k1 while y<(y0+2xc-k1+0.0001) do  
  begin FF:=if ((x-x0)/c)2+((y-y0)/c)2≤1  
    then 1/(p1xc2) else 0;  
    dodgy(x,y,FF);  
  end;
```

comment 3;

```
  q1:=p1:=k1;w:=x:=x0-p1;  
  for x:=x+p1 while x≤a, a do  
  begin p1:=p1xc1;m:=x-w;w:=x;q1:=m/c1;y:=y0-q1;  
  Repeat 1: for y:=y+q1 while y≤b do  
    begin if x<2xc+x0 and y<2xc+y0  
      then goto Repeat 1;  
      dodgy(x,y,0);q1:=q1xc1;  
    end;
```

```
if  $x > 2x_c + x_0$  or  $b > 2x_c + y_0$  then dodgy(x,b,0);  
end;
```

comment 4;

```
q1:=p1:=k1;w:=x:=x0-p1;  
for  $x:=x+p1$  while  $x \leq a$ , a do  
begin  $p1:=p1 \times c1$ ;  $m:=x-w$ ;  $w:=x$ ;  $q1:=m/c1$ ;  $y:=y_0+q1$ ;  
Repeat 2: for  $y:=y-q1$  while  $y \geq 0$  do  
begin if  $x < 2x_c + x_0$  and  $y > y_0 - 2x_c$   
then goto Repeat 2;  
dodgy(x,y,0);  $q1:=q1 \times c1$ ;  
end;  
if  $x > 2x_c + x_0$  or  $0 < y_0 - 2x_c$  then dodgy(x,0,0);  
end;
```

comment 5;

```
q1:=p1:=k1;w:=x:=x0+p1;  
for  $x:=x-p1$  while  $x \geq 0$ , 0 do  
begin  $p1:=p1 \times c1$ ;  $m:=w-x$ ;  $w:=x$ ;  $q1:=m/c1$ ;  $y:=y_0+q1$ ;  
Repeat 3: for  $y:=y-q1$  while  $y \geq 0$  do  
begin if  $x > x_0 - 2x_c$  and  $y > y_0 - 2x_c$   
then goto Repeat 3;  
dodgy(x,y,0);  $q1:=q1 \times c1$ ;  
end;  
if  $x < x_0 - 2x_c$  or  $0 < y_0 - 2x_c$  then dodgy(x,0,0);  
end;
```

comment 6;

```
q1:=p1:=k1;w:=x:=x0+p1;  
for  $x:=x-p1$  while  $x \geq 0$ , 0 do  
begin  $p1:=p1 \times c1$ ;  $m:=w-x$ ;  $w:=x$ ;  $q1:=m/c1$ ;  $y:=y_0-q1$ ;  
Repeat 4: for  $y:=y+q1$  while  $y < b$  do
```

```
begin if x>x0-2xc and y<2xc+y0  
  then goto Repeat 4;  
  dodgy(x,y,0);q1:=q1xc1;  
end;  
  if x<x0-2xc or b>2xc+y0 then dodgy(x,b,0);  
end;  
end of DATMAKER;
```

```
procedure NORMEQ(N,n,store);  
value N,n; integer N,n; real array store;  
begin integer p1,p2,ii,jj,dd,ff,kk,p1f,p1i,  
  p1fk,p1ij,if,jk;  
  real array A[1:(n+1)x(n+1),1:(n+1)x(n+1)],  
  B[1:(n+1)x(n+1)];  
  procedure pos div(m,A,B);  
  value m;integer m;array A,B;  
  begin integer i,j,k;  
    real procedure dot(a,b,ppp,qqq);  
    value qqq; real a,b; integer ppp,qqq;  
    begin real s; s:=0;  
      for ppp:=1 step 1 until qqq do s:=s+aXb;  
      dot:=s  
    end dot;  
  end;
```

comment 7;

```
for i:=1 step 1 until m do  
  begin A[i,i]:=sqrt(A[i,i]  
    -dot(A[j,i]2,1,j,i-1));  
    for j:=i+1 step 1 until m do  
      A[i,j]:=(A[i,j]  
        -dot(A[k,i],A[k,j],k,i-1))/A[i,i]  
    end;
```

comment 8;

```
for i:=1 step 1 until m do  
B[i]:=(B[i]-dot(A[k,i],B[k],k,i-1))/A[i,i];
```

comment 9;

```
for i:=m step -1 until 1 do  
B[i]:=(B[i]-dot(A[i,m+1-k],B[m+1-k],k,m-1))  
      /A[i,i];  
for i:=1 step 1 until m do  
p[i]:=B[i];  
  
end of pos div;  
p1:=n+1;p2:=p1↑2;  
for kk:=1 step 1 until p2 do  
begin for ii:=1 step 1 until p2 do  
  A[kk,ii]:=0;  
  B[kk]:=0;  
end;
```

comment 10;

```
for ii:=0 step 1 until n do  
begin p1i:=p1×ii+1;  
  for jj:=0 step 1 until n do  
  begin p1ij:=p1i+jj;  
    for ff:=0 step 1 until ii-1 do  
    begin p1f:=p1×ff+1;if:=ii+ff;  
      for kk:=0 step 1 until n do  
      begin p1fk:=p1f+kk;jk:=jj+kk;  
        for dd:=1 step 1 until N do  
        A[p1fk,p1ij]:=  
          (if if=0 then 1 else store[dd,1]↑if)×  
          (if jk=0 then 1 else store[dd,2]↑jk)+
```

```
        A[p1fk,p1ij];
    end;
end;
ff:=i1;p1f:=p1xff+1;i1f:=i1+ff;
for kk:=0 step 1 until jj do
begin p1fk:=p1f+kk;jk:=jj+kk;
    for dd:=1 step 1 until N do
        A[p1fk,p1ij]:=
            (if i1f=0 then 1 else store[dd,1]↑i1f)×
            (if jk=0 then 1 else store[dd,2]↑jk)+
            A[p1fk,p1ij];
    end;
end;
end;
```

comment 11;

```
for ff:=0 step 1 until n do
begin p1f:=p1xff+1;
    for l1:=0 step 1 until n do
        begin p1fk:=p1f+kk;
            for dd:=1 step 1 until N do
                B[p1fk]:=
                    (if ff=0 then 1 else store[dd,1]↑ff)×
                    (if kk=0 then 1 else store[dd,2]↑kk)×
                    store[dd,3]+B[p1fk];
            end;
        end;
    end;
```

```
pos div(p2,A,B);
end of NORMEQ;
```

comment 12;

```
procedure POWERCOEFF;  
begin integer f1,f2,f3;real i,j;  
  f1:=format([4snd]);f2:=format([2snd]);  
  f3:=format([4s-d.ddddd10-ndc]);  
  writetext(70,[[3c5s]I[3s]J[5s]COEFF[2c]]);  
  for i:=0 step 1 until n do  
  for j:=0 step 1 until n do  
  begin write(70,f1,i);  
    write(70,f2,j);  
    write(70,f3,p[(n+1)x i+j+1]);  
  end;  
end of POWERCOEFF;
```

comment 13;

```
procedure POWERSURFACE;  
begin integer f4,f5,f6;  
  real pp1,pp2,qq1,qq2,x,y;  
  real procedure POWERPOINT(X,Y);  
  value X,Y;real X,Y;  
  begin real P;integer iz,jz;  
    P:=p[1];  
    for iz:=1 step 1 until n do  
    P:=(Y↑iz)xp[iz+1]+P;  
    for jz:=1 step 1 until n do  
    P:=(X↑jz)xp[(n+1)xjz+1]+P;  
    for iz:=1 step 1 until n do  
    for jz:=1 step 1 until n do  
    P:=(X↑iz×Y↑jz)xp[(n+1)xiz+jz+1]+P;  
    POWERPOINT:=P;  
  end of POWERPOINT;  
  f4:=format([4sddd.dd]);
```

```
f5:=format([2sndd.dd]);
f6:=format([3s-ndd.dddddcc]);
pp2:=a/pp;qq2:=b/qq;pp1:=a-pp2+0.0001;
qq1:=b-qq2+0.0001;
writetext(70,[[3c6s]X[7s]Y[9s]LOAD[2c]]);
for x:=0,x+pp2 while x<pp1,a do
for y:=0,y+qq2 while y<qq1,b do
begin write(70,f4,x);
      write(70,f5,y);
      write(70,f6,POWERPOINT(x,y));
end;
for i2:=1 step 1 until tt do
begin x:=xx[i2];y:=yy[i2];
      write(70,f4,x);
      write(70,f5,y);
      write(70,f6,POWERPOINT(x,y));
end;
end of POWERSURFACE;
```

comment 14;

```
for i2:=1 step 1 until tt do
begin xx[i2]:=read(20);
      yy[i2]:=read(20);
end;
```

```
close(20);
for i2:=1 step 1 until ee do
p[i2]:=0;
```

DATMAKER;

```
NORMEQ(N,n,store);  
POWERCOEFF;  
POWERSURFACE;  
close(70);  
end;  
end  
→
```

Wheel-Load Expressed as a Chebyshev Series

```
begin library A0,A6,A14;  
  integer n,pp,qq,tt,1,j;  
  real a,b,c,x0,y0,p1;  
  
comment 1;  
  open(20);open(70);copytext(20,70,[_<>_]);  
  a:=read(20);b:=read(20);x0:=read(20);y0:=read(20);  
  c:=read(20);n:=1+read(20);pp:=read(20);  
  qq:=read(20);tt:=read(20);p1:=3.141592654;  
  
  begin real array t[1:n,1:n],xx,yy[1:tt];  
    procedure CHEBCOEFF;  
      begin integer ALPHA,BETA,f1,f2,f3;  
        real pis,ns,pit;  
        real array functco,Tstar[1:n,1:n],nalpha[1:n];  
  comment 2;  
    real procedure THAT(I,J);  
    value I,J; integer I,J;  
    begin real tone;
```

```
tone:=0;
for ALPHA:=0 step 1 until n-1 do
for BETA:=0 step 1 until n-1 do
tone:=functco[ALPHA+1,BETA+1]×
    Tstar[I+1,ALPHA+1]×Tstar[J+1,BETA+1]+tone;
THAT:=ns×tone;
end of THAT;
```

comment 3;

```
pis:=pi/(4×n);ns:=4/(n↑2);pit:=1/(pi×c↑2);
for ALPHA:=0 step 1 until n-1 do
begin nalpha[ALPHA+1]:=(cos(pis×(2×ALPHA+1)
    +0.5))↑2;
    Tstar[1,ALPHA+1]:=1;
    Tstar[2,ALPHA+1]:=2×nalpha[ALPHA+1]-1;
    for i:=2 step 1 until n-1 do
    Tstar[i+1,ALPHA+1]:=(4×nalpha[ALPHA+1]-2)
        ×Tstar[i,ALPHA+1]-Tstar[i-1,ALPHA+1];
    end;
```

comment 4;

```
for ALPHA:=0 step 1 until n-1 do
for BETA:=0 step 1 until n-1 do
functco[ALPHA+1,BETA+1]:=if ((a×nalpha[ALPHA
    +1]-x0)↑2+(b×nalpha[BETA+1]-y0)↑2-c↑2)
    <0 then pit else 0;
```

comment 5;

```
t[1,1]:=0.25×THAT(0,0);
for i:=1 step 1 until n-1 do
t[i+1,1]:=0.5×THAT(i,0);
for j:=1 step 1 until n-1 do
```

```
t[1,j+1]:=0.5×THAT(0,j);  
for i:=1 step 1 until n-1 do  
for j:=1 step 1 until n-1 do  
t[i+1,j+1]:=THAT(i,j);  
f1:=format([4snd]);f2:=format([2snd]);  
f3:=format([4s-d.ddddd0-ndc]);  
writetext(70,[[3c5s]I[3s]J[5s]COEFF[2c]]);
```

comment 6;

```
for i:=0 step 1 until n-1 do  
for j:=0 step 1 until n-1 do  
begin write(70,f1,i);  
    write(70,f2,j);  
    write(70,f3,t[i+1,j+1]);  
end;  
end of CHEBCOEFF;
```

comment 7;

```
procedure CHEBSURFACE;  
begin integer k1,k2,f4,f5,f6;  
    real pp1,pp2,x,y,xt,qq1,qq2,yt,SP;  
    real array Tn[1:n,1:pp+1],Te[1:n,1:qq+1],  
    Tnn,Tee[1:n];  
    procedure TERM(X,K1,ARR);  
    value X,K1;real X;integer K1;real array ARR;  
    begin ARR[1,K1]:=1; ARR[2,K1]:=2×X-1;  
        for i:=2 step 1 until n-1 do  
            ARR[i+1,K1]:=(4×X-2)×ARR[i,K1]-ARR[i-1,K1];  
    end of TERM;  
    real procedure SUM(kk1,kk2);  
    value kk1,kk2; integer kk1,kk2;
```

```
begin real F1;F1:=0;  
  for i:=0 step 1 until n-1 do  
    for j:=0 step 1 until n-1 do  
      F1:=t[i+1,j+1]×Tn[i+1,kk1]×Te[j+1,kk2]+F1;  
      SUM:=F1;  
end of SUM;
```

```
k1:=0;pp2:=a/pp;pp1:=a-pp2+0.0001;  
for x:=0,x+pp2 while x<pp1,a do  
begin k1:=k1+1;xt:=x/a;  
  TERM(xt,k1,Tn);  
end;
```

```
k1:=0;qq2:=b/qq;qq1:=b-qq2+0.0001;  
for y:=0,y+qq2 while y<qq1,b do  
begin k1:=k1+1;yt:=y/b;  
  TERM(yt,k1,Te);  
end;
```

```
k1:=0;f4:=format([4sndd.dd]);  
f5:=format([2sndd.dd]);  
f6:=format([3s-ndd.ddddddc]);  
writetext(70,[[3c6s]X[7s]Y[9s]LOAD[2c]]);
```

```
for x:=0,x+pp2 while x<pp1,a do  
begin k1:=k1+1;k2:=0;  
  for y:=0,y+qq2 while y<qq1,b do  
    begin k2:=k2+1;  
      write(70,f4,x);  
      write(70,f5,y);  
      write(70,f6,SUM(k1,k2));  
    end;  
end;
```

```
end;  
for k1:=1 step 1 until tt do
```

```
begin xt:=xx[k1]/a;yt:=yy[k1]/b;  
  Tnn[1]:=Tee[1]:=1;  
  Tnn[2]:=2xt-1;Tee[2]:=2yt-1;  
  for i:=2 step 1 until n-1 do  
    begin Tnn[i+1]:=(4xt-2)×Tnn[i]-Tnn[i-1];  
      Tee[i+1]:=(4yt-2)×Tee[i]-Tee[i-1];  
    end;  
  SP:=0;  
  for i:=0 step 1 until n-1 do  
    for j:=0 step 1 until n-1 do  
      SP:=t[i+1,j+1]×Tnn[i+1]×Tee[j+1]+SP;  
      write(70,f4,xx[k1]);  
      write(70,f5,yy[k1]);  
      write(70,f6,SP);  
    end;  
  end of CHEBSURFACE;
```

```
comment 8;  
  for i:=1 step 1 until tt do  
    begin xx[i]:=read(20);  
      yy[i]:=read(20);  
    end;  
  
  close(20);  
  CHEBCOEFF;  
  CHEBSURFACE;  
  close(70);  
  end;
```

end

→

Wheel-Load Expressed as a Fourier Series

```
begin library AO,A6,A14;  
  integer 1,j,n,pp,qq,tt,12;  
  real a,b,c,x0,y0,p1,x,y;  
  
comment 1;  
  open(20);open(70);copytext(20,70, [<>]);  
  a:=read(20);b:=read(20);x0:=read(20);y0:=read(20);  
  c:=read(20);n:=read(20);pp:=read(20);qq:=read(20);  
  tt:=read(20);p1:=3.141592654;  
  
  begin real array LOAD[1:n+1,1:n+1],xx,yy[1:tt];  
  procedure FOURSERIES;  
    begin integer f1,f2,f3; real as,bs,abc,X13,Eta3;  
  
comment 2;  
    real procedure BESSEL(X);  
    value X; real X;  
    begin integer R,RR,RRR; real Q,QQ;  
      QQ:=Q:=X/2;R:=0;RR:=RRR:=1;  
    Repeat: R:=R+1; RR:=R×RR; RRR:=(R+1)×RRR;QQ:=Q;  
      Q:=Q+(((−1)↑R)×((X/2)↑(1+2×R)))/(RR+RRR);  
      if (QQ-Q)/Q>1.010-12 then goto Repeat  
        else BESSEL:=Q;  
    end of BESSEL;  
  
comment 3;  
    real procedure FOURCOEFF(I,J,BESSEL);  
    integer I,J; real procedure BESSEL;  
    begin real A,B;
```

```
B:=pi*sqrt((I↑2)/as+(J↑2)/bs);  
A:=abc/Bxcos(IXX13)xcos(JXEta3)xBESSEL(Bxc);  
FOURCOEFF:=A;  
end of FOURCOEFF;
```

```
as:=a↑2;bs:=b↑2;abc:=8/(a×b×c);X13:=pi×x0;  
Eta3:=pi×y0;f1:=format([4snd]);  
f2:=format([2snd]);  
f3:=format([4s-d. ddddd10-ndc]);  
writetext(70,[[3c5s]I[3s]J[5s]COEFF[2c]]);
```

comment 4;

```
LOAD[1,1]:=1/(a×b);  
write(70,f1,0);  
write(70,f2,0);  
write(70,f3,LOAD[1,1]);
```

comment 5;

```
for j:=1 step 1 until n do  
begin write(70,f1,0);  
write(70,f2,j);  
LOAD[1,j+1]:=(FOURCOEFF(0,j,BESSEL))/2;  
write(70,f3,LOAD[1,j+1]);  
end;
```

comment 6;

```
for i:=1 step 1 until n do  
begin write(70,f1,1);  
write(70,f2,0);  
LOAD[i+1,1]:=(FOURCOEFF(1,0,BESSEL))/2;  
write(70,f3,LOAD[i+1,1]);
```

```
end;  
for i:=1 step 1 until n do  
for j:=1 step 1 until n do  
begin write(70,f1,i);  
    write(70,f2,j);  
    LOAD[i+1,j+1]:=(FOURCOEFF(i,j,BESSEL));  
    write(70,f3,LOAD[i+1,j+1]);  
end;  
end of FOURSERIES;
```

comment 7;

```
procedure FOURCHECK;  
begin integer f4,f5,f6; real pp1,pp2,qq2,qq1;
```

```
    real procedure FOURVALUE(X,Y);  
    value X,Y; real X,Y;  
    begin real HH,X1,Y1;  
        HH:=0;X1:=p1X/a;Y1:=p1Y/b;  
        for i:=0 step 1 until n do  
        for j:=0 step 1 until n do  
            HH:=HH+LOAD[i+1,j+1]xcos(iX1)xcos(jY1);  
        FOURVALUE:=HH;  
    end of FOURVALUE;
```

```
    f4:=format([4s $\text{ndd}$ . $\text{dd}$ ]);f5:=format([2s $\text{ndd}$ . $\text{dd}$ ]);  
    f6:=format([3s- $\text{ndd}$ . $\text{ddddddc}$ ]);  
    pp2:=a/pp;qq2:=b/qq;pp1:=a-pp2+0.0001;  
    qq1:=b-qq2+0.0001;  
    writetext(70,[[3c6s]X[7s]Y[9s]LOAD[2c]]);  
    for x:=0,x+pp2 while x<pp1,a do  
    for y:=0,y+qq2 while y<qq1,b do  
    begin write(70,f4,x);
```

```
        write(70,f5,y);
        write(70,f6,FOURVALUE(x,y));
    end;
    for i2:=1 step 1 until tt do
    begin x:=xx[i2];y:=yy[i2];
        write(70,f4,x);
        write(70,f5,y);
        write(70,f6,FOURVALUE(x,y));
    end;
end of FOURCHECK;

comment 8;
for i:=1 step 1 until tt do
begin xx[i]:=read(20);
    yy[i]:=read(20);
end;

close(20);
FOURSERIES;
FOURCHECK;
close(70);
end;
end
→
```

APPENDIX C: PROGRAMS FOR THE COMPUTATION OF PAVEMENT
STRESSES AND DEFORMATIONS

The following three computer programs are written in order to calculate, in a rectangular slab resting on an elastic foundation, the stresses, strains and deflections which result from the application of a given load intensity distribution, expressed in terms of a truncated power series, to the upper surface of the slab. The mathematical model representing this slab/foundation system is re-expressed in the form of a set of simultaneous algebraic equations by the use of a power series solution to this model. The first program sets up the simultaneous algebraic equations and the second program solves these equations for the coefficients of the power series which describe the unknown stress resultants and weighted average displacement. The third program determines stresses, strains and deflections in the rectangular plate from the power series representation of the stress resultants, weighted average displacement and the load intensity distribution.

Setting-up the Simultaneous Algebraic Equations

```
begin library A0,A3,A6,A13,A14;  
      integer n,F,z;  
      real a,b,h,mu,E,k;
```



```
P[g,h1]:=0;  
Q[g]:=0;  
end;
```

comment 5;

```
P[2,1]:=P[7,1]:=P[13,1]:=P[19,1]:=P[24,1]:=  
P[25,1]:=P[29,1]:=P[30,1]:=P[32,1]:=P[34,1]:=  
P[40,1]:=P[41,1]:=P[45,1]:=P[49,1]:=1;  
P[8,1]:=P[20,1]:=P[26,1]:=P[27,1]:=P[31,1]:=  
P[33,1]:=P[35,1]:=P[50,1]:=2;
```

comment 6;

```
for g:=1 step 1 until 52 do  
P[g,2]:=P[g,4]:=n;  
for g:=19 step 1 until 27 do  
P[g,2]:=P[g,4]:=n-1;  
P[38,2]:=P[39,2]:=P[30,4]:=P[31,4]:=n-1;  
P[5,2]:=P[15,2]:=P[6,4]:=P[14,4]:=n-2;
```

comment 7;

```
P[4,3]:=P[11,3]:=P[16,3]:=P[21,3]:=P[24,3]:=  
P[26,3]:=P[32,3]:=P[33,3]:=P[37,3]:=P[38,3]:=  
P[40,3]:=P[42,3]:=P[47,3]:=P[51,3]:=1;  
P[17,3]:=P[22,3]:=P[25,3]:=P[27,3]:=P[39,3]:=  
P[41,3]:=P[43,3]:=P[52,3]:=2;
```

comment 8;

```
P[2,5]:=P[7,5]:=P[13,5]:=P[19,5]:=P[24,5]:=  
P[25,5]:=P[29,5]:=P[30,5]:=P[32,5]:=P[34,5]:=  
P[40,5]:=P[41,5]:=P[45,5]:=P[49,5]]=-1;  
P[8,5]:=P[20,5]:=P[26,5]:=P[27,5]:=P[31,5]:=  
P[33,5]:=P[35,5]:=P[50,5]]=-2;
```

```
P[21,5]:=P[22,5]:=P[23,5]:=1;  
P[5,5]:=P[15,5]:=2;
```

comment 9;

```
P[4,6]:=P[11,6]:=P[16,6]:=P[21,6]:=P[24,6]:=  
P[26,6]:=P[32,6]:=P[33,6]:=P[37,6]:=P[38,6]:=  
P[40,6]:=P[42,6]:=P[47,6]:=P[51,6]:=-1;  
P[17,6]:=P[22,6]:=P[25,6]:=P[27,6]:=P[39,6]:=  
P[41,6]:=P[43,6]:=P[52,6]:=-2;  
P[19,6]:=P[20,6]:=P[23,6]:=1;  
P[6,6]:=P[14,6]:=2;
```

comment 10;

```
for g:=1 step 1 until 52 do  
P[g,7]:=P[g,9]:=n;  
for g:=19 step 1 until 27 do  
P[g,7]:=n-1;  
P[24,9]:=P[25,9]:=P[26,9]:=P[27,9]:=P[30,9]:=  
P[31,9]:=P[32,9]:=P[33,9]:=P[38,9]:=P[39,9]:=  
P[40,9]:=P[41,9]:=n-1;
```

comment 11;

```
for g:=1 step 1 until 8 do  
begin P[g,8]:=B[1];  
P[g+9,8]:=B[2];  
P[g+18,8]:=B[3];  
P[g+27,8]:=B[4];  
P[g+35,8]:=B[5];  
P[g+43,8]:=B[6];  
end;  
P[9,8]:=B[1];P[18,8]:=B[2];P[27,8]:=B[3];
```

P[52,8]:=B[6];

comment 12;

P[1,10]:=P[2,10]:=P[12,10]:=P[13,10]:=
P[19,10]:=P[20,10]:=P[34,10]:=P[35,10]:=
P[44,10]:=P[45,10]:=B[1];
P[3,10]:=P[4,10]:=P[10,10]:=P[11,10]:=
P[21,10]:=P[22,10]:=P[42,10]:=P[43,10]:=
P[46,10]:=P[47,10]:=B[2];
P[24,10]:=P[25,10]:=P[26,10]:=P[27,10]:=
P[30,10]:=P[31,10]:=P[32,10]:=P[33,10]:=
P[38,10]:=P[39,10]:=P[40,10]:=P[41,10]:=B[3];
P[7,10]:=P[8,10]:=P[28,10]:=P[29,10]:=
P[49,10]:=P[50,10]:=B[4];
P[16,10]:=P[17,10]:=P[36,10]:=P[37,10]:=
P[51,10]:=P[52,10]:=B[5];
P[5,10]:=P[6,10]:=P[9,10]:=P[14,10]:=
P[15,10]:=P[18,10]:=P[23,10]:=P[48,10]:=B[6];

comment 13;

Q[7]:=-axt;Q[8]:=Q[17]:=t;Q[9]:=Q[18]:=-Tx
kxf/d;Q[16]:=-bxt;Q[24]:=axbxm;Q[25]:=-ax m;
Q[26]:=-bxm;Q[27]:=m;Q[34]:=-a;Q[35]:=
Q[43]:=1;Q[42]:=-b;Q[48]:=k/d;Q[49]:=-ax
kxT/d;Q[50]:=Q[52]:=kxT/d;Q[51]:=-bxkxT/d;

comment 14;

TT:=0;

for g:=1 step 1 until 52 do

if(P[g,2]-P[g,1])>0 and (P[g,4]-P[g,3])>0 then

TT:=(P[g,2]-P[g,1]+1)×(P[g,4]-P[g,3]+1)+TT;

comment 15;

```
for z:=1 step 1 until (n+1)×(n+1) do  
begin R[z]:=R[z+B[2]]:=+T×C×f×R[z];  
      R[z+B[6]]:=-R[z]/(T×f);  
end;
```

```
begin integer array NUM[1:2],BB[1:2,1:TT];  
      real array BBB[1:TT];
```

comment 16;

```
procedure varcoeff(VAR,G);  
value G; integer G; real VAR;  
begin for i:=P[G,1] step 1 until P[G,2] do  
      for j:=P[G,3] step 1 until P[G,4] do  
        begin rr:=(P[G,7]+1)×i+j+1+P[G,8];  
          u:=(P[G,9]+1)×(i+P[G,5])+j  
            +P[G,6]+1+P[G,10];  
          move:=move+1;  
          BB[1,move]:=rr;  
          BB[2,move]:=u;  
          BBB[move]:=VAR;  
        end;  
end of varcoeff;
```

```
move:=0;  
NUM[1]:=F;NUM[2]:=TT;
```

comment 17;

```
for g:=7,8,9,16,17,18,24,25,26,27,34,35,42,  
43,48,49,50,51,52 do varcoeff(Q[g],g);
```

comment 18;

```
varcoeff(rXaX(1+1),1);
varcoeff(-rX(1+1),2);
varcoeff(sXrXbX(j+1),3);
varcoeff(-sXrX(j+1),4);
varcoeff(-(1+1)X(1+2),5);
varcoeff(-sX(j+1)X(j+2),6);
varcoeff(rXbX(j+1),10);
varcoeff(-rX(j+1),11);
varcoeff(sXrXaX(1+1),12);
varcoeff(-sXrX(1+1),13);
varcoeff(-(j+1)X(j+2),14);
varcoeff(-sX(1+1)X(1+2),15);
varcoeff(-rXaX(j+1),19);
varcoeff(rX(j+1),20);
varcoeff(-rXbX(1+1),21);
varcoeff(rX(1+1),22);
varcoeff(2X(1+1)X(j+1),23);
varcoeff(aX(1+1),28);
varcoeff(-(1+1),29);
varcoeff(aXbX(j+1),30);
varcoeff(-bX(j+1),31);
varcoeff(-aX(j+1),32);
varcoeff((j+1),33);
varcoeff(bX(j+1),36);
varcoeff(-(j+1),37);
varcoeff(aXbX(1+1),38);
varcoeff(-aX(1+1),39);
varcoeff(-bX(1+1),40);
varcoeff((1+1),41);
varcoeff(-aX(1+1),44);
varcoeff((1+1),45);
```

```
varcoeff(-bx(j+1),46);  
varcoeff((j+1),47);
```

comment 19;

```
  for z:=1 step 1 until 2 do  
    output(10,NUM[z]);  
  for z:=1 step 1 until F do  
    output(10,R[z]);  
  for z:=1 step 1 until TT do  
    begin write(10,f1,BB[1,z]);  
      write(10,f1,BB[2,z]);  
    end;  
  for z:=1 step 1 until TT do  
    write(10,f2,BBB[z]);  
  charout(10,61);
```

```
  end;  
end of DATPREP;
```

comment 20;

```
  for z:=1 step 1 until (n+1)x(n+1) do  
    R[z]:=read(20);
```

```
  close(20);  
  DATPREP;  
  close(10);
```

end;

end

→

Solving the Simultaneous Algebraic Equations

```
begin library AO,A6,A14;  
  integer Z,s1,s2,Q,TT;  
  
comment 1;  
  open(20);open(70);copytext(20,70,[_<>]);  
  Z:=read(20);TT:=read(20);  
  
  begin real array R,H[1:Z],BBB[1:TT],  
    CC[1:Z*(Z+1)+2];  
  integer array BB[1:2,1:TT];  
  
comment 2;  
  procedure symdiv(m,A,B);  
  value m; integer m; array A,B;  
  begin integer i,j,k;  
    boolean array d[1:m];  
    real procedure dot(a,b,p,q);  
    value q; real a,b; integer p,q;  
    begin real s; s:=0;  
      for p:=1 step 1 until q do s:=s+a*xb;  
      dot:=s  
    end dot;  
    for i:=1 step 1 until m do  
      begin real w;  
        w:=A[i+(i-1)*i+2]-dot(A[j+(i-1)*i+2]i,  
          if d[j] then -1 else 1,j,i-1);  
        d[i]:=w<0;  
        A[i+(i-1)*i+2]:=sqrt(if d[i] then -w else w);  
        for j:=i+1 step 1 until m do
```

```
A[1+(j-1)xj+2]:=A[1+(j-1)xj+2]
-dot(if d[k] then -A[k+(i-1)x1+2]
else A[k+(i-1)x1+2],A[k+(j-1)xj+2],
k,i-1))/(if d[1] then -A[1+(i-1)x1+2]
else A[1+(i-1)x1+2]);
end;
for i:=1 step 1 until m do
B[i]:=B[i]-dot(A[k+(i-1)x1+2],if d[k]
then -B[k] else B[k],k,i-1))/(if d[1] then
-A[1+(i-1)x1+2] else A[1+(i-1)x1+2]);
for i:=m step -1 until 1 do
B[i]:=B[i] -dot(A[1+(m-k)x(m+1-k)+2],
B[m+1-k],k,m-1))/A[1+(i-1)x1+2];
end of symdiv;
```

comment 3;

```
for s1:=1 step 1 until Z do
R[s1]:=1.010read(20);
for s1:=1 step 1 until TT do
begin BB[1,s1]:=read(20);
BB[2,s1]:=read(20);
end;
for s1:=1 step 1 until TT do
BBB[s1]:=1.010read(20);

close(20);
for s1:=1 step 1 until Zx(Z+1)+2 do CC[s1]:=0;
```

comment 4;

```
for s1:=1 step 1 until TT do
for s2:=s1 step 1 until TT do
```

```
begin if BB[1,s1]=BB[1,s2] then  
  begin Q:=if BB[2,s2]>BB[2,s1]  
    then BB[2,s1]+(BB[2,s2]-1)×BB[2,s2]+2  
    else BB[2,s2]+(BB[2,s1]-1)×BB[2,s1]+2;  
    CC[Q]:=BBB[s1]×BBB[s2]+CC[Q];  
  end;  
end;  
  
  for s1:=1 step 1 until Z do H[s1]:=0;  
  
comment 5;  
  for s1:=1 step 1 until TT do  
    H[BB[2,s1]]:=BBB[s1]×R[BB[1,s1]]+H[BB[2,s1]];  
  
    symdiv(Z,CC,H);  
  
comment 6;  
  for s1:=1 step 1 until Z do  
    output(70,H[s1]);  
  
    close(70);  
  end;  
end  
→
```

Determination of Stresses, Strains and Deflections

```
begin library AO,A6,A14;  
  integer n,F,tt,pp,qq,N,pd;  
  real h,a,b,mu,E,k,x,y,g,D,T;
```

comment 1;

```
open(20);open(70);copytext(20,70,[<>]);  
a:=read(20);b:=read(20);h:=read(20);mu:=read(20);  
E:=read(20);k:=read(20);n:=read(20);pp:=read(20);  
qq:=read(20);tt:=read(20);
```

```
g:=(1+26xkxh/(70xE));T:=6xmu/(5XhxE);  
D:=9Xh/(70xE);F:=(n+1)x(n+1)x4+n↑2;N:=(n+1)↑2;
```

```
begin real array kk[1:F],xx,yy[1:tt];
```

```
procedure POWERSURFACE;
```

```
begin integer f9,f10; real pp1,pp2,qq1,qq2;
```

```
procedure POWERPOINT(X,Y);
```

```
value X,Y; real X,Y;
```

```
begin real P,W,WL,Mx,My,H,phi,sigma x,  
sigma y,tor xy,fmax,fmin;
```

```
integer p,q,sks;
```

comment 2;

```
P:=W:=Mx:=My:=H:=0;
```

```
P:=kk[1];W:=kk[N+1];Mx:=kk[2×N+1];
```

```
My:=kk[3×N+1];H:=kk[4×N+1];
```

```
for q:=1 step 1 until n do
```

```
begin sks:=q+1;P:=(Y↑q)×kk[sks]+P;
```

```
sks:=sks+N;W:=(Y↑q)×kk[sks]+W;
```

```
sks:=sks+N;Mx:=(Y↑q)×kk[sks]+Mx;
```

```
sks:=sks+N;My:=(Y↑q)×kk[sks]+My;
```

```
end;
```

```
for q:=1 step 1 until n-1 do
```

```
begin sks:=q+1+N×4;H:=(Y↑q)×kk[sks]+H;
```

```
end;
```

```
for p:=1 step 1 until n do
```

```
begin sks:=(n+1)×p+1;P:=(X↑p)×kk[sks]+P;
```

```
sks := sks + N; W := (X↑p) × kk[sk] + W;
sks := sks + N; Mx := (X↑p) × kk[sk] + Mx;
sks := sks + N; My := (X↑p) × kk[sk] + My;
end;
for p := 1 step 1 until n-1 do
begin sks := n × p + 1 + N × 4; H := (X↑p) × kk[sk] + H;
end;
for p := 1 step 1 until n do
for q := 1 step 1 until n do
begin
sks := (n+1) × p + q + 1; P := (X↑p × Y↑q) × kk[sk] + P;
sks := sks + N; W := (X↑p × Y↑q) × kk[sk] + W;
sks := sks + N; Mx := (X↑p × Y↑q) × kk[sk] + Mx;
sks := sks + N; My := (X↑p × Y↑q) × kk[sk] + My;
end;
for p := 1 step 1 until n-1 do
for q := 1 step 1 until n-1 do
begin
sks := n × p + q + 1 + N × 4; H := (X↑p × Y↑q) × kk[sk] + H;
end;
Mx := Mx × (a × X - X↑2); My := My × (b × Y - Y↑2);
```

comment 3;

```
WL := (W - T × (Mx + My) + D × P) / g;
```

comment 4;

```
sigma x := 6 × Mx / h↑2; sigma y := 6 × My / h↑2;
tor xy := 6 × (H × (a × X - X↑2) × (b × Y - Y↑2)) / h↑2;
```

comment 5;

```
fmin := (sigma x + sigma y) / 2
-sqrt(((sigma x - sigma y) / 2)↑2 + tor xy↑2);
```

```
fmax:=(sigma x+sigma y)/2
      +sqrt(((sigma x-sigma y)/2)2+tor xy2);
writetext(70,[[2c]]);
write(70,f10,X);
write(70,f10,Y);
write(70,f9,P);
write(70,f9,W);
write(70,f9,WL);
write(70,f9,fmax);
write(70,f9,fmin);
write(70,f9,(fmax-muxfmin)/E);
write(70,f9,(fmin-muxfmax)/E);
```

comment 6;

```
if abs(sigma x- sigma y)<1.010-20
then begin writetext(70,[[13s]]);
      goto next;
      end;
phi:=(arctan((2xtor xy)/(sigma x-sigma y)))
      x45/1.5708;
phi:=if(sigma x-sigma y)>0 then phi
      else 90+phi;
write(70,f9,-phi);
next: end of POWERPOINT;
```

```
f9:=format([s-d. dddd10-nd]);
f10:=format([s-ndd.d]);
pp2:=a/pp;qq2:=b/qq;pp1:=(a-pp2+0.0001);
qq1:=(b-qq2+0.0001);
writetext(70,[[4c5s]CO-ORDS[7s]LOAD[8s]PLATE
[6s]INTERFACE[5s]MAXIMUM[6s]MINIMUM[6s]
MAXIMUM[6s]MINIMUM[5s]PRINCIP [c5s]X[6s]
```

```
Y[3s]INTENSITY[4s]DEFLECTION[3s]DEFLECTION[4s]  
STRESS[7s]STRESS[7s]STRAIN[7s]STRAIN[6s]  
DIRECTION[c]);
```

comment 7;

```
for x:=0,x+pp2 while x<pp1,a do  
for y:=0,y+qq2 while y<qq1,b do  
POWERPOINT(x,y);
```

comment 8;

```
for pd:=1 step 1 until tt do  
begin x:=xx[pd]; y:=yy[pd];  
POWERPOINT(x,y);  
end;
```

end of POWERSURFACE;

comment 9;

```
for pd:=1 step 1 until F do  
kk[pd]:=read(20);
```

comment 10;

```
for pd:=1 step 1 until tt do  
begin xx[pd]:=read(20);  
yy[pd]:=read(20);  
end;
```

```
close(20);  
POWERSURFACE;  
close(70);
```

end;

end

→